5-2017

VISUALIZING THE DYNAMICS OF IMMUNE SURVEILLANCE IN BRAIN TUMORS BY INTRAVITAL MULTIPHOTON MICROSCOPY

Felix Nwajei

Visualizing the dynamics of immune surveillance in brain tumors by intravital multiphoton microscopy

by

Felix I. Nwajei, MD

APPROVED:

_____
Tomasz Zal, Ph.D.
Supervisory Professor

_____
Kimberly Schluns, Ph.D.

_____
Amy Heimberger, M.D.

_____
Joya Chandra, Ph.D.

_____
Robert Dantzer, DVM, Ph.D.

APPROVED:

_____
Dean, The University of Texas
Graduate School of Biomedical Sciences at Houston

VISUALIZING THE DYNAMICS OF IMMUNE SURVEILLANCE IN BRAIN TUMORS BY INTRAVITAL MULTIPHOTON MICROSCOPY

A

DISSERTATION

Presented to the Faculty of

The University of Texas

M.D. Anderson Cancer Center UTHealth

Graduate School of Biomedical Sciences

In Partial Fulfillment

of the Requirements

for the Degree of

DOCTOR OF PHILOSOPHY

By

Felix I. Nwajei, MD

Houston, TX

May, 2017

DEDICATION

To my parents, Felix and Felicia Nwajei, I have seen further because of you.

Thank you for being an embodiment of dignity and integrity.

To my siblings Michael, Tony, and Francisca, you have been the best examples of true optimism and perseverance.

ACKNOWLEDGEMENTS

I am indebted to a lot of people for walking this journey with me. First, I would like to thank my mentor Dr. Tomasz Zal, for allowing me to explore my passion and creativity in his lab; I honestly did not think that it was possible to be given free reins to pursue new areas with relatively little experience in the basic sciences. I have truly discovered science as a personal passion. Thank you for guiding me, providing helpful criticisms and helping me think like a scientist. My experience here has left an indelible mark for my future endeavors.

I would like to thank my current and previous committee members, Drs. Kimberly Schluns, Amy Heimberger, Joya Chandra, Robert Dantzer and Bradley McIntyre for all your valuable advice and support. Dr. Schluns, you have been an invaluable personal mentor; Dr. Heimberger, thank you for accepting me into your lab, mentoring me on the translational aspect of brain tumor immunology, and providing me with plenty avenues for professional growth. I feel very lucky and truly privileged to have experienced the entire spectrum of basic and translational tumor immunology; Dr. Chandra, thank you for always reminding me that you all want the best for me; Dr. Dantzer, thank you for making me statistically conscious. Also, to my PhD examination members; thank you Dr. Stephen Ullrich for volunteering to chair my exam and for helping me enhance my public speaking through your seminars; Dr. Greg Lizee, thank you for volunteering and challenging me during my candidacy exam. This experience has helped mold me into a better scientist.

Many thanks to past and present Zal lab members Meena Shanmugasundaram, Figen Beceren-Braun, Chodaczek Grzegorz, Anna Zal, Sungho Lee, Todd Bartkowiak,

Ivy Wuenyue Wu, and Dana Paine. Thank you for your contributions toward my research project, your advice and technical help. I wouldn't have been able to finish all of this without your mental and physical assistance. To the Heimberger past and present lab members, Konrad, Edjah, John, Tiffany, Ling, Yuuri, Anantha, Martina, Ryuma, Hillary, Nasser, thank you for your suggestions and encouragement. Further, I have been blessed to have completed a rotation at the Konopleva lab. Thank you, Dr. Konopleva for all the recommendation letters that you have generously provided and to all the lab members including Juliana, Karina, and Polina. Finally, I will be forever grateful to Shouhao Zhou, who helped analyze my "big data" collection with advanced statistical models.

To Shailbala, Nahum, Laura, Elizabetta, thank you for providing advice and encouragement every time you could. Thank you Stephanie for providing me with useful resources during the completion of this thesis; I owe a lot of it to your generosity. To Tonya, Lauren, Bonnie, Rosie, Doretha, Patrice, Toretta, thank you for your help when I needed it.

Many thanks to the many doctors, nurses, and patient care assistants of CHI-St. Luke's hospital that helped nurse me back to health just three weeks before the completion of this thesis and my public defense. You made this possible.

To my friends, Ayokunle, Vincent, Akhil, Evans, Mimi, Tony (too many of you), Mark, Kingsley, Duben, thank you for making my journey lighter throughout all these years.

Lastly, I am grateful to all the institutes and organizations that have funded my work during the past few years including grants from the NIH/NCI, Schissler fellowship

for translational research at the University of Texas MD Anderson Cancer Center, T.C. Hsu memorial scholarship, The University of Texas MD Anderson Cancer Center MRP fund, and CPRIT. This work would not have been possible without your generous support.

VISUALIZING THE DYNAMICS OF IMMUNE SURVEILLANCE IN BRAIN TUMORS BY INTRAVITAL MULTIPHOTON MICROSCOPY

By

Felix I. Nwajei, MD

Supervisory Professor: Tomasz Zal, Ph.D.

Brain tumors (BTs) generally have a bad prognosis despite conventional treatment strategies. Immunotherapy is a relatively novel treatment approach that has shown benefit for durable treatment of melanoma, and is a promising candidate for different tumor types including BTs. Immunotherapeutic strategies work by exploiting and/or enhancing natural anti-tumor immune response, a process that is critically dependent on adaptive immunity, T cell infiltration and surveillance of tumor. However, little is known about the dynamics and regulation of T cell surveillance in BTs. Resident immune cells of the myeloid lineage known as microglia are ubiquitous in the brain parenchyma while tissue-resident myeloid dendritic cells (DCs) known to activate T cells are relatively rare in the brain compared to DCs in other organs. Accumulating evidence indicates that myeloid cells infiltrate and create an immune suppressive microenvironment in BTs, but the identity of these myeloid cells and their role in the adaptive immune surveillance of BTs by T cells is unclear. Based on the predominance of microglia in the brain tissue, studies focused on understanding how BT immune surveillance is regulated, have been skewed toward microglia. Many conclusions regarding microglia function have been deduced from *in vitro* experiments. Nonetheless, *in vivo* studies in parallel models such as EAE indicate that DCs are superior to microglia in antigen presentation to T cells in the brain and to date, there is

no direct *in vivo* evidence to suggest otherwise. In addition, DCs are well-established cellular regulators of T cell surveillance in extracranial tumors. Therefore, I hypothesized that DCs, rather than microglia, play a major role in regulating T cell surveillance in BTs. To address this hypothesis, I have developed experimental imaging systems for longitudinal intravital multiphoton microscopy of immune cell dynamics in BTs in living mice and used this approach to interrogate T cell behavior in orthotopic glioma and in experimental intracranial metastases *in vivo*. I found that the myeloid infiltration of BTs was dominated by CD11c+ DC cells rather than microglia. Quantitative *in situ* tissue cell image cytometry further revealed that myeloid-derived CCR2+ monocytes accumulated in the BT core, CD11c+ DCs at the tumor margin, and CX3CR1+ microglia outside the tumor. T cells formed clusters around CD11c+ DCs, but not the microglia. Within these clusters, T cells vigorously interacted directly with CD11c+ DCs. CD11c+ DCs retained T cells and controlled their motility patterns, indicating that CD11c+ DCs play a major role in regulating T cell retention and motility in BT. Corresponding to the preferential distribution of CD11c+ DCs at BT margins was expression of the neuronal chemokine Fractalkine (CX3CL1). Deficiency of the Fractalkine receptor CX3CR1 resulted in decreased CD11c+ DC recruitment. In addition, decreased CD11c+ DC recruitment was accompanied by decreased T cell recruitment, an increase in the spatial diffusion of the few BT-infiltrating T cells, and subsequent outgrowth of a fibrosarcoma BT, which spontaneously regresses in the brain of control wild type mice in a CD8 T cell dependent manner.

In summary, by using novel intravital imaging systems for longitudinal visualization of BT immune surveillance across several types of cancer, I showed that the recruitment, migration and retention of tumor infiltrating T cells in the brain is

mediated by incoming CD11c+ DCs rather than by the brain-resident CX3CR1 microglia, and identified the neuronal chemokine Fractalkine as a key molecule that promotes T cell surveillance in BTs by recruiting CD11c+ DCs.

These findings suggest that the non-microglial tumor-associating CD11c+ myeloid cells and the fractalkine/CX3CR1 chemokine pathway control T cell surveillance in BT and represent attractive immunotherapeutic targets that could be modulated for guiding endogenous or adoptive transfer of T cells to BT sites and for therapeutic modulation to enhance immunity against BTs.

TABLE OF CONTENTS

COPYRIGHT

LIST OF FIGURES

LIST OF ABBREVIATIONS

BT—Brain tumor

CNS—Central nervous system

CSF—Cerebrospinal fluid

GBM—Glioblastoma multiforme

GFAP—Glial Fibrillary Acidic Protein

WHO—World Health Organization

TCGA—The Cancer Genome Atlas

EMT—epithelial-mesenchymal transition

MDP—Macrophage Dendritic cell precursor

DC—Dendritic cell

CTLA4—Cytotoxic T-lymphocyte associated protein 4 (CD152)

PD1—Programmed death 1 (CD279)

PM—Patrolling monocyte

CM—Classical monocyte

NR4A1—Nuclear receptor subfamily 4 group A member 1

MDSC—Myeloid derived suppressor cell

pMHC—Peptide-Major histocompatibility complex

ICOS—Inducible T-cell costimulator (CD278)

ICA—Internal carotid artery

ICr—Intracranial

OX40 or TNFRSF4—Tumor necrosis factor receptor superfamily member 4 (CD134)

IDO—Indoleamine 2,3-dioxygenase

FoxP3—Forkhead box P3 transcription factor

nTregs—Natural regulatory T cells

iTregs—Induced regulatory T cells

MMPs—Matrix Metalloproteinases

ADAM —A disintegrin and metalloproteinase domain-containing protein

SHG—Second harmonic generation

RAG1—Recombination activating gene 1

ECs—Endothelial cells

ITGAX—Integrin subunit alpha X

ITGAM—Integrin subunit alpha M

ISF—Interstitial fluid

CSF1R—Colony stimulating factor 1 receptor (CD115)

HSVTK—Thymidine kinase of herpes simplex virus

DAMPs—Danger associated molecular patterns

PAMPs—Pathogen associated molecular patterns

PBS—Phosphate-buffered saline

PRR—Pattern recognition receptor

ATP—Adenosine triphosphate

DNA—Deoxyribonucleotide adenosine triphosphate

RNA—Ribonucleotide adenosine triphosphate

ROS—Reactive oxygen species

SCID—Subacute combined immune-deficient

TABLES

CHAPTER 1:

BACKGROUND

1.1. General Introduction

Mammalian tissues are under constant surveillance by the immune system[1,2]. The primary function of the immune system is to protect organisms from environmental pathogens such as bacteria or viruses that could prove fatal if left unchecked. Generally, the immune system recognizes molecular aspects of pathogens and mounts a rapid response in a two-layered manner to resist host organ invasion and damage. In contrast, nonviral cancer is a more sinister pathological event as it involves intrinsic mutational changes in an organism's own cells that may be barely detectable by the immune system during cancer initiation. These mutations trigger a cascade of events including cellular transformation, immortalization, unabated proliferation, and a diminished survival capacity of the host organism. Although cancer cell-intrinsic factors play key roles in tumor development and progression, and cancerous cells were once thought to be undetectable by the immune system[3-24], it is now established that during a natural anti-tumor immune response, immune cells are capable of detecting specific peptide antigens in transformed cancer cells. In addition, immune cells play a major role in both tumor progression and eradication, and have more recently been shown to be attractive targets for cancer therapy[24-34].

Cancer has been aptly described as "wounds that do not heal[35]." This notion is based on decades of research uncovering striking similarities between chronic wounds and cancer. Importantly, both disease conditions are usually characterized by rich immune cell infiltrates and abundant immune cell-derived molecular signals, and epidemiological and mechanistic studies have linked chronic inflammation to cancer progression, indicating a pro-tumorigenic effect of immune cell infiltrates[36-42]. However, the significance of the immune system as a key antagonist of cancer growth has been

recognized due to better understanding of the immune system through finely-tuned molecular mechanistic studies and immunotherapeutic applications[43-45]. More than a decade ago, in a landmark review, Hanahan and Weinberg condensed the multitude of research data elaborating the mechanistic underpinnings of the cellular and molecular aspects of cancer progression into a handful of principles known as the “Hallmarks of Cancer.” These hallmarks include self-sufficiency in growth signals, insensitivity to anti-growth signals, evading apoptosis, limitless replicative potential, sustained angiogenesis, and tissue invasion and metastasis[46]. This extensive review excluded the role of the immune system because there was only weak mechanistic evidence available to support the hypothesis of tumor immune surveillance proposed by Burnet and Thomas in 1957. More recently, however, the inflammatory and immune evasive properties of cancer have been included as part of cancer hallmarks based on mounting evidence that the immune system can in fact detect and eliminate cancer cells, and paradoxically also aid in cancer progression[24,47,48]. While each of the initially prescribed hallmarks were viewed from a mostly cancer cell-intrinsic angle, myriad studies have been extensively reviewed in the updated version of the “Hallmarks of Cancer,” emphasizing that tumor immune infiltrates and immune-derived molecules play either major or supporting roles in almost all of the initially described hallmarks of cancer[47,49-55].

A reinvigorated interest in the historically controversial field of cancer immunology is due to a better understanding of molecular immunology and the accepted role of immunotherapy in the care of the cancer patient. [56-60] Nonetheless, a significant proportion of patients receiving immunotherapy do not respond. Therefore, to increase the efficacy of immunotherapy, it is pertinent to answer key questions

pertaining to why some tumors elicit robust immune responses while others do not. For example, it was hypothesized that differences in tumor neoantigenic load could explain differences in response to immunotherapy in different tumor types, and advances are already being made in understanding the impact of tumor mutational load and as a consequence, neo-antigens in response to T cell immunotherapy[61-64]. It is also known that immune cell compositions in different tissues are distinct in steady state and in cancer progression[65-67], and this may play a role in determining the extent to which an adaptive T cell immune response to cancer works to eradicate cancer cells. A deepening of our understanding on immune response to tumors in the context of the complex biological milieu in which they might exist is essential for a better grasp of immune surveillance in specific tumor types.

The brain is one such complex environment that presents a challenge for proper understanding of an immune response to tumors because of its distinct anatomy and immunological makeup. I will address brain tumors (BTs), the immunological composition of the brain, its anatomical barriers (blood brain barrier and CNS lymphatic), and the concept of brain immune privilege in different sections below. In this thesis, I have sought to investigate the extent to which BTs are infiltrated by T cells, the dynamics of potentially-infiltrated T cells in BTs, and the mechanisms by which T cell surveillance in BT is regulated. A comprehensive understanding of the mechanisms guiding T cell immune surveillance in BTs may reveal strategies that may be important for the development of potent immunotherapy for BT treatment and may pave the way for an organ-specific approach to immunotherapy application in cancer.

1.2. A brief historical perspective on brain tumor immunology research:

Brain tumors constitute one of the most deadly types of cancer. Relative to other tumor types, BTs are one of the less well-understood in the context of tumor immunology. On the basis of research conducted by Medawar more than half a century ago, the brain was claimed to be an immune privileged site[68,69]. About the same time, the inability to identify classical lymphatic vessels in the brain, which were known to be present in other mammalian tissues and organs and critical for immune cell trafficking, lent credence to the notion of brain immune privilege. Subsequent studies conducted a few decades after Medawar's findings revealed no role for the immune system in controlling BTs in athymic immune-deficient nude mice and further bolstered the idea of brain immune privilege[70,71]. These findings led to the erroneous conclusion that the brain is shielded from surveillance by adaptive immune cells such as T cells, and likely has impeded progress in understanding the mechanisms of T cell surveillance of BTs. However, the idea of an immune-privileged brain was first challenged in observational studies showing the presence of dural lymphatic-like vessels and subsequent findings in which fluorescent tracers injected directly into mouse brain parenchyma were identified within non-vascular pathways in the olfactory lobe region, which were traceable to the cervical lymph nodes[72]. In the absence of a conventional channel for drainage of brain interstitial fluid (ISF) to the cervical lymph nodes, non-vascular tracks were proposed to serve as substitutes for lymphatics. Since then, studies have documented the presence of brain-derived myelin antigen-specific T cells in the parenchyma, brain meninges, and cervical lymph nodes in mouse models of multiple sclerosis and brain infections[73-79]. The latter studies suggested a model in which antigens in the brain can be transported to the cervical lymph nodes for potential

activation of naïve T cells [72,80]. In support of this model, recent studies confirmed and extended these previous observations by identifying and describing distinct networks of lymphatic channels that drain directly into the cervical lymph nodes, indicating that lymphatic drainage of the brain is similar to extracranial peripheral tissues. In addition, it suggested that the brain is not sequestered from immune cell surveillance. Based on this, there is more impetus in the field of neuroimmunology to investigate the dynamics of antigen presenting cells and T cells in various brain pathologies.

Historically, BTs have been classified according to histological appearance and studied as separate entities, and treatments have been applied differently according to the histological diagnosis[81]. In the section below, I will be discussing BT types and examine how immune infiltrates in such tumors could serve as a predictive/prognostic tool in patient survival. [82-88].

1.3. Brain Tumors

Brain tumors are heterogeneous and are classified into two main types according to the organ of origin. Primary BTs arise from within the brain tissue and secondary BTs or brain metastases originate from extracranial organs.

I will briefly elaborate on the complexity in BTs types and subtypes based on the World Health Organization (WHO) and The Cancer Genome Atlas (TCGA) classifications[5,89].

1.3.1. Primary brain tumors

Primary BTs arise within distinct anatomical brain regions in the pediatric patient relative to the adult patient. BTs in pediatric patients frequently develop in the infratentorial (brainstem) region, while they are mostly supratentorial (cerebral

hemispheres) in adults. However, the cell-specific origin for such tumors is not well understood[90-94]. Because of similar marker expression with several precursor or differentiated cell types, primary BTs are thought to originate from poorly differentiated glial cells such as oligodendrocytes, astrocytes, neural progenitor cells, and ependymal cells. For instance, astrocytomas share glial fibrillary acid protein (GFAP) expression with astrocytes and oligodendrogliomas stain for myelin basic protein (MBP), an oligodendrocyte marker. Based on aggressive histological characteristics and rapid patient mortality, a deadly type commonly known as glioblastoma multiforme (GBM) has become well-recognized among the multitude of primary BTs types and is thought to arise from astrocytes as it characteristically has GFAP expression. Recent studies based on gene-expression from TCGA dataset has further classified GBMs according to molecular characteristics[95]. Differential gene-expression and somatic molecular characteristics delineate GBM into four recognized subtypes including pro-neural, classical, and mesenchymal, thus indicating distinct molecular subtypes within the GBM histological subtype with associated differences in the inflammatory responses[95,96]. In this new classification, it is now recognized that in both primary and recurrent GBM, the mesenchymal subtype has the highest immune signature, characteristically infiltrated by neutrophils, both pro-inflammatory “M1” and immune suppressive “M2” macrophages, but reduced presence of activated natural killer T (NKT) cells in comparison with other molecular subtypes[96]. The proneural subtype has decreased resting memory CD4 T cells and the classical subtype has increased dendritic cell signature[96]. Despite the differences in the composition of immune infiltrates, in recurrent GBM of all subtypes, there is increased infiltration by regulatory T cells. Patients with primary or recurrent GBM of the mesenchymal subtype have the

worst overall or progression-free survival while the proneural subtype has the best[96]. In sum, differences in immune cell presence may be exploited for effective immunotherapy in different GBM molecular subtypes. However, as these studies were nonfunctional, mechanistic work is required for better understanding of immune surveillance in BTs and could provide new knowledge for developing novel immune therapeutic strategies to improve patient survival.

1.3.2. Brain metastases

In contrast to primary BTs, brain metastases originate from cancers of extracranial tissues[97]. The epithelial to mesenchymal transition (EMT) process enables conditions favorable for cancer cells to migrate and penetrate the tissue basement membrane and gain access into the circulation[98,99]. Subsequently, disseminated cancer cells undergo a cascade of events that end with successful engraftment and growth of cancer cells in peripheral organs including brain tissue[27,100]. Brain metastasis is an event that can potentially occur during the progression of any malignant primary cancer type[100]. In the United States alone, it is estimated that approximately 170,000 new patients will be diagnosed with brain metastases annually, a number 10 times higher than in primary BTs[101]. Primary cancer types such as lung cancer, breast cancer, and melanoma have a high propensity to metastasize to the brain[102] (**Table 1**). In contrast, brain metastases derived from soft tissue fibrosarcoma, cervical, prostate, and liver cancers are relatively rare[103-106]. Patients who develop brain metastases have very poor prognosis with a median overall survival ranging from a few weeks to months[100]. Present treatment strategies such as surgical resection, radiation therapy, and

chemotherapy have shown only modest benefit in extending survival of patients with brain metastases[107,108].

In comparison with GBM, the link between the immune system and brain metastases is even less well-understood despite its high incidence. Although there is no comprehensive comparison of immune cell infiltrates between distinct brain metastases types, recent characterization of patient brain metastases aggregated regardless of tissue of origin demonstrated that T cells can infiltrate brain metastases generally[109,110]. Further, it was shown that the density of T cells infiltrating brain metastases foci ranged from sparse to very dense[109]. In addition, T cell localization was found to correlate with “peritumoral edema” as defined by the flare region in pre-operative magnetic resonance imaging, and higher T cell infiltration into brain metastases correlated with better overall survival time of patients[109]. These observations and associations are potentially translatable as they could serve as prognostic or predictive tools for patient outcome; however, the extent to which T cells infiltrate brain metastases foci originating from distinct primary tumor types is unclear. In addition, how T cells localize and are organized in BT and what mechanisms regulate T cell localization in the tumor and their interaction with other cells in the BT microenvironment remain unknown. These are questions that I will be probing in chapters 3 and 4 of this thesis. In sum, a better understanding of T cell surveillance in brain metastases is urgently needed. The knowledge gained may provide new insights into the development of novel immunotherapeutic strategies for brain metastases. Overall, the brain tissue is a common denominator for growth of both primary BTs such as GBM and brain metastases. Therefore, knowledge of immune response gained from studying one cancer type may be relevant for the other and vice versa.

Table 1 | **Typical sites of metastatic relapse for solid tumours**

Tumour type	Principal sites of metastasis
Breast	Bone, lungs, liver and brain
Lung adenocarcinoma	Brain, bones, adrenal gland and liver
Skin melanoma	Lungs, brain, skin and liver
Colorectal	Liver and lungs
Pancreatic	Liver and lungs
Prostate	Bones
Sarcoma	Lungs
Uveal melanoma	Liver

***Primary tumors that frequently metastasize to the brain are highlighted in red rectangles**

Nguyen DX, Bos PD and Massague J; Nature Reviews Cancer, 2009.

Adapted by permission from Macmillan Publishers Ltd: [Nat Rev Cancer] (Nguyen DX et al., *Metastasis: from dissemination to organ-specific colonization* 2009. Apr; 9(4):274-84. Copyright Clearance Center.

1.4. Mechanisms of tumor immune surveillance in the brain

1.4.1 An overview of the immune system and anti-tumor immune surveillance

The immune system is divided into two arms—innate and adaptive (**Figure 1**). The innate arm of the immune system is naturally wired with evolutionary conserved receptors that can sense conserved structures on pathogens and sterile tissues such as pathogen associated molecular patterns (PAMPs) and danger associated molecular patterns (DAMPs), respectively[111-114]. Innate immunity functions as the first line of defense during an immune response and responds rapidly relative to the adaptive immune system; however, this response is generally non-specific. In contrast, the adaptive arm of the immune system takes several days to respond during an immune

response, but its actions are highly specific. The specificity of adaptive immune cells is determined by an incredible capacity to recombine their receptors to recognize different antigens in a major histocompatibility complex (MHC)-restricted manner. Upon resolution of a disease, the adaptive immune cells can evolve a memory phenotype. Due to their intrinsic cellular properties, antigen-specific memory adaptive immune cells are capable of initiating very strong and rapid adaptive recall responses in the event of a re-encounter of the same antigen[1,115,116]. Innate immune responses are executed by myeloid cells including macrophages, microglia, monocytes, dendritic cells; granulocytes such as neutrophils, eosinophils, basophils, and mast cells; γδ-TCR T cells; and natural killer (NK) cells. On the other hand, adaptive immune cells include αβ-TCR T cells and B cells. For the purpose of this thesis, I will be focusing on how innate myeloid cells including microglia, monocytes, macrophages, and dendritic cells, and the adaptive T cells interact in BTs.

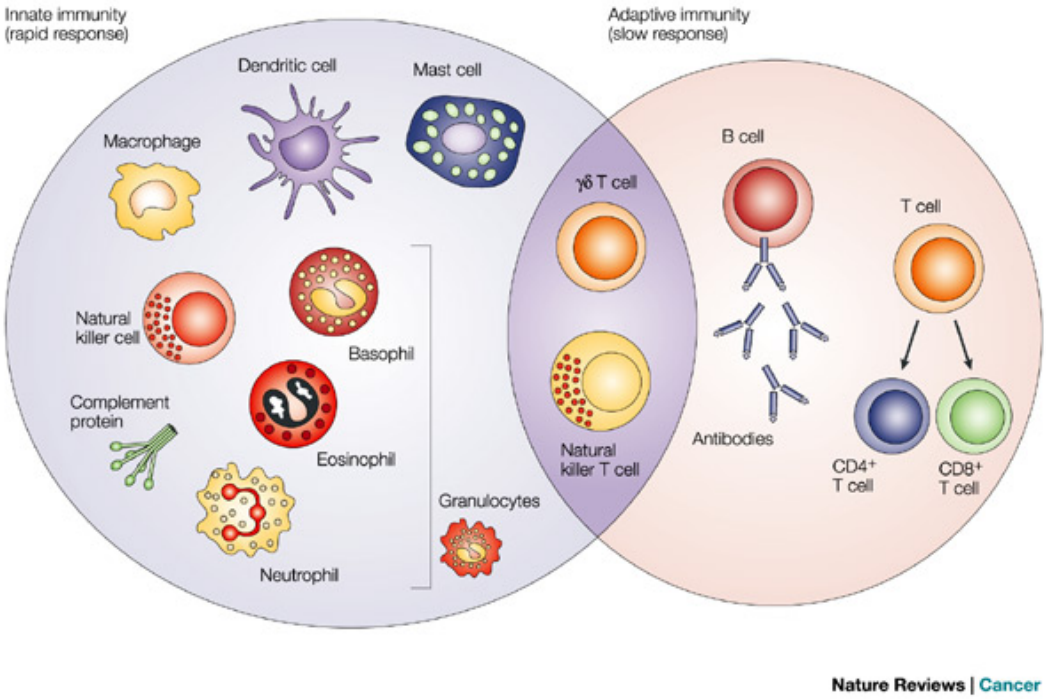

Figure 1. Classification of cells in innate and adaptive immunity. Cells that participate in innate and adaptive immunity are illustrated within the bright lavender (left) and pink (right) colored circles, respectively. Natural killer (NK) and γδ T cells have characteristics that overlap between innate and adaptive immunity and are represented within the overlapping segment between both circles. Adapted by permission from Macmillan Publishers Ltd: [Nat Rev Cancer] (Glenn Dranoff, *Cytokines in cancer pathogenesis and cancer therapy* 2004. Jan; 4(1):11-22. Copyright Clearance Center.

Immune surveillance of a tumor is based on the fact that immune cells are highly dynamic and can detect and recognize tumor-specific antigens (TSA) and/or tumor-associated antigens (TAA). Tumors are composed of highly mutated cells that may provide a plethora of antigenic materials that are potentially ingested by antigen presenting cells such as dendritic cells (DCs) and macrophages, and transported via tumor-draining lymphatics to secondary lymphoid tissues for presentation to naïve T cells (**Figure 2**). Following T cell recognition of TSA/TAA displayed by DCs, T cells become activated, egress from the lymph node, and potentially migrate to the target

organ invaded by cancer to perform effector functions including an attempt to eradicate the tumor.

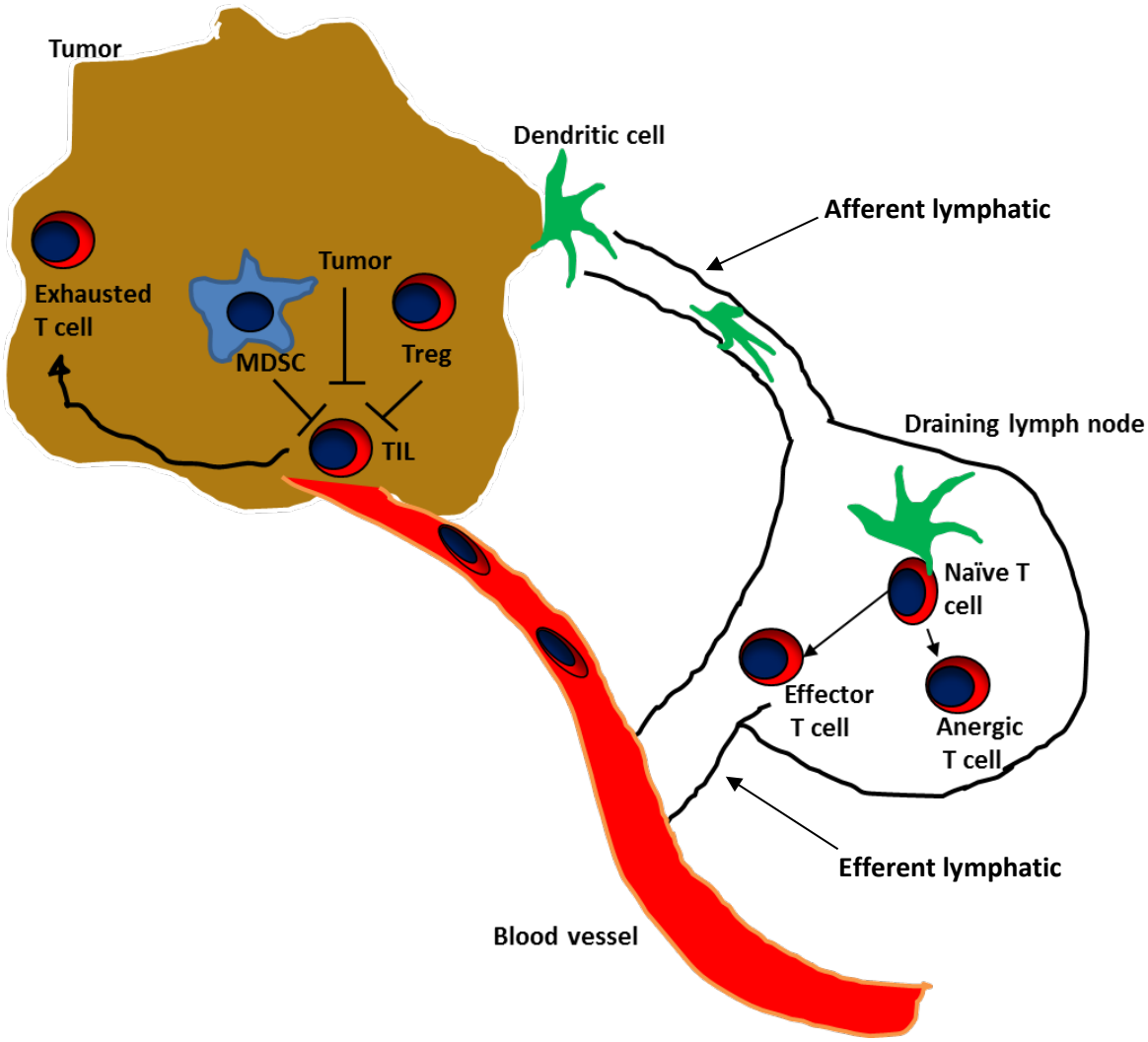

Figure 2. Illustration of the dynamics of antitumor immune surveillance.

Dendritic cells (green) engulf antigens from the tumor; process it, and present processed antigens to naïve T cells in the tumor-draining lymph node. Effective antigen presentation involves 3 signals (1. Peptide-MHC complex; 2. costimulatory molecules; and 3. cytokines), which lead to T cell activation, differentiation and proliferation of effector T cell that then migrate to the tumor (tumor infiltrating lymphocytes; TIL) to perform effector functions. In the absence of costimulation, T cells become anergic. Several cellular [myeloid derived suppressor cells (MDSCs) and regulatory T cells (Tregs)] and molecular (PD-1/PD-L1) regulatory mechanisms are present in the tumor or the lymph node to maintain tight control of this process and may cause immune suppression through a variety of mechanisms leading to T cell exhaustion.

The idea of tumor immune surveillance was first hypothesized by Thomas and Burnet in 1957 based on observations made in organ transplantation and subsequent studies in tumor graft transplantation[24,117]. Essentially, it was discovered at that time that following transplantation in rabbits, a donor tissue such as skin was frequently met with vigorous rejection by the recipient's immune system[118,119]. In tumor transplantation experiments, it was observed that tumor transplantation into a non-syngeneic host resulted in tumor rejection, indicating that the recipient's immune system was capable of recognizing what was likely a tumor antigen. Therefore, it was postulated that the infrequency of cancer occurrence in humans could be explained by an immune surveillance mechanism that continuously prevents the outgrowth of cancerous cells[117,120]. However, this idea was controversial because there was no mechanistic insight into how the immune system could recognize and eliminate a tumor, which was believed to express self-antigens as it originates from aberrant host cells[117,121,122]. Also, spontaneously arising tumors were rarely rejected despite the induction of an immune response[123]. Subsequent experiments by Osias Stutman revealed no difference in the development of tumor in immune-deficient athymic nude mice in comparison with control immune-competent mice, suggesting that the immune system played no role in the control of tumor progression, and discredited the immunosurveillance concept[71]. Despite these early setbacks, the first tumor antigen was eventually identified in 1991[124], athymic nude mice are now known to be "leaky" and not absolutely immune-compromised[125-128], and robust concrete evidence has accumulated in support of tumor immune surveillance in both animal models and humans leading to renewed enthusiasm for the immune surveillance hypothesis[24,129-132]. With advancements in the field of molecular biology and the availability of new tools including knockout (KO) mice,

the immune surveillance hypothesis has been overwhelmingly supported by observations from studies conducted in the laboratory of Robert Schreiber and others[24,133-140]. For example, sarcomas that were induced by a chemical carcinogen in recombination activation gene (Rag)-KO mice, which unlike nude mice completely lack adaptive immune cells, showed significant outgrowth in comparison with wild type mice, indicating that tumor growth is controlled by the adaptive immune system. Similar results were obtained in interferon-gamma receptor (IFNyR)-KO mice, STAT1-KO (lacking the gene responsible for IFNy signaling), perforin-KO, αβ T cell KO (lacking the TCR β-chain), and γδ T cell KO (lacking the TCR δ-chain) mice, all indicating that components of the immune system are involved in controlling tumor growth[24,133-140] . Although the immune system plays a tumor surveillance role, spontaneous tumors tend to progress lethally from presumably immune-resistant cancer cell clones. In a set of experiments to test the role of the immune system in the development of tumor resistance clones, transplantation of a carcinogen-induced tumor from a primary wild type host to a secondary wild type recipient resulted in lethally progressive tumor. In contrast, transplantation of a similar tumor from a primary immune-deficient Rag-KO host to a secondary wild type recipient showed significant decrease in tumor growth. Together, these results suggested that the intact immune system in the primary immune-competent wild type host provided selective pressure for development of less immunogenic and resistant tumor clones while the lack of immune selective pressure in the primary immune-deficient RagKO host was necessary for the retention of tumor immunogenicity. This phenomenon of tumor sculpting by the immune system was conceptualized as the process of cancer immunoediting. [132,141-143]. Cancer immunoediting is a process that includes three phases including elimination,

equilibrium, and escape (**Figure 3**). In effect, this concept includes tumor immunosurveillance during which tumor eradication occurs (elimination phase), immunological sculpting of the tumor leading to selection for resistant cancer cell clones, which are potentially less immunogenic or have acquired mechanisms of immune evasion or suppression (equilibrium phase), and subsequent uninhibited tumor progression (escape phase)[24,130,144].

Despite our present understanding of cancer immune surveillance and aspects of immunoediting, most of the data is borrowed from research conducted in extracranial organs. In the brain, however, the mechanisms regulating immune surveillance in tumors remain unclear partly due to the idea of brain immune privilege. This idea first came to light following an experiment by Medawar[69]. He observed that skin to skin transplantation in rabbits caused the recipient rabbit to mount strong immune response with subsequent rejection of the transplanted tissue. However, when the same tissue was transplanted into recipient rabbit brain, the tissue was not rejected. In contrast, when he first transplanted donor skin tissue into the skin of recipient rabbits and waited a few days before transplanting similar donor skin tissue into the brain of the same recipient rabbits, the transplanted tissue in the brain was rejected[69]. This suggested that the brain is immunologically quiescent or privileged in comparison with peripheral tissues. Since then, in support of an immune-privileged brain, countless studies have demonstrated unique features of the brain that could prevent the development of robust immune response within the brain tissue[68,145-148].

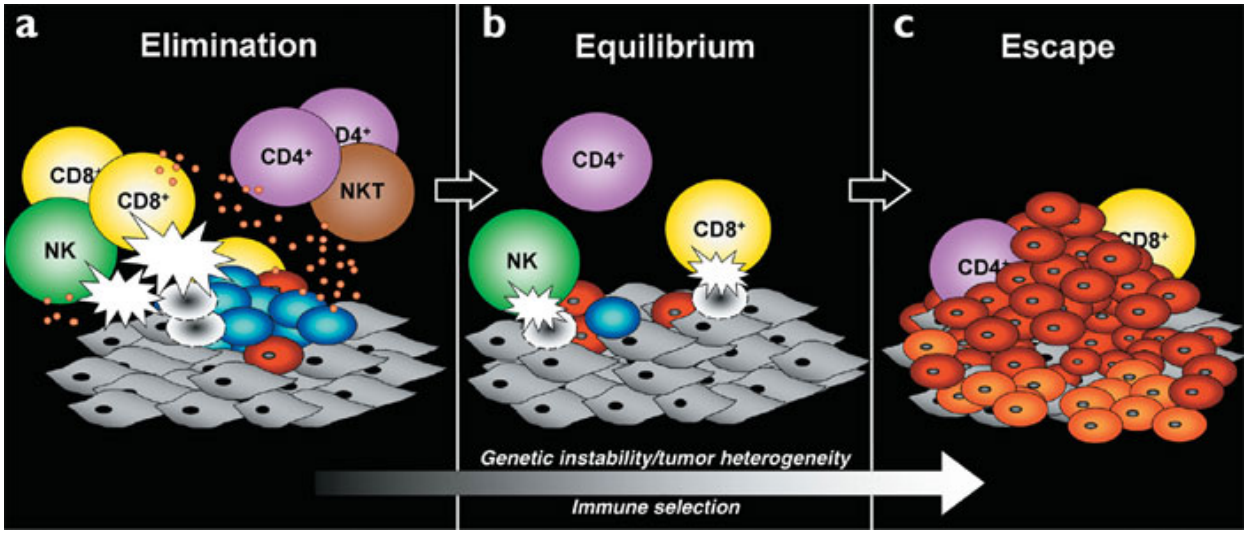

Figure 3. The process of cancer immunoediting.

Cancer immunoediting encompasses three processes. (**a**) Elimination corresponds to immunosurveillance (**b**) Equilibrium represents the process by which the immune system iteratively selects and/or promotes the generation of tumor cell variants with increasing capacities to survive immune attack. (**c**) Escape is the process wherein the immunologically sculpted tumor expands in an uncontrolled manner in immunocompetent host. In **a** and **b**, developing tumor cells (blue), tumor cell variants (red) and underlying stroma and nontransformed cells (gray) are shown; in **c**, additional tumor variants (orange) that have formed as a result of the equilibrium process are shown. Different lymphocyte populations are as marked. The small orange circles represent cytokines and the white flashes represent cytotoxic activity of lymphocytes against tumor cells. Reprinted by permission from Macmillan Publishers Ltd: [Nature Immunology] (Dunn GP, Bruce AT, Ikeda H, Old LJ, Schreiber RD. Cancer immunoediting: from immunosurveillance to tumor escape. 2002;3:991-8); Copyright (2002). Copyright Clearance Center.

1.4.2. The Blood-Brain Barrier (BBB) in steady state and inflammation

The BBB has been pivotal in the debate on brain immune privilege and is believed to play a critical role in regulating interactions between the brain and immune cells in extracranial peripheral tissues. The BBB serves to tightly regulate the influx of molecules or cells from the circulation into the brain tissue in normal homeostatic conditions[146,149,150]. Unlike fenestrated capillaries in the extracranial peripheral tissues, the BBB is made up of endothelial cells that are bound together by tight junctions. This

basic endothelial structure is further reinforced by pericytes, astrocytic foot processes, and smooth muscle cells[151]. BBB tight junctions and efflux pumps are mechanisms that prevent small molecules from penetrating the brain parenchyma[152-155]. Consequently, delivery of small molecules such as kinase inhibitors and targeted therapy to treat brain pathologies such as brain tumors has been shown to be inefficient[154]. In contrast, systemic immune cells such as memory T cells have been found to be present in the brain at steady state[156-158]; however, only very small numbers of these cells have been identified in comparison with extracranial peripheral tissues[147,158159]. Furthermore, transmigration of T cells via the BBB into the brain parenchyma frequently occurs in diseases such as multiple sclerosis and viral encephalitis in humans[74,79,160,161], or experimental acute encephalomyelitis (EAE) in mice[79,162,163].

As an early model system to understand how immune cells breach the BBB and penetrate into the brain parenchyma, several mechanisms have been proposed as to how the initiation of EAE occurs. Activated or encephalitogenic T cells, but not resting T cells were found to be able to penetrate the BBB after intravenous injection in rats[164,165]. This event was found to be independent of antigen recognition or MHC compatibility, but dependent on the activation and the blast stage of the T cell, indicating that T cell activation alone was sufficient for T cells to breach the BBB[166]. Subsequent studies showed that this process is dependent on P-selectin to access the leptomeningeal vascular endothelium, and lymphocyte function-associated antigen 1 (LFA-1) and α4-integrins to penetrate the BBB[167]. Additionally, based on the constitutive expression of CCL19 in CNS endothelia, a CCR7/CCL19-chemokine-dependent mechanism has been proposed for CCR7-expressing T cells to cross the BBB via the leptomeninges[162,164,168,169]. In another study, entry of T helper-17 cells into

the CNS via the choroid plexus into the brain ventricles was found to be a CCR6/CCL20-dependent process, required for the initiation of EAE[170]. Cumulatively, these data indicate that encephalitogenic T cells can access multiple brain interface sites to penetrate the BBB and induce neuroinflammation. Although the prior studies were based on a model in which autoreactive T cells are constantly circulating in the bloodstream and are able to directly penetrate the BBB, a recent study showed that circulating T cell blasts lack the capacity to penetrate the BBB and initiate EAE in a rat model unless they are first licensed in the lungs[171]. In fact, after local stimulation of resting myelin-reactive memory T cells in the lungs of rats, those cells proliferated profoundly, migrated to the CNS, and caused paralysis in the rats[171]. This indicated that the lung is a site of reactivation for autoaggressive T cells prior to induction of EAE.

More recently, another study detailed the events that occur after the BBB has been breached following induction of EAE[163]. Shortly after cerebral vessel disruption following EAE induction with subcutaneous injection of myelin oligodendrocyte glycoprotein (MOG) peptide, Incomplete Freund's Adjuvant (IFA), and intraperitoneal injection of pertussis toxin, microglia become activated, and this was followed by infiltration of DCs and T cells[163]. This latter study suggested a model in which activated microglia are the primary initiators of autoaggressive T cell entry into the CNS. However, only the green fluorescent protein-tagged receptor CX3CR1, which is broadly expressed by microglia, macrophages, and some DCs, was used to identify microglia[163]. In addition, the mechanisms by which T cells accumulate and are retained at sites of EAE remain unknown. In sum, there appear to be different mechanisms involved in the initiation of EAE. Whether the various mechanisms involved in EAE initiation are interconnected or work separately is an important question that is still

being dissected. Importantly, whether similar mechanisms are operational in brain tumors is being investigated.

In patient GBM tissues, studies conducted in the 1970s and 1980s revealed high numbers of infiltrated microglia and macrophages, but rare infiltrating T cells. In addition, GBM patients were found to be highly lymphopenic, bearing resemblance to patients with immune-deficient disorders[172-175]. On one hand, it was believed that GBM patients were generally lymphopenic and on the other, due to the prevailing idea of brain immune privilege, it was thought that antigen presenting cells such as DCs and adaptive immune T cells were likely restricted from being present within these tumors. Regulatory T cells have been found in high numbers in peripheral blood and tumor tissue in patients with GBM, and have been suggested as an immune suppressive mechanism in GBM patients[176-179]. Hence, it is unlikely that the BBB preferentially restricts effector T cells from migrating into GBM tumor tissue. Alternatively, it was thought that inefficient or lack of antigen presentation to naïve T cells could explain the limited number of effector T cells in GBM tissue[180-189]. This latter theory seemed plausible partly due to the fact that classical lymphatics in the CNS had not been identified at the time[190-192]. As it would turn out, there is now evidence to support the idea of inefficient or lack of antigen presentation in GBM, and CNS lymphatics have been identified[62,63,82]. Thus, by using appropriate models in which antigen presentation is operational, one could address several important questions pertaining to the dynamics of T cell migration into BT, potential local proliferation in the tumor, and interaction with antigen presenting cells in the tumor microenvironment. These are questions that I will probe in chapter 3 of this thesis.

1.4.3. The role of CNS Lymphatics in immune response to brain tumor

Lymphatics are critical in the generation of an immune response during tumor progression. Conventional lymphatic vessels are made up of endothelial cells that are identified by the expression of Prox1, CD31, LYVE-1, podoplanin, VEGFR3, and CCL21[82,193,194]. Similar to peripheral tissue capillaries, lymphatics are generally permeable, allowing for ISF, macromolecules, and cellular entry[195]. Anatomically, there are two types of lymphatics, including afferent and efferent lymphatics; the afferent lymphatic channel transports lymph and cells from the tissue to the draining lymph node while cells exit the efferent lymphatic into the bloodstream to a potential target tissue (**Figure 2**). Functionally, lymphatic vessels are classified into initial and collecting vessels[195-198]. Importantly, the collecting vessels possess bi-leaflet valves to allow for unidirectional flow of lymph. Antigen presentation generally involves the migration of antigen presenting cells such as DCs via the afferent lymphatic vessel to the tissue-draining lymph node where antigen presentation to naïve T cells occurs. The efferent lymphatic vessel serves as a conduit for activated effector T cells exit the lymph node into the bloodstream and migrate to a target tissue.

In the brain, the mechanism of antigen transport is still been unraveled. In the 1960s, lymphatic vessels were described to be present at the base of the skull [199]. Subsequently, dural lymphatics were described in rats[200]. It was in the 1980/ 1990s that Cserr H.F. *et al*. first showed using functional experiments that tracer dyes that were directly injected into the CSF or brain parenchyma could be traced from beneath the olfactory lobe to the nasal lymphatics and the cervical lymph nodes[72,80] (**Figure 4**). Recently, mechanistic studies have confirmed earlier findings and demonstrated that brain parenchymal ISF drains into cerebral perivascular spaces, termed “glymphatics”,

and that both ISF and cerebrospinal fluid (CSF) eventually drain into a recently described perisinusoidal conventional lymphatic network in the mouse meninges[82,194] (**Figure 5a &b**). In addition, a direct connection between the meningeal lymphatics and the cervical lymph node has been demonstrated. In light of these findings, the routes of antigen-presentation in EAE that I elaborated on in the BBB section are being reexamined[193,201,202].

In BTs, prior studies showed that vaccination of BT-bearing mice and GBM patients in the flank region with dendritic cells loaded with tumor antigen can induce antigen presentation in the inguinal lymph node and result in BT eradication[86,203,204]. This supported the idea that antigen presentation is likely defective in GBM patients. It also suggests a model in which antigen-presentation in a distal secondary lymphoid tissue from the brain can elicit robust immune response to BT. In addition, in a recent study, Dunn G.P. *et al.*, identified the presence of neoantigens in GBM mouse tumor models including GL261[63]. Interestingly, these mouse tumor models were found to contain very high mutational load of up to 26, 000 compared to less than 100 in GBM tissues[22,63]. Following direct inoculation of mice with cancer cells into the brain, antigen-specific T cells for the same previously identified neoantigens were recovered with tetramers from both the tumor mass and the cervical lymph node. These findings suggest a model in which BT antigens are transported from the brain parenchyma to the cervical lymph node likely via the “glymphatic” and meningeal lymphatic routes described above. Whether BT antigen-presentation occurs at multiple sites other than the cervical lymph node or whether the extent of BT antigen presentation varies in different lymphoid tissues remains to be elucidated. In sum, the brain appears to be open to surveillance by immune cells such as T cells. This gives further support for the

questions I aim to answer pertaining to T cell surveillance in BTs. In the next few sections I will go into details into the key cells involved in tumor immune surveillance, the distinct immune cells found in the brain, and the roles they might play in BT surveillance.

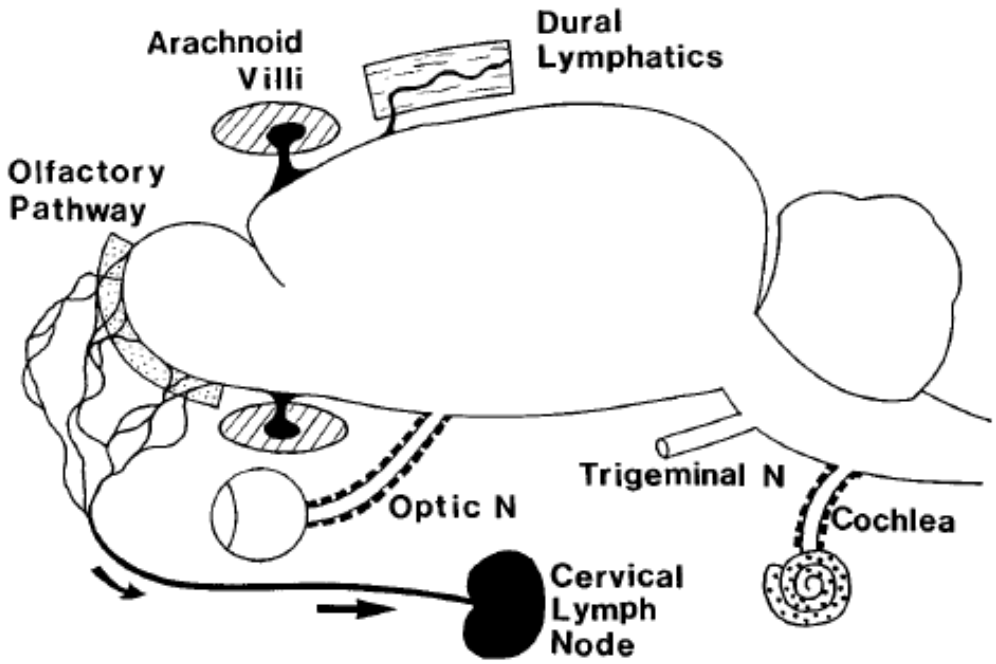

Figure 4. Prior view of CNS lymphatics. Schematic showing the drainage paths of lymphatics in a rat brain (Black arrows). Adapted by permission from John Wiley &Sons, Inc.: [Neuropathol Appl Neurobiol.] (Kida, S., CSF drains directly from the subarachnoid space into nasal lymphatics in the rat. Anatomy, histology and immunological significance 1993 Dec; 19(6):480-8.). Copyright Clearance Center.

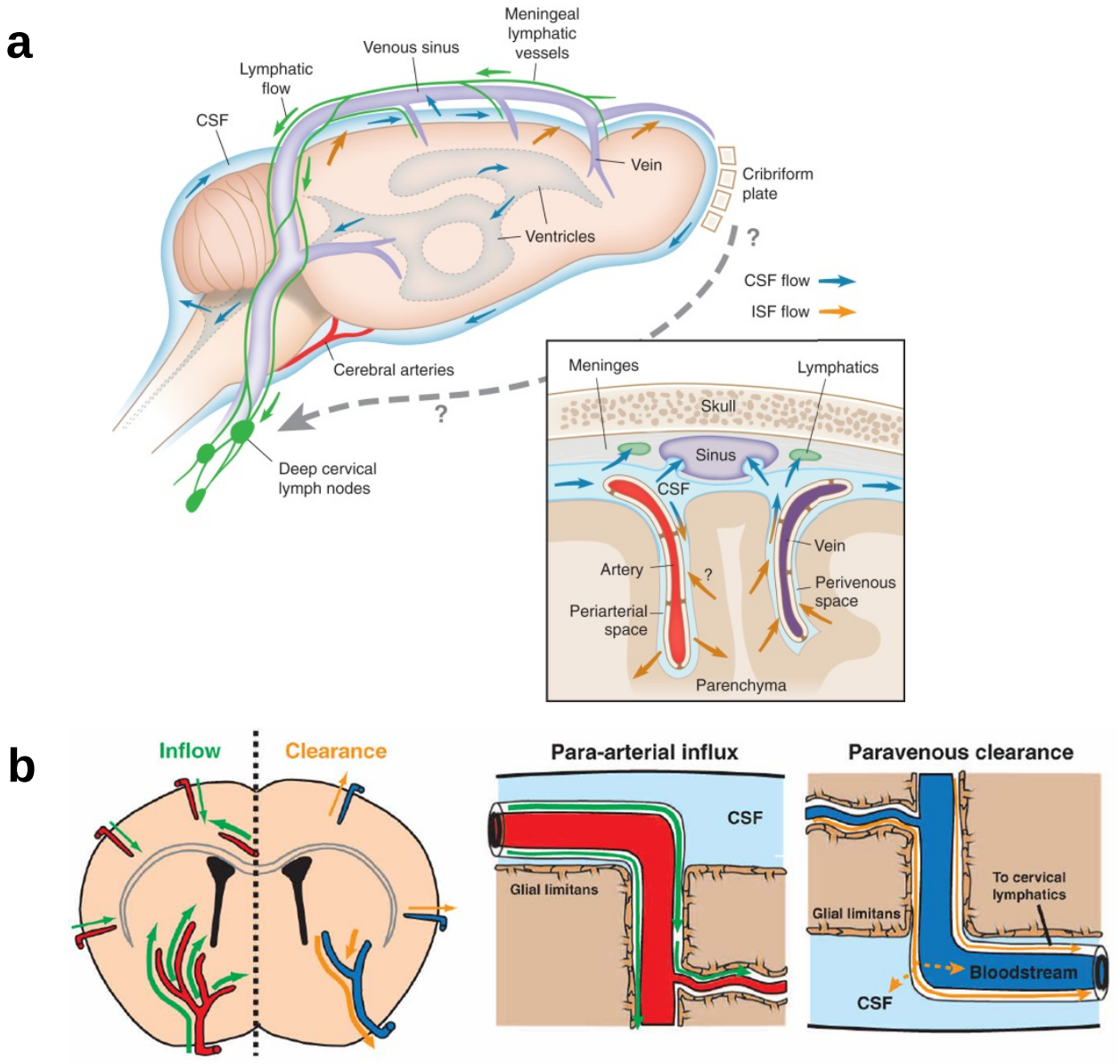

Figure 5. New view of CNS lymphatics.

a. Schematic showing the drainage paths of lymphatics in a mouse brain (Green arrows). The blue and orange arrows show the flow of CSF and ISF, respectively. Adapted by permission from *Elsevier: [Neuron] (*Louveau A.*, Lymphatics in Neurological Disorders: A Neuro-Lympho-Vascular Component of Multiple Sclerosis and Alzheimer's Disease?* 2016 Sep 7;91(5):957-73.). Copyright Clearance Center.

b. Schematic depiction of the glymphatic pathway. In this brain-wide pathway, CSF enters the brain along para-arterial routes, whereas ISF is cleared from the brain along paravenous routes. From here, solutes and fluid may be dispersed into the subarachnoid CSF, enter the bloodstream across the postcapillary vasculature, or follow the walls of the draining veins to reach the cervical lymphatics. "From [Iliff, Jeffrey J. et al. "A Paravascular Pathway Facilitates CSF Flow Through the Brain Parenchyma and the Clearance of Interstitial Solutes, Including Amyloid B." *Science translational medicine* 4.147 (2012): 147ra111. *PMC*. Web. 11 Mar. 2017.]" Reprinted with permission from AAAS. Copyright Clearance Center.

1.4.4 Myeloid cells

Macrophages

Macrophages are critical in regulating tissue homeostasis, and controlling tissue inflammation involving pathogens and cancer[53,205]. Macrophages originate from the yolk sac during embryogenesis in mice and migrate into tissues to become tissue resident cells such as Kuppfer cells in the liver, microglia in the brain, Langerhan cell in the dermis, and alveolar macrophages in the lungs. During inflammatory conditions, macrophages presumably originate from circulating monocytes, which are derived from the bone marrow common macrophage dendritic precursor (MDP) cells[206]. However, the specific population of blood monocytes that differentiates into macrophages in tissue is yet to be identified. Within different tissues, the mechanisms by which macrophages are sustained vary. In general, macrophages are able to self-renew in tissue by local proliferation while a portion of tissue-resident macrophages are replenished from the circulation by blood monocytes[207]. Macrophages in mice and humans can be identified by a combination of surface markers including CD11b (mouse/human), F4/80 (mouse), CD68 (mouse/human), CSF1R (mouse/human), MAC2 (mouse/human), CD11c (mouse/human), Ly6G (mouse), Ly6C (mouse), IL-4Ralpha (mouse/human), and CD163 (human)[208]. Importantly, there is no single marker that defines macrophages exclusively and typically a combination of high CD11b, F4/80, and low CD11c (enriched in DCs), Ly6G (enriched in granulocytes), and Ly6C (enriched in monocytes) are used to identify them. In addition, other surface markers such as CX3CR1 and Iba1 together with cellular morphology are utilized for identifying specialized tissue macrophages such as microglia and other CNS macrophages residing at brain interfaces[209,210].

Microglia and CNS macrophages

In the adult steady state brain, microglia make up the highest number of resident myeloid cells in the brain parenchyma [75,211,212] (**Figure 6**). Microglia play critical roles during neural development and in maintaining tissue homeostasis in the adult brain by pruning developing neurons and engulfing cellular debris, respectively[211,213]. In steady state, microglia soma are fixed, and they rely on highly motile cell processes that continuously extend and retract to survey the surrounding brain region for potential dead cells[214]. In a recent finding, TAM (named after receptor tyrosine kinases **T**yro3, **A**xl, and **M**er) receptor tyrosine kinases Mer and Axl, and corresponding ligands Gas6 and protein S, which are known regulators of innate immune response, were found to control phagocytic functions of microglia at steady state[215]. However, in the presence of inflammatory signals such as IL6, TNFalpha, and nitric oxide (NO), microglia become sensitized to neural-derived factors such as adenosine triphosphate (ATP), glutamate, and the chemokine fractalkine (CX3CL1)[216-219]. They then become activated, transform into an amoeboid form, and subsequently migrate to areas of perturbation to prevent further damage to the brain tissue or, in some cases, exacerbate the inflammation[215]. For a long time, microglia were thought to arise from bone marrow progenitor cells, which give rise to some tissue macrophages[220-223]. Fate mapping studies in mice, however, have revealed a colonization of the brain by microglia during only embryogenesis[224] (**Figure 7**). Around embryonic day 9.5 (E9.5), yolk sac myeloid cells migrate to the brain to become the brain microglia. It was also believed that circulating monocytes could replenish microglia in an adult brain[221]. However, numerous studies have now shown that microglia in an adult brain are not replenished by peripheral myeloid cells, indicating that microglia self-renew and that resident microglia and

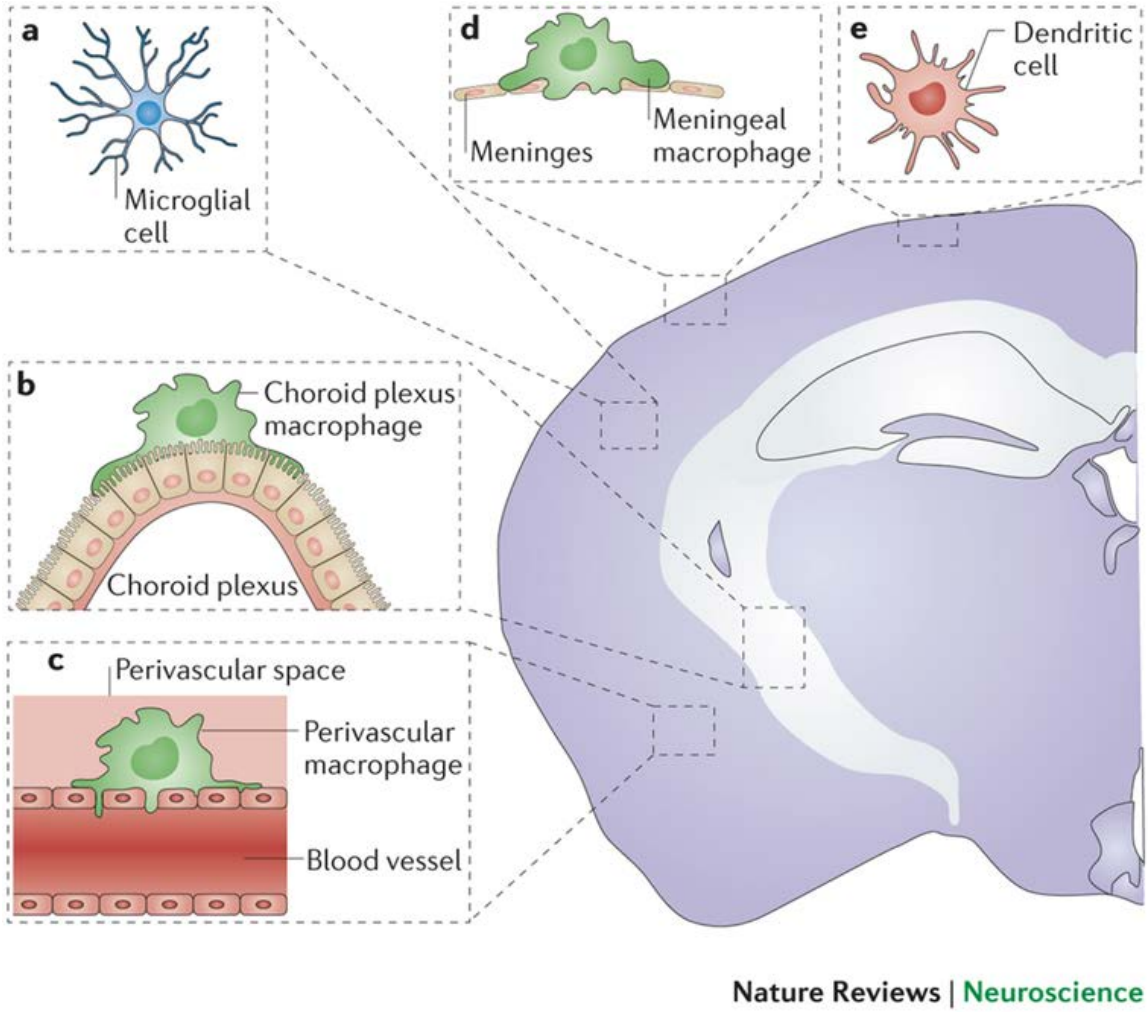

Figure 6. Organization of innate myeloid cells in the healthy brain. Microglia are present within the parenchyma of the brain in steady state. Other myeloid cells are named according to location occupied in the cranial compartment including choroid plexus macrophages (location: choroid plexus in the ventricles); perivascular macrophage (location: perivascular space); meningeal macrophage (location: meninges); and dendritic cells (location: meninges and perivascular space). Adapted by permission from Macmillan Publishers Ltd: [Nat Rev Neuroscience] (Marco Prinz and Josef Priller, *Microglia and brain macrophages in the molecular age: from origin to neuropsychiatric disease* 2014 May; 15(5):300-12. Copyright Clearance Center.

infiltrating monocytes/macrophages derived from the circulation may play distinct roles in steady state and pathological conditions[206]. However, the radioresistant nature of microglia as well as the quick regenerative properties of monocytes/macrophages have

made it technically challenging in delineating the distinct roles played by each of these subsets in chronic diseases such as cancer[225,226].

Apart from microglia which are the resident intraparenchymal myeloid cells of the CNS, there are other resident macrophages that reside within specific niches at brain parenchyma interfaces including meningeal (mMF), perivascular (pMF), and choroid plexus macrophages (cpMF). Recent studies have provided a better understanding of the relationship between these cell types[209]. Despite the believe that other CNS macrophage subsets originate from the fetal liver and can be replenished by circulating bone marrow-derived monocytes, recent findings indicate that CNS macrophages and microglia are actually ontogenically related[209] (**Table 2**). Apart from cpMFs which originate from both the yolk sac and fetal liver myeloid precursor cells and can be replenished by circulating Ly6C+ monocytes in a CCR2 dependent manner, mMFs and pMFs were demonstrated to originate from only the yolk sac and migrate into their distinct niches in the brain at similar times with microglia[209]. And both mMFs and pMFs are not replenished by circulating monocytes in similarity to microglia. At the transcriptional level, CNS macrophage subsets and microglia depend on the transcription factor PU.1, but not Myb, Batf3, and Nr4a1. In addition, they share surface expression of CX3CR1, CSF1R, and Iba1. Notwithstanding, all CNS macrophage subsets showed higher expression of Ptprc (CD45) at both the mRNA and protein level when compared with microglia, while perivascular macrophages were enriched for Mrc1 (CD206) and CD36 in addition to CD45[209]. Furthermore, CNS meningeal and perivascular macrophage development was shown to be independent of Flt3+ multipotent hematopoietic precursors in the BM, indicating that CNS macrophages are distinct from BM derived cells.

Table 2. Characteristics of resident myeloid cells in the brain parenchyma and at central nervous system interfaces

	Microglia	Meningeal macrophage (mMF)	Perivascular macrophage (pMF)	Choroid plexus macrophage (cpMF)
Location	Brain parenchyma	Meninges	Perivascular niche	Choroid plexus
Origin	Yolk sac	Yolk sac	Yolk sac	Yolk sac and fetal liver
Transcriptional factor(s)	PU.1 & Irf8 (Not dependent on Myb and Batf3)	PU.1 & Irf8 (Not dependent on Myb and Batf3)	PU.1 (Not dependent Batf3)	PU.1 (Not dependent on Myb, Irf8, and Batf3)
Surface markers	CX3CR1, CSF-1R, Iba-1	CX3CR1, CSF-1R, Iba-1	CX3CR1, CSF-1R, Iba-1	CX3CR1, CSF-1R, Iba-1
CD45 mRNA (Ptprc) expression	+	+++	+++	+++
CD45 protein expression	+	+++	+++	+++
CD206	-	NA	+++	NA
Replenishment	Self-renew	Self-renew	Self-renew	Self-renew/circulating Ly6C+ monocytes
Flt-3 dependence	-	-	-	+/-
Morphology	Ramified	Amoeboid	Elongated	

In fact, it was demonstrated that previous observations of BM-derived cells infiltrating the brain interfaces in chimera experiments was due to irradiation-induced CNS tissue inflammation, which could damage the BBB and artificially attract BM cells to the brain[221]. Morphologically, microglia are ramified, meningeal macrophages are amoeboid, and perivascular macrophages are elongated in alignment with proximal blood vessels. Therefore, they can be distinguished by imaging studies. In addition,

intravital imaging has shown that microglia and CNS macrophages extend and retract cell protrusions differently[209]. However, whether CNS macrophage subsets play distinct roles from bone marrow-derived macrophages or microglia is not yet known. In sum, different myeloid cell subsets have to be taken into consideration when investigating the role of myeloid cells in BTs.

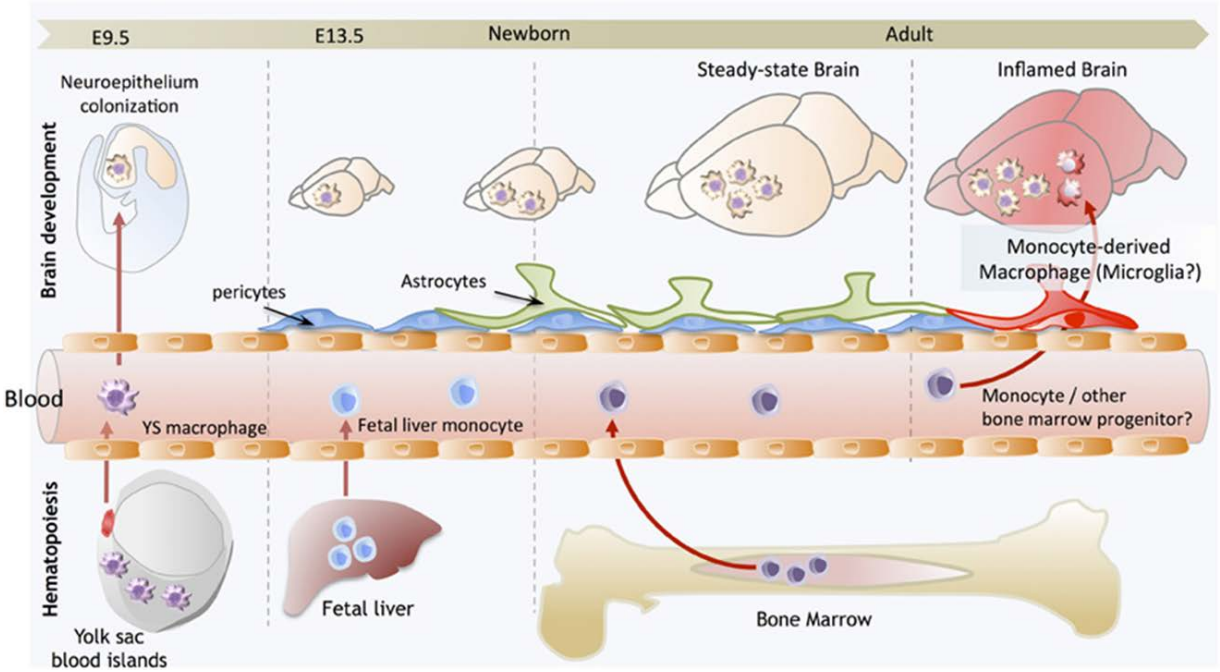

Figure 7. Myeloid cell colonization of the brain from embryonic to adult life in mice. At embryonic day 9.5 (E9.5), Yolk-sac (YS)-derived macrophages gain access into the circulation, migrate, and localize in the embryonic brain to give rise to microglia. Other brain macrophages depicted in **Figure 6** differentiate from YS and fetal liver-derived monocytes, and the bone marrow becomes a major source of monocytes in adult steady state or inflamed brain. Adapted from Frontiers open-access publisher: [Front Cell Neurosci.] (Ginhoux F, *Origin and differentiation of microglia* 2013 Apr 17;7:45.)

Role of Macrophages and Microglia in brain tumors

In the context of cancer, macrophages constitute a widely researched population in the tumor microenvironment termed tumor-associated macrophages (TAMs)[227-231].

Early investigations into immune response to BTs revealed that BTs are largely infiltrated by classical macrophages and the brain resident microglia[205,232]. Since then, there has been immense interest in understanding macrophage plasticity and its role in BT progression. Based on the availability of certain molecular factors such as IFN-gamma, IL-1, and TNF-α, TAMs can be skewed to an "M1" anti-tumor or "classical" phenotype, while immune suppressive cytokines such as IL-4, TGF-beta, and IL10, tend to skew TAMs to an "M2" pro-tumor or "alternative" phenotype[233,234]. However, most of these studies are *in vitro* and may not rigidly translate *in vivo* as represented by a recent study that found that these macrophage phenotypes do not exist at polar ends of a spectrum but rather in continuum, with more resemblance of an unpolarized "M0" phenotype[235]. Depletion of presumably "M2" TAMs by various strategies including small molecule inhibitors such as colony stimulating factor 1 receptor (CSF1R) inhibitors *in vivo* has shown reversal in tumor growth, and this is presently an area of intense research as CSF1R inhibitors are currently being tested in clinical trials[236-239].

However, the origin of TAMs in brain tumor remains very controversial. Experiments in mice have shown that TAMs are mostly composed of infiltrating cells from peripheral tissues such as the bone marrow; however, a recent study claims that TAMs in BT are composed of mainly microglia and not circulating monocytes, and that microglia drive BTs progression[240]. In the latter study, head-shielded mice were irradiated, leading to eradication of only bone marrow hematopoietic cells and circulating cells in the periphery but not the cranial compartment. Microglia but not blood-derived macrophages or monocytes were found to be diffusely infiltrating the tumors. Conflicting with other investigators, the authors claimed that microglia have high expression of CD45 (a marker that has been shown to be strikingly low in

microglia and used as a separation marker for microglia and CD45hi-expressing macrophages)[240] and suggested that the literature on microglia should be reevaluated. Furthermore, the authors failed to consider CNS macrophage subsets at brain interfaces, skull bone marrow myeloid cells, and brain dendritic cells that were not eliminated with irradiation [209,212,241]. In fact, a more recent study showed that macrophages residing at CNS interfaces express high levels of CD45 at both the mRNA and protein levels, in contrast to microglia, and may play a crucial role in neuro-oncologic diseases[209]. As such, the composition of myeloid cells in BTs is still unclear and deserves thorough scrutiny. In this thesis, I have generated a novel reporter mouse model and developed a new method of analysis in an attempt to better characterize myeloid cell subsets in BTs.

For a long time, there has been uncertainty as to whether DCs could play a major role in antigen presentation in BTs since only very small numbers have been detected in BT tissue[242]. Due the predominance of microglia and macrophages, which have been estimated to make up about 30% of BT tissue, it has been suggested that these are the cells that play a major role in regulating immune surveillance in BT progression. In studying immune regulators in BTs, microglia and macrophages are commonly lumped together due to the difficulty in distinguishing between both cell types. Thus, it is unclear as to whether both cell types play distinct roles in immune response to BTs. Nevertheless, glioma-infiltrating microglia/macrophages show high expression of TLRs, but are inefficient at producing inflammatory cytokines such as TNF-α, IL-1, and IL-6. In addition, despite showing high expression of MHC-II, they lack expression of costimulatory molecules CD80 and CD86[242,243]. This would suggest that they are likely ineffective at presenting antigens to T cells. Interestingly, *in vivo*

stimulation of glioma-infiltrating microglia/macrophages in rats by intratumoral injection of CpG-containing oligonucleotides, which engage TLRs, in glioma-bearing rats resulted in increased glioma growth and a reduction in cytotoxic T cell tumor lysis capacity[244]. This indicates that attempts at stimulating glioma-infiltrated microglia/macrophages, at least with CpG-containing oligonucleotides, may be ineffective in activating adaptive T cells and could be deleterious. In BT-bearing mice, microglia have been shown to express Fas ligand, a molecule involved in cell-mediated apoptosis. Inhibition of Fas ligand activity resulted in increased infiltration of leukocytes into the tumor mass. Thus, glioma-infiltrating microglia/macrophages are thought to be polarized to an “M2” tumor-promoting phenotype, in which form they suppress effective immune surveillance of BT[245]. Importantly, interventions aimed at skewing presumable “M2” macrophages to an “M1” proinflammatory or anti-tumor phenotype or depleting glioma-infiltrating microglia/macrophages have resulted in extended survival in tumor-bearing mice[235,236,246 247]. However, it is still unknown whether depletion by CSF-1R inhibitors actually acts on distinct “M2” macrophages since “M1/M2” macrophages are now known to be closely related and bear semblance to an unpolarized “M0” phenotype at least in human glioma, which may extend in a similar manner in mice. Nonetheless, the results indicate that glioma-infiltrating microglia/macrophages have an immune suppressive role in BTs, but does not reflect on their capacity to directly control T cell surveillance in BTs. In addition, depleting glioma-infiltrating microglia/macrophages is inefficient as tumors recur frequently[237].

Monocytes

Monocytes play key roles in tumor progression[248]. They are thought to differentiate and replenish macrophages or DCs in tissue[249,250]. Monocytes originate from a common macrophage dendritic cell precursor (MDP) in the bone marrow[250] (**Figure 8**), and are classified into Ly6C+ classical monocytes (CM) and Ly6C- patrolling monocytes (PM)[250].

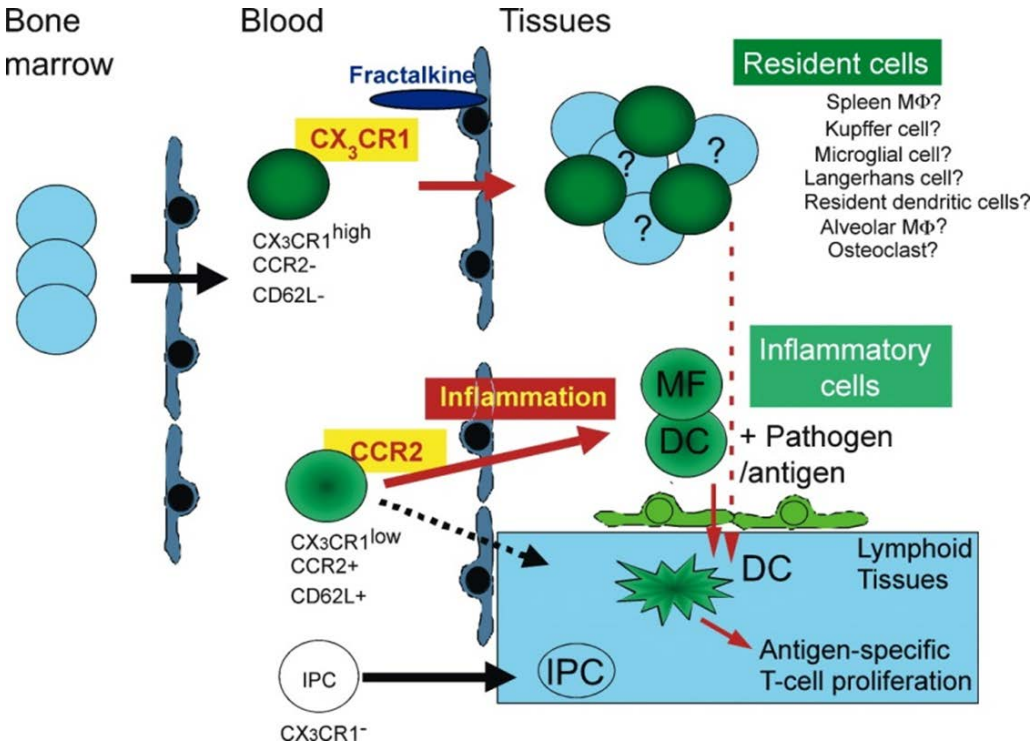

Figure 8. Monocyte derivatives in peripheral tissues in health and disease. Resident monocytes express high levels of CX_3CR1 which, upon interaction with fractalkine, facilitates extravasation into tissues, where these cells give rise to specialized cell types. Inflammatory monocytes express lower levels of CX_3CR1 but have high levels of other receptors like CCR2 that respond to inflammatory chemokines, resulting in migration of the cells to sites of inflammation, where they subsequently differentiate into dendritic cells (DCs) or macrophage/myeloid derived suppressor cells. Monocytes with no expression of CX3CR1 give rise to interferon producing cells (IPC) also called plasmacytoid DCs (PDC). Adapted by permission from Macmillan Publishers Ltd: [Immunity] (Geissmann F. et al., *Blood Monocytes Consist of Two Principal Subsets with Distinct Migratory Properties* 2003 Jul;19(1):71-82.) Copyright Clearance Center.

Several transcription factors including PU.1, JunB, C/EBP-a, C/EBP-b and IRF8 play key roles in the development of myeloid cells in general and especially in CM. In contrast, development of hematopoietic cells into PM has only been recently shown to be dependent on Nuclear Receptor Subfamily 4 Group A Member 1 (NR4A1) expression[251,252]. Although it was previously believed that CMs differentiate into PM, it is now known that CM and PM utilize distinct and independent pathways during development and likely perform different functions[252]. The CM subset is identified by the surface expression of $Ly6C^{+}$ $CCR2^{+}$ $CX3CR1^{lo}$ $CD62L^{+}$. Functionally, CMs migrate to tissues invaded by infectious agents or into inflamed tissues, and can differentiate into antigen presenting DCs and potentially mediate acute pathogen clearance or differentiate into monocytic myeloid derived suppressor cells (MDSC), in which case they contribute to immune tolerance in chronic disease states[253]. Importantly, CMs have also been shown to robustly migrate and infiltrate tumors, where they contribute to an immune suppressive population of monocytic cells also referred to as Ly6C+ CD11b+ Gr1+ CCR2+ monocytic MDSC as opposed to the neutrophilic population of Ly6G+ CD11b+ Gr+ granulocytic MDSCs. Both populations promote tumor growth and there is active research in this area to gain better understanding about their regulation[254,255]. Despite the availability of more evidence skewed toward revealing CM as pro-tumorigenic cells, some studies have also demonstrated an anti-tumor role for CM in the control of cancer cell metastasis, reminiscent of its capacity to also serve as precursor for antigen presenting DCs in infection and indicative of a dual role during inflammation[256-258].

Table 3. Classification and characteristics of monocytes

	Classical monocytes (CM)	Patrolling monocytes (PM)
Origin	Macrophage dendritic cell precursor (MDP)	MDP
Transcriptional factor(s)	PU.1, JunB, c/EBP-α, c/EBP-β, IRF-8	NR4A1
Surface markers	CD11b, Ly6C^{+}, CCR2^{+}, CX3CR1^{lo}, CD62L^{+}, Gr1^{+}	Ly6C^{-}, CCR2^{lo}, CX3CR1^{+}, CD62L^{-}
Function	Differentiation into dendritic cells (antigen presentation, anti-tumor role) or myeloid derived suppressor cells (MDSCs: cancer immune suppression/tolerance)	Surveillance of healthy vascular endothelium Anti-tumor role

In contrast, patrolling monocytes, which are identified by the surface expression of Ly6C^{-} CCR2^{lo} CX3CR1^{+} CD62L^{-}, were known for long a long time to only survey healthy vasculature for potential damage[259,260]; however, recent intravital imaging studies in a model of lung tumor revealed a new role for PMs in preventing the adhesion of circulating cancer cells to lung tissue vasculature. In situations where cancer cells succeeded in engrafting into the lung tissue, PMs were found to be capable of transmigrating through the pulmonary vascular endothelium and infiltrating the established tumor. In addition, signaling via the Fractalkine chemokine receptor CX3CR1 was found to be required by PM to inhibit lung tumor initiation[261]. However, the extent to which CMs and PMs infiltrate brain tumor and their organization in the tumor microenvironment is unknown. In this thesis, I have attempted to analyze the

extent to which CMs and PMs are prevalent in BT. Nevertheless, it will be crucial to distinguish the functions of these monocyte subsets in BT progression.

Dendritic cells

Dendritic cells (DCs) are professional antigen presenting cells (APCs) and serve as a major link between the innate and the adaptive arms of the immune system[212,262-265]. DCs utilize a diverse repertoire of receptors expressed on the cell surface to scan and recognize PAMPs in microbial infections[266-273] Consequently, they endocytose and process such infectious microbial agents into peptides that are eventually presented to naïve T cells in the lymph node via peptide-MHC complexes I and II (pMHC-I and pMHC-II)[274-276]. Precisely, the engulfed tumor materials are processed through complex intracellular machinery such as the proteasome into distinct peptide antigens, which are then loaded unto MHCs in the endoplasmic reticulum, and eventually routed through the golgi apparatus and displayed on the surface of DCs[277]. During this process, DCs migrate through afferent lymphatic channels to the tumor-draining lymph node paracortical regions, where they encounter naïve T cells.

Importantly, unlike other APCs such as macrophages, after phagocytosis of antigens, the acidic milieu in DCs is tightly regulated by NOX2 to prevent destruction of potential peptide antigens necessary for T cell activation[278]. In addition, DCs have an extensive capacity to process and present/cross-present antigens from both intracellular and extracellular pathways via pMHC I and II[278]. Further, in contrast to other APCs, DCs express costimulatory ligands CD80 and CD86 that are necessary for T cell priming. Regardless, a clear distinction between DCs and macrophages still

remains controversial as there is no specific marker that delineates these two described cell types.

DCs are recognized by their expression of a combination of several surface markers, including CD45+ CD11chi MHC-II+ CD11b+. Although CD11b is widely shared by myeloid cells including DCs and macrophages, CD11c is highly expressed on all subsets of DCs in mice in contrast to a low expression on macrophages (which have high expression of F4/80), while CD11b is expressed by only a few subsets of DCs. Therefore, CD11c expression has become almost interchangeable with the presence of DCs; however, care must be taken in interpreting results using this marker. CD11c is an integrin also referred to as integrin gamma X (ITGAX) and its functional role is unknown. Fluorescent transgene encoded by the CD11c promoter has been used to create a reporter mouse that has helped dissect the myeloid lineage within *in vitro* studies and has played a major role in increasing our understanding and appreciation of dynamic interactions between DCs and T cells in *in vivo* imaging studies.

Two subsets of DCs have been recognized based on differences in phenotype and function. They include CD8α+ and CD8α- DC subsets. CD8α+ DCs are found in the spleen of mice[279] and are critical in the activation of CD8+ cytotoxic T cells (CTLs). In peripheral tissues, however, similar DCs do not classically express CD8α. Instead, they are recognized by the expression of CD103[280]. Importantly, CD8α+/CD103+ DCs are efficient at engulfing and processing apoptotic cell bodies at sites of infection or cancer, and subsequently cross-present the peptide product of apoptotic cells to CD8+ T cells within the same vicinity[281,282]. Thus, it is likely that efficient T cell surveillance of BT will involve interactions between DCs, such as CD8α+ DCs, and T cells in the tumor

microenvironment. CD8α+/CD103+ DCs rely on several transcription factors for development including Batf3, IRF8, and Zbtb46[283]. In Batf3 knockout mice in which CD8α+ DCs are absent, there is poor control of infections such as Toxoplasma gondii, and enhanced growth of tumor in cancer models[284-286]. This would suggest a possible role for CD8α+ DCs in BT control. The second subset of DCs identified as CD8α- DCs are delineated by other surface markers including CD11b+ and CD4+. Importantly, they are involved in the activation of CD4+ T cells. CD8α- DCs are required in T_h2 T cell responses in allergic diseases[279,287]. Apart from these latter DC subsets, a small population of resident DCs has been found to reside in certain regions of the brain involved in neurogenesis[212]. Based on marker expression such as CD115, Gr-1, and Ly-6C, it is thought that they are mucosal and monocyte-derived[288]. In addition, they can be identified by expression of CD11c, but some populations express CD11b and CD103. Interestingly, brain DCs can proliferate under the influence of IFN-gamma, can upregulate MHC-II, and can stimulate naïve CD8 T cells[241,289]. However, they are known to be largely radioresistant, in similarity to microglia, and their role in BTs needs to be determined. In sum, DCs are likely to play a major role in controlling T cell surveillance in BT. In the next section, I will discuss T cells and the mechanisms by which DCs prime T cells during an immune response.

1.4.5 T cell biology, T cell priming, and role of T cell subsets in cancer

T cells are the main effectors of the adaptive arm of the immune system involved in cell-mediated immunity[1]. For T cells to function effectively, they must recognize antigens presented as peptides on MHCs via the T cell receptor (TCR). The TCR is a heterodimeric protein in the T cell membrane that consists of an alpha and a beta chain

(αβ-T cells); however, in a different type of T cells, the TCR is made up of a gamma and a delta chain (γδ T cells). Within the scope of this thesis, I will be focusing strictly on the role of αβ-T cells in BT surveillance. Developmentally, T cell precursors, which originate from the bone marrow, migrate to the thymus where they rearrange alpha and beta TCR chains and undergo positive and negative selection in the thymic cortical and medullary regions, respectively. During this selection process, T cells that bind strongly to self-antigens are clonally deleted[290]. T cells that are not deleted undergo clonal diversion to become regulatory T cells (Tregs), which play crucial roles in both autoimmunity and cancer progression. Following completion of T cell selection, mature CD4 and CD8 T cells exit the thymus into the systemic circulation and eventually localize and reside in secondary lymphoid organs such as lymph nodes (SLOs) and spleen[291]. Within SLOs such as lymph nodes, T cells continuously scan for cognate antigens in the para-cortical region. However, for efficient antigen presentation, pMHC-DCs rely on chemokine receptors like CCR7 to migrate to paracortical T cell areas in the draining lymph node over a CCL19/CCL21 chemokine gradient[78,292,293]. Correspondingly, naïve T cells also utilize CCR7 in addition to DC-CK1 (a DC-expressed chemokine, which preferentially attracts naïve T cells[294]) to scan for pMHC-bearing DCs. Upon making contact with pMHC-bearing DCs, a three-signal model of T cell activation ensues[295-298].

The first step in T cell activation involves the engagement of T cells with the pMHC on DCs via the TCR. The avidity and affinity of the TCR for cognate pMHC determines the strength of the signaling cascade downstream of the TCR[299,300]. This TCR signaling can be monitored by use of transgenic mouse models such as nuclear factor of activated T cells (NFAT) or NR4A1-GFP reporter mice[301-303], in which the

green fluorescent protein (GFP) transgene is expressed under the orphan nuclear receptor NR4A1/Nurr77 promoter. By using a reporter mouse such as NR4A1-GFP transgenic mouse, early T cell activation involving only the ligation of the TCR can be detected in the form of GFP accumulation in the T cell nucleus. The mechanism behind this involves TCR ligation to pMHC complex, which leads to translocation of the NR4A1 transcription factor from the cytoplasm to the nucleus where it binds to DNA cassettes to promote further downstream signaling.

Following TCR ligation, cell-cell contact between the T cell and pMHC-expressing DCs initiate the second signal[299,304]; this is mediated by binding of constitutively-expressed CD28 on T cells to costimulatory molecules on pMHC-DC including CD80 (B7-H1) and CD86 (B7-H2). Efficient binding of CD28 to CD80/86, is a necessary step in T cell activation without which T cells become anergic[305]. This step also helps to amplify the TCR signal strength. In some situations, very high TCR signal strengths that could be deleterious to the host are potentially possible and could cause T cells to function in an auto-reactive manner. To prevent this from occurring, peripheral tolerance regulatory mechanisms involving the upregulation of co-inhibitory molecules such as CTLA-4 on the surface of T cells, which has a high affinity for B7/H1 and B7/H2, competitively bind to and work to out-compete CD28 for the same cognate receptors, preventing cell cycle progression[306]. Furthermore, the programmed death receptor receptor (PD-1), which is upregulated by chronically activated or exhausted T cells and binds to its cognate ligands (PDL1 and PDL2) on tolerogenic DCs, inhibits T cell activation by recruiting SHP1/2 to the TCR. SHP1/2 dephosphorylate early downstream signaling events[307-311]. Cancers appropriate the upregulation of these natural homeostatic mechanisms of immunity to prevent

immunological clearance. In addition to the immune checkpoints, cellular (Tregs and MDSCs) and other molecular factors including T cell Fas/Fas-ligand interaction, transforming growth factor-beta (TGF-b), IL-10, and indoleamine 2,3-dioxygenase 1 (IDO1), and immune suppressive cytokines contribute to peripheral tolerance mechanisms in physiologic or pathologic states[312,313]. These factors are known to be involved in inhibiting T cell activation. This would imply that in situations such as viral diseases and cancer, the inhibition of T cells by upregulation of these factors could subdue effector functions of T cells including interferon-gamma (IFN-γ), perforins, and granzymes[139]. In fact, a number of studies have revealed the utility of blocking these inhibitory signals in the tumor microenvironment in preclinical models of a diverse type of cancers including BTs[314]. The results from those studies showed that inhibition of such inhibitory signals slows the rate of tumor progression and is associated with increased presence of cytotoxic effector T cells[314-319].

The third signal includes a variety of stimulating cytokines including type 1 interferon (IFN-I) and IL-12. Mechanistically, IFN-I and IL-12 enhance T cell response to basal IL-2 by prolonging the surface expression of IL-2 high-affinity receptor, CD25, thereby activating downstream phosphoinositol-3-kinase (PI3K) pathway and cell cycle progression genes via FoxM1[320]. As such, the third signal maintains long-term T cell proliferation.

CD4 effector T cells

A subset of CD4 T helper cells enhance the activation of CD8 cytotoxic T cells and also perform effector functions such as tumor killing. The T_h1 subset of CD4 effector T cells is induced by IL-12 and IFN-γ and is identified by the expression of the

Tbet transcription factor and production of cytokines including IFN-γ, IL-2, and TNF-α[321]. This subset is involved in cell-mediated immunity and inflammatory conditions, elimination of intracellular pathogens, and autoimmunity. Importantly, during T cell activation, inhibition of the co-inhibitory molecules such as CTLA-4 resulted in a T_h1-mediated control of tumor[322].

The T_h2 subset is induced by a cytokine milieu in which IL-4 and IL-2 predominate[323,324]. Such T cells are identified by the expression of GATA-3 transcription factor and the production of IL-4, IL-5, IL-6, IL-10, and IL-13. This subset is primarily involved in the production of antibodies by B cells, in elimination of extracellular pathogens, and in allergic diseases such as asthma.

In chronic diseases, a different subset known as Th17 is induced by TGF-beta and IL-6, and identified by the expression of RORγt and production of IL-17, IL-21, and IL-22. Th17 cells play a role in the exacerbation of autoimmune conditions such as Crohn's disease and in the elimination of extracellular pathogens and fungal infections[325]. Although their function remains controversial, elimination of Th17 cells resulted in decreased tumor-bearing mouse survival[326,327].

CD4 Regulatory T cells (Tregs)

CD4 regulatory T cells are a subpopulation of T cells that are usually characterized by FoxP3 expression. In steady state, Tregs maintain immune tolerance to self-antigens. Within inflammatory diseases, Tregs suppress T cell activation[328-332]. Tregs are similar to other T cells in that they originate from the same lymphoid precursor that populates the thymus. However, Tregs only acquire a distinct signature during the later stages of T cell development in the medullary region of the thymus by

binding to intermediate levels of self-antigen presented by autoimmune regulator (AIRE+)-expressing medullary thymic epithelial cells[333,334]. In addition, before exiting the thymus, they begin expressing high levels of the forkhead box P3 transcription factor (FoxP3)[335], a hallmark feature of functional regulatory T cells (Tregs). Deficiency of Tregs in mice and humans leads to the rapidly fatal autoimmune condition known as immunodysregulation polyendocrinopathy enteropathy X-linked syndrome (IPEX)[336,337], demonstrating the key role of Treg cells in the maintenance of immune tolerance. The thymus-derived Tregs are termed natural Tregs and are best defined by the expression of CD4+, CD25+, and FoxP3+[338]. In addition, an inducible form of Tregs, which can be identified with a similar set of markers, are potentially generated from effector T cells in disease microenvironment such as cancer due to abundant immune suppressive and differentiation cytokines such as TGF-beta[339,340]. Importantly, Tregs are highly enriched in tumors and play an immune suppressive role by producing cytokines such as IL-10 and TGF-b[305,334,341-343]. Previous work showed that Tregs accumulate preferentially in high-grade human gliomas, such as GBMs, altered effector function of non-Treg T cell fraction *in vitro*, but there was no impact of Treg presence on patient survival[179,344,345]. However, following similar observations in glioma-bearing mice, depletion of Tregs with anti-CD25 antibody resulted in prolonged mouse survival indicating that Tregs play an immune suppressive role in the glioma microenvironment[178,179,318,319,346]. Mechanistically, the CCL2/CCR4 chemokine axis has been implicated in the recruitment of Tregs in human glioma and strategies have been tested to modulate this pathway[347]. In addition, small molecule inhibitors acting on pathways utilized by Tregs such as the signal transduction and activation of transcription 3 (STAT3) pathway have been shown to deplete Tregs and are about to be tested in clinical trials[348,349].

Furthermore, checkpoint blockade therapies including CTLA4, which have been shown to alter the CD4 T cell compartment and prolong survival in glioma-bearing mice, are already in clinical trials[315]. Thus, there is great interest in understanding immune suppressive mechanisms that might be utilized by Tregs to subvert immune-eradication of cancer and potentially resist these promising treatment strategies. However, it is unknown how Tregs are regulated by DCs in brain tumor. This thesis will address how Treg dynamics might be regulated in the BT microenvironment.

CD8 T cells

CD8 T cells are crucial in the elimination of viral infectious agents and in controlling cancerous growths[341,350-355]. Depletion of CD8 T cells with monoclonal antibodies is known to result in increased tumor growth and decreased mouse survival[356,357]. CD8 T cell engagement with cancer cells *in vitro* results in the polarization of cytolytic granules including perforins and granzymes toward the contact area if effector function is maintained[358]. Perforins are released and contribute to cell killing, in part, by creating pores in the target cell membrane thereby enabling the penetration of granzymes and subsequent target cell lysis[359,360]. Because CD8 T cells are effective in eliminating cancer during cancer immunotherapy, CD8 T cell proportion in tumor has been applied clinically, to some extent, as a surrogate for response to treatment[361-367]. Following the clearance of cancer cells or pathogens, CD8 T cells contract and form a memory pool that can be rapidly recalled upon secondary challenge by the same cancer or pathogen.

Memory CD8 T cells are also an attractive target in immunotherapy especially in formulating anti-tumor vaccines because of its potential to prevent tumor occurrence or

recurrence after successful treatment. An active area of tumor immunology research is trying to understand how endogenous or exogenous transferred CD8 T cells can be retained in tumor to promote tumor cell killing. Some survival molecules that are being investigated include cytokines such as IL-2, IL-7, IL-15, and IL-21[368,369], because they are critical in both naïve T cell function and in maintaining memory CD8 T cell pool. In the brain, CD8 T cells have been shown to form a tissue-resident memory pool after the elimination of a model virus pathogen in mice[370]. This memory pool correlated with the presence of a subset of CD11c+ DCs[371], indicating that memory T cells may require CD11c+ DCs after resolution of an infection, at least in the brain. In general, however, how T cells interact with DCs and may be retained in BTs is unknown. I will be investigating the retention and interaction dynamics of T cells in this thesis.

1.4.6. Dynamics of DCs and T cells in anti-tumor immune surveillance

Anti-tumor immune surveillance is a very dynamic process. For this to occur during a natural anti-tumor immune response there must be cell-to-cell interaction between myeloid cells and T cells, and between T cells and the tumor[372-375]. Classical immunological techniques such as flow cytometry, immunohistochemistry, and animal cell transfers or chimera experiments have been used to establish a basis for immune cell infiltration and interactions in tissue; however, they have limited primary utility, but a significant complementary role in dissecting, understanding, and defining distinct real time cell dynamics and interactions within the immune circuit. Recent advances in intravital confocal and two photon microscopy have played a major role in the investigation of cell interactions in various organs and tissues including the eye, skin, lung, liver, intestine, brain, and lymph nodes[376]. While this technical application has

advanced our understanding of immune cell interactions especially in the lymph node[295,377-379], it has only been recently deployed to study immune surveillance of tumors in peripheral organs including the lungs, skin, brain, mammary fat pad, and abdomen[374,380].

Through intravital multiphoton microscopy and complementary *in vitro* live cell studies of mostly infectious diseases[373,379,381-383], it has been established that naïve T cells in the lymph node are highly motile. Naïve T cells display high average velocities of between 10-15μm/min, show non-directed random motility, and high instantaneous speeds of up to 25μm/min. However, upon making contact with antigen-loaded DCs, T cells show reduced velocity and instantaneous speed and persist in long-lived contacts[384]. Thus, the exceptionally high speeds displayed by T cells in the lymph node have been explained as a mechanism to enhance the scanning efficiency of naïve T cells for peptide-loaded DCs.

Super-resolved *in vitro* microscopy studies of peptide-loaded DCs and T cells have enhanced our understanding of immune synapse formation between cytotoxic T cells (CTLs) and DCs[385-393]. This highly dynamic process involves a feedback mechanism between CTL actin cytoskeleton polarization and TCR signaling. The mechanism entails the polarization of CTL actin cytoskeleton toward the immune synapse, upregulation of adhesive molecules such ICAM-1 and LFA-1, ligation of the TCR to the pMHC-DCs, and subsequent TCR downstream signaling that eventually results in the activation of the CTLs. Calcium imaging studies and model antigens such as ovalbumin have also enhanced the appreciation of the level of strength of T cell activation during such interactions[394-396]. In addition to the TCR ligation, the expression of co-stimulatory ligands such as CD28 and its interaction with its cognate B7-H1/B7-

H2 receptors on DCs has been detailed[296,306,397]. As these processes are critical for T cell function, it will be important to study these processes in the BT microenvironment, as there may be differences in how T cells interact with DCs *in vivo*.

In the tumor, the dynamics of immune cells in general are less well-understood[398,399]. Nevertheless, in time-lapse movies, antigen-experienced T cells engage cancer cells and potentially a myriad other immune and stromal cells. Although it was predicted that an activated T cell could make sequential one to one contacts to kill cancer cells as had been observed *in vitro*, it has become apparent that this is a more complicated process *in vivo*[400]. For example, intravital imaging has shown that it takes approximately 6 hours for one cytotoxic T cell to kill one cancer cell[372]. This indicates that cancer killing, *in vivo,* is a very slow process, and supports the idea that large numbers of cytotoxic T cells are required to make any meaningful impact in tumor progression. However, possibly due to antigen recognition, T cells display a variety of migration patterns *in vivo* such as maintaining prolonged interactions, less prolonged interactions ("kiss and run"), or no interaction[401]. Therefore, it is likely that given a certain number of cytotoxic T cells in the tumor, only a proportion of those T cells may be involved in active killing of cancer cells. Despite these potential limitations, valuable knowledge has been obtained by direct visualization of T cell surveillance in tumor. For example, in a a model of subcutaneous tumor, OVA-expressing EG7 thymoma cells were implanted in mice and subsequently infused with exogenous TCR transgenic OT-I-CTLs.Tumor-antigen specific CTLs infiltrated the tumor and show high expression of CD69 and IFN-y, indicating T cell activation. They exhibited reduced velocity, their migratory pattern became more confined, and they showed increased arrest in the tumor relative to non-OT-I-expressing CTLs[372,402,403]. Recent studies in mammary fat

pad of mice also utilizing the model OVA-antigen have shown that exogenously transferred OT-I-CTLs can persist in prolonged contact with DCs at the margin of the tumor, where they undergo reactivation[375]. These findings indicate that T cells must recognize cancer antigens in order to engage in prolonged interactions in the tumor microenvironment, potentially with cells such as DCs, macrophages, and/or tumor. It must be recognized that despite the ease of using model antigens in mouse studies to simplify our understanding of anti-tumor immune response, parallel studies in human tissues require analysis of highly polymorphic MHCs expressing a vast array of tumor associated-antigens, and variably recombined TCRs may have different reactivity to T cell epitopes[404]. A more recent study utilizing intravital imaging within a subcutaneous tumor suggested that during tumor progression, DCs “trap” CTLs; however, little is known about the role of DCs in the regulation of T cell surveillance in tumor. Specifically, much less is known within BT. Therefore, I will be devoting chapter 3 of this thesis to comprehensively address some questions pertaining to the role of DCs in BT immune surveillance and their interaction with T cells.

1.4.7. Role of chemokines in immune cell recruitment and surveillance in brain tumors

For immune cells to establish cell to cell contact, they must first migrate to the tissue of interest. Immune cells are highly dynamic and can migrate over long and short distances[405,406]. Myeloid cells such as DCs are generally generated from monocytes that migrate from the bone marrow and seed tissues while adaptive T cells egress from lymph nodes to tissue after undergoing priming. Chemokines are cytokines involved in the chemoattraction of cells in normal homeostatic conditions and at sites of

inflammation[407]. Several chemokines have been identified and they are grouped into four subfamilies including C-, CC-, CXC-, and CX3C- based on the number and spacing of cysteines.

During inflammation, chemokines may be expressed at tissue endothelial surfaces in a bound form or released as a soluble form into serum. Importantly, immune cells migrate over chemokine gradients and utilize adhesion molecules such as integrins to bind to endothelial-bound chemokines in order to transmigrate into tissues via the vasculature[408,409]. Interestingly, DCs have been shown to exhibit differential migration patterns depending on the form of chemokine available. For example, surface-immobilized CCL21 was found to induce random migration of DCs, whereas a soluble CCL21 induced a directional motility pattern[408]. Although the repertoire of chemokines necessary for myeloid and T cell migration is vast, the specifics of how immune cells migrate and organize themselves in BT remains unclear and the regulation of this process is largely unknown.

In the brain, several factors have been implicated in immune cell recruitment during inflammation including chemokines, neurotransmitters, molecules of the complement pathway, and ATP[216]. In BTs, glioma cells have been shown to produce a host of chemoattractants, which have been implicated in the recruitment of TAMs. including CSF-1, monocyte chemoattractant protein-3 (MCP-3), monocyte chemoattractant protein-1 (MCP-1/CCL2), hepatocyte growth factor and scatter factor (HGF/SF), fractalkine (CX3CL1), glial cell-derived neurotrophic factor (GDNF), CXCL12 (SDF-1), and granulocyte macrophage-colony stimulating factor (GM-CSF). This indicates that there are a multitude of chemoattractants that can mediate immune cell recruitment in BTs. However, many of these studies have been conducted *in vitro* using

microglia cell lines, and *in vivo* studies on the importance of some chemoattractants such as MCP-1 have been challenged[216]. Out of all these, fractalkine is a particularly compelling candidate since it is highly expressed at steady state in brain tissue in comparison with other organs and has been termed the “neuronal chemokine.” Yet, its role in BT immune surveillance is unknown.

Fractalkine is constitutively expressed in a membrane-bound form by neurons in a healthy brain and can be subsequently cleaved into a soluble form by metalloproteinases (MMPs) such as ADAM10 and 17 following tissue damage[210]. In the membrane-bound form, fractalkine exists as a 373 amino acid with an extracellular domain and mucin-like stalk, a transmembrane domain, and a cytoplasmic tail[410]. Following MMP cleavage, however, the soluble form acts as a chemokine that has an extracellular domain and the mucin-like stalk. Thus, fractalkine can serve both adhesive and chemotactic functions depending on the state of the tissue[411,412].

Fractalkine acts on and signals via its only known receptor, CX3CR1[413,414]. CX3CR1 is a G-protein coupled receptor[413]. CX3CR1 has been studied extensively with respect to microglia and macrophages in the context of cellular adhesion, apoptosis, and migration (**Figure 9**) but CX3CR1 is also expressed on the surface membrane of monocytes, and some DCs as such CX3CR1 may mediate DC and monocyte migration and function in both physiological and pathological conditions[210,409-411,414,415]. In steady state, CX3CR1 is ubiquitously expressed by microglia in the brain parenchyma.

The expression of both fractalkine and CX3CR1 has been intensively studied in neurogenesis, neurodegenerative diseases such as Alzheimer’s, and in brain

tumors[213,416]. The disruption of CX3CR1 has been shown to affect neural pruning, suggesting that microglia is critical in brain development[211,213]. In addition, CX3CR1 deficiency may or may not have a role in mediating microglia function duringplaque removal and neuronal damage in models of Alzheimers[417,418]. Recently, CX3CR1 deficiency was found to be associated with Ly6C+ classical monocytes infiltration in BTs and reduced survival in BT-bearing mice; however, DCs and T cells were not studied[419]. In addition, this process was determined to be orchestrated by IL-1 since fractalkine showed very low expression in mouse or human GBM cells/tumor mass, where the monocytes/macrophages were localized.[419]. However, it seems unlikely that fractalkine that is constitutively and highly expressed in healthy neuronal cells and a major chemokine would be dormant during an inflammatory process involving tumor-induced tissue stress/damage and immune cell recruitment[237]. In the brain, it is possible that aggressively progressing tumors damage neurons and induce of the release of soluble fractalkine, which is an ideal candidate to regulate the dynamics of anti-tumor immune surveillance.

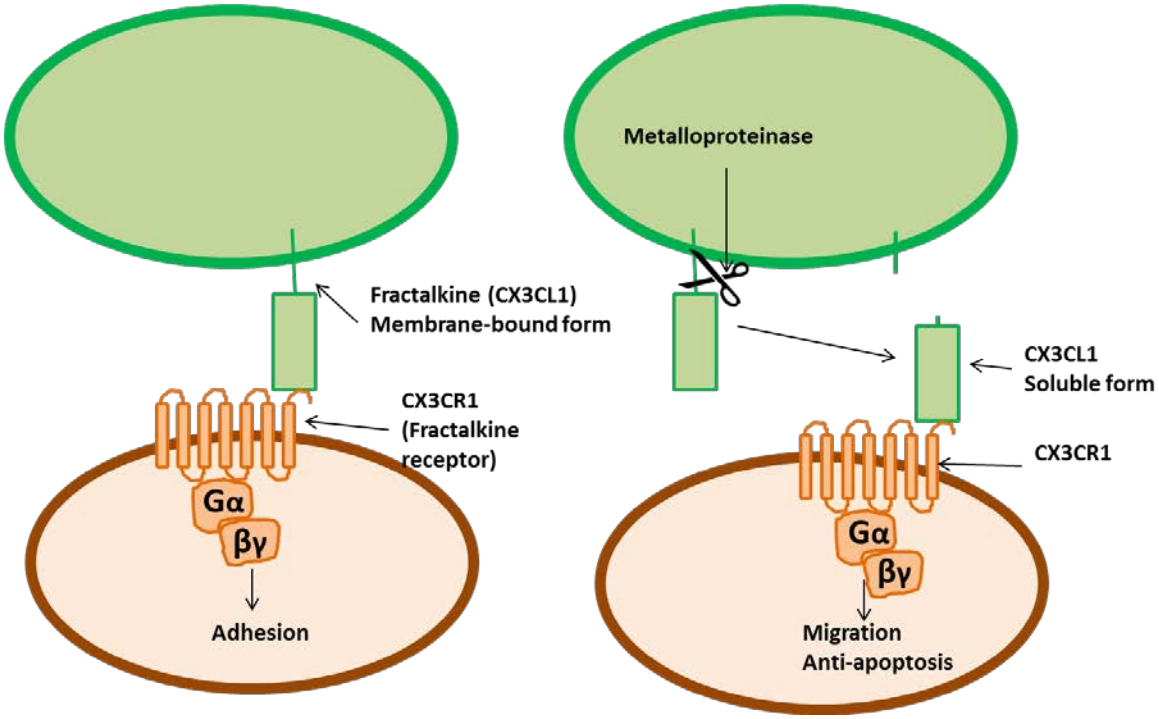

Figure 9. Role of Fractalkine/CX3CR1 chemokine pathway.

The roles of Fractalkine are illustrated in the figure. It shows membrane bound and soluble Fractalkine (cleaved by metalloproteinases) participating in cellular adhesion and survival anti-apoptosis/migration, respectively.

1.5. Specific aims

Based on the information in this chapter, my central hypothesis is that brain antitumor immune surveillance by T cells is regulated by extracranial myeloid cells, such as BM-derived DCs through the neuronal chemokine fractalkine. I will present results from the investigation of this hypothesis in two specific aims:

1. Determine the role of antigen presenting cells in the recruitment and dynamics of T cells in brain tumor microenvironment by employing real time imaging techniques

2. Determine the role of fractalkine/CX3CR1 signaling pathway in the dynamics of immune response to brain tumors by utilizing genetic knockout mouse models and intravital microscopy.

The work in this thesis is aimed at determining the identity and composition of myeloid cells infiltrating BT and understanding the fundamental cellular mechanisms regulating anti-tumor T cell immune surveillance. In addition, I have examined a molecular mechanism involving how a local chemokine produced in the brain tissue governs immune response to BTs. The results obtained from the experiments conducted in this thesis will increase our understanding of BT immune surveillance and will be relevant in developing strategies to enhance conventional immunotherapy.

1.6. Overall approach and rationale

The studies conducted in this thesis will help in constructing a brain tumor landscape of immune cellular localization, migration, and interaction. For this to be accomplished, appropriate tumor models will be used. Genetically engineered mouse models of spontaneously developing tumors (GEMMs) are the gold standard for studying tumor progression in preclinical settings. However, these models are driven by mostly oncogenic mutations and lack the endogenous passenger mutational load that may be relevant for proper antigenic immune cell recognition and function. Similarly, cancer cells derived from human BTs contain genetic mutations that may be closest to those detected in human patients with cancer; however, they have to be grown within immune deficient mice to prevent rejection. Thus immune response to such tumors cannot be adequately studied. In contrast, experimental tumor models derived from cell cultures of carcinogen-induced cancer types from different tissues including the brain,

lungs, skin, and soft tissues can potentially develop in immune-competent syngeneic animals when re-implanted. Importantly, it has been shown that tumors derived from such cancer cell types possess high mutational loads[63] and are strongly immunogenic[117,139], suggesting that there is likely to be endogenous immune reactivity when implanted *in vivo* in immune competent mice and as such help in the understanding of T cell surveillance in tumor. Therefore, to investigate the dynamics and regulation of endogenous immune cells in BTs, I have employed longitudinal intravital multiphoton microscopy of immune cells in experimental BT models including GL261 glioma, Lewis lung carcinoma (LLC), B16 melanoma, and MCA fibrosarcoma brain metastases. The rationale for employing intravital two-photon microscopy is to provide high spatiotemporal 3-dimensional resolution time-lapse images to better understand T cell surveillance in BTs in a dynamic fashion.

Two-photon microscopy:

Two-photon microscopy is a powerful imaging technique in biological research. In contrast to a confocal microscope that generates single high-energy photons from ultraviolet lasers to excite molecules in a volume of tissue, a 2-photon microscope works by simultaneously directing two separate low-energy photons of long wavelengths generated by ultra-fast femto-pulsed infrared lasers at a molecule. In confocal microscopy, excitation works linearly, while it is non-linear in 2-photon microscopy, meaning that, theoretically, image resolution is better with confocal microscopy; however, practical adjustments can be made in 2-photon microscopy to produce confocal-like resolution images.

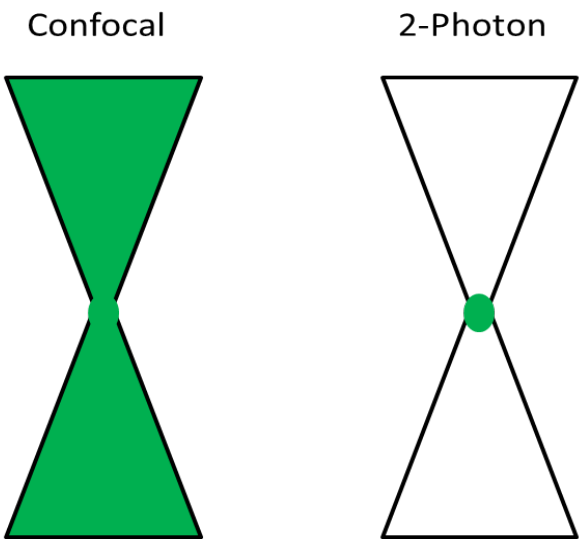

Figure 10. Illustration of tissue excitation and emission in confocal and 2-photon microscopy. The green region represents the volume of tissue excited by photons. The green sphere at the intersection of the inverted cones represents the volume of tissue at the focal plane of interest. The region within the inverted cones represents the volume of tissue above and below the focal region of interest.

It is worth noting that low-energy photons are significantly less absorbed by molecules such as fluorophores than high-energy photons. Based on this principle, several advantages of using a 2-photon microscope become apparent. First, in contrast to confocal microscopy in which high-energy photons excite molecules above and below the focal plane in a volume of tissue illuminated (**Figure 10**), the low-energy photons of a 2-photon microscope only excite molecules in a focal plane, where the probability of two separate photons converging on a single molecule is highest. Further, because a large volume of tissue is excited during confocal microscopy, there is a lot of light scattering that occurs from out-of-focus planes leading to a blurred image. Hence

a pinhole is required to prevent the collection of out-of-focus scattered light. In contrast, since a 2-photon microscope restricts excitation of a molecule to a single plane, scattering from out-of-focus planes is greatly diminished and a pinhole is therefore not required. This enables deeper penetration of more low-energy photons into the brain tissue, resulting in better signal-to-noise. Interestingly, a very good example of a tissue that is highly light-scattering is the brain. In addition, exposure of large volumes of tissue to excitation in confocal imaging can potentially lead to photobleaching/photodamage and possible loss in tissue viability, while photobleaching/photodamage are limited to the focal plane of interest in 2-photon imaging and as such better preserves tissue viability. Especially relevant to brain imaging, low-energy photons in 2-photon microscopy can penetrate deeper into biological tissues to depths of up to 600um to 1mm[420-425], while confocal imaging is usually limited to the surface of tissues to a depth of about 100um from the surface. Apart from the advantages above, 2-photon imaging also has the capacity to produce signals from unlabeled tissue samples such as collagen and muscle based on second-harmonic generation (SHG). In this thesis, SHG will be used during imaging to visualize skull and meninges without any labeling, which will enable differentiation from the underlying brain cortex.

Despite the advantages of 2-photon microscopes, the image resolution is usually lower than with confocal imaging. This is immediately understandable because a microscope's scale resolution is inversely proportional to the wavelength of light used[420]. As such, 2-photon imaging requires expensive objectives with high numerical apertures. In addition, thermal damage arises during imaging of pigmented specimen

and could be potentially problematic during imaging of pigmented tumors such as melanoma.

The use of intravital two photon microscopy here is innovative because it has not been used previously to the extent of its application in the studies conducted in this thesis. In addition, it will reveal information such as real time *in vivo* single cell-cell interactions in a multidimensional manner that cannot be accessed otherwise.

Tumor models

The tumor types that will be utilized include fluorescent-labelled syngeneic GL261 glioma, Lewis Lung Carcinoma (LLC), MCA-fibrosarcoma, and B16-F10 melanoma. I have selected these cancer types because they recapitulate the most prevalent and deadly of patient primary BT and brain metastases to a certain extent, at least in an experimental setting. Importantly, as described earlier, each of these models is syngeneic to the immune competent hosts in which they will be studied, and thus can implanted to be studied in an orthotopic or heterotopic manner. To visualize tumor growth by intravital imaging, the cancer cells have been made fluorescent. As it is likely that fluorescent cancer cells may have higher immunogenicity due to the fluorescent proteins, appropriate controls have been used for proper interpretation of the data.

Experimental strategies

To visualize immune cell interaction with tumor, a broad range of multi-color reporter mice have been used to visualize distinct groups of immune cell populations including microglia, monocytes, DCs, T cells, and Tregs. For further visualization of T cell subsets and important molecules involved in T cell interaction, cells have been

stained by tissue immunofluorescence. To increase the robustness of the investigations in this thesis, genetic knockout mice, cell-specific *in vivo* depletion experiments such as in cell-specific diphtheria-toxin receptor mice, and bone marrow transfer studies have been conducted. In addition, to ascertain relevance to human patients with brain tumors, selected studies have been conducted on human tumors. It is hoped that the studies completed here will reveal relevant mechanisms underpinning anti-tumor T cell surveillance in the brain and provide new insight into how to optimize immunotherapies for brain tumor patients.

CHAPTER 2:

MATERIALS AND METHOD

Cell lines

MCA-205 fibrosarcoma cell line was obtained from Dr. Xiao-Feng Qin (The University of Texas MD Anderson Cancer Center (UTMDACC)) B16-F10 was obtained from Dr. Willem Overwijk (UTMDACC), LLC was obtained from Dr. Limo Chen (UTMDACC), and GL261 was purchased from American Type Culture Collection (ATCC). Cell lines were confirmed to be mycoplasma free. Cancer cells were maintained in RPMI culture medium containing 5% fetal bovine serum (FBS), 1% Penicillin/Streptomycin (P/S), 1% beta-mercaptoethanol or in DMEM/high glucose media containing 10% FBS and 1% P/S. Cells in culture were stored in incubators at 37^0C and 5% CO_2. To render the cells fluorescent for intravital microscopy, MCA-205 fibrosarcoma, B16-F10 melanoma, Lewis-lung carcinoma (LLC), and GL261 glioma cell lines were transduced with VECTOR DESCRIPTION encoding the mCerulean fluorescent protein as previously described.[426]

Animals

Use of animals was approved by the institutional use and care committee (IACUC) under protocol number 00000878-RN01. All animals were on the C57Bl/6 background and bred in-house or commercially purchased. C57Bl/6 wild type (WT), $Rag1^{-/-}$, CX3CR1-GFP, and CCR2-RFP mice were purchased from the Jackson Laboratories (Bar Harbor, ME). Additional C57Bl/6 WT mice were purchased from the Radiation Oncology Department at UTMDACC. CD11c-EYFP mice were obtained from Dr. Michel Nussenzweig, The Rockefeller University, New York, NY; hCD2-DsRed mice

were from Dr. Dimitris Kioussis, The National Institute for Medical Research, Mill Hill, London, U.K.; and ROSA$^{mT/mG}$ mice were obtained from Dr. M. Konopleva, Dept. of Leukemia, UTMDACC. Various combinations of these strains were generated by interbreeding and genotyping. For experiments, mice of both sexes were used at ~1.5 to 6 months old and euthanized by CO_2 inhalation and cervical dislocation in line with the IACUC guidelines.

Brain Tumor Models

To generate tumors in mouse brain, cancer cells were prepared and injected either directly by intracranial injections or indirectly via the internal carotid artery. Cancer cells were harvested from 10 cm cell culture dishes at logarithmic growth phase by washing with 1x PBS and trypsinizing with 2ml of 0.05% trypsin for about 2 minutes and detaching the cells by gentle agitation of the dish, followed by trypsin neutralization with 8 ml media and cell concentration by centrifuging at 1,350rpm, 4^0C, for 10 minutes, repeated for a second wash in HBSS. Cell concentration was measured with a hemocytometer and adjusted for injections as described later. Cells were kept on ice throughout the length of the injection procedure.

Preparation of intravital thinned skull windows

To create skull window for longitudinal imaging, the mouse was anesthetized with a loading dose of 10µl/g mouse of 10mg/mL ketamine and 1mg/mL xylazine cocktail intraperitoneally, followed by 50µl of same concentration every 15-20 minutes to maintain anesthesia until completion of surgery. Fur was depilated from the cranial vault, which extended to the nasal bridge anteriorly, the temporal skull regions laterally,

and the occipital region posteriorly. The skin was then decontaminated using swabs of betadine and 70% alcohol. The skin overlying the cranium was excised and the pericranium was gently detached from the underlying skull bone. Mouse was restrained with tapes on a surgical stage and warmed with a heating blanket for the entire length of the surgery. A 5-6 mm diameter parietal skull region to be thinned was marked using a pen 1-mm lateral to the sagittal suture and 1-mm posterior to the coronal suture. Vetbond glue was then applied on the dry skull except within the region marked with a pen. The marked skull region was thinned to about 10-20 μm in thickness using a high-speed diamond drill with saline cooling. Specifically, the outer table or cortical bone and spongy medullary cavity of the mouse skull were surgically shaved off, leaving an intact inner table. Further shaving was done with cone-shaped drill bits to increase the optical quality of the inner table. Thereafter, the thinned skull was reinforced with a 5mm-diameter/1mm-thickness round cover glass that was lightly attached to the inner table to prevent indentation of the thinned skull into the cranial compartment. Further strengthening of the window preparation was done using dental cement.

Internal carotid artery injection for metastasis models

Brain tumors were induced by injection of cancer cells into the internal carotid artery (ICA). Specifically, the mice were anesthetized, the fur was depilated on the anterior region of the neck, and the exposed skin was decontaminated with betadine and 70% alcohol. After this, a 1 cm midline incision was made on the anterior aspect of the neck, followed by exposure of the common, external, and internal carotid arteries. The common carotid and external carotid arteries were ligated and 1 x 10^5 cancer cells in 0.1 ml volume of saline were infused via the patent part of the common carotid artery

into the internal carotid artery, which supplies the brain. Infusion of cancer cells was done slowly over 30 seconds to 1 minute. After this, the patent part of the common carotid artery was then ligated, and skin was closed using surgical staples.

Orthotopic cancer injection for the GL261 glioma model

For direct intracranial injection, the mice were anesthetized, the fur was depilated on the head, and the exposed skin was decontaminated with betadine and 70% alcohol. A 5-6 mm burr hole was placed in the parietal skull while preventing damage to the dura mater. 2×10^4 cancer cells were implanted using a glass pipette attached to a micromanipulator system (Sutter, Novato, CA). The glass pipette was stereotactically oriented at the center of the exposed brain region and inserted to a depth of 200-250 μm. Cancer cells were injected in 2 μl volume of phosphate-buffered saline (PBS) over a period of 2 to 5 minutes and the pipette was then withdrawn slowly over a period of 15 to 20 minutes. An air-brain interface was created by applying PBS or artificial CSF[427,428] on the exposed brain. This was followed by closure of the brain by use of a glass coverslip that was adhered with Vetbond glue to the adjacent skull and further reinforced with dental cement.

Tail vein injection

For tail vein injection, cells were harvested with trypsin and washed twice in PBS. 10^5 cells were injected via the tail vein into mice.

In vivo depletion of CD8 T cells

For CD8 T cell depletions, mice were injected with 100 mg/ml anti-CD8α antibody (Clone #53-6.72, BioXcell, San Diego, CA) intraperitoneally, either one day before or on day 5 after injection of cancer cells and then every other day until the experiment was terminated at day 20 after cancer cell injection. Control animals were injected with PBS. Depletion was verified by flow cytometry analysis of CD8 T cell levels in mouse peripheral blood.

Depletion of CD11c-YFP cells

Mouse expressing both YFP and diphtheria toxin receptor (DTR) under the CD11c promoter was used for depletion of CD11c cells in longitudinal imaging studies. Specifically, CD11c cells were depleted by consecutive injections of100ng/day of diphtheria toxin (DT) on days 11 and 12 after a baseline time-lapse movie of CD11c-YFP cells in the tumor had been acquired. Depletion of CD11c-YFP cells was confirmed by *in vivo* visualization of CD11c-YFP cells in the tumor on day 13.

Bone marrow transfer studies

CD11c-EYFP/hCD2-DsRed and CX3CR1$^{GFP/GFP}$ mice were used as donor and recipient, respectively. Bone marrow (BM) was harvested from CD11c-EYFP/hCD2-DsRed mice, resuspended in RPMI media, and injected intravenously via the tail vein into unirradiated CX3CR1$^{GFP/GFP}$ mice (7 x 10^6 cells/mouse). BM infusion was done either one day before cancer cells were injected into mice via the ICA or five days after ICA cancer cell injection. Brains of recipient mice were harvested, and brain tumors were analyzed at day 20 after ICA cancer cell injection.

Immunofluorescence

Brain tissue was embedded in optimal cutting temperature (OCT) medium and stored at -80^{0}C immediately after mice were euthanized. Embedded brain tissues were cryotome sectioned into 5-8 µm thin sections. Sectioned fresh brain tissues were stained with various antibodies, either alone or in combinations including, anti-mouse MHC-II biotin conjugated antibody (1:100; Clone M5/114.15.2; eBioscience) as a primary and APC streptavidin (1:500; Cat.#554067; BD Pharmingen) as secondary; and purified rabbit anti-mouse fractalkine (1:100; Cat.#TP233; Torrey Pines Biolabs Inc.) as the primary and Alexafluor-647 goat anti-rabbit (1:500; Cat.#A31633; Invitrogen Molecular Probes) as the secondary. Antibodies were used in a 1:100 dilution ratio in blocking buffer. Specifically, frozen tissues were first washed with PBS to get rid of the OCT. After this, the tissues were incubated with blocking buffer (SuperBlock blocking buffer; Thermo scientific; #37517) for 30 minutes. Subsequently, tissue samples were washed twice in PBS, and then incubated with antibodies overnight as described. Finally, the antibody was washed off of tissues by using PBS. For fresh tissue sections, the specimens were immediately incubated in blocking buffer for 30 minutes to 1 hr before proceeding through similar steps as with the frozen sections. Tissues were mounted with Prolong Gold (Invitrogen) and imaged using a Leica SP8 confocal laser scanning microscope (Leica Microsystems, Buffalo Grove, IL).

In vivo dynamic *microscopy*

Intravital microscopy was performed using a customized two-photon confocal SP5 laser scanning microscope (Leica Microsystems, Buffalo Grove, IL) with four

channel non-descanned detectors, including two hybrid (HyD) detectors, and two femtosecond lasers (Spectra-Physics). The system was operated in a fast resonant scanning mode with frame averaging or in a conventional galvo-scanning mode. Mice were anesthetized as earlier described. After confirming complete anesthesia, mice were head-immobilized with a custom-made stereotactic holder on a heated motorized microscope stage maintained at 37^0C throughout the entire imaging procedure. To highlight the vasculature, TRITC-dextran; 155kD (10mg/ml; Sigma Aldrich; #T1287-50MG) was diluted at a concentration of 1:5 in PBS and 50µl injected via the tail vein or retro-orbital route. Time-lapse stacks of images were acquired using Nikon objectives (16X, NA = 0.8 or 25X, NA = 1.1), at a distance of 5 µm between Z-planes and a 20 to 30 seconds inter-stack interval, for a period of 30 minutes to 2 hours. Interline sequential excitation at two femtosecond-pulsed wavelengths was used to enhance channel separation as follows: 840 nm excitation: CFP, GFP and TRITC emission; 990 nm excitation: SHG, YFP and DsRed emission. Typical image format was 512 x 512 pixels. Some sequences were acquired in 1024 x 1024 pixel format. For longitudinal studies, imaging was repeated on the same area using the vasculature as landmark at set time points after cancer cell implantation until about 30 days.

Ex vivo imaging

For *ex vivo* imaging, brain was harvested after mouse circulation fixation with 4% paraformaldehyde under anesthesia. The brain was sectioned into 4-5 equal thick coronal sections (~2mm each) with a sharp blade, sections were overlaid with a PBS-moistened cover glass and imaged through a 2X and 4X objectives (Olympus), or a 16X NA = 0.8 objective (Nikon).

Image processing

Prior to analysis, acquired images were subjected to processing using the Leica Application Suite version 1.7.0 build 1240 (Leica Microsystems). Images were parsed through several stages. For example, if images were noisy, filtering was performed by applying a median filter width of 3. Next, crosstalk correction was performed on each channel to eliminate channel bleed-through. Subsequently, images were analyzed in xy-2-dimension maximum intensity projections created from all images, xyz-3-dimension images, or xyzt-4-dimension time-lapse images.

Image analysis: cell tracking

For three-dimensional cell tracking and contextual analyses, Leica Image Format (lif) files were opened using Bitplane Imaris analysis software versions 7 to 8.3.1 (Bitplane AG, Saint Paul, MN). Voxel dimensions were specified according to the objective used for image acquisition. If drift was present, it was corrected based on averaged landmark features such as cancer cell groups. T cell motility was analyzed by tracking individual T cells using the spot and surface tools of Imaris. For time-lapse images obtained from the open skull window experiments, cells at a depth of >100 μm below the cover glass were analyzed to avoid potential confounding surface tissue artifacts. Cells were tracked by initial automated spot detection followed by autoregressive spot tracking and manual tracking. Quantitative analyses were done on all tracks with a duration > 10 min. Contextual analyses, which involves determining the behavior of cells in context of other cells or anatomical structures, were based on surface detection followed by distance transformation.

Image analysis: static analyses

Large area imaging by image stitching

For gross analysis of the brain, multiple images were acquired and stitched. Each individual image was generated from a z-stack by projecting in 2-dimensions using maximum intensity projection in Leica processing software. Image stitching (tile alignment) was done in Photoshop CS6. Line intensity profiles were generated from images using the Line tool on Slidebook version 5/6 or ImageJ.

Cells were counted using the spot function in Imaris. If direct counting of cells was not possible due to dense cellular clustering and insufficient image resolution in the image of the data set, then cell counts were obtained using a volumetric approach implemented in Imaris software[429,430]. Thus, volumes of either CD11c-EYFP or hCD2-DsRed T cell objects were delineated in 3-dimensions by thresholding. Cell numbers were calculated by dividing each volume by the average calculated volume of a given cell type, which was calibrated in the same data set based on averaging individually measured volumes of multiple well-isolated single cells (10-20 cells). Overall cell densities were calculated by dividing the number of cells by the z-stack volume. Sphericity is the extent to which the shape of a cell closely approaches that of a mathematically perfect sphere. It is calculated by using the surface tool in Imaris to represent a cell, and the software models the cell's shape and does calculations to determine the extent of sphericity, which ranges from 0 to 1.

Cell-cell spatial correlation

To analyze the degree of spatial correlation between cell types, each primary image was divided into nine equal sub-fields. In each sub-field, total areas of each cell

type were obtained by segmentation of images in respective channels. Resulting paired values (measured in pixels) were analyzed for correlation using GraphPad Prism Software.

Contextual image analyses

Proximity of T cells to DC or cancer cells.

For calculating cellular densities inside and outside tumors, and at tumor margins, each of these regions was determined using the surface tool and distance transformation, followed by splitting the DC and T cell volumes (or spots) in each measured tumor region volume. Distances of T cell to CD11c-YFP DC was generated after converting T cells to spot objects by using the spot tool and CD11c-YFP cells to surface object by using the surface tool. Imaris Distance Transformation function was then used to create certain threshold distances outside CD11c-YFP cell surface objects. Finally T cell distance to CD11c-YFP cells was generated using the Filter and distance threshold functions.

Analysis of myeloid cell subset numbers and densities within the tumor, at the margin, and within the extratumoral region or brain parenchyma.

To identify all highlighted myeloid cells, CX3CR1$^{+/GFP/}$CD11c-YFP/CCR2-RFP channels were all normalized and added together by using the Arithmetic processing function on Imaris to create a single “myeloid” channel. Each cell in the “myeloid” channel was then represented as a spot by using the spot tool. The Surface tool was then used to create tumor surface object, and the Distance Transformation tool/Filter and Distance threshold functions were used to generate distances from outside or

inside the edge of the tumor surface object and used to segregate spots (CX3CR1$^{+/GFP}$ /CD11c-YFP/CCR2-RFP) into different compartments (tumor outside, tumor margin, and tumor core) from the “myeloid” spot population.

Human Samples

Human GBM tissue and blood samples were obtained by Dr. A. Heimberger under approval from the Institutional Review Board of UTMDACC LAB03-0687. Informed consent was obtained from each participant. Patients’ tumors were graded pathologically as newly diagnosed glioblastoma (glioblastoma, n = 11) by a neuropathologist according to the World Health Organization (WHO) classification. Peripheral blood was drawn from the patients intra-operatively or healthy donors (n=11). Control CD14^{+} cells [a general marker of monocytes and monocyte-derived macrophages [431] (n = 4, age range of 26-35) from intractable epilepsy brain tissue was provided by Prof. Jack P. Antel (Montreal Neurological Institute). CD11b^{+} cells from postmortem brain tissue (n = 4, age 67 and 78, gray and white matter, post mortem delay 7-9 h) were obtained from The Netherlands Brain Bank (NBB), Netherlands Institute for Neuroscience, Amsterdam (open access: www.brainbank.nl). All Material has been collected from donors who provided a written informed consent for a brain autopsy and the use of the material and clinical information for research purposes obtained by the NBB. Human glioma or CNS tissue was digested with Liberase TM enzyme which contains highly purified collagenase I and II. This approach significantly improves cell isolation when compared with standard collagenase digestion.[432] After enzymatic digestion, the myelin was removed by centrifugation using

a Percoll gradient which has previously been shown to result in the highest viability of $CD11b^+$ cells.[433]

Statistics

GraphPad Prism version 6.00 (GraphPad Software), Microsoft Excel (Microsoft office package), and statistical software R v3.3.1 with packages nestedRanksTest v0.2 and nlme v3.1-128 were used for statistical analyses. Student t-test was used to analyze normal-distributed data while the non-parametric Mann-Whitney test (two-group comparison) was used to analyze non-normal distributed data. When appropriate, non-normal-distributed data were transformed by logarithm for the parametric analysis. For data including several mice in which T cells were followed longitudinally in the same mouse, the mixed effects regression model was applied to account for variability in T cell behavior and heterogeneity between mice. The mixed effects regression model[434] was employed to examine the change of T cell velocity after CD11c-DC depletion. Each observation of velocity was first normalized using logarithmic transformation. T cell arrest coefficients were arranged in [0,1] with significantly inflated 0s and 1s, with 0 and 1 representing T cell values pre- and post-CD11c-DC depletion, respectively.

For the mixed effects regression model:

Suppose y_{ij} is the velocity of jth T cell from the ith mouse. AP_{ij} takes value of either 0 or 1, where 1 indicates that the jth T cell from the ith mouse is after depletion, 0 before depletion. β_{i0} and β_{i1} are between-mouse random effects for intercept and slope. To examine the change of T cell velocity after depletion, we test whether H_0: α_1=0 against H_0: α_1!=0.

This can be mathematically represented as follows:

$log(y_{ij}) = \alpha_0 + \beta_{i0} + (\alpha_1 + \beta_{i1})*AP_{ij} + \varepsilon_{ij}$

$\beta_{i0} \sim N(0, \sigma_0^2)$

$\beta_{i1} \sim N(0, \sigma_1^2)$

$\varepsilon_{i1} \sim N(0, \sigma_\varepsilon^2)$

Since we failed to transform arrest coefficient values to fit a Gaussian distribution, we applied non-parametric nested Mann-Whitney-Wilcoxon Test[435] to make comparison before and after CD11c-DC depletion.

Horizontal bars represent the means, and vertical bars represent +/- Standard Deviation (SD). P values of less than 0.05 were considered statistically significant (*p<0.05, **p<0.01, ***p<0.001, and ****p<0.0001).

CHAPTER 3: LONGITUDINAL INTRAVITAL VISUALIZATION OF ENDOGENOUS INNATE AND ADAPTIVE IMMUNE SURVEILLANCE IN BRAIN TUMORS

Part I: Development of an intravital imaging system to investigate immune response to brain tumors.

Introduction

Multiple physiological mechanisms exist to protect the brain from immune-mediated neuronal damage[150]. However, these same protective mechanisms make it challenging to tease apart physiological responses of brain immune cells in intravital BT imaging as traumatic brain preparations are involved. From the exterior; the pericranium, skull, dura, arachnoid and pia maters, and vascular barriers prevent the accessibility of the brain parenchyma to environmental pathogens, blood-borne infectious agents, molecules, and antibodies. Such barriers include the blood-brain barrier and the blood-CSF barrier[68,145,146,148,149,152,155,436-439]. In addition to these exterior deterrents, in the event that the brain vasculature is breached, there is rapid migration of microglia to the site of vascular damage, and is a process that is not clearly understood in the context of brain metastases initiation[76,214]. Recent studies have also shown in intravital movies how the brain vasculature is immediately repaired by macrophages, which are required to “glue” breached endothelial tips together[440]. All of these support a model in which the homeostatic state of brain resident immune cell populations changes rapidly upon direct mechanical manipulation of the brain.

Multiphoton intravital imaging has provided unprecedented direct visualization of immune cell dynamics in various organs and tissues including the brain[214,380]. Despite the application of thinned and open skull imaging windows to answer fundamental questions[214,428,441], studying the initial immune response to tumors in a physiological state is nearly impossible due to the surgical procedures involved. For example, mechanical trauma to the dura or arachnoid initiates a strong response by the resident

immune cells including the microglia and potentially the peripheral innate and adaptive immune cells[214]. Although it was previously thought that immune cells isolated from BTs in mice and humans were mostly microglia, recent understanding of broadly shared surface markers between microglia and peripheral immune monocytes and macrophages blurs the lines of distinction[209]. Thus, making conclusions about the contribution of immune cell populations to brain tumor immune surveillance during the various stages of tumor progression could be confounded by traumatic events during cancer cell implantation. Progress in intravital imaging has been made by the use of sliced brain organotypic cultures[419]; however, this isolates the brain from the systemic circulation and traumatizes the tissue as well. Recent methods now enable intravital imaging of tumors in intact brain tissue in living mice, but the studies still involve significant traumatic preparations and have been mostly limited to immune-deficient nude and subacute combined immune-deficient (SCID) mice[441-449]. Intravital imaging in immune competent mice has been conducted, but in some cases mice have been treated with immune suppressants such as dexamethasone, which prevents immune cell proliferation and effector functions[441]. To overcome these technical limitations in brain tumor imaging, which conventionally involves 1) brain trauma due to full-thickness skull bone removal and 2) cancer cell deposition by direct intracranial injection, I have developed a novel experimental model of intravital imaging of *in vivo* brain tumor immune surveillance. This system consists of a thinned skull window that is combined with internal carotid cancer cell injection. Thinned skull window preparations have been used in the past to study multiple physiological processes involving neurons, microglia, and the cerebral vasculature in pathological conditions such as Alzheimers and stroke[417,450]. Likewise, internal carotid injections have been conducted in previous

studies to answer a variety of questions related to the process of brain metastasis and stem cell biology[100]. Both techniques, when done separately, do not involve mechanical trauma to the brain parenchyma. Therefore, a combined system involving both techniques was developed for visualization of immune cells in brain metastases.This method was selected because it does not inflict mechanical injury to the brain tissue, when performed with appropriate expertise. I present data that reveals this approach does not produce artefactual immunological activation and specifically, cancer cells engraft and grow from within the vasculature into the brain tissue beginning from single cancer cells closely recapitulating the clinical scenario. As a read-out of brain tissue injury, morphological response of microglia has been visualized in CX3CR1$^{+/GFP}$ mice as microglia are known to respond rapidly to regions of brain parenchyma or vasculature injury[211,214]. In addition, I have compared the behavior of microglia in response to cancer cells between models in which tumor is initiated by delivery via the internal carotid artery relative to cerebral injection. The experiments conducted here were focused on early tumor time points ending at day 7, which represents a phase in which acute mechanical trauma is potentially most detectable.

Results

3.1a. *Intravital imaging experimental setup*

To verify that skull thinning does not inflict mechanical trauma to the brain, CX3CR1$^{+/GFP}$/hCD2-DsRed mice were used. In this mouse strain, GFP reporter gene has been knocked into the CX3CR1 locus encoding CX3CR1 protein expression and DsRed is expressed under the CD2 promoter; CX3CR1 is expressed by all microglia, and T cells can be visualized by the expression of Ds-Red. Importantly, the CX3CR1$^{+/GFP}$ reporter mouse strain faithfully reports very rapid reaction of microglia to injury within very brief time periods[214]. The CD2-DsRed mice have been used to show the influx of T cells into the brain parenchyma during stroke[450].

To first visualize microglia in the steady state brain, mice with thinned skull windows that were not injected with cancer cells were head-restrained with a custom-designed mouse skull frame and stabilized on a heated custom-made motorized imaging stage. Imaging was performed transcranially via the glass window 5 to 10 minutes after thinning of mouse skull, by using multiphoton microscopy settings as described in the methods section. Mouse body temperature and anesthesia was maintained throughout imaging, as described in the methods. A schema demonstrating this process is shown in **Figure 11a**.

Second harmonic generation (SHG) was applied during multiphoton imaging to differentiate the thinned bone and underlying meninges from the underlying brain cortex. This is possible because biological structures such as collagen, which constitute skull and meninges, exhibit inversion asymmetry and a structural arrangement that show a second order non-linear optical property[451-453]. This property can be harnessed during photonic molecular polarization to generate fluorescent signals from such

endogenous tissues without prior dye labeling and is known as SHG. Within the brain cortex, microglia were observed to be discretely distributed in both two-dimensional orientation and three-dimensional optical sections, with multiple dendrites extending from each cell soma (**Figure 12a & movie 1**). The soma and dendrites of some of the microglia appeared to be in direct contact with the cerebral vasculature. Time-lapse imaging revealed motile microglia dendrites around the relatively sessile soma, scanning the brain especially around vessels and presumably other adjacent brain structures such as neurons and astrocytes, as previously described[214] (**Figure 12b and movie 1**). This observation was consistent with previous studies that have investigated the dynamics of microglia in healthy *in vivo* brain tissue[214,215]. Importantly, T cells were observed to travel within the lumina of microglia-associated blood vessels, but not extraluminally. This observation is similar to those made in sham controls in a previous study of T cell influx into the brains of mice with stroke[450]. Overall, these findings indicate that the proposed model does not cause changes in microglia dynamics and perturb the blood-brain barrier in mice.

Figure 11

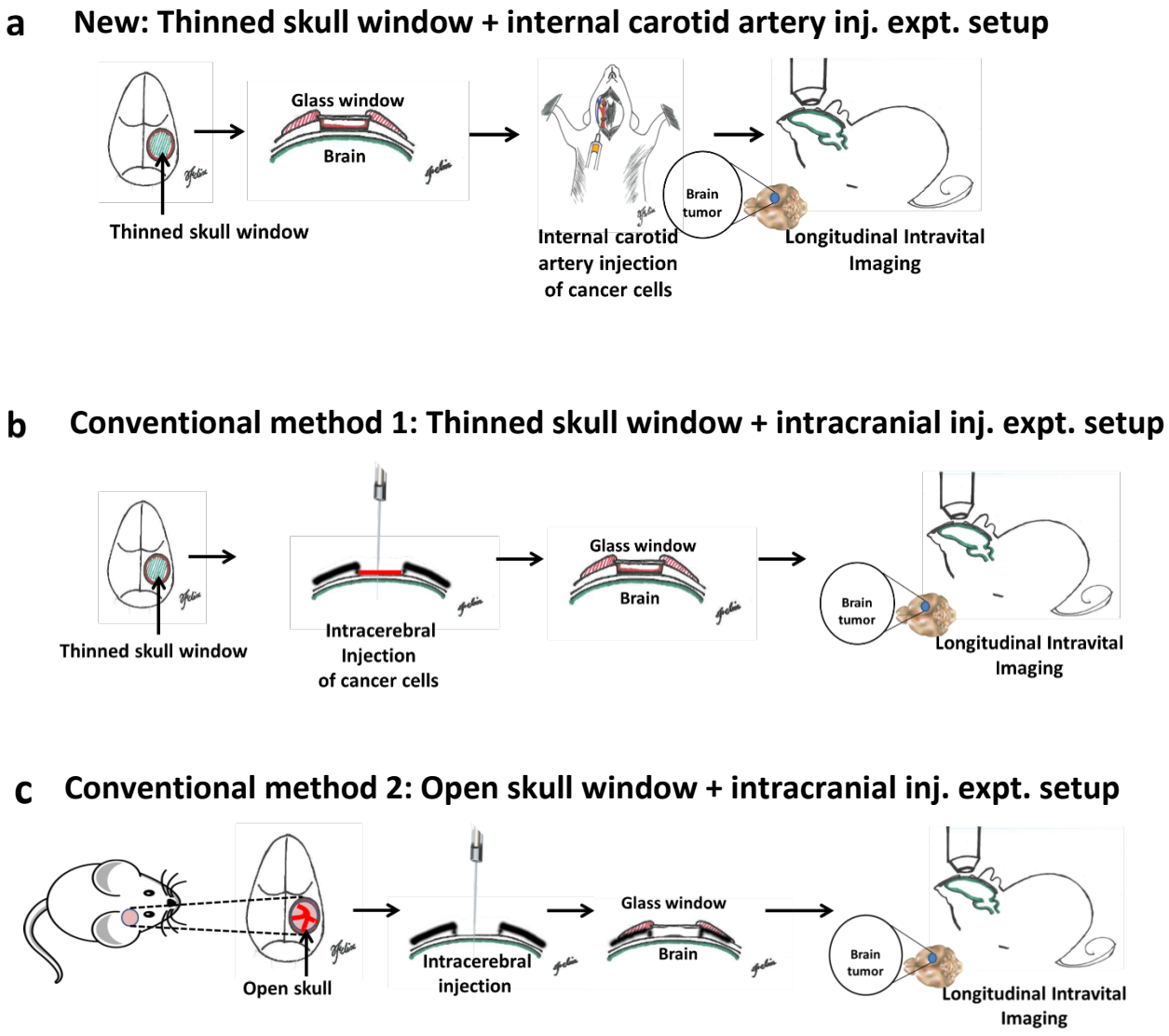

Figure 11. Schematic diagram of skull window experimental systems for intravital imaging of brain metastases.

a. A schematic of a new system combining thinned skull window and ICA injection. The model consists of thinning a 5-6mm diameter of a mouse skull leaving an eggshell osteotomy, followed by bonding of a cover glass to the edges of intact calvaria. Cancer

cells are then injected to the brain via the ICA, and non-survival or longitudinal survival intravital imaging is performed.

b. A schematic of a conventional system for intravital imaging system of brain tumor through a thinned mouse skull. A 5-6mm diameter of mouse skull is thinned as in (**a**), but cancer cells are implanted directly into the brain through the thinned skull at a depth of ~200-250μm by using an automated glass pipette, then the thinned skull window is secured with cover glass as in (**a**). Non-survival or longitudinal survival intravital imaging is performed.

c. A schematic depicting open skull window imaging of brain tumor. Craniotomy is performed to completely excise a 5-6mm diameter piece of mouse skull unlike in (b) where an eggshell osteotomy is left. In similarity to (**b**), cancer cells are injected directly into the brain at a depth of ~200-250μm below the dura mater by using an automated glass pipette. Artificial CSF or PBS is applied to the exposed brain, and a round glass coverslip is used to protect the brain tissue from dehydration and reinforced with Vetbond glue and dental cement on the edges. Intravital imaging can be done through the window to obtain time-lapse images longitudinally, and tumor size can be followed by acquiring tumor mosaics.

Figure 12

a.

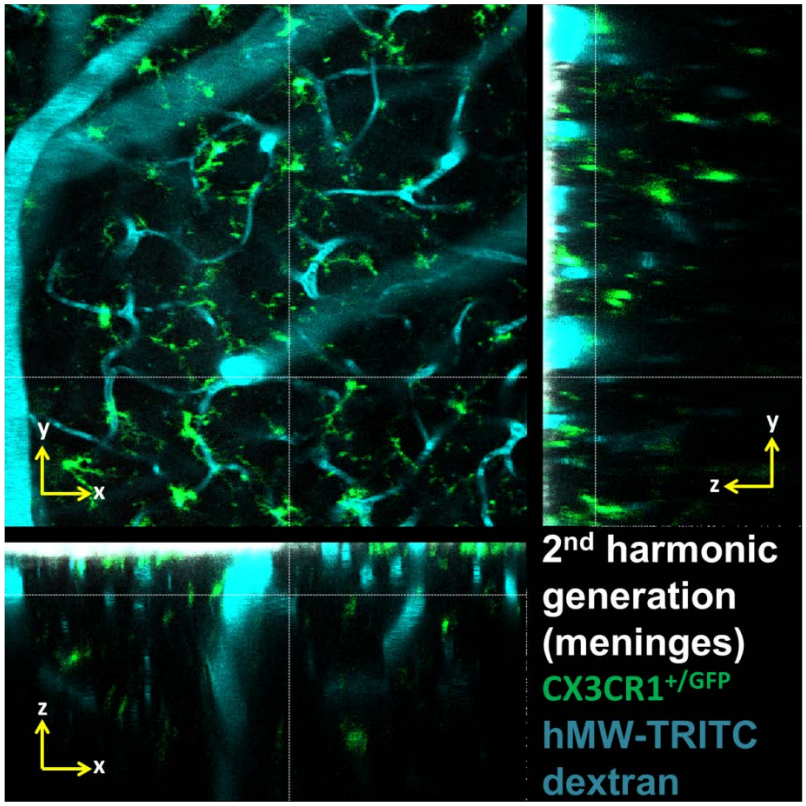
y
x
y
z
z
x
2nd harmonic generation (meninges)
CX3CR1+/GFP
hMW-TRITC dextran

b.

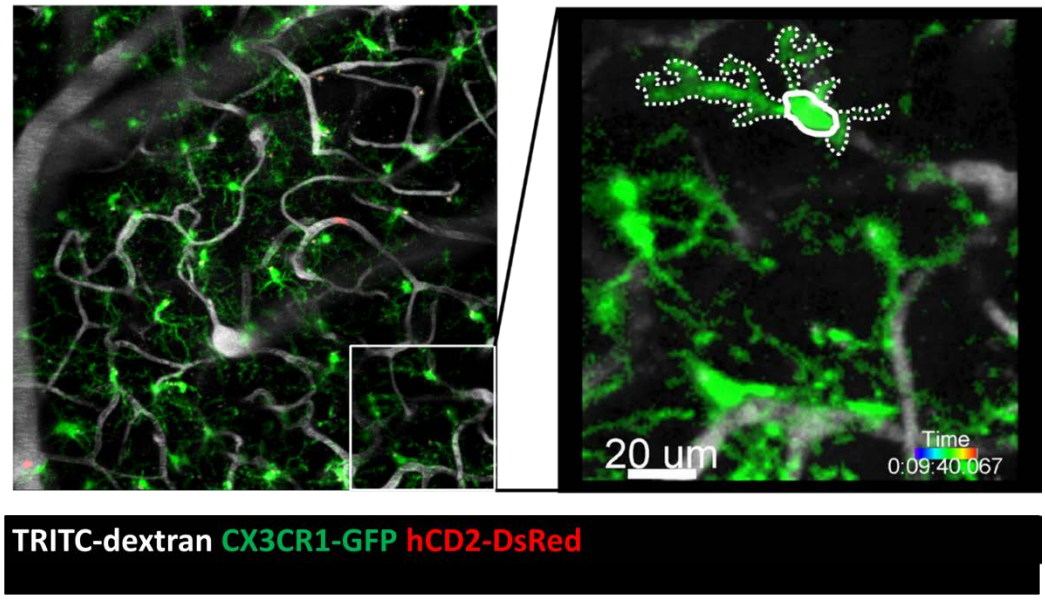
20 um
Time
0:09:40.067
TRITC-dextran CX3CR1-GFP hCD2-DsRed

Figure 12. Intravital imaging of healthy mouse brain.

a. Representative image from z-stack imaging of healthy mouse brain showing meninges (white) in the xz/yz axes, distribution of microglia ($CX3CR1^{+/GFP}$; green) within the brain cortex, and brain vasculature (cyan) in a three-dimensional xyz space. High molecular weight TRITC dextran dye was injected intravenously via the tail vein to visualize the vasculature. Imaging depth is up to 200µm (M**ovie 1**).

b. Representative still image from intravital time-lapse imaging of healthy mouse brain showing motility of microglia ($CX3CR1^{+/GFP}$; green) and T cells (hCD2-DsRed), and brain vasculature (hMW-TRITC-Dextran; White). Inset represents zoomed-in region showing close-up structure (white lines; thick line represent microglia soma, dotted lines represents the dendrites) and motility of microglia dendrites (**Movie 1**)

3.2a. Internal carotid artery injection is a more physiologically relevant method than intracranial injection for studying the immune response to brain tumors from a single cancer cell level

Direct implantation of cancer cells in mouse brain confounds the understanding of microglia dynamics in response to brain tumor initiation. To test the extent of microglia reactivity to BTs beginning at a single cell level and without local mechanical trauma, the new model was used in syngeneic CX3CR1$^{+/GFP}$ mice on the C57BL6 background (**Figure 11a**). In these reporter mice, microglia can be visualized in a healthy brain based on morphological characteristics (**Figure 12a**) while CX3CR1$^{+/GFP}$ monocytes from extracranial tissues are absent in the healthy brain. CX3CR1$^{+/GFP}$ monocytes are present in the brain only after trauma, in which case their morphology is ameboidal (**Figure 13a & movie 2**).

In the new model, within two days after mice wereinfused with cancer cells derived from methylcholanthrene (MCA)-induced fibrosarcomas by internal carotid artery injection, single cancer cells were found to be lodgedwithin cerebral microvasculature and the microglia mostly retained their typical ramified morphology as in **Figure 12a & b**. Seven days after ICA-inj., I could still visualize features of resting microglia including relatively immobile microglia soma as well as arrays of highly dynamic dendritic extensions. In contrast, in the conventional model (**Figure 11b**), mice receiving cancer cells directly into the brain showed CX3CR1$^{+/GFP}$ cell accumulation around the site of the injection and lost the typical microglia morphology, and the BBB appeared to have been breached as indicated by dye leakage from vessels in the brain parenchyma (**Figure 13a & movie 2**). At day 7 after cancer cell injection by intracranial (ICr) injection in the conventional model, I could not identify any distinct morphological

features of CX3CR1$^{+/GFP}$ cells resembling that of resting microglia, and analysis of CX3CR1$^{+/GFP}$ cell sphericity became technically challenging as the cells appeared to have clustered into “bee hive” formations. Quantitatively, the density of CX3CR1$^{+/GFP}$ cells in the imaging field of view increased after direct ICr-inj. while there was no observable change after indirect ICA-inj. of cancer cells to mice brain in comparison with healthy brain (**Figure 13c**). In addition, CX3CR1$^{+/GFP}$ cells in ICr-injected mice increased in sphericity as opposed to cells in ICA-injected mice and in steady-state, indicative of the potential activation status of microglia and/or infiltrating monocytes/macrophages following ICr injection. (**Figure 13d**). Importantly, it is impossible to distinguish activated microglia from infiltrating monocytes/macrophages in an inflamed brain as they both appear amoeboid in shape. Together, these results suggest that ICA injection of cancer cells coupled with transcranial intravital imaging via thinned skull window provides a better physiological platform than direct ICr injection for studying the initial events of immune response to BTs.

3.3a. CX3CR1$^{+/GFP}$ *cells become motile after ICr (conventional model) but not ICA-induced (new model) cancer cell injection*.

To determine the motility pattern of CX3CR1$^{+/GFP}$ cells in both systems, I tracked individual CX3CR1$^{+/GFP}$ cells two days after cancer cell injection (**Figure 14a**). In mice that were injected with cancer cells via ICr-inj., multiple elongated time color-coded tracks of varying lengths were found to be present around the site of cancer cell injection suggesting CX3CR1$^{+/GFP}$ cell motility. In contrast, after ICA-induced cancer cell injection or in the healthy brain, only dots of single colors were observed indicating that no CX3CR1$^{+/GFP}$ cell displacement had occurred (**Figure 14a**). Further, CX3CR1$^{+/GFP}$

cells in the conventional model had significantly increased average velocity in comparison with the relatively immotile cells in the new model or steady-state microglia (**Figure 14b**). We were unable, however, to quantify the motility of distinct CX3CR1$^{+/GFP}$ cells seven days after ICr-inj. due to the extensive infiltration, cluster formation of the CX3CR1$^{+/GFP}$ cells around the injection site, and extremely blurred morphological features of individual cells (**Figure 14b**). Again, this indicates that the new model is a better system than the conventional model at least in terms of maintenance of CX3CR1$^{+/GFP}$ cell motility behavior as in the healthy steady state brain.

Figure 13

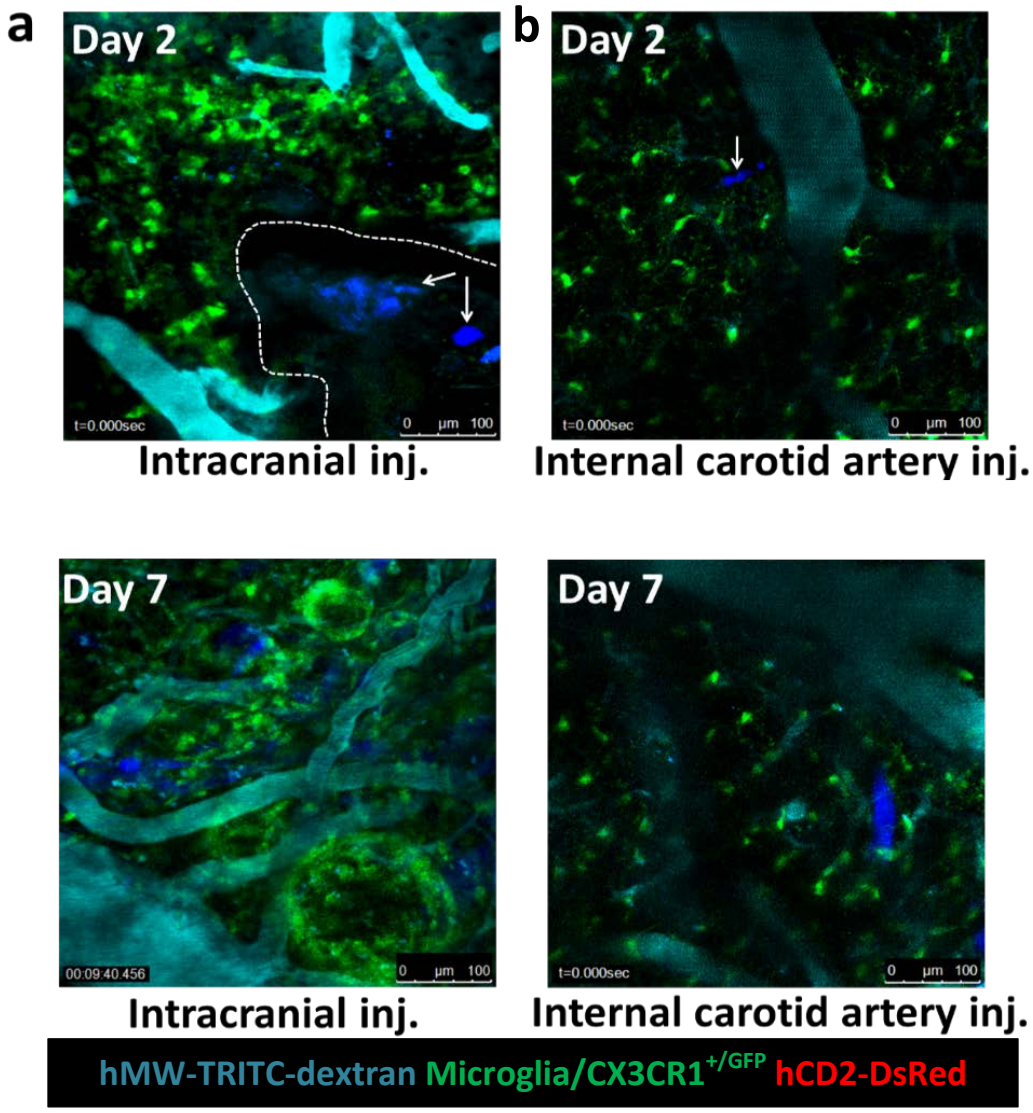
a
Day 2
t=0.000sec
0 µm 100
Intracranial inj.
b
Day 2
t=0.000sec
0 µm 100
Internal carotid artery inj.
Day 7
00:09:40.456
0 µm 100
Intracranial inj.
Day 7
t=0.000sec
0 µm 100
Internal carotid artery inj.
hMW-TRITC-dextran Microglia/CX3CR1+/GFP hCD2-DsRed
C
CX3CR1+ cell density
Healthy brain
ICA D2
ICr D2
d
Frequency
Sphericity
Healthy brain
ICr day 2
ICA day 2

Figure 13. Intravital imaging of brain tumor within the New Vs Conventional murine model systems.

a. Representative still image from intravital time-lapse imaging of MCA brain tumor-bearing mouse in the conventional model showing MCA cancer cells/tumor (blue), microglia/monocytes ($CX3CR1^{+/GFP}$; green), and brain vasculature (hMW-TRITC-dextran; cyan), 2 and 7 days after cancer cell injection by intracranial injection via a thinned skull window. The day 7 panel shows abnormally tortuous vasculature, and "bee hives" of $CX3CR1^{+/GFP}$ cells. Scale bar represents 100μm.

b. Representative still image from intravital time-lapse imaging of MCA brain tumor-bearing mouse in the new model showing MCA cancer cell/tumor (blue), microglia ($CX3CR1^{+/GFP}$), and brain vasculature (hMW-TRITC-dextran; cyan), 2 and 7 days after cancer cell injection by the ICA injection method. The top panel shows MCA cancer cell trapped in brain vasculature, and microglia (based on morphology), 2 days after ICA cancer cell injection The right panel shows MCA cancer cell(s), brain vasculature, and microglia (based on morphology), 7 days after ICA cancer cell injection. Scale bar represents 100μm.

c. Density of $CX3CR1^{+/GFP}$ cells in healthy brain and in MCA brain tumor-bearing mice 2 days after ICr- or ICA-induced MCA tumor (n = 3 from 2 separate experiments; each dot represents the density of all cells in a field of view in a mouse brain; data analysis was done by unpaired t test; $*P < 0.05$).

d. Sphericity of $CX3CR1^{+/GFP}$ cells in healthy brain and in MCA brain tumor-bearing mice 2 days after ICr- or ICA-induced tumor (Representative of 3 animals from 2 separate experiments).

Figure 14

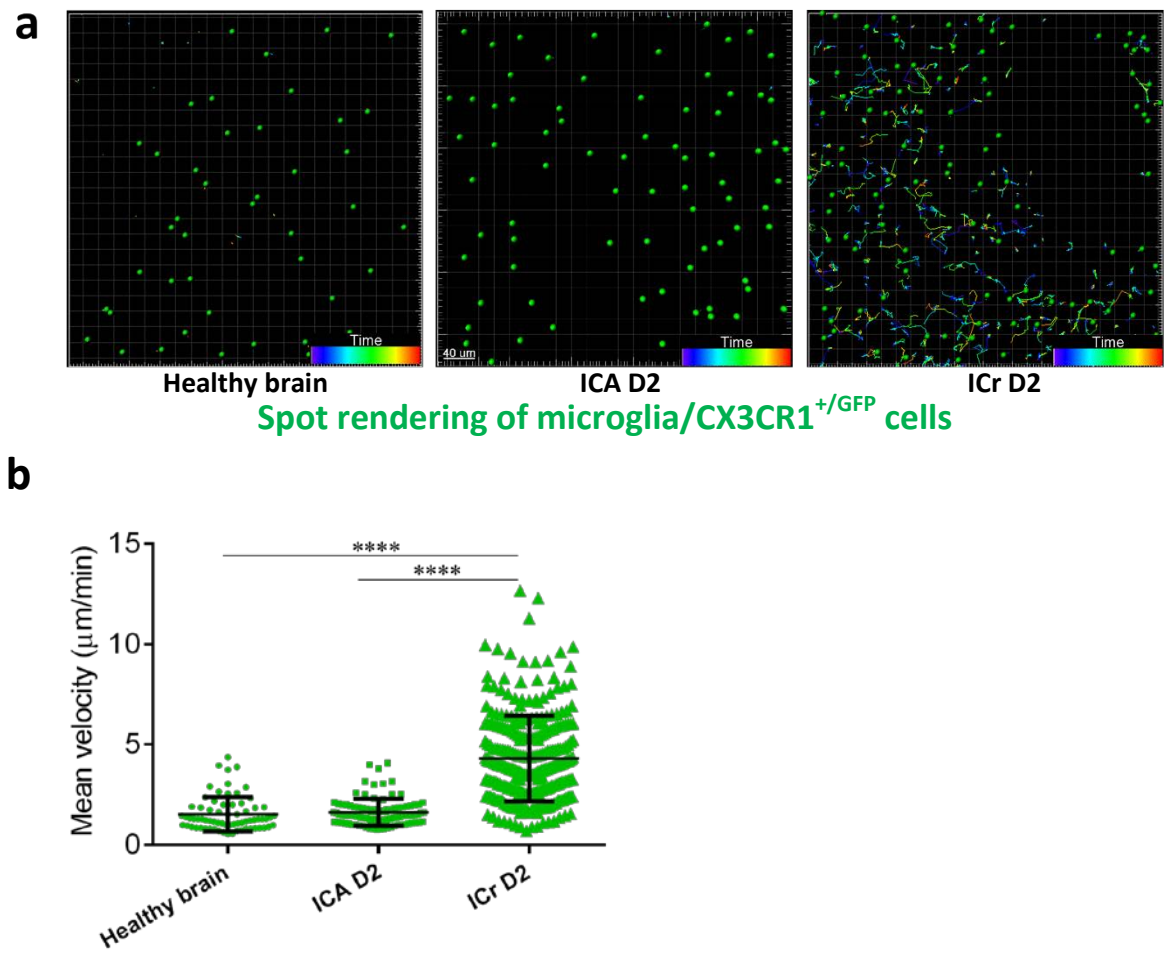

Figure 14. Window-located CX3CR1$^{+/GFP}$ cells become highly motile after IC injection, but not after ICA injection.

a. Representative still images from Imaris cell tracking of CX3CR1$^{+/GFP}$ cells in mice brain in intravital time-lapse movies. The left and middle panels show green spots, which represent the positions of microglia over the duration of 9 min and 45 min, respectively. The right panel shows the positions of CX3CR1$^{+/GFP}$ cells (green spots) and their migratory tracks (time-scale color-coded lines) over 40min. Scale bar represents 40µm.

b. Mean velocity of CX3CR1$^{+/GFP}$ cells in the imaging field of view within the skull window region in healthy brain and MCA tumor-bearing mouse brain after ICA- and ICr-induction of BT (n = 2 from 2 separate experiments; the average velocity of individual CX3CR1$^{+/GFP}$ cells acquired over 20min to >1 hr of time-lapse movies were accumulated for comparison by using the non-linear mixed effects regression model; ****$P < 0.0001$).

Discussion

In this study, I successfully developed an experimental setup to study the immune response to BTs in near-physiological brain tissue in living mice and showed that ICA injection combined with thinned skull window imaging is better than the ICr injection approach with regards to non-specific immune cell motility. While the combination of open skull windows and ICr injection is conceptually superior to the thinned skull window technique because it enables direct penetration of photons into the brain tissue and ultimately enhances better imaging and visualization of cells located in deep remote brain regions, it is a more traumatic alternative. In general, a unique advantage of the conventional thinned skull approach is that it aids relatively easy manipulation and cancer cell implantation[454]. In addition, it enables better predictability of tumor growth location, which potentially increases the extent of experimental reproducibility in terms of imaging different animals at similar time points, in longitudinal experiments. However, it carries an attendant risk of causing brain parenchymal damage before cancer cells engraft in the tissue and is associated with artifacts of early immune cell activation and response, with the disruption of the BBB. The study by Zhang L. *et al*. supports the conclusion above, in that following ICr injection, mouse brain develops gliosis due to injection injury as revealed by increased GFAP staining at the injection site[454]. By combining thinned skull window and ICA-inj., I have solved these problems; however, I cannot exclude effects that the procedure may have on aspects of microglia physiology that were not investigated such as molecular signaling pathways. In addition, because the cancer cells that are lodged in the brain after ICA injection are better at reproducing brain metastasis from extracranial tumors but may not truly recapitulate the early phase of tumor development in primary BTs, a

better physiological system for studying primary BTs would be one in which thinned skull windows are combined with spontaneously developing BT in GEMM models in which resident immune cells such as microglia can be visualized. Nevertheless, experiments conducted in part II of this chapter reveal the power of the ICA-inj./thinned skull imaging method in understanding the distribution of both resident and infiltrating myeloid cells in late stage BTs when ICA-induced tumors have engrafted extensively into the brain parenchyma.

The novel system established here preserves intact brain vascular structures and perfusion. In contrast to the direct injection approach which traumatizes blood vessels and causes leakage of injected dyes into the brain tissue, vessels appeared normal in the system developed here suggesting an intact BBB[442]. However, we did not explore potential molecular changes such as signaling pathways in the cells composing the BBB[145]. Previous studies have shown that microglia respond rapidly to secure even very tiny breaches in the vasculature[214]. Since I did not observe such protective or crowding behavior of microglia around the vasculature at early time points, I suspect that cancer cells engraft into brain tissue by a mechanism that may not damage the vasculature and maybe undetectable by microglia.

Microglia can potentially transform from a dendritic morphology to an amoeboid form, one that is strikingly similar to blood-derived monocyte and macrophages[455]. This makes it difficult to interpret studies using the conventional approach, as the traumatic nature of cancer cell deposition causes an increase in the sphericity of the CX3CR1$^{+/GFP}$ cells around the site of injection. In addition, the cells accumulate in clusters, making it difficult to assess the morphology of adjacent cells that may retain a dendritic morphology within the clusters. Increased motility of CX3CR1$^{+/GFP}$ cells

obscures the early physiologic response and behavior of microglia to cancer cells[214]. Therefore, this novel approach may provide better clarity in studying immune cell response to cancer cells in the brain at the single cell level.

Since BTs in humans are thought to begin from single mutated cells or disseminated malignant cancer cells from secondary tumors, this approach now opens an avenue to study the different aspects of immune response to tumor initiation including the contribution of innate cells such as neutrophils, patrolling monocytes, dendritic cells, classical monocytes, and NK cells, and the subsequent onset of adaptive T cell immune response. Although microglia are brain resident and are quick to respond to pathologies such as brain parenchyma injury, there are other innate immune cells from the periphery such as neutrophils that are capable of initiating rapid response to a variety of disease conditions including trauma and even cancer cells[261]. However, the impact of the new system developed here on the early phase homeostasis of other innate cells such as neutrophils was not investigated as previous studies that utilized an approach similar to the conventional thinned skull method described here did not observe any recruitment of neutrophils to traumatized site in brain tissue after direct injection; however, changes in microglia were not investigated in those studies[456].

This new approach developed is not without limitations. With ICA-induced cancer cell injection, there is markedly reduced power of predicting the location of cancer cell entrapment and hence increased variability in timing longitudinal intravital imaging of tumor growth within the brain in different mice. This is especially pronounced given the small imaging window dimensions in mouse skull and the limits posed by anatomical skull suture lines in extending such windows. In addition, since

the intact skull can add to light scattering caused by brain tissue, the extent to which imaging of immune response in deep brain regions can be accomplished is reduced. Our approach may also be limited in use due to the requirements of specialized expertise with manipulating microvessels such as the common or internal carotid artery during cancer cell injection in mice and the longer duration it takes to complete the same procedure in several mice as opposed to conventional intracranial injection approaches. Nevertheless, both ICA and ICr injection systems may be combined to answer some questions by taking the strengths and limitations of each approach into consideration. In the future, additional ways of improving these model systems would include developing lasers or optical adaptors capable of deeper photon penetration through brain tissue and creation of GEMM BT reporter models.

Part II: Identification of a cellular mechanism for the regulation of T cell surveillance in brain tumors

Introduction

Immune surveillance is a critical aspect of tumor progression. Effective immune surveillance depends on a tightly regulated migration of immune cells between peripheral organs and secondary lymphoid tissues[68,457]. However, little is known about the dynamic behavior and interactions of immune cells in tissues invaded by cancer. In the brain, the dynamics and regulation of immune response in tumors has been masked for a long time by the idea of brain immune privilege, and has detracted from a comprehensive understanding of immune response in BTs and development of immunotherapy[68,69]. Further, our present understanding of anti-tumor immune response through *in vivo* intravital imaging experiments and analysis has been largely derived from studies utilizing model tumor antigens, such as ovalbumin, and exogenously transferred cognate antigen-specific clonal T cell populations. Despite the immense knowledge on immune cellular dynamics and interactions gained from model antigen experiments, tumors in humans have great diversity in antigens and the associated potential T cell response is most likely polyclonal. As such, the true biology in human patient tumor may not be recapitulated in such experiments.[372,375,402]. Moreover, in the brain, intravital visualization and analysis of anti-tumor T cell response is lacking[442].

Previous studies have attempted to understand brain tumor immune response by using brain slices[419], thereby isolating the brain from the systemic circulation and extra-cranial immune response; other attempts at BT *in vivo* imaging studies have been limited technically by experimental systems and the range of reporter mouse models

available for concrete immune response readout[444,446]. Here, I have applied an array of longitudinal intravital imaging systems and reporter mice to visualize endogenous innate and adaptive immune surveillance in brain tumors. Specifically, I employed thinned skull window in mice in combination with ICA injection to visualize the innate and adaptive immune cell response to metastatic tumor types such as MCA and LLC. In addition, I used the open skull approach to image immune cell response to ICr-inj. orthotopic GL261 because of the inefficiency of this cancer cell type to engraft into the brain tissue after ICA injection. Also, this approach aided imaging of GL261 cancer cells and associated immune cells in deeper brain regions beyond the extent achieved by the thinned skull/ICA injection approach. The CD11c-YFP mouse strain has been developed and established for use in dissecting the dynamics of myeloid cells especially DCs, which have high expression of CD11c. In this study, I used the CD11c-YFP mouse strain to visualize a population of innate myeloid cells that I will refer to as DCs based on their morphology; however, other myeloid cells such as macrophages can express the YFP fluorophore encoded by the CD11c promoter as elaborated on in chapter 1. In addition, I have used other myeloid cell reporter mouse strains including fractalkine and CCL2 chemokine receptors, CX3CR1 and CCR2, encoding GFP and RFP fluorophores, respectively, to better characterize the myeloid cell repertoire in BT. hCD2-DsRed mice were used to visualize T cells, which express DsRed that is encoded by the CD2 promoter. Finally, I have bred the mouse strains above to obtain double or triple reporter mouse strains to dissect the interactions between the innate and adaptive immune cells in BTs by intravital imaging.

Results

3.1b. Longitudinal intravital imaging reveals differential immune response patterns in different brain tumor types.

It is well established that for a natural immune response to be generated there must be an effective coordination between myeloid antigen presenting cells (APCs) and T cells in the lymph node[379,397,458,459]. At sites of inflammation, T cells are known to undergo a cyclical process of reactivation between contacting tumor and tumor-associated APCs[301]. Therefore, to directly visualize the endogenous immune surveillance in various brain tumor types in a longitudinal manner, I employed appropriate experimental intravital imaging systems (**Fig. 11**). These systems enabled me to capture longitudinal evolution of endogenous anti-tumor immune response (**Figure 15**). As shown in **Figure 16 & movie 3**, orthotopic GL261 glioma was visualized from about 10 minutes after cancer cell implantation up to a 28-day terminal time point. GL261 tumor progressed lethally, and although CD11c-YFP cells and T cells were robustly recruited temporally, the pace was slower than tumor growth. GL261 tumor-associated T cells steadily increased in migration velocity in the tumor microenvironment from 8μm/min up to a peak of 13μm/min) between day 7 and 13, but decreased to ~9um/min at day 28.

Lewis lung carcinoma (LLC) brain metastasis, which was generated by ICA, progressed lethally over a 19-day period (**Fig. 17 & movie 4**). In this model, CD11c-YFP cells and T cells were recruited robustly up to day 11, but sharply reduced afterwards. LLC-associated T cells showed relatively high average velocity at day 5 of ~8μm/min at day 5, and decreased to ~6μm/min at day 11 after cancer injection. The decrease in T cell velocity continued steadily until day 19 (~4μm/min).

Figure 15

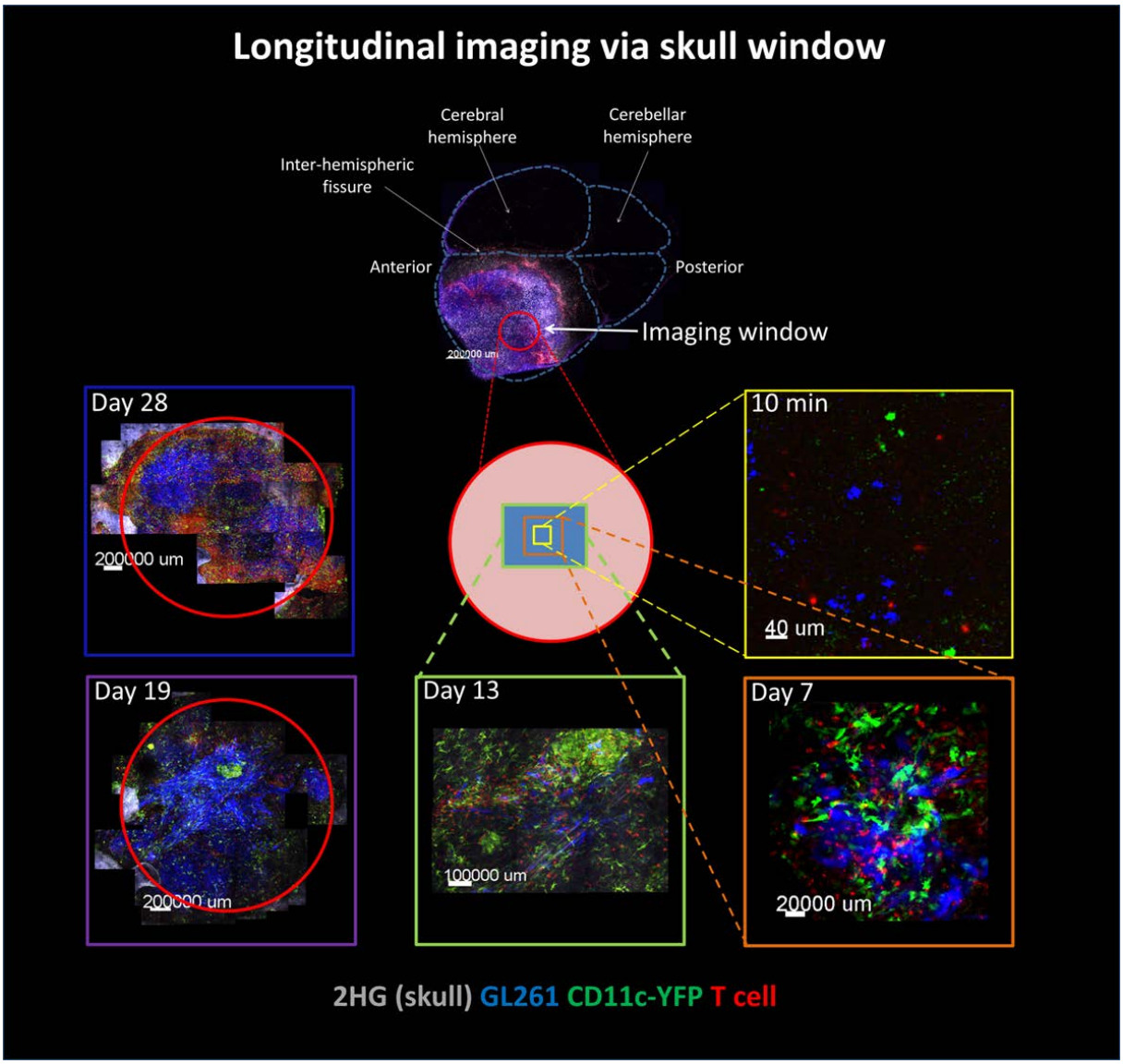

Figure 15: Schematic and confocal images representing a mouse brain with anatomical location of late stage brain tumor, and longitudinal appearance of tumor and immune cells via imaging window.

The continuous blue line schematic above the image panels represents the anatomical boundaries of a mouse brain, defining the brain into specific regions and is

superimposed on a representative confocal image of *ex vivo* whole brain with mosaic of GL261 tumor (blue), CD11c-YFP cells (white) and T cells (red). The red continuous circle indicates the region of the brain tissue directly underneath a virtual open skull window and protected by glass cover slip through which longitudinal intravital imaging was performed.

The panels below the schema are arranged in a clockwise fashion and show representative mosaics of tumor (blue), CD11c-YFP cells (green) and T cells (hCD2-DsRed) acquired longitudinally by 2-photon microscopy via imaging skull window. Some regions of mouse skull (white/gray) can be visualized by SHG at late stage time points when the brain tumor size is near or beyond the edges of the skull window.

Lastly, in contrast to GL261 and LLC, MCA fibro-sarcoma cancer cells engrafted and progressed until day 7 (**Fig. 18 & movie 5**). Interestingly, the recruitment of CD11c-YFP cells and T cells continued in the tumor region, surpassed tumor coverage in the imaging field of view, and only began declining after observable tumor regression between days 10 and 12. MCA-associated T cells did not show any significant change in average velocity throughout the imaging time points (~9μm/min). These data suggest that robust anti-tumor immune response is mounted in the brain contrary to the notion of brain immune privilege, that the recruitment of CD11c-YFP cells and T cells correlate in a time-dependent manner, and that the average velocity of T cells exhibited during migration vary in different brain tumor types spanning from relatively high migratory activity throughout the length of observation in MCA and GL261 tumors to very low activity in late stage LLC tumors.

Figure 16

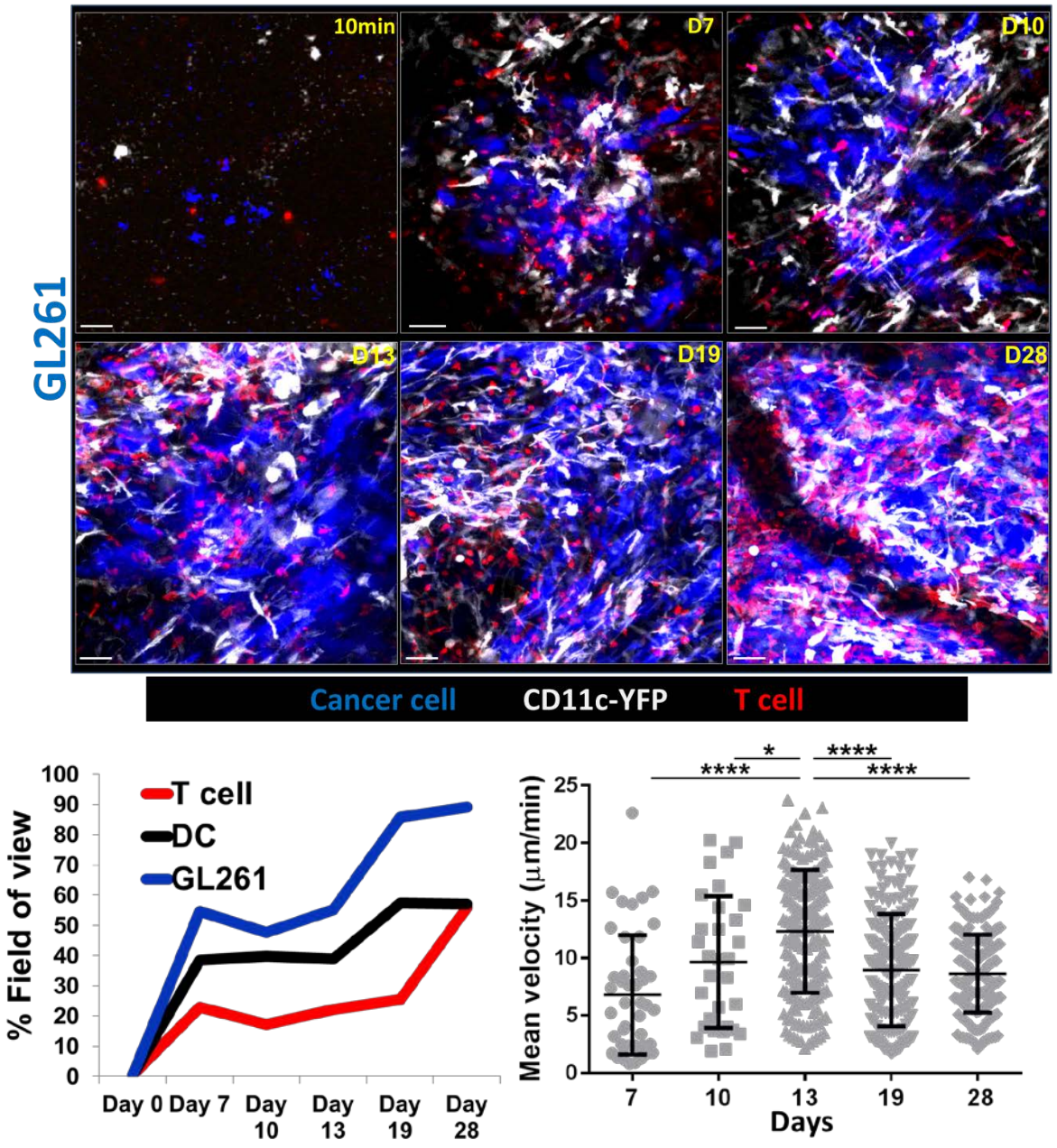

Figure 16. Longitudinal intravital imaging of immune response in GL261 brain tumor.

Representative still intravital images from time-lapse imaging of DCs (CD11c-YFP; white) and T cells (hCD2-DsRed) in GL261 brain tumor (blue) from 10 min to 28 days

after intracranial implantation. The graphs below the image panels show the temporal dynamics of GL261 tumor growth and infiltration of CD11c-YFP cells and T cells in the field of view and the mean velocity of T cells over the time period of imaging (n = 1 mouse; represents longitudinal imaging sessions conducted in 5-6 different experiments; *$P < 0.05$, ****$P < 0.0001$; mean velocity was analyzed by using the non-linear mixed effects regression model). Scale bar represents 50μm.

Figure 17

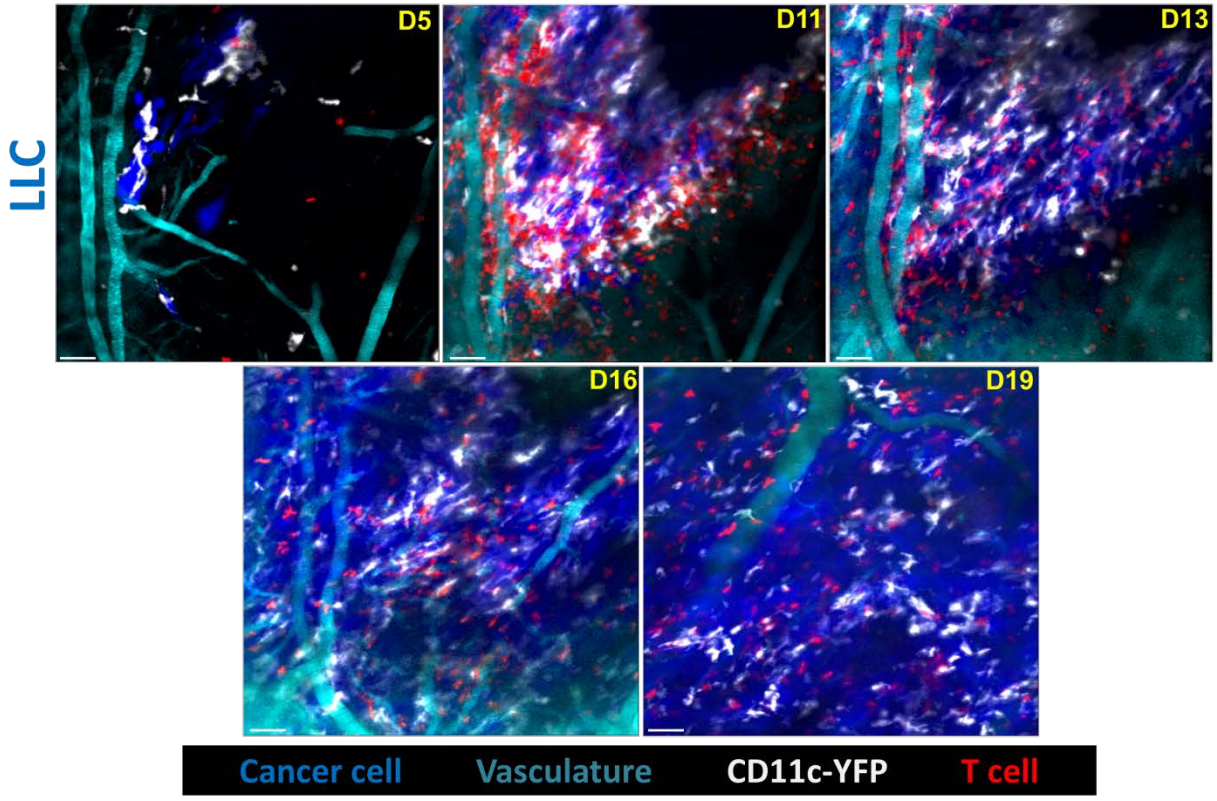

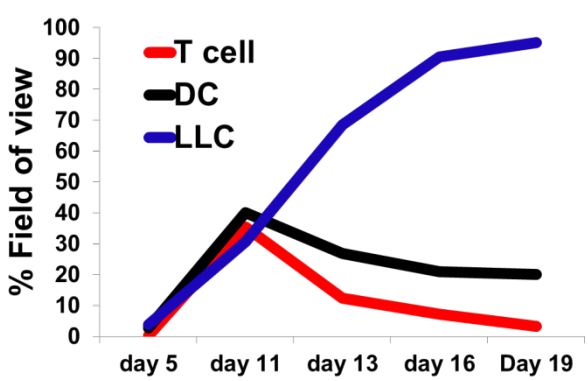

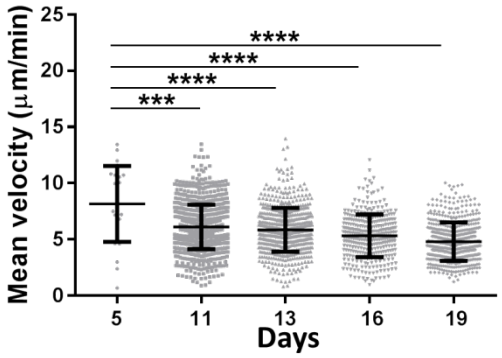

Figure 17. Longitudinal intravital imaging of immune response in LLC brain tumor.

Representative still intravital images from time-lapse imaging of DC (CD11c-YFP; white) and T cells (hCD2-DsRed) in LLC brain tumor (blue) from 5 days to 19 days after LLC cancer cell injection via the ICA using the thinned skull window approach. The

graphs below the image panels show the temporal dynamics of LLC tumor growth and infiltration of DC cells and T cells in the field of view and the mean velocity of T cells over the time period of imaging. (n = 1 mouse; represents longitudinal imaging sessions conducted in 3-4 different experiments ns = not significant; ***$P < 0.001$, ****$P < 0.0001$; mean velocity was analyzed by using the non-linear mixed effects regression model). Scale bar represents 50μm.

Figure 18

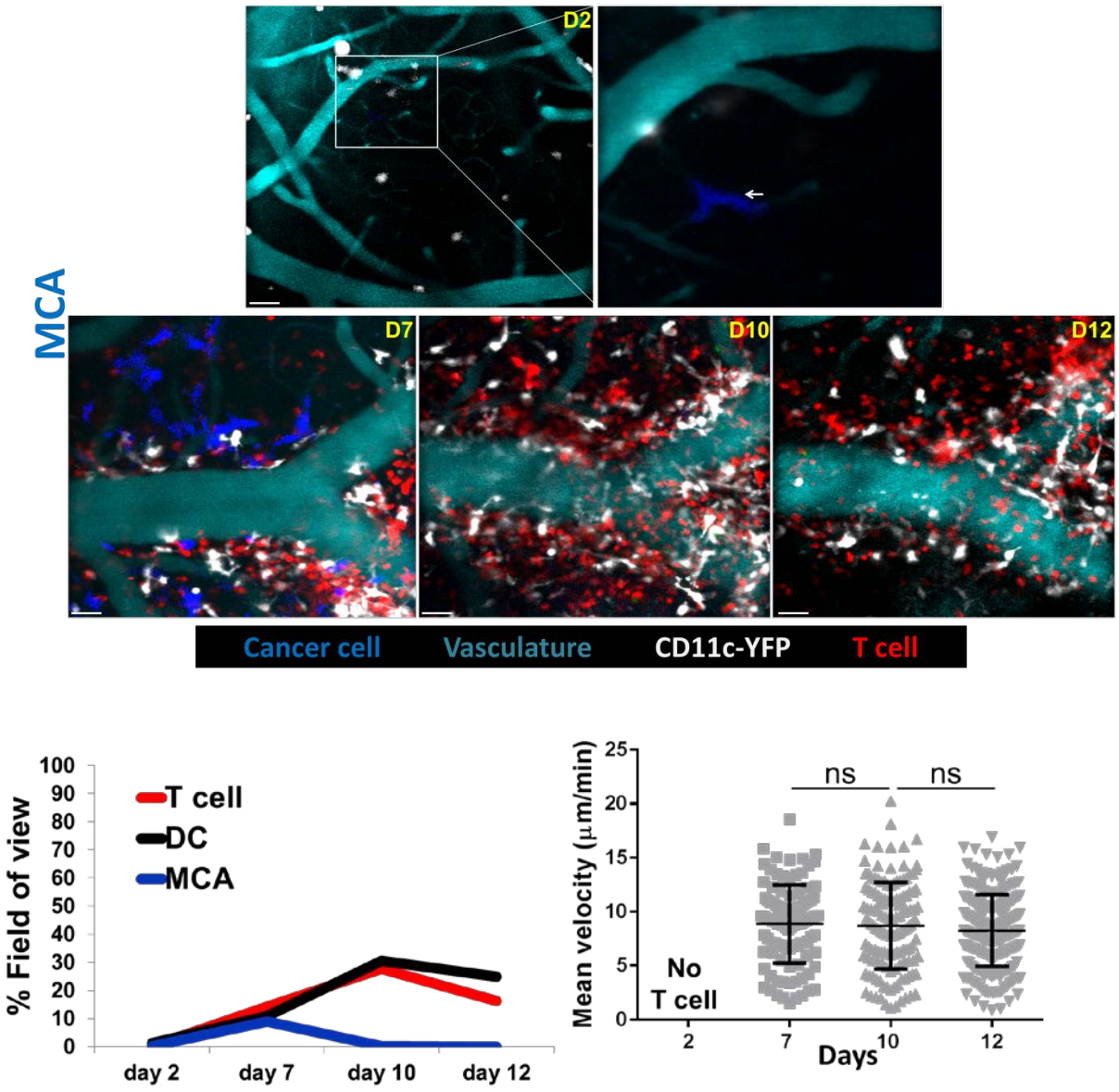

Figure 18. Longitudinal intravital imaging of immune response in MCA brain tumor.

Representative still intravital images from time-lapse imaging of CD11c-YFP (white) and T cells (hCD2-DsRed) in MCA brain tumor from 7 days to 12 days after LLC cancer cell injection via the ICA using the thinned skull window approach. MCA tumor regresses at day 10 and is not evident at day 12. The graphs below the image panels

show the temporal dynamics of MCA tumor growth and infiltration of CD11c-YFP cells and T cells in the field of view and the mean velocity of T cells over the time period of imaging. (n = 1 mouse; represents longitudinal imaging sessions conducted in 5 mice in 3 different experiments; ns = not significant; mean velocity was analyzed by using the non-linear mixed effects regression model). Scale bar represents 50μm.

3.2b. CD11c-YFP cells preferentially associate with tumor and T cells relative to microglia

I reasoned that since CD11c-YFP cells and T cells correlate temporally during recruitment and population of brain tumor types longitudinally, they may also correlate in space, in spatially organized niches within the brain tumor microenvironment. Remarkably, across different brain tumors including GL261, LLC, MCA, and B16-F10, I observed that tumors that were infiltrated by T cells were those that contained high densities of CD11c-YFP cells, which unlike the CD11c-negative microglia, are relatively rare in normal brain (**Fig. 19 and 20**). T cell densities strikingly correlated with CD11c-YFP densities spatially in tumor at both the microscopic (single brain regions acquired by high-magnification objective) and macroscopic scales (whole brain) (**Fig. 19c and Fig. 21**). In macroscopic tumors, both T cells and CD11c+ DCs were found in high densities around tumor margins (**Fig. 21**). However, very few CD11c-YFP and T cells was observed in B16-F10 brain tumor with only a weak correlation between both cell types (**Fig. 19a & b**) This was not surprising, as this tumor type is historically known to be poorly immunogenic.

It is conventionally believed that microglia are the predominant immune cell population in brain tumors and potentially regulate anti-tumor immune response[191,246,460,461]. Based on this, I evaluated the correlation of the area density of microglia to the area of the image field of view occupied by MCA brain metastatic tumors, and found only a weak correlation between the density of microglia, MCA tumor, or MCA tumor-infiltrating T cells. In contrast, the density of CD11c-YFP cells was strongly correlated with the area occupied by MCA tumor (**Fig. 19a & c**). This

suggested a critical role for CD11c-YFP cells in the regulation of T cell immune response in brain tumors.

Based on such striking spatial correlation between CD11c-YFP cells and T cells, I next assessed the interaction pattern between these two cell populations by using intravital two-photon microscopy. In the spontaneously regressive MCA tumor, T cells migrated preferentially closer to CD11c-YFP cells and adjacent blood vessels than with the tumor itself (**Fig. 22**). Similarly, in the progressive GL261 tumor, T cells also migrated in swarms around CD11c-YFP cells (**Fig. 23a & movie 6**). Analysis of T cell motility tracks revealed that the T cells centered around CD11c-YFP cells over a distance of 8-12μm, which is close to the range obtained in a previous study involving *in vivo* intravital imaging studies of lymph node DC/T cell interactions[462]. However, T cells maintained a high local migration speed around CD11c-YFP cells over time despite their proximity, and this contrasts to previous observations in the lymph node where T cells proximal to DCs showed reduced speed[295,379] (**Fig. 23b**). This would indicate presumably very transient contacts between the T cells and CD11c-YFP cells in GL261 brain tumor despite the clustered pattern of T cell swarms that could be easily presumed for prolonged interaction with CD11c-YFP cells. Further, in GL261, although T cells appeared confined, the confinement was relatively weak with a confinement radius of ~73um that became apparent only during long observations. In contrast to GL261, T cells in MCA brain tumor were more tightly confined around CD11c-YFP cells with a confinement radius of 33um (**Fig. 23c**). Together, CD11c-YFP cells and T cells correlate in brain tumor niches and T cells are organized and motile around CD11c-YFP cells.

Figure 19

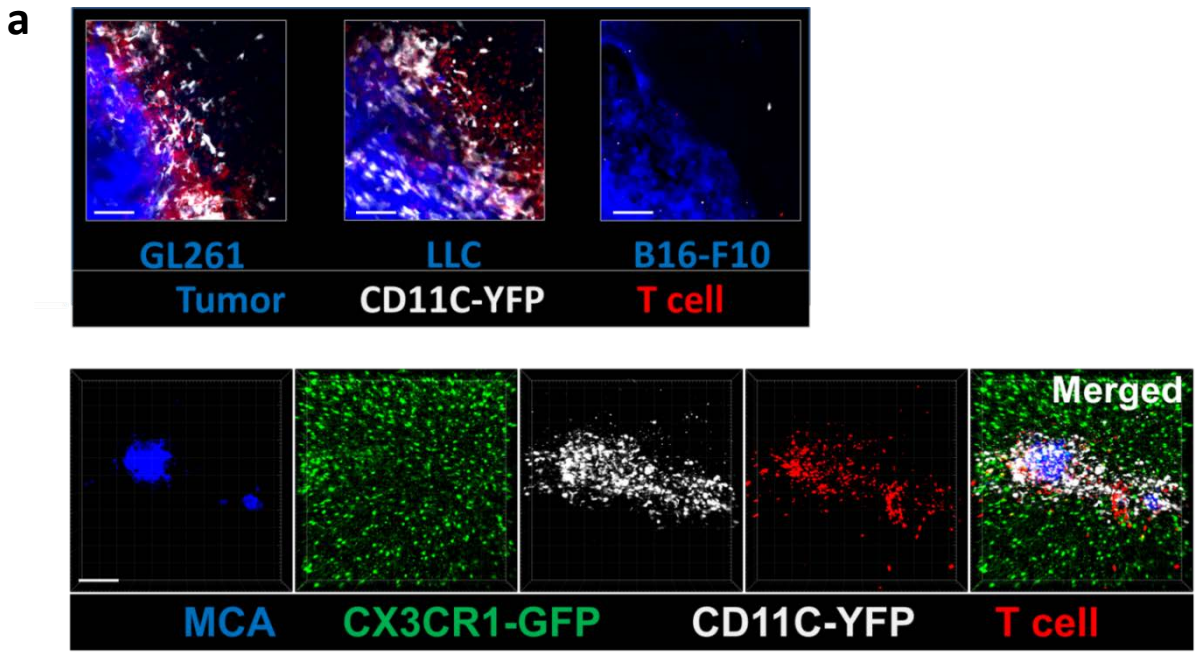
a
GL261
LLC
B16-F10
Tumor
CD11C-YFP
T cell
Merged
MCA
CX3CR1-GFP
CD11C-YFP
T cell
b
GL261
R2 = 0.72
T cells
CD11c+DC
LLC
R2 = 0.55
T Cells
CD11c+DC
B16-F10
R2 = 0.03
T cells
CD11c+DC
c
R2 = 0.26
Microglia
MCA
R2 = 0.55
CD11c+DC
MCA
MCA
R2 = 0.68
T Cells
CD11c+DC
MCA
R2 = 0.26
T Cells
Microglia

Figure 19: CD11c-YFP cells preferentially associated with tumor and T cells relative to microglia.

a. *Top*: Representative confocal images showing localization of endogenous CD11c-YFP cells (white) and T cells (hCD2-DsRed) in different types of brain tumor including GL261 glioma, LLC, and B16-F10 melanoma (blue) captured between days 13 and 19. Tumor types were generated by direct intracranial injection (GL261) and ICA injection (LLC and B16-F10). *Bottom*: Confocal images show localization of endogenous CX3CR1 cells (identified as mostly microglia based on distribution and morphology as described in chapter 3), CD11c-YFP cells, and T cells in MCA brain tumor induced by ICA injection. Scale bar represents 50 μm.

b. The first three graphs show the correlation between T cells and CD11c-YFP cells in various tumor types (n = 2-4 mice/tumor type; 9 areas of tumor-associated immune cells were analyzed from an average of 2 tumor nodules per mouse; each dot represents a single area analyzed).

c. Graphs show the correlation of CX3CR1-GFP microglia and CD11c-YFP cells to MCA tumor, and the correlation of T cells to CD11c-YFP cells and CX3CR1-GFP microglia cells (n = 4 mice; 9 areas of tumor-associated immune cells were analyzed from an average of 2 tumor nodules per mouse; each dot represents a single area analyzed).

Figure 20

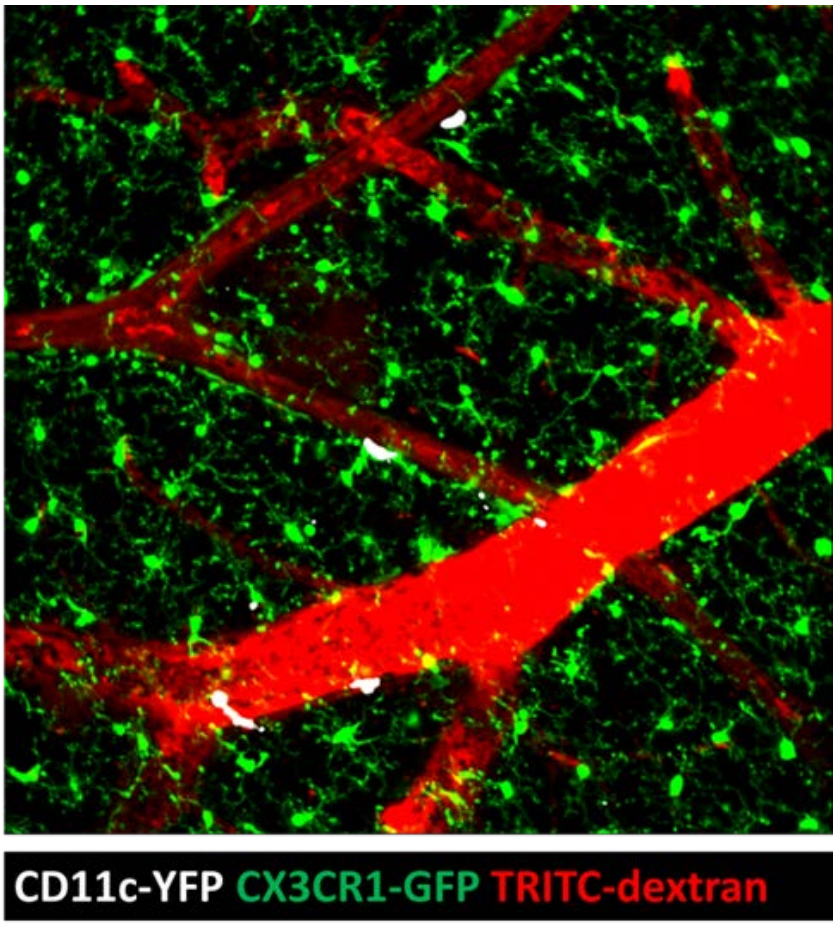

Figure 20. Confocal image of healthy mouse brain

Representative still image from a healthy mouse brain showing brain vasculature (TRITC-Dextran; red), microglia (green), and CD11c-YFP DCs (white).

Figure 21

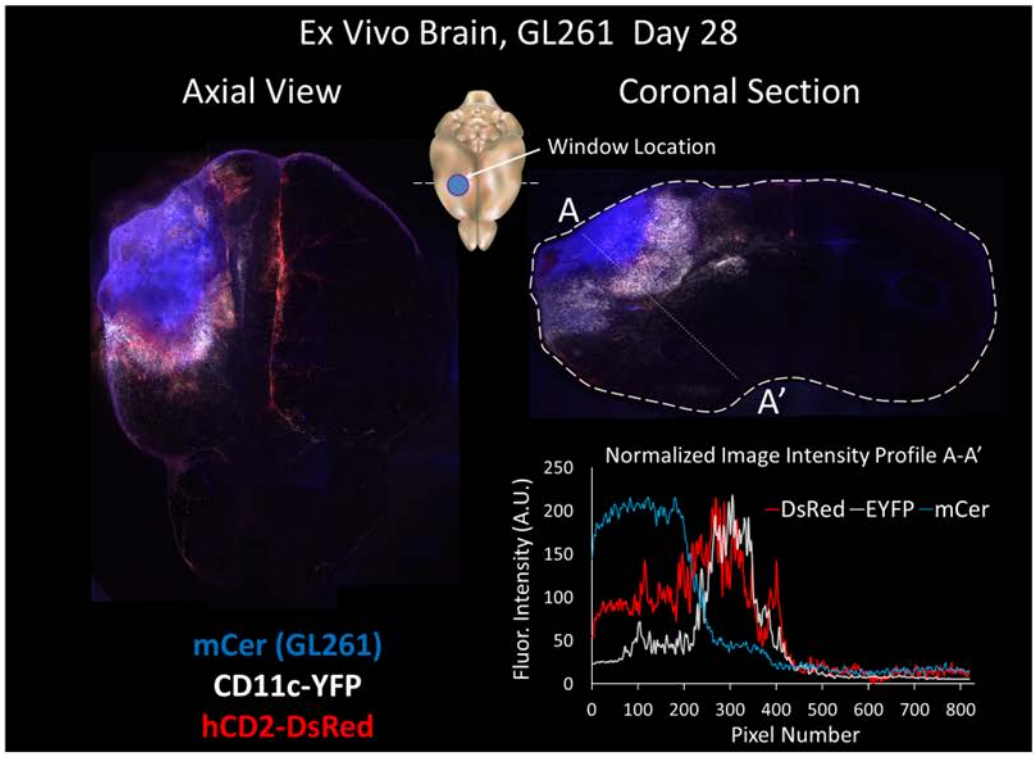

Figure 21. Distribution of CD11c+ DCs and T cells correlate in brain tumor at a macroscopic level.

Representative image of the axial (left) and coronal (right) planes GL261 brain tumor (blue) with associated CD11c-YFP DCs (white) and T cells (hCD2-DsRed), respectively. The cartoon in the middle depicts a mouse brain and the approximate location of the GL261 brain tumor. The dotted line demonstrates the margin of the brain and the straight line cuts through the midsection of the tumor. The corresponding line profile graph to the straight line shows the distribution of CD11c-YFP DCs and T cells in relation to GL261 brain tumor. (Represents experiments conducted in 5 different mice)

Figure 22

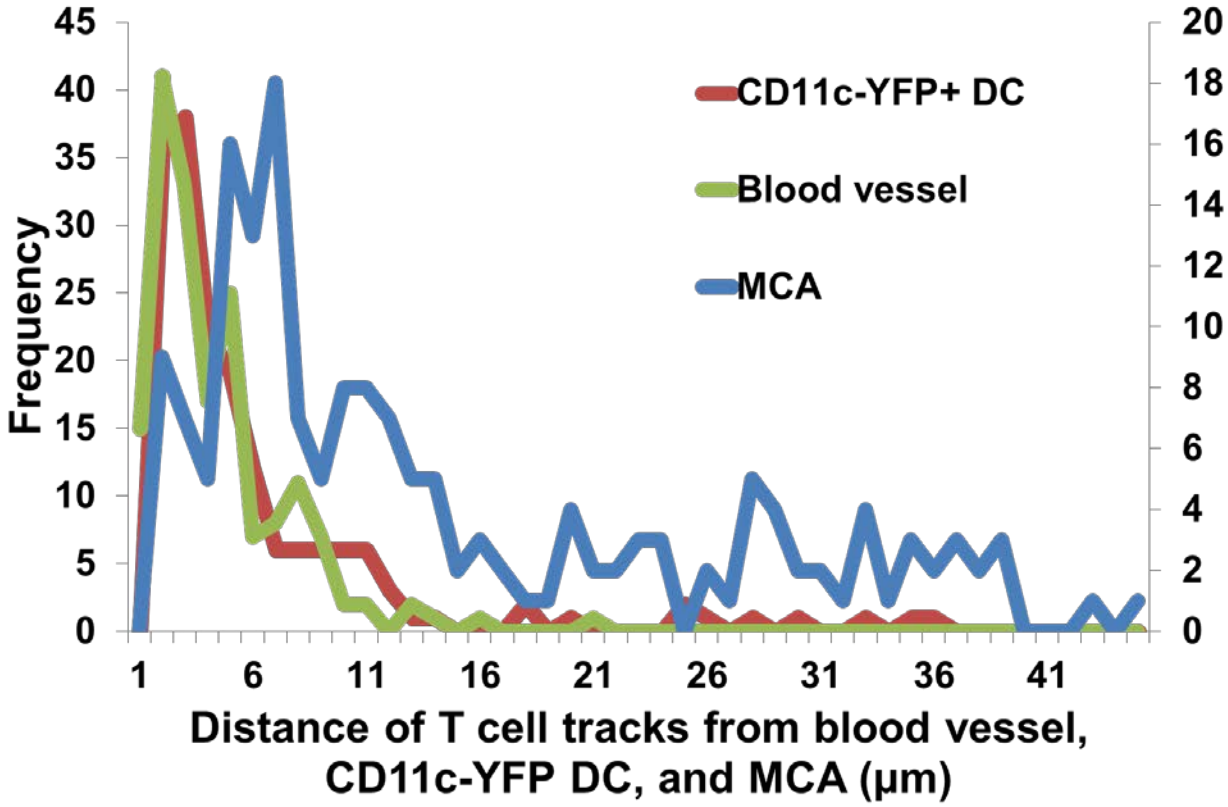

Figure 22: T cells preferentially associate with CD11c-YFP cells and the brain vasculature Graph shows an example of the frequency of T cells migrating at a given distance relative to vasculature, MCA tumor, and CD11c-YFP cells in intravital time-lapse imaging in a day 7 MCA tumor. Individual tumor-infiltrating T cells were tracked, and the frequency of the distance between the mean positions of T cell tracks to vasculature, MCA tumor, and CD11c-YFP cells were plotted in the same graph. The left axis represents frequency of CD11c-YFP+ DC and blood vessel, while the right axis represents frequency of MCA tumor (n =4).

Figure 23

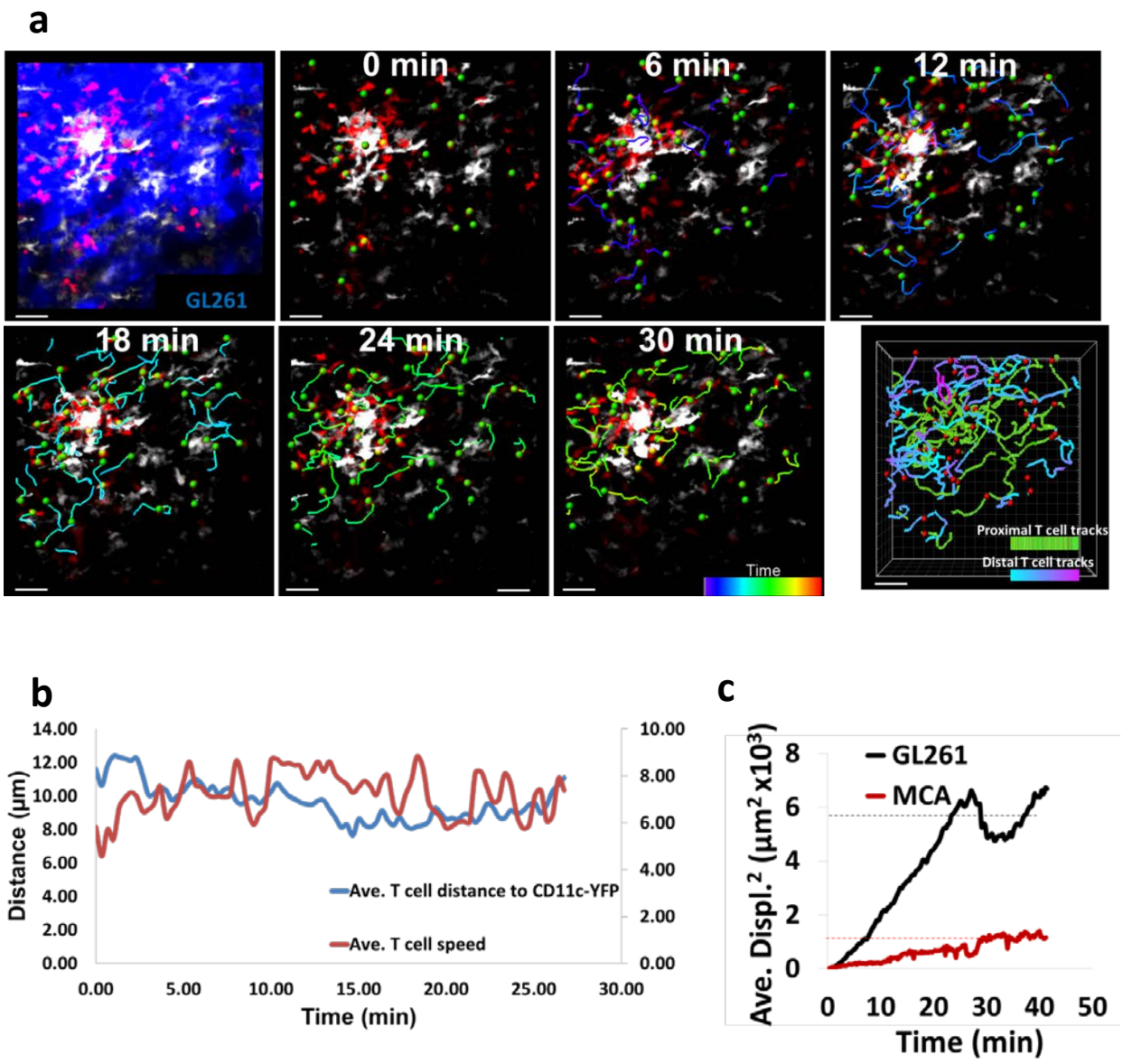

Figure 23: Brain tumor infiltrating T cells are organized in clusters around CD11c-YFP cells.

a. Representative still intravital images of CD11c-YFP and T cellular interactions from 0 – 30 min in a day 10 GL261 brain tumor (blue). The green spots are superimposed on T cells and represent the positions of T cells in the tumor. The color-coded lines

represent the tracks of T cells during the duration of acquisition of time-lapse images. In the bottom right image panel, the T cell track lines are segregated according to nearness to CD11c-YFP cells. The green lines represent tracks of proximal (defined as 0-7μm from the CD11c-YFP cell margin) T cells while the blue/violet lines indicate tracks of distal (defined as 9μm to infinity from CD11c-YFP cell margin) T cells. Scale bar represents 50μm.

b. Graph shows the average distance of all T cells to CD11c-YFP cells (blue line; left Y axis) and the average speed of T cells (red line; right Y axis) in relation to the length of T cell migration time acquired (Represents experiments conducted 5-6 different times).

c. Graphs show the squared average displacement of all T cells in GL261 and MCA tumor over the length of T cell migration time acquired (represents experiments conducted separately for ~5-6 different times).

*3.3b. In situ imaging and quantification of myeloid cells in a novel myeloid reporter mouse reveals distinct localization of myeloid cell subsets in brain tumor***.**

A better understanding of the myeloid immune cell composition of brain tumors is complicated by the presence of the brain resident microglia and infiltrating macrophages and monocytes.There are no reporter mouse models to properly delineate these two populations appropriately. Therefore, to characterize the myeloid cells in the brain tumor microenvironment, I generated a novel triple myeloid reporter mouse in which I could visualize different myeloid cells under the CX3CR1-GFP, CD11c-YFP, and CCR2-RFP promoters[210,212,463]. With this new model, five myeloid cell types including microglia, patrolling monocytes (PMs), classical monocytes (CMs), mature and immature dendritic cells (DCs) can be potentially identified according to different combinations of fluorophore expression (**Table 2**).

To gain insight into the composition and localization of brain tumor-associated myeloid cells, I then injected MCA cancer cells via the ICA and subsequently imaged engrafted brain tumors in fixed *ex vivo* thick brain tissue sections by using confocal microscopy. Imaging revealed distinct localizations of the different myeloid cells in the tumor microenvironment (**Fig.24a**).

Next, I developed a novel method of quantifying the myeloid cell populations directly from their actual localizations in the tumor and termed this method *in situ* tumor immune cytometry (iTIC). This method is detailed in chapter 2 and represents an advancement in cellular quantification in the field of imaging as it is the first method employing Imaris imaging software Spot detection tool and the recently developed Vantage analysis and plotting tool for cytometry purposes. The closest competing method to iTIC utilizes the colocalization tool on the same Imaris imaging software, but

has certain technical drawbacks[464]. For example, the colocalization values calculated and exported do not efficiently reproduce true fluorophore colocalization from an arithmetic and computational standpoint. In addition, the exported values have to be transported to Flowjo software for further analysis and graphing into dot plots. In contrast, the iTIC method utilizes the mean fluorophore intensity in a cell to calculate the extent of expression of different fluorophores expressed by the same cell of interest. Further, the dot plots are generated within the same software by using the Vantage tool. This allows for back and forth validation of the data as each spot can be visualized and interrogated by any user. Overall this approach is superior to conventional flow cytometry because cells are analyzed within retained tissue architecture and multi-layered tissue and does not involve cell processing as in flow cytometry tissue preparation, which could result in cell loss. Using the iTIC method, I was able to identify five distinct myeloid cell populations in the tumor microenvironment (**Table 2**) and account for their spatial localization in the tumor (**Fig. 24b**).

After tissue analysis with iTIC, I identified the same five populations of myeloid cells outside the tumor and in the tumor regions (**Fig. 24c**). Interestingly, CD11c-YFP DCs were highly enriched in the tumor and were composed mainly of CD11c+ CX3CR1- and CD11c+ CX3CR1+ cells. In contrast, CX3CR1+ CD11c- cells were predominating outside the tumor region (**Fig. 25a & b**). In an attempt to better understand the composition of the tumor-infiltrating myeloid cells, I stratified the cells according to localization in the tumor core or tumor margin. I then analyzed the populations residing within each of these compartments and found a preferential enrichment of CD11c-YFP DCs (CD11c+ CX3CR1+ and CD11c+ CX3CR1-) at the tumor margin, while the CCR2 monocytes (CCR2+ CD11c- and CCR2+ CD11c+) were

preferentially enriched within the tumor core (**Fig. 25c & d**). More specifically, both mature and immature DCs dominated the margin and core of the tumor relative to the region outside the tumor denoted as the Extratumoral region ((ET); **Fig. 24c**). Interestingly, CMs as defined in **Table 2,** were preferentially enriched in the tumor core relative to the tumor margin or the region outside the tumor. Patrolling monocytes were few and were mostly localized in the core of the tumor and outside the tumor region. In support of our earlier observation (**Fig. 19b**), microglia were mostly present outside the tumor region relative to the tumor core and margin; however, there was no change in the density of microglia in the tumor versus the ET region (**Fig.24c**), suggesting that the tumor is not enriched for microglia as opposed to DCs and CMs.

3.4b. CD11c-YFP cells are competent antigen presenting cells and T cell proliferation occurs in proximity to CD11c-YFP cells

To determine the competence of CD11c-YFP cells to perform professional APC functions, I stained tumor-bearing brain tissue sections with MHC-II and by confocal imaging; I found preferential expression of MHC-II in tumor-associated CD11c-YFP cells compared to the surrounding CX3CR1+ CD11c- microglia (**Fig. 26a**). In addition, there were several examples of T cells undergoing proliferation in the brain tumor microenvironment. In most cases these events occurred in proximity to CD11c-YFP cells (**Fig. 26b & movie 7**). These data support the idea that CD11c-YFP cells are a key professional APC population in the brain tumor microenvironment.

Figure 24

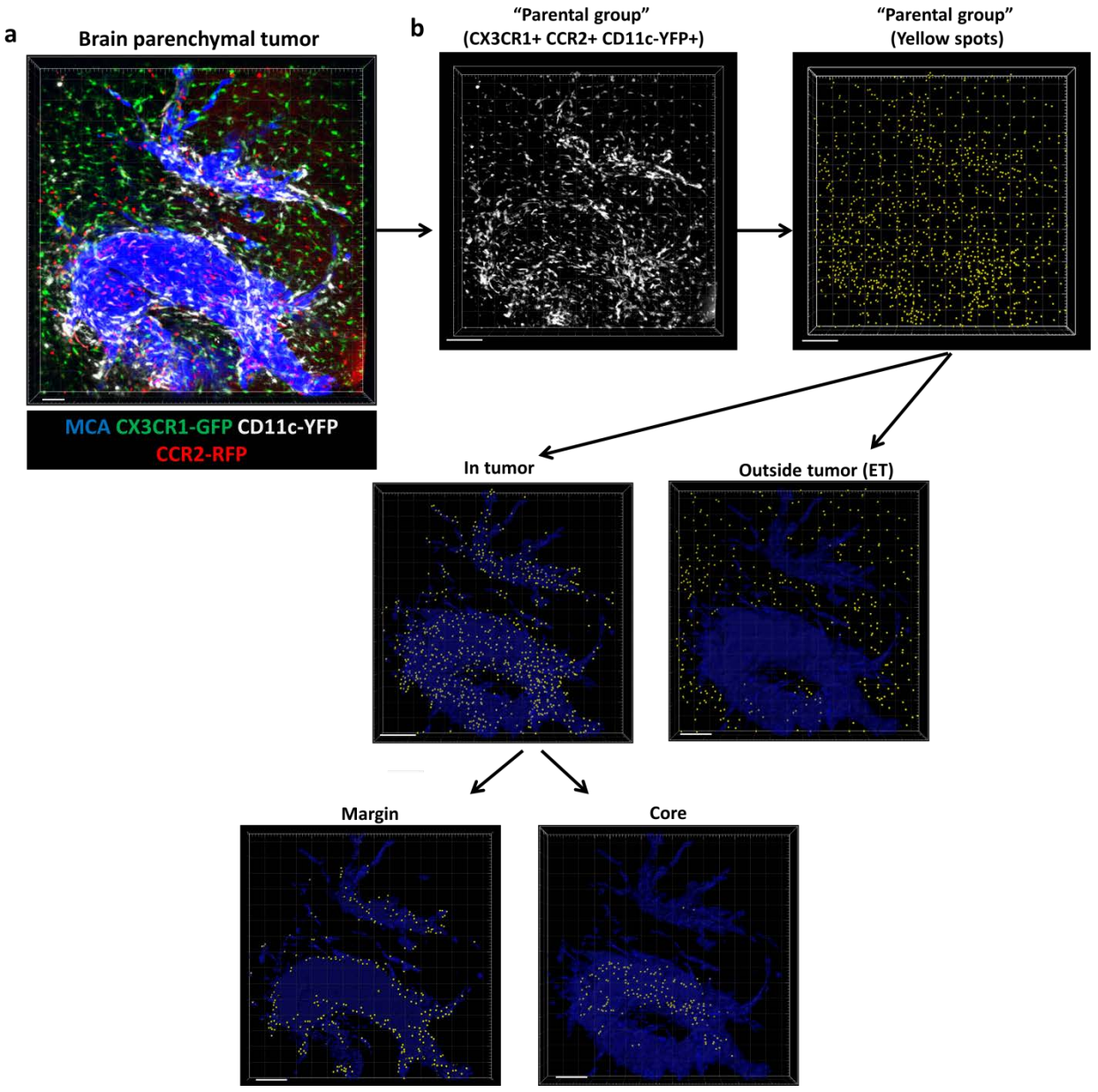
a
Brain parenchymal tumor
MCA CX3CR1-GFP CD11c-YFP
CCR2-RFP
b
"Parental group"
(CX3CR1+ CCR2+ CD11c-YFP+)
"Parental group"
(Yellow spots)
In tumor
Outside tumor (ET)
Margin
Core

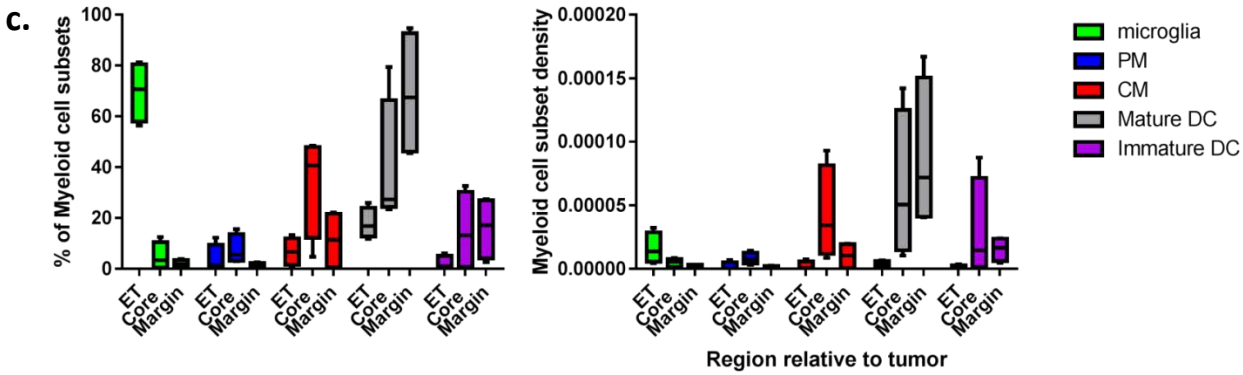
c.
% of Myeloid cell subsets
100
80
60
40
20
0
ET
Core
Margin
Myeloid cell subset density
0.00020
0.00015
0.00010
0.00005
0.00000
Region relative to tumor
microglia
PM
CM
Mature DC
Immature DC

Figure 24. In situ imaging and quantification of myeloid cells in a novel myeloid reporter mouse reveals distinct localization of myeloid cell subsets in brain tumor.

a. Representative confocal maximum intensity projection of a 3-dimensional image of MCA brain tumor (blue) induced by ICA injection, CX3CR1-GFP (green), CD11c-YFP (white), and CCR2-RFP (red) cells.

b. Arithmetic summation of individual myeloid subsets including CX3CR1-GFP, CD11c-YFP, and CCR2-RFP cells on Imaris imaging software into a group defined as “parental group” (white). The parental group cells is split into two compartments, represented by spots (yellow), relative to the tumor; “in tumor” and “outside tumor”. The cells (spots) in tumor are further split with respect to the edge or core of the tumor as tumor margin and tumor core, respectively. CM = classical monocytes, PM = patrolling monocytes, and DC = dendritic cells.

c. Graphs to the left and right show percentage and density, respectively, of myeloid cell subsets residing “outside tumor” or extratumoral (ET), “tumor core”, and “tumor margin.” (n = 4 mice from 2 different experiments).

Table 4.

	Markers	Identity
1.	CX3CR1 + CD11c- CCR2-	microglia
2.	CX3CR1 + CD11c- CCR2+	PM
3.	CX3CR1 - CD11c- CCR2+	CM
4.	CX3CR1 + CD11c+ CCR2-	Mature DC
	CX3CR1 - CD11c+ CCR2-	Mature DC
5.	CX3CR1 + CD11c+ CCR2+	Immature DC
	CX3CR1 - CD11c+ CCR2+	Immature DC

Table 2. Phenotypic myeloid cell markers used in this study. To define myeloid cell subsets based on these phenotypic markers, novel triple myeloid reporter mice were created to then define what populations may be operational within our brain tumor models.

Different combinations of fluorophore marker expression were used to identify distinct myeloid cell subtypes including microglia, patrolling monocytes (PM), classical monocytes (CMs), and mature and immature DCs.

Figure 25

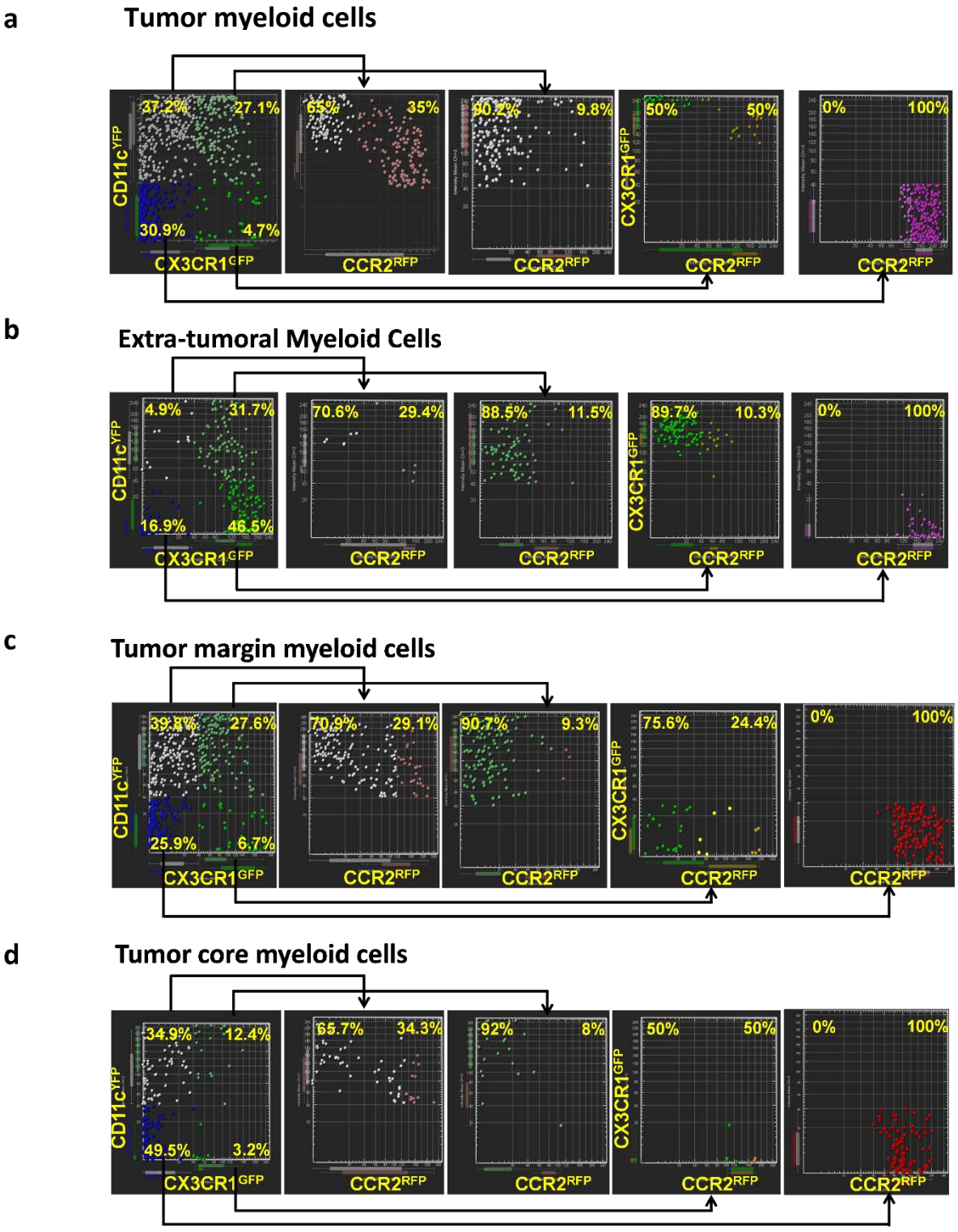
a
Tumor myeloid cells
37.2%
27.1%
30.9%
4.7%
65%
35%
90.2%
9.8%
50%
50%
0%
100%
b
Extra-tumoral Myeloid Cells
4.9%
31.7%
16.9%
46.5%
70.6%
29.4%
88.5%
11.5%
89.7%
10.3%
0%
100%
c
Tumor margin myeloid cells
39.8%
27.6%
25.9%
6.7%
70.9%
29.1%
90.7%
9.3%
75.6%
24.4%
0%
100%
d
Tumor core myeloid cells
34.9%
12.4%
49.5%
3.2%
65.7%
34.3%
92%
8%
50%
50%
0%
100%
CD11c YFP
CX3CR1 GFP
CCR2 RFP

Figure 25. Various myeloid-derived immune populations have differential distribution in brain tumors.

Vantage mode dot plots were generated using Imaris imaging software. Distinct myeloid cell subsets were identified based on genetically-tagged fluorophore expression in a triple myeloid reporter mouse strain based on relative in situ tissue location to brain tumor. Colors used in the dot plots are pseudo-colors and only indicate populations identified by the markers on the x and y axis. Representative dot plot to the left shows the percentage of the various tumor-infiltrating myeloid cells *in situ,* in (**a**) tumor, (**b**) extratumoral, (**c**) margin, and (**d**) core regions of MCA brain tumor. The 4 dot plots to the right show the percentage expression of CCR2-RFP by individual groups of myeloid cells in the leftmost panel.

Figure 26

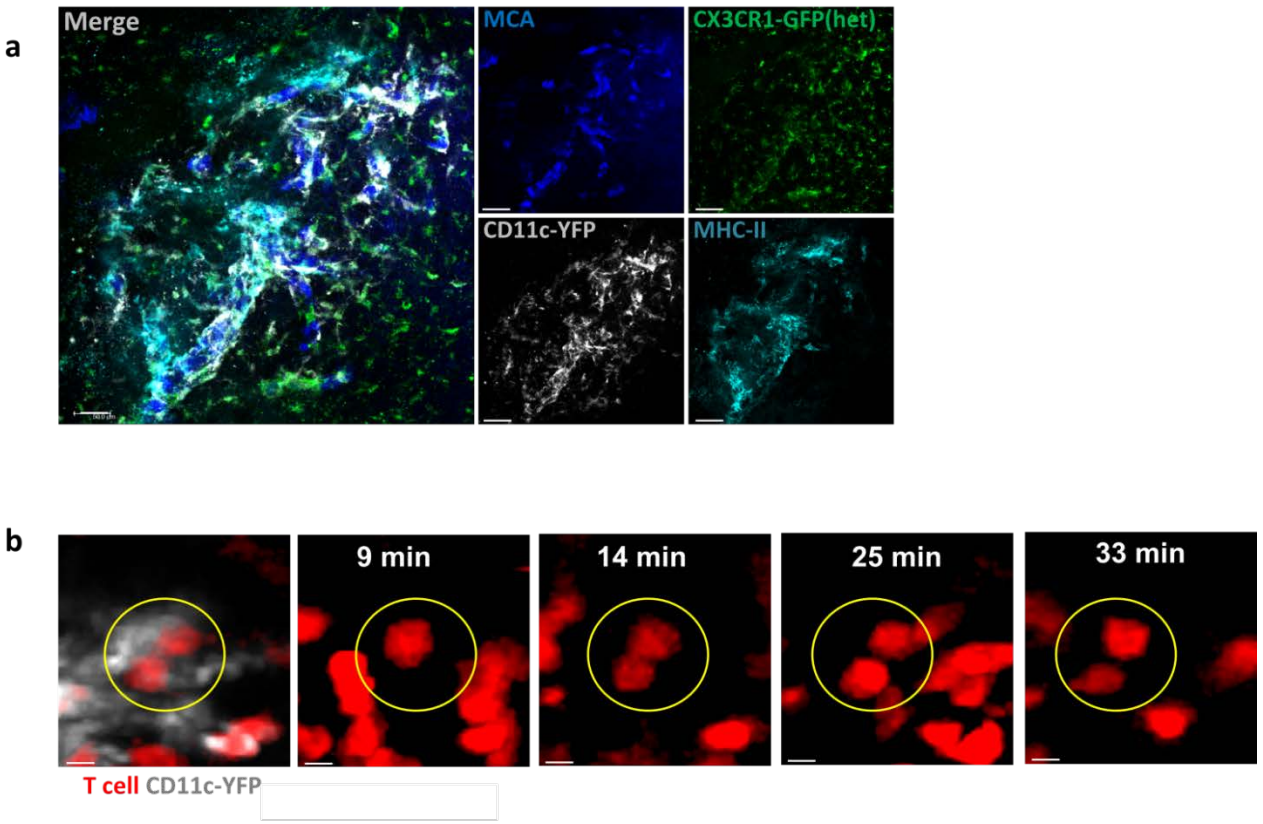

Figure 26. Confocal image and intravital microscopy reveal the presence of competent CD11c-YFP APC and T cell proliferation in brain tumor

a. Representative left merged confocal image of MCA brain tumor-associated CD11c-YFP cells and CX3CR1-GFP cells, reveals coexpression of CD11c-YFP and MHC-II. Single panels to the right show MCA tumor, CX3CR1-GFP, CD11c-YFP, and MHC-II expresson.

b. Representative still images showing intravital time-lapse imaging capture of a T cell (hCD2-DsRed) undergoing proliferation in association with CD11c-DCs. Yellow sphere

marks the boundary of a T cell undergoing cell division (Observed in >5 different experiments).

3.5b. Localization of BM-derived CD11c-YFP cells and T cells in brain tumor correlate after adoptive co-transfer

Non-microglial myeloid cells such as monocytes are robustly mobilized from the BM during tissue inflammation including brain cancer[248,419]. Therefore, I wanted to test the idea that BM-derived CD11c-YFP cells localize in brain tumors and serve as precursors for tumor-associated DCs. In addition, I wanted to determine whether tumor-infiltrating T cells localize in BM-derived CD11c-YFP cell niches in the brain tumor microenvironment. To accomplish this, I isolated whole bone marrow (BM) cells from wild type double reporter mice in which I could visualize CD11c-YFP cells and T cells, and transferred fresh BM isolates into CX3CR1-Knockout tumor-bearing mice. BM cells were transferred into animals in two different groups; the first group received BM cells one day before MCA cancer cells were injected to the brain via the ICA, and the second group received BM cells fourteen days after cancer cell injection. Upon imaging of late stage tumor-bearing tissue sections at day twenty after cancer cell injection, I found that BM-derived CD11c-YFP cells localized in brain tumor and surprisingly, T cells also localized in tumor-associated CD11c-YFP cell niches within brain tumor microenvironment in both groups of mice receiving BM cells at an early and late time point (**Fig. 27a**). The CD11c-YFP cells also bore striking morphological resemblance to endogenous brain tumor associated-DCs previously observed. Quantitatively, the CD11c-YFP cells were specifically localized in tumor in comparison with non-tumor regions (**Fig. 27b**). In addition, T cells correlated strongly with CD11c-YFP cells in brain tumors from mice that received CD11c-YFP cells and T cells a day before or 14 days after cancer injection (**Fig. 27c**). This indicates that BM-derived CD11c-YFP monocytes populate brain tumors and presumably differentiate into

competent antigen presenting DCs at different stages of brain tumor growth. In addition, it supported the idea that CD11c-DCs play a role in the localization of T cells in brain tumor.

3.6b. CD11c-YFP cells are important for the retention and motility of T cell subsets in brain tumor

I reasoned that since T cells localize and tend to form clusters around CD11c-YFP cells in the local tumor milieu that CD11c-YFP cells might be important in regulating T cell dynamics. To test this idea, I evaluated double reporter mice in which I could both visualize CD11c-YFP cells and T cells and also manipulate CD11c-YFP cells; this was possible because the double reporter mouse strain also expressed diphtheria toxin receptor (DTR) under the CD11c promoter. In CD11c-DTR expressing mice, CD11c cells can be specifically depleted by consecutive injections of small concentrations (100ng/day) of diphtheria toxin (DT). I then implanted GL261 cancer cells intra-cranially into DTR-expressing or DTR-non-expressing control mouse brain, and imaged the tumor longitudinally. I chose an intermediate tumor growth time point of day 10 to begin imaging as this time point showed robust CD11c-YFP and T cell recruitment in the tumor in most mice. I then obtained baseline time-lapse movies of CD11c-YFP cells and T cells in the tumor at day 10 and this was followed by injecting mice with DT intraperitoneally (100ng/day) at days 11 and 12, before eventually obtaining post-DT treatment time-lapse movies at day 13 and day 16. I used 100ng/day of DT because it produced the most optimal and consistent depletion of CD11c-YFP cells over a short duration of only two days in my experience. Following treatment with DT, as expected, CD11c-YFP cells were almost completely eliminated in the tumor (**Fig. 28a & movie 8**). The numbers of T cells also decreased sharply (**Fig. 28a & b**); this was unexpected

because I had hypothesized that in the GL261 progressive tumor, T cells were “held” by DCs in presumably unproductive interactions and I anticipated that after elimination of the DCs, T cells would be released from interacting with CD11c-YFP cells, redistribute in the tumor and potentially show cytotoxic behavior. I then analyzed the motility of T cells and found a significant reduction in the mean velocity of T cells post-DT treatment when compared to the pre-DT baseline. Correspondingly, T cells showed more arrest after DT treatment in comparison with the baseline (**Fig. 29a-c and movie 9**). In contrast, there was no significant change in the motility of T cells in the DTR-non-expressing control mice between pre-DT and post-DT scenarios. (**Fig. 29b-c & movie 9**). This indicates that CD11c-YFP cells are important for the retention of T cells in the tumor microenvironment and in controlling their motility. When I analyzed for FoxP3 Tregs, which are much fewer than non-FoxP3 expressing T cells in brain tumor, I found that Treg motility was significantly decreased but less affected than T cells (**Fig. 30 and movie 10**). Overall, the experiments conducted here showed a critical role for CD11c-DCs in retaining T cells and Tregs in GL261 brain tumor and in regulating their motility behavior.

Figure 27

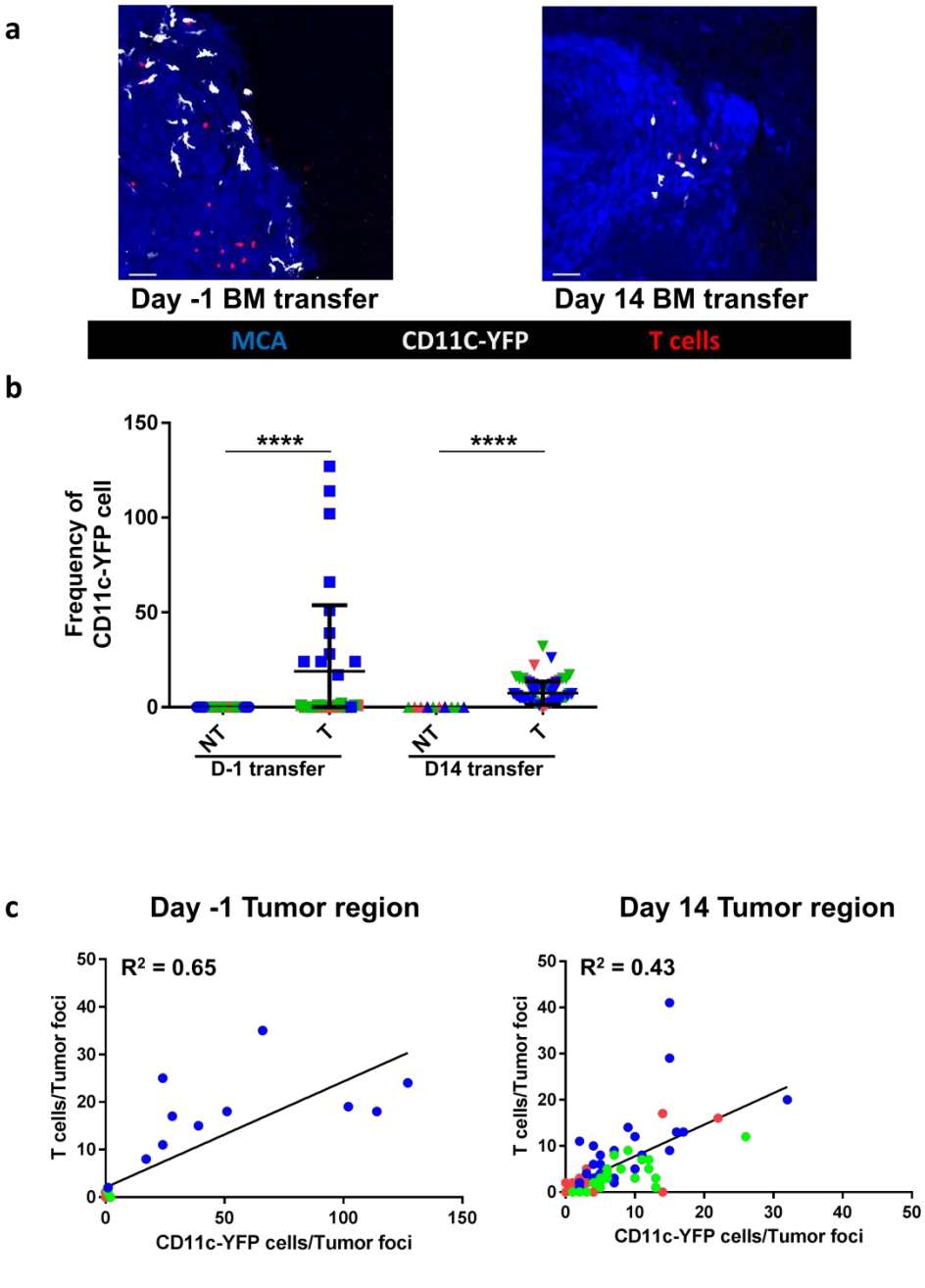

Figure 27. Transfer of bone marrow cells into brain tumor-bearing mice reveals correlation of CD11c-YFP and T cell localization in tumor.

a. Representative images showing the localization of CD11c-YFP cells (white) and T cells (hCD2-DsRed) in a 21-day MCA brain tumor after BM transfer. The left panel

represents cell localization in tumor after BM cells were transferred a day before cancer cell injection via ICA. The right panel represents cell localization in tumor after BM transfer 14 days after cancer cell injection via ICA.

b. Frequency of CD11c-YFP cells in MCA brain tumor (T) in comparison with non-tumor (NT) regions of the brain. A group of colored dots in the graph represent all metastatic tumor nodules randomly imaged and analyzed from a single mouse. Each dot represents the number of CD11c-YFP cells localized within a single metastatic tumor nodule or field of view (n = 3 mice/group; ****P <0.0001; frequency of CD11c-YFP cell analysis was done by non-linear mixed effects regression model).

c. Correlation of total T cells per tumor nodule or field of view and CD11c-YFP cells in the same field of view. Left graph represents cell correlation in tumor in experiments in which BM was transferred to tumor-bearing mice 1 day before cancer cell injection and right graph represents cell correlation in tumor from experiment in which BM was transferred to tumor-bearing mice 14 days after cancer cell injection (n = 3 mice/group). Different colors represent tumor nodules from different mice. A group of dots of the same color in the graph represent all metastatic tumor nodules randomly imaged and analyzed from a single mouse. Each dot represents the correlation of the area of distribution of CD11c-YFP DC and T cell in a tumor nodule or field of view.

Figure 28

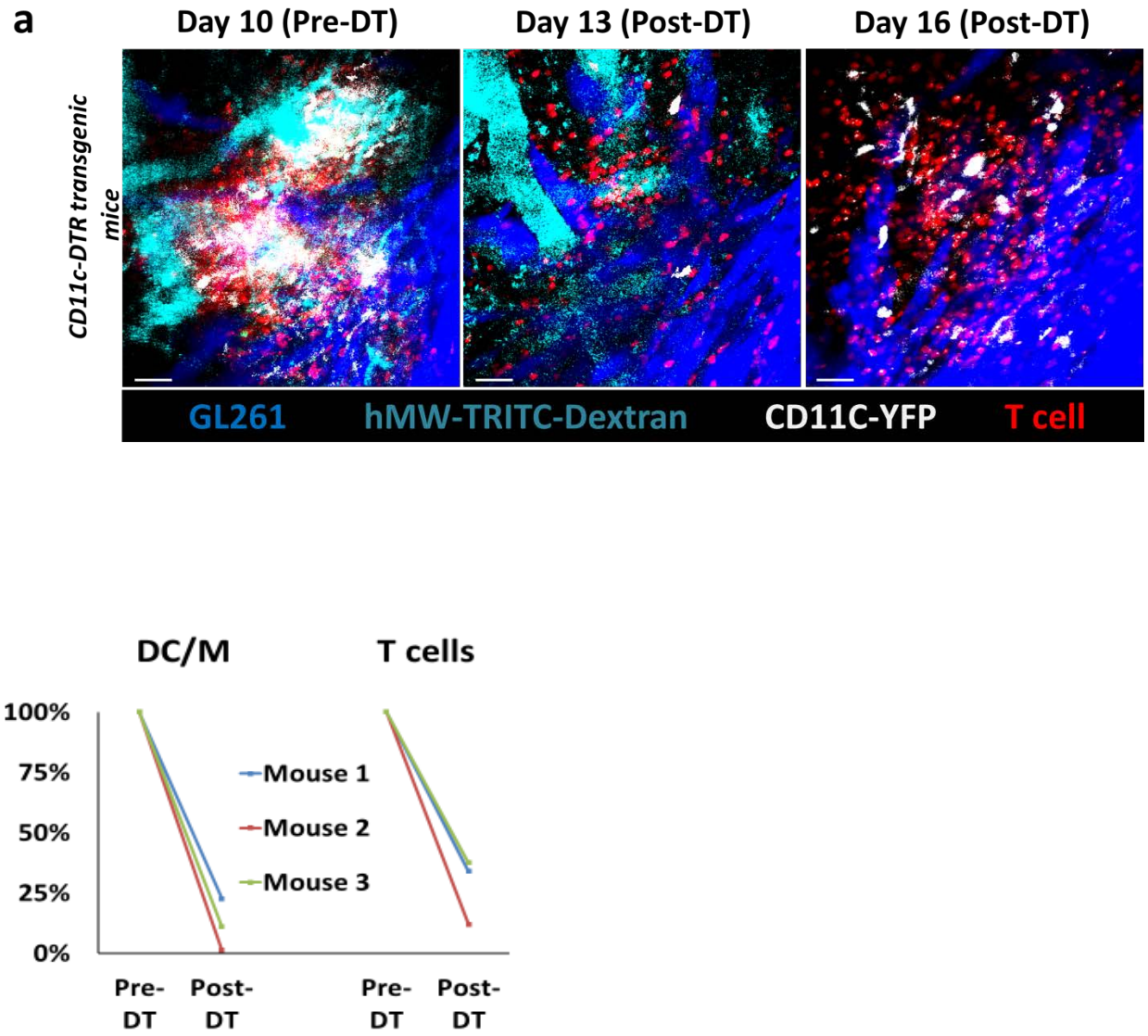

Figure 28. Longitudinal intravital imaging reveals CD11c-YFP cells are important for the retention and motility of T cell subsets in brain tumor.

a. Representative still images of longitudinal imaging sessions of endogenous CD11c-YFP cells (white), total T cells (red) and Gl261 brain tumor (blue) in CD11c-DTR transgenic mice at days 10, 13 and 16. Mice were treated with intraperitoneal injections

of DT at days 11 and 12 (n = 5 mice in 5 different longitudinal experiments). Scale bar represents 50μm.

b. Percentage of CD11c-YFP cells and T cells in the imaging field of view on days 10 and 13 before and after depletion of CD11c-YFP cells, respectively. Each colored line represents longitudinal depletion of CD11c-YFP DCs and associated change in T cell numbers per field of view in a GL261 brain tumor-bearing mouse.

Figure 29

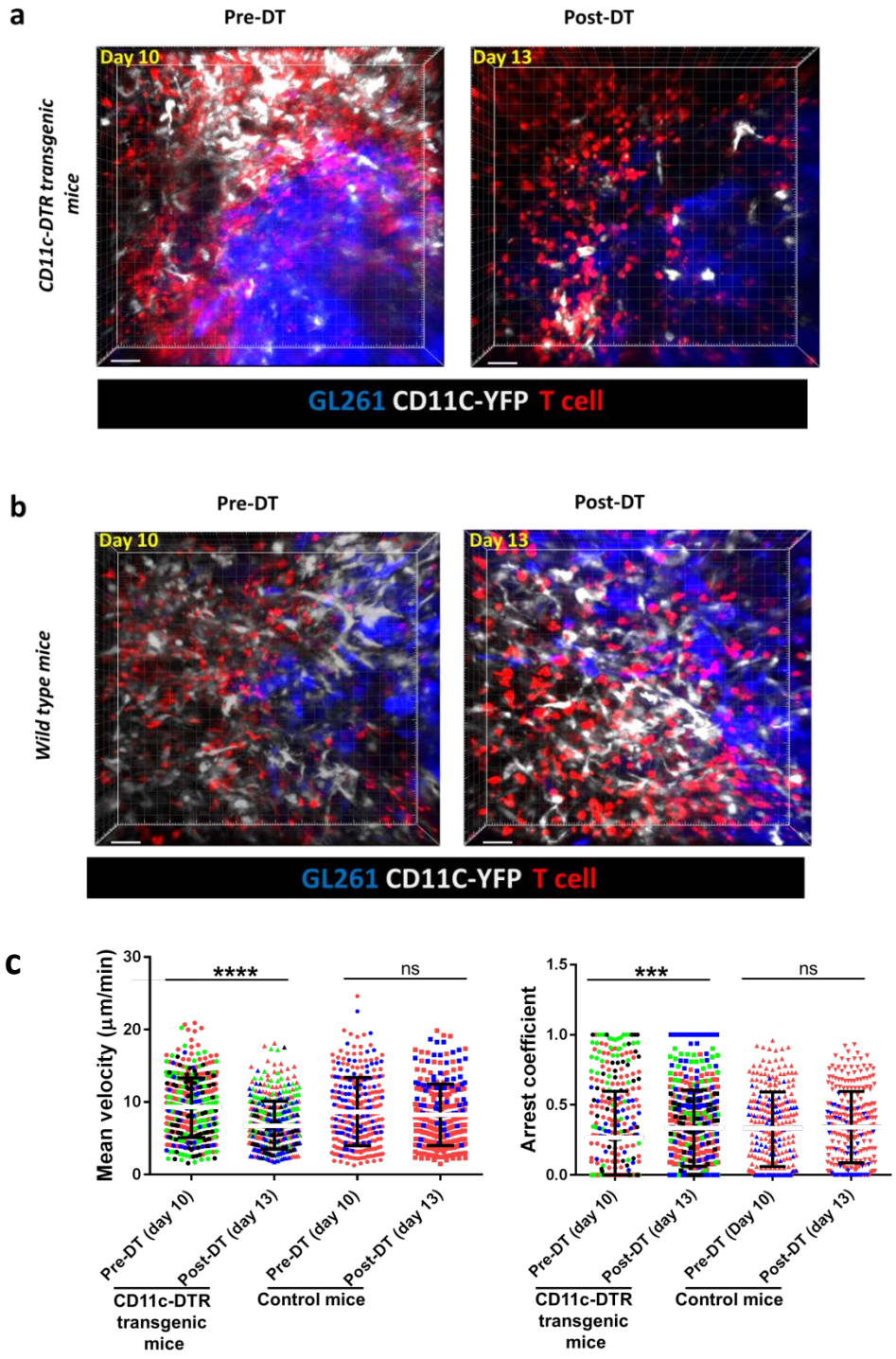

Figure 29. Longitudinal intravital imaging reveals CD11c-YFP cells are important for the retention and motility of T cell subsets in brain tumor.

a & b. Representative still images of longitudinal imaging sessions of endogenous CD11c-YFP cells, total T cells and Gl261-mCerulean glioma tumor in CD11c-DTR transgenic mice (upper image panels) and wild type mice (lower image panels) at days 10 and 13. Mice were treated with intraperitoneal injections of DT at only days 11 and 12.

c. Graphs show mean velocity and arrest coefficient of T cells at days 10 and 13 before and after treatment of CD11c-DTR transgenic mice (n = 4 mice accumulated from 4 different longitudinal experiments; experiment was repeated ~8 times and only movies with trackable T cells were included for analysis; mean velocity and arrest coefficient analysis were done by non-linear mixed effects regression model and Nested Mann-Whitney-Wilcoxon Test, respectively; ***$P < 0.001$, ****$P < 0.0001$, ns = not significant) and wild type mice with DT, respectively (n = 2 accumulated from 2 different longitudinal experiments; experiment was repeated ~6 times). Different colors represent T cells from different mice.

Figure 30

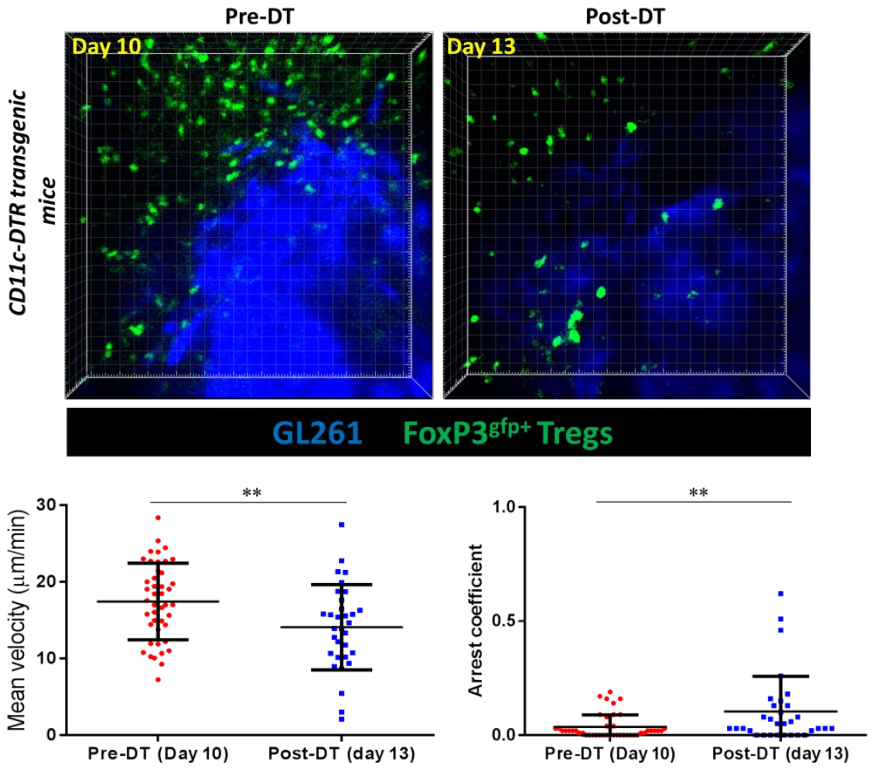

Figure 30: Longitudinal intravital imaging reveals CD11c-YFP cells are important for the retention and motility of Tregs in brain tumor.

Representative still images obtained from longitudinal 2-photon intravital imaging sessions of GL261-mCerulean tumor, and endogenous Tregs at day 10 and 13. CD11c-DTR mice were treated by intraperitoneal injection of DT at days 11 and 12. Graphs show the mean velocity and arrest coefficient of Tregs before and after depletion of CD11c-YFP cells (n = 2 mice accumulated from 2 different longitudinal experiments; ns = not significant; ***P* = 0.01; experiment was conducted ~5 times and only movies with trackable T cells were included for analysis). Scale bar represents 50µm. (Mean velocity and arrest coefficient analysis were done by Non-linear mixed effects regression model and Nested Mann-Whitney-Wilcoxon Test)

3.7b. Batf3 transcription is not important for CD11c-DC-mediated control of brain tumor.

Effective control of tumors generated in peripheral organs has been associated with efficient cross-presentation of antigens by Batf3-dependent DCs to CD8 T cells in the tumor bed[279]. As introduced in chapter 1, Batf3 is a transcription factor that regulates the development and function of CD8α+/CD103 DCs. In Batf3-KO mice, CD8α+/CD103 DCs are absent, and antigen cross-presentation is deficient. Therefore, I sought to test the role of Batf3-dependent CD8α+ DCs in the control of brain tumor growth. To test this, I injected MCA cancer cells into the brains of WT or Batf3-KO mice via the internal carotid artery. Following visualization of sections of tumor-bearing brain tissues and quantification, tumor growth in Batf3-KO mice appeared comparable to growth in WT mice (**Fig. 31a & b**), indicating that MCA brain tumor growth is not dependent on the Batf3 transcriptional network in DCs, at least in the model tested here. In addition, visualization of CD11c-YFP cells and T cells in Batf3-KO mice revealed qualitatively comparable infiltration of CD11c-YFP cells and T cells in the tumor.

Figure 31

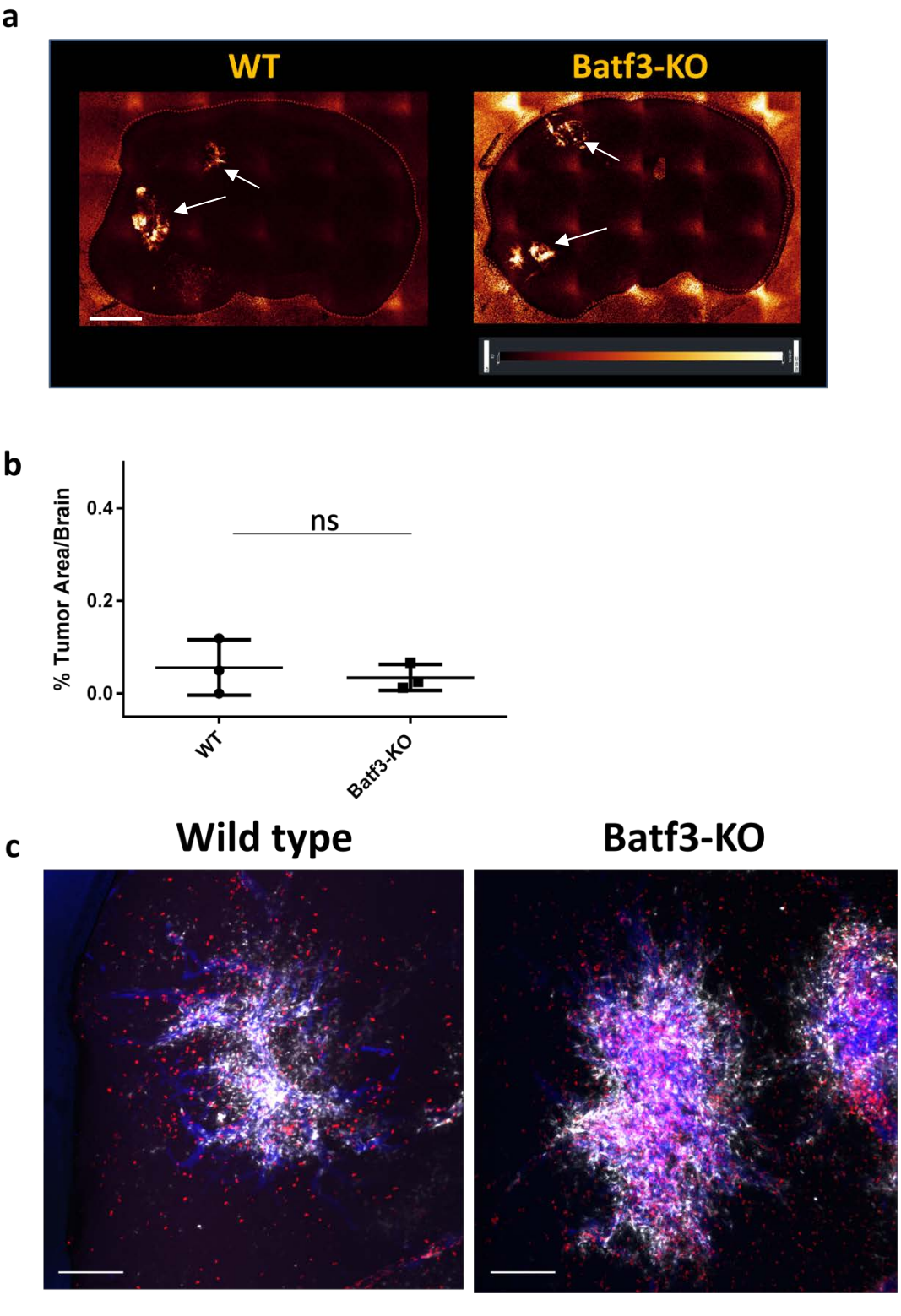
a
WT
Batf3-KO
b
% Tumor Area/Brain
0.4
0.2
0.0
ns
WT
Batf3-KO
c
Wild type
Batf3-KO

Figure 31. Batf3 is not important for CD11c-DC-mediated control of brain tumor.

A. Growth of MCA fibrosarcoma in the brains of wild-type and Batf3-KO mice at day 20 following injection of 10^5 fluorescent-labeled MCA- cells via the internal carotid artery. Tumor is in glow-scale and indicated by the white arrows. Scale bar represents 1mm.

B. Graph shows percentage of brain tissue covered by tumor and each dot represents a mouse (n = 3 mice/group; ns = not significant; unpaired t test).

C. Representative confocal images obtained from brain tissue sections from wild type and Batf3-KO mice at day 20 showing CD11c-YFP and T cells in association with MCA tumor.

Discussion

To our knowledge, this is the first documented evidence of real time T cell dynamics in brain tumors. By applying different methods including direct and indirect cancer cell injection and longitudinal intravital imaging, I have uncovered a spatiotemporal relationship between T cells and CD11c DCs in brain tumors. Interestingly, this was pervasive across different tumor types evaluated, except for the poorly immunogenic B16-F10 melanoma, which had very few T cells and CD11c DCs present in the tumor to begin with. Overall, T cells formed clusters around CD11c DCs but this was not terribly surprising as this finding is consistent with a previous study that documented the "entrapment" of T cells in CD11c DC network[465]; however, the fact that T cells continued to migrate around CD11c DCs in a random pattern in such confined area was unexpected. Although migration of T cells in clusters or confined spaces usually reflect decreased velocity and prolonged interactions between T cells and CD11c DCs in studies utilizing model tumor antigens, I detected few events of long-lived contacts between T cells and CD11c DCs in a model presumably involving polyclonal T cells. This suggests that T cells could be transiently interacting with CD11c DCs to gather signals for reactivation in the tumor or T cells are only organized in such patterns by yet unidentified CD11c DC-associated molecules or chemokine gradient(s). In support of the former, tumor associated CD11c DCs showed preferential expression of MHC-II and correspondingly, I observed multiple instances of T cell proliferation in MCA and GL261 tumor–a phenomenon that may be a more common than previously believed. On the other hand, given the above observations it is also possible that T cells engaging CD11c DCs in short-lived contacts in the progressive GL261 model may

be undergoing tolerization in similarity to a DC/T cell interaction pattern previously detailed in the lymph node[379].

A key finding of this study is the demonstration that myeloid cells including dendritic cells and classical monocytes, rather than microglia, are preferentially enriched in brain tumors and play a dominant role in T cell tumor surveillance. This is in contrast with previous studies that have highlighted the predominance of microglia-like cells in various brain tumor types and their immune suppressive properties[216,232,446,460,461,466-468]. This discovery was made possible by the iTIC method, which I used to delineate and identify major myeloid cell subsets and their spatial localization in the brain tumor microenvironment. The distinct localization of mature dendritic cells and classical monocytes to the margin and core of the tumor, respectively, was particularly striking. These two cell populations have been documented to play distinct roles in tumor, with mature DCs playing mostly an anti-tumor role, while the classical monocytes are known to be tumor supportive, at least in other types of extracranial tumor models[28,255,258,356,419]. In addition, the revelation of distinct organization patterns of “mature” and “immature DC” populations at the margin and core of the tumor by iTIC quantification methodology suggests likely ongoing differentiation of “immature DCs” or monocytes to mature DCs in the tumor and may involve cytokine or antigen-dependent differentiation mechanisms. However, it is also possible that the localization of mature DCs at the tumor margin and CM in the tumor core represent opposing forces during brain tumor progression, as mature DCs and CM have been shown to be mostly anti-tumor and pro-tumor[258,419], respectively.

Another surprising discovery in this study is that CD11c DCs control T cell retention and their migratory pattern in brain tumors. Although we nurtured the idea that

we could eliminate CD11c DCs to “free-up” T cells from CD11c DC “entrapment[465],” the numbers of T cells decreased dramatically, rather than redistribute in the tumor, and the T cells became relatively less motile when compared to controls. This suggests that CD11c DCs are necessary for effective T cell surveillance in the tumor. It also suggests a role for strategies that enhance infiltration of DCs into the tumor microenvironment or combine DC and T cell for tumor immunotherapy as opposed to conventional strategies employing either DCs or T cells exclusively. For example, adoptive transfer of TILs or engineered chimeric antigen receptor (CAR) T cells may profit from an additional strategy of enhancing DC infiltration into the tumor to potentially aid in the retention and anti-tumor function of TILs or CAR-T cells at the tumor. This finding also aligns well with the recent observation of a subset of rare tumor-associated CD103+ DCs mediating the anti-tumor effects of anti-CTLA4 checkpoint blockade in melanoma[457,469,470]. Although we could not implicate the Batf3-dependent CD8α+ DCs, which shares the same transcription factors as CD103+ DCs, several compensatory transcriptional pathways such as Irf4 and Irf8 have recently been elucidated that allow the development of CD8α+ DCs. Importantly, Batf3-dependent CD8α+ DCs are absent in Batf3-knockout mice on the 129 SvEV mouse background but not the C57Bl6 background, suggesting that mouse background may impact encoding of the Batf3-knockout transgene[471]. In this study, C57Bl6 mice were used and this could further account for the disparity between our results and published findings[279,280,285,286,471]. Future experiments utilizing mice with complete absence of CD8a+/CD103+ in C57Bl6 mice or other Batf3-KO mouse strains will be important in determining the role of this DC population in the immune control of brain tumors.

One limitation of this study is the lack of specificity of CD11c expression as a marker to distinguish DCs from other macrophages. While the CD11c-YFP transgenic mouse model remains very useful in gaining unprecedented appreciation of the dynamics of “DCs” and T cells in intravital imaging experiments, better mouse models that specifically identify only DCs will be important in clarifying the specific functions of DCs relative to other macrophage subtypes. However, theoretically, it may be impossible to distinguish all DCs from macrophages, as both cell types arise from a common macrophage dendritic progenitor (MDP) cell, and these cells utilize very similar signaling pathways and genetic programs during differentiation[472-475]. In addition, given present technology, it is almost impossible to predict MDP differentiation into specific lineages and may present a challenge for developing a transgenic reporter mouse that fatefully reveals a single lineage. Also, confounding issues with local tissue factors such as cytokines altering the plasticity of potentially differentiated cell types cannot be excluded. This may add to the complexity of achieving a goal of cellular specificity for DC fluorescent reporter mouse models. Regardless, distinct DC subsets such as conventional DCs regulated by Zbtb46 transcription factor have been recently engineered for studies on conventional DCs[457,476].

The discovery of distinct myeloid cell organization in different tumor regions by the iTIC method provides a framework to begin understanding brain tumor-associated myeloid cells. Although this finding needs to be validated in more tumor types, it calls into question the long-held notions about myeloid cell types believed to be dominant in controlling brain tumor immune surveillance. In the literature, methods that appear to have been confounded by the techniques used to initiate brain tumors (intracranial injection) and process/analyse brain tumor specimens (flow cytometry procedures) may

have introduced immune cell artifacts such as trauma-induced inflammation and cell loss due to tissue processing, respectively, and led to confusion about the composition of tumor-infiltrating myeloid cells in brain tumor[444-446]. Presumably due to these limitations, most studies have pooled different tumor-associated myeloid cells under a single arc usually coined as the “microglia/macrophages” entity[216,477-489]. Regardless, distinguishing myeloid cell populations is still a difficult task as techniques and distinct surface markers to separate different subsets of myeloid cells infiltrating brain tumor in their native tumor microenvironment *in situ* are still being developed. With availability of more reporter mice tagged with cell lineage-specific fluorophores[210,212] myeloid cell lineages may likely be better teased apart to better understand the composition of myeloid cell types and their spatial organization in tumor. In fact, when this approach is potentially combined with conventional gene profiling methods such as *in situ* hybridization, a lot of new knowledge may be obtained in terms of associating gene expression to cellular phenotype, tissue localization, and dynamic cellular behavior.

Based on the findings presented here, the presence of CD11c+ DC in tumor or similar DCs identified by more robust markers in human tissues may positively impact the prognosis of brain tumor patients being treated with immunotherapy. In support of this idea, a recent study showed that high expression of CD11c cells[469] or DCs was a good prognostic factor for patients with different cancer types[490,491]. However, further experiments are needed to determine whether CD11c+ DC population is necessary during immunotherapy in brain tumor models.

CHAPTER 4: IMMUNE RESPONSE TOWARD BRAIN METASTASIS DEPENDS ON THE FRACTALKINE- CX3CR1 RECEPTOR AXIS

Introduction

Immune surveillance of tumor is highly dependent on dynamic cell migration and cell-cell contact[372,379,400,492,493]. For effective immune surveillance to occur, T cells must travel to the site of the tumor after being primed by antigen presenting cells in tumor-draining lymph nodes[372,375,379,398]. In tumor, T cells show migratory patterns that must be regulated for effective tumor control[372]. However, little is known about the molecular mechanisms regulating the dynamics of T cell tumor surveillance in the brain. Chemokines are widely known to regulate immune cell migration in host homeostasis, defense, and tolerance[294,494]. Studies of inflammatory disorders in mouse models have revealed the importance of chemokines in mediating innate and adaptive immune responses in autoimmunity, infection, and anti-tumor immune surveillance[407,414,495].

There are numerous chemokines that mediate immune responses within different tissues and they are organized in an organ-specific manner[413,496]. The stromal-derived factor 1 (SDF1) chemokine and its receptors CXCR4/CXCR7 are necessary for embryonic survival including neuronal migration and vasculogenesis, and has been the most studied chemokine pathway in brain tumors[497]. Importantly, SDF1 and CXCR7 are upregulated in tumor endothelium, microglia, and glioma cancer cells in glioma tissue while CXCR4 has been shown to be highly expressed in high grade GBM and in glioma stem-like cells[498-500]. The SDF1 pathway works by preventing apoptosis in glioma cells and inducing increased tumor angiogenesis/vasculogenesis[501-503]; however, inhibition of CXCR4 or CXCR7 has resulted in increased apoptosis and decreased proliferation of glioma cells[504-506]. The monocyte chemoattractant protein 1 (MCP-1/CCL2) is another chemokine that is produced by microglia in inflammatory conditions or in glioma tissue and known to attract Tregs, effector T cells, and inflammatory monocytes

via its receptor CCR2[347,419,502,507,508]. In addition, the CCL22/CCR4 pathway has been implicated in recruiting T cells to brain tumor[508-510]. Microglia express CCR5 and inhibition of CCR5 prevented transition to an “M2” immune suppressive phenotype[511,512]. CXCL2-CXCR2 is up-regulated by brain resident perivascular myeloid cells and inhibition reduced tumor vessel density and glioma size[513]. Other chemokines expressed in glioma or implicated in glioma progression include CXCR3, CCL20/CCR6, CXCL16/CXCR6, CCL27/CCR10[514-518].

However, the aforementioned chemokines are inducible in glioma tissue and presumably operate equally in inflammatory conditions in other mammalian tissues as in glioma. In contrast, there may be chemokines that operate in an organ-specific manner even in the brain. Fractalkine is one such chemokine that is highly expressed by neurons in the healthy brain, and to a lesser extent by epithelia in other tissues such as the kidney, lung, and uterus[411,519]. Fractalkine is known to control the migration of several myeloid cell types and some T cells via its only known receptor, CX3CR1[419]. Because of its high expression in the brain, Fractalkine could be a key regulator of anti-tumor immunity in the brain; however, its involvement in brain tumor T cell immune surveillance is largely unexplored. Fractalkine is unique as it is the only member of the fourth class of CX3C- family of chemokines. It is constitutively membrane-bound on neurons and is produced as a long protein with cytoplasmic, transmembrane, mucin-like stalk, and chemokine domains. In addition, it can assume a soluble form following cleavage by metalloproteinases such as ADAM10 and 17[520]. This form accesses the circulation and is important for the recruitment of CX3CR1-expressing cells[412,519,520]. Fractalkine may be released into the tissue and circulation in the setting of CNS injury[521,522]. In this regard, brain tumors show striking similarity to CNS injury events as

they progressively invade the surrounding tissue architecture and potentially induces responses from the surrounding brain tissue including neurons. Therefore, the possibility that traumatized neurons surrounding brain tumors could upregulate expression or release soluble Fractalkine is likely. The process of brain tumor growth is associated with increased expression of metalloproteinases[27,523] . Therefore it is probable that this process may be utilized in upregulating relevant metalloproteinases such as ADAM10 and 17, which could then cleave fractalkine into the circulation.

CX3CR1 is a G-protein coupled receptor that is expressed on the surface membrane of various immune cell types including microglia, macrophages, monocytes, DCs, and T cells[210,413]. CX3CR1 is known to be important in cell migration and adhesion[524-526]. Using genetically engineered mice, CX3CR1 has been shown to be important in the pathogenesis of Alzheimer's disease, atherosclerosis, diabetes mellitus, atopy, HIV, and cancer[414,415,419,527,528]. In addition, single nucleotide polymorphisms of CX3CR1 have been implicated in several inflammatory disease conditions such as atherosclerosis, HIV/AIDs, and atopic dermatitis[529-531]. Although deficiency of CX3CR1 was recently shown to regulate infiltration of immune suppressive monocytes in glioma progression[419], its role in the regulation of brain tumor immune surveillance is lacking especially with regards to T cell involvement, and in the regulation of antigen presenting myeloid and T cell dynamics in brain tumor. Therefore, based on the expression of Fractalkine in the brain, I hypothesized that the Fractalkine-CX3CR1 axis counteracts brain tumor progression by regulating anti-tumor immune responses.

Results

4.1. MCA brain tumor progression is controlled by T cells

Different tumor lines were found to have a differential propensity to grow within the brain of mice. Specifically, B16 melanoma and Lewis Lung Carcinoma (LLC) demonstrated engraftment and rapid growth within 14-21 days after *in vivo* injection. In contrast, the fibrosarcoma line, MCA, initially demonstrated engraftment in the brain but failed to grow. This was not an issue of tissue kinetics or cancer cell viability since MCA demonstrated robust growth *in vivo* in the lung (**Fig 32**), indicating that there was a unique property of the MCA line that allowed immunological recognition and clearance.

To determine whether adaptive immune surveillance is critical for progression of MCA brain tumor, I injected MCA cancer cells via the ICA to the brain of Rag-KO mice, which are deficient in T and B cells. After mice were sacrificed at late time points of day 18-20, brain sections visualized by confocal microscopy revealed significantly larger tumor in brain of Rag-KO mice in comparison to wild type (WT) mice (**Fig 33a &b**). This established the role of the adaptive immune system in the control of ICA-induced MCA brain tumor.

To specifically test the role of T cells in MCA anti-tumor immunity, CD8 cytotoxic T cells known to play a major role in killing cancer cells were depleted one day before or 5 days after MCA cancer cells were injected into C57Bl/6 WT mice as described in chapter 2. After depletion of CD8 T cells one day before cancer cell injection, MCA brain tumors were found to be significantly larger relative to WT control mice, indicating that CD8 T cells control MCA brain tumor growth (**Figure 33c**). However, depletion of CD8 T cells 5 days after injection of cancer cells resulted only in a trend towards increased MCA brain tumor growth. Furthermore, intravital microscopy of MCA brain

tumor in WT reporter mice revealed fragmentation of MCA tumor (**Figure 33d and movie 11**). This coincided with persistence of T cells in association with CD11c-YFP cells in the fragmenting tumor nodule, reminiscent of observations documented in chapter 4. Although T cells in associating with the tumor exhibited stable engagement, other T cells within the vicinity of the tumor showed less stable engagement or no engagement.

4.2. The Fractalkine/CX3CR1 axis is dysregulated in glioblastoma patient myeloid cells and control of MCA brain metastases in mice depends on the Fractalkine/CX3CR1 pathway

To identify molecular candidates that may regulate brain tumor immune surveillance by T cells, I mined several databases including BioGPS which I analyzed for mRNA expression of chemokines in different mammalian tissues. Fractalkine was identified as a lead candidate based on species conservation and relatively higher expression in the brain in comparison with other mammalian tissues in mice and humans. (**Fig. 34 & 35**). In a bid to explore the role of Fractalkine in regulating brain tumor immune surveillance, healthy and tumor-bearing mice brain tissue sections were stained with anti-Fractalkine antibody in order to visualize the expression of Fractalkine. By using confocal microscopy, I found high expression of Fractalkine at the margin of MCA and GL261 tumor as opposed to its discrete cellular localization in healthy brain tissue, presumably within neurons as has been previously documented[410,519] (**Fig. 36a & b**).

Figure 32

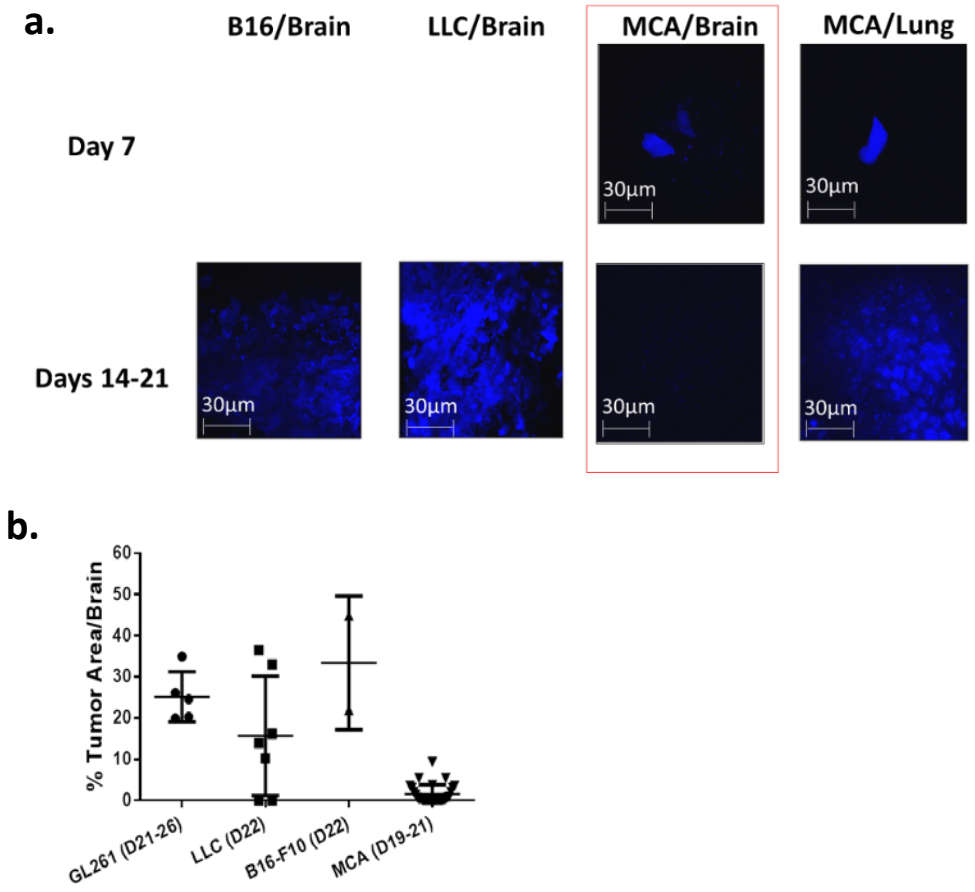

Figure 32: MCA brain metastases establish efficiently in lung but not brain.

a. Growth of B16, LLC, and MCA tumors (blue) in the brains or lungs of wild-type mice after injection of 10^5 fluorescent-labeled cancer cells via the internal carotid artery or tail vein, respectively. Panels within the red line rectangle indicate inefficient growth of MCA in the brains of mice at later time points

b. Percentage of brain parenchyma area in coronal plane infiltrated by tumor. Each dot represents one mouse [GL261 (n = 5), LLC (n = 7), B16-F10 (n = 2), and MCA (n = 29); mice were pooled from >2 experiments]. The numbers in parenthesis in the x-axis represent the range of time points when mice were sacrificed for analysis.

Figure 33

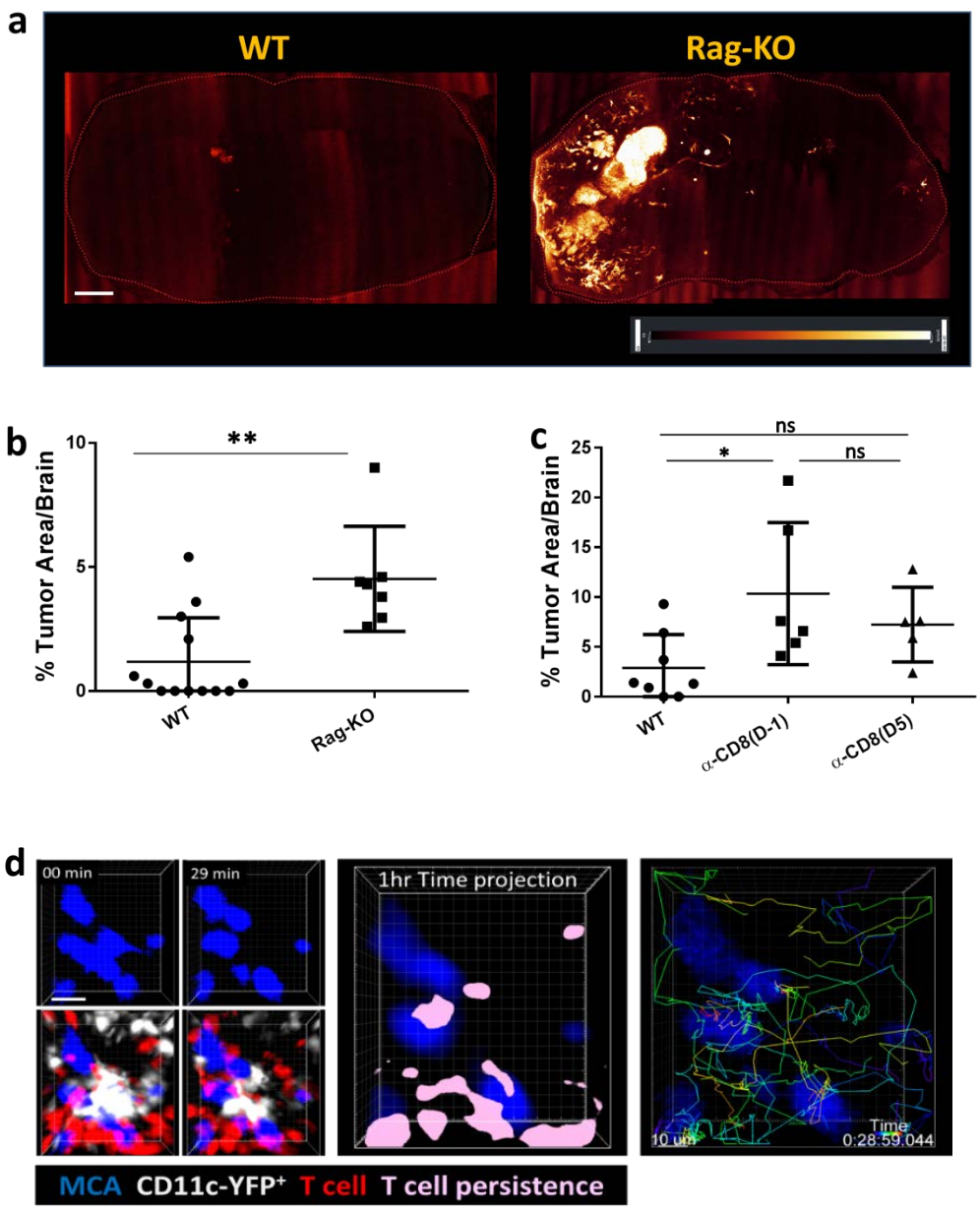

Figure 33: Growth of MCA is controlled by CD8 T cells.

a. Confocal images of coronal brain sections from WT and Rag-KO mice showing growth of MCA at day 20 following ICA cancer cell injection. Scale bar represents 1mm.

b. Graph shows the percentage of brain parenchyma infiltrated by tumor in the coronal plane and each dot represents a mouse (**$P < 0.001$; n = 7-13 mice/group; pooled from 2 different experiments; Mann-Whitney non-parametric test).

c. Growth of MCA in the brains of control mice or mice injected with anti-CD8α depleting antibody (100mg/ml; intraperitoneally; Clone #53-6.72, BioXcell, San Diego, CA) at day 20 following injection of MCA cancer cells via the ICA. Graph shows the percentage of the brain parenchyma area in coronal plane infiltrated by tumor and each dot represents a mouse (n = 5-8 mice/group, pooled from 2 different experiments). Scale bar represents 1mm. D-1 and D5 represent two different groups of mice that were treated with CD8 depleting antibody beginning one day before they were injected with cancer cells via the ICA or five days after cancer cells were injected in mice. *$P < 0.05$, ns = not significant.

d. Representative image panels to the left show MCA-mCerulean fibrosarcoma brain tumor (blue) undergoing fragmentation in association with $CD11c^{+}$DCs (white) and T cells (hCD2-DsRed; time span of active fragmentation is shown in the top left corner of the upper panels). Representative time-projection image panel in the middle shows areas of T cell persistence (pink) at the tumor site during a 1-hour time-lapse image acquisition. In the right panel, time color-coded tracks indicate T cell migration tracks over 1 hour; T cell migration tracks proximal to tumor/CD11c-YFP DCs appear more clustered in comparison with distal tracks. Scale bar represents 10μm.

To test for the relevance of Fractalkine signaling pathway in human brain tumor patients, NanoString digital color-coded barcode technology was used to measure the mRNA expression of Fractalkine receptor, CX3CR1. This was done using CD14+ peripheral blood monocytes from healthy donors and GBM patients, and CD14+ myeloid cells from normal post-mortem/epilepsy brain tissue and tumor-infiltrating GBM myeloid cells. Interestingly, CX3CR1 mRNA levels were significantly reduced in CD14+ PBMCs and GBM tumor-myeloid cells in almost all GBM patient specimens tested in comparison with control samples (**Fig. 36c & d**). Therefore, to test for the importance of Fractalkine signaling via CX3CR1 in brain tumor progression, MCA cancer cells were injected via the ICA into CX3CR1-KO mice, and wild type (WT) and CX3CR1-heterozygous mice were used as controls. This was based on the reasoning that knockout of CX3CR1 would disrupt Fractalkine signaling and the consequent immune surveillance, thereby enabling progression of the spontaneously regressing MCA brain tumor. After confocal imaging of MCA tumor-bearing brain tissue sections and analysis, significantly larger tumors were found in CX3CR1-KO mice in comparison with WT mice. Unexpectedly, MCA tumors in CX3CR1 heterozygous mice were also significantly larger than in WT mice (**Fig. 37**). This suggested that Fractalkine signaling via CX3CR1 is important at different levels of its expression in counteracting the progression of brain tumors, at least in the MCA tumor model.

In line with a role for Fractalkine/CX3CR1 signaling in tumor progression, I reasoned that absence of fractalkine signaling could impact the dynamics of CD11c-YFP cells and T cells. Interestingly, when the density of T cells and CD11c-YFP cells was quantified in MCA tumor, both populations were highly reduced in CX3CR1-heterozygous and CX3CR1-KO mice in comparison with WT mice (**Fig. 38a-c**). In

addition, the surface of tumor covered by T cells was reduced in CX3CR1-heterozygous and CX3CR1-KO mice relative to WT controls; however, the capacity of T cells to contact cancer cells was not significantly altered (**Fig. 39**)**.** This suggested that the Fractalkine/CX3CR1 signaling pathway supports the recruitment of CD11c-YFP cells and T cells to MCA brain tumor.

4.3. CX3CR1 controls T cell motility patterns in the tumor

Finally, I investigated the role of Fractalkine/CX3CR1 signaling in regulation of T cell motility in brain tumor. To test this, MCA cancer cells were injected via the ICA WT and CX3CR1-KO mice. By acquiring time-lapse movies of T cells in tumor-bearing WT or CX3CR1-KO mice between 7-10 days after cancer cell injection and tracking the T cells (**Fig. 40a and movie 12**), radial tracking plots of T cells showed that T cells in CX3CR1-KO mice diverged more from their track origin whereas those in WT mice were in swarmed or clustered in the tumor region and remained closer to their track origins (**Fig. 40b**). No difference in T cell velocity and meandering was found between CX3CR1-KO and WT mice; however, T cells in CX3CR1-KO mice were more diffuse, and were less arrested at the tumor (**Fig. 40c**). These data supports the idea that the lack of Fractalkine signaling via CX3CR1 leads to altered and inefficient anti-tumor T cell motility patterns in brain tumor.

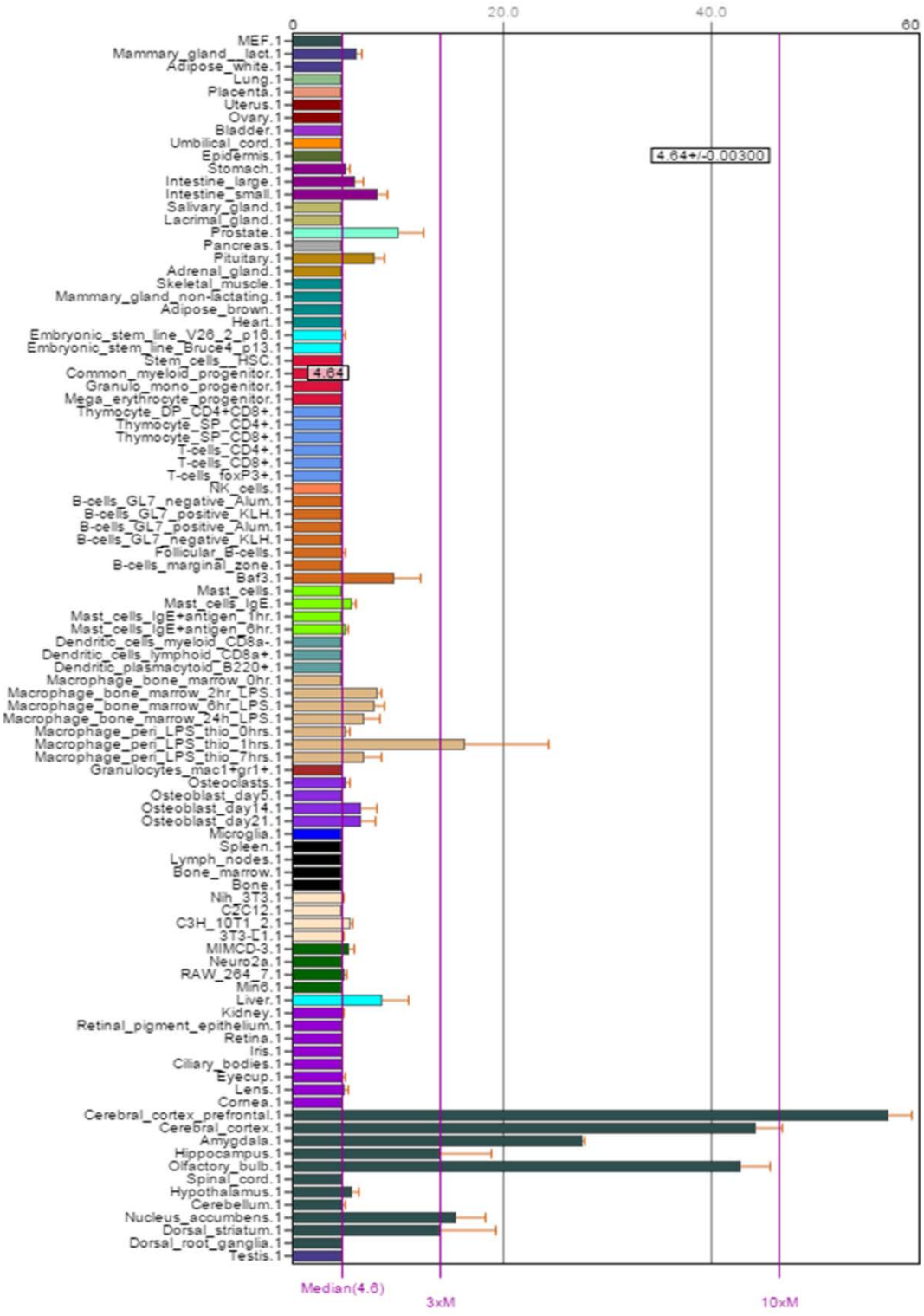

Figure 34: Histogram showing gene expression level of fractalkine in different tissues and organs in mice (http://biogps.org/#goto=genereport&id=20312).

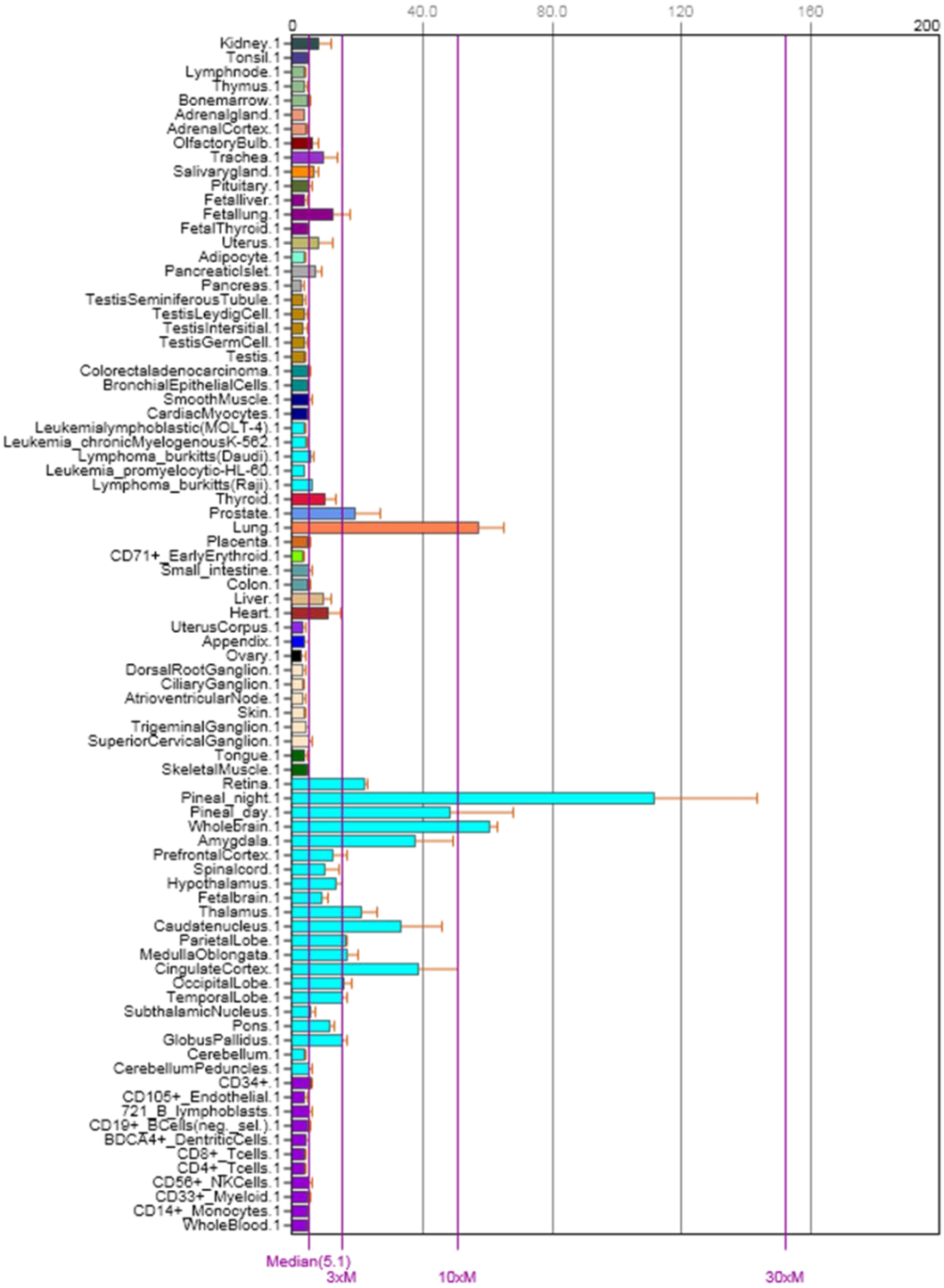

Figure 35: Histogram showing gene expression level of fractalkine in different tissues and organs in human tissue specimens http://biogps.org/#goto=genereport&id=20312).

Figure 36

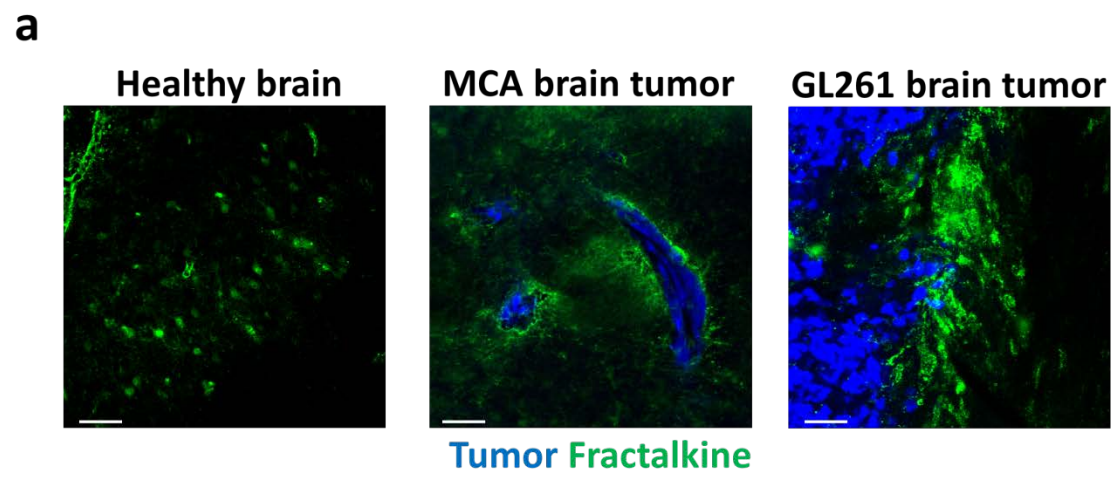
a
Healthy brain
MCA brain tumor
GL261 brain tumor
Tumor Fractalkine

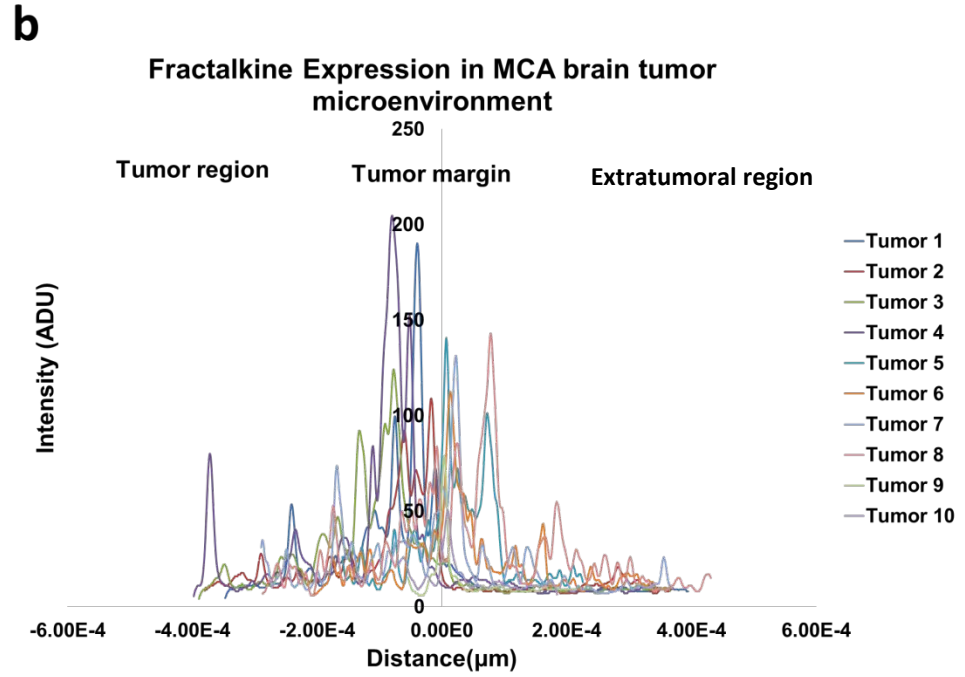
b
Fractalkine Expression in MCA brain tumor microenvironment
Tumor region
Tumor margin
Extratumoral region
Intensity (ADU)
250
200
150
100
50
0
-6.00E-4
-4.00E-4
-2.00E-4
0.00E0
2.00E-4
4.00E-4
6.00E-4
Distance(μm)
Tumor 1
Tumor 2
Tumor 3
Tumor 4
Tumor 5
Tumor 6
Tumor 7
Tumor 8
Tumor 9
Tumor 10

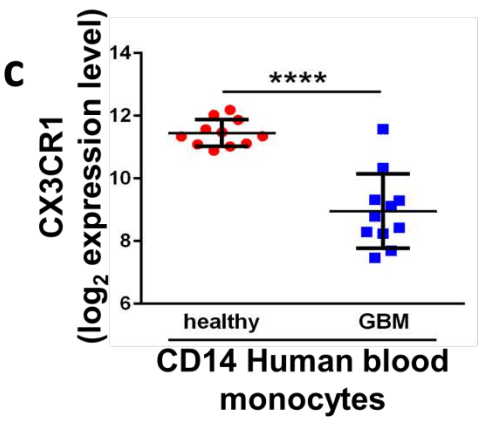
c
CX3CR1 (log2 expression level)
****
healthy
GBM
CD14 Human blood monocytes

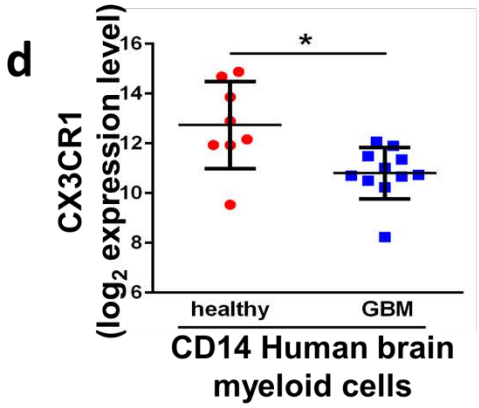
d
CX3CR1 (log2 expression level)
*
healthy
GBM
CD14 Human brain myeloid cells

Figure 36. Fractalkine is highly expressed at the margin of brain tumors, and expression of its receptor CX3CR1, is reduced in GBM patients.

a. Representative confocal images of *ex vivo* brain tumor tissue sections showing expression of Fractalkine in normal brain, and MCA and GL261 brain tumors. MCA tumor was generated by ICA injection while GL261 was directly implanted by ICr-injection. Scale bar represents 50μm.

b. Intensity profile of Fractalkine obtained from 10 different MCA tumor nodules (n = 3). The intensity line profile cuts across the margin of the tumor beginning from inside the tumor and extending to relatively normal brain tissue.

c. Gene expression level of CX3CR1 on CD14+ monocytes obtained from peripheral blood of healthy donors and GBM patients (n = 11; unpaired t test).

d. Gene expression level of CD14+ myeloid cells obtained from normal brain tissue (post mortem/epilepsy patients) and GBM patients. Each dot represents a patient (n = 11; unpaired t test).

*Sungho Lee, MD PhD was helpful in staining normal brain tissues for Fractalkine in **figure a**.

*****Konrad Gabrusiewicz, PhD and Amy Heimberger, MD, were helpful in conducting and discussing experiments in **figures c and d**, and kindly shared the results for this thesis.

Figure 37

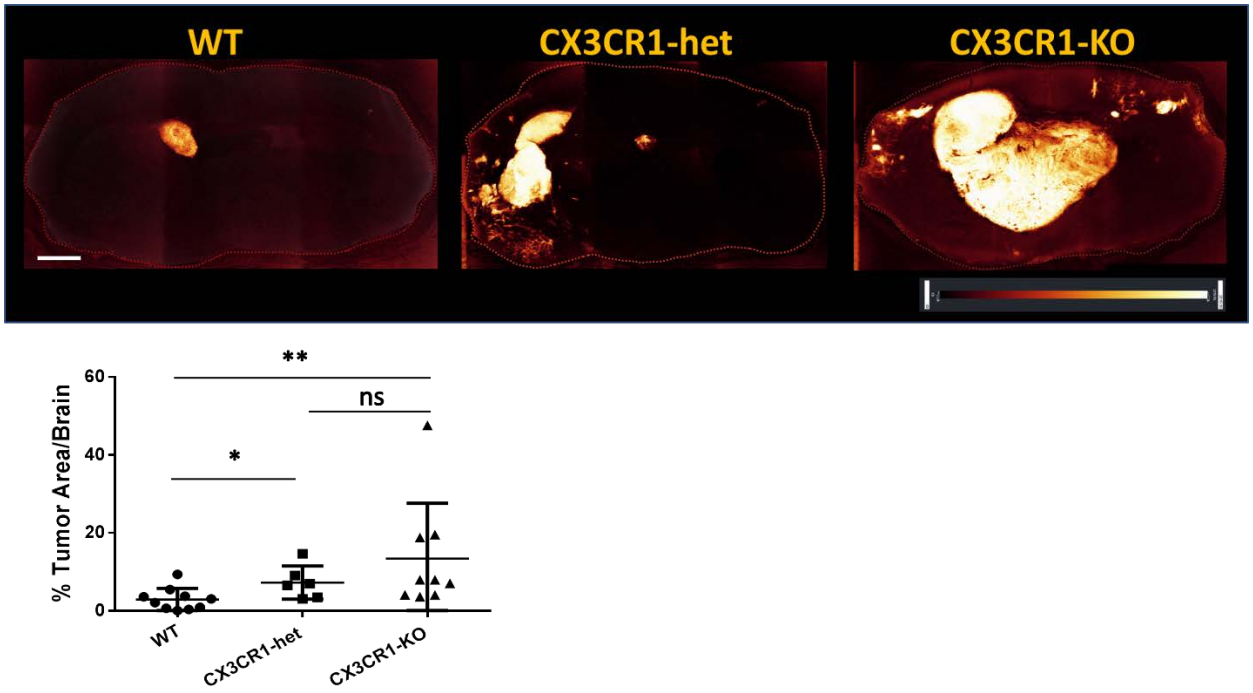

Figure 37. CX3CR1 deficiency in mice is important for efficient establishment of brain tumor.

a. Representative confocal images of MCA cancer cell growth in the brains of WT, CX3CR1-heterozygous, and CX3CR1-KO mice at day 20 after injection via the ICA. Images are shown in glow-scale; white represents the maximum fluorescence intensity, red represents the minimum, and black indicates the lack of fluorescent signal. Brain parenchyma is outlined with red dashed lines for clarity.

b. Graph to the right of the image panel shows the percentage of the brain parenchyma area in coronal plane infiltrated by tumor and each dot represents a mouse (n = 7-10; pooled from 3 different experiments; unpaired t test). Scale bar represents 9 mm. *P = 0.04, **P = 0.003, ns = not significant.

Figure 38

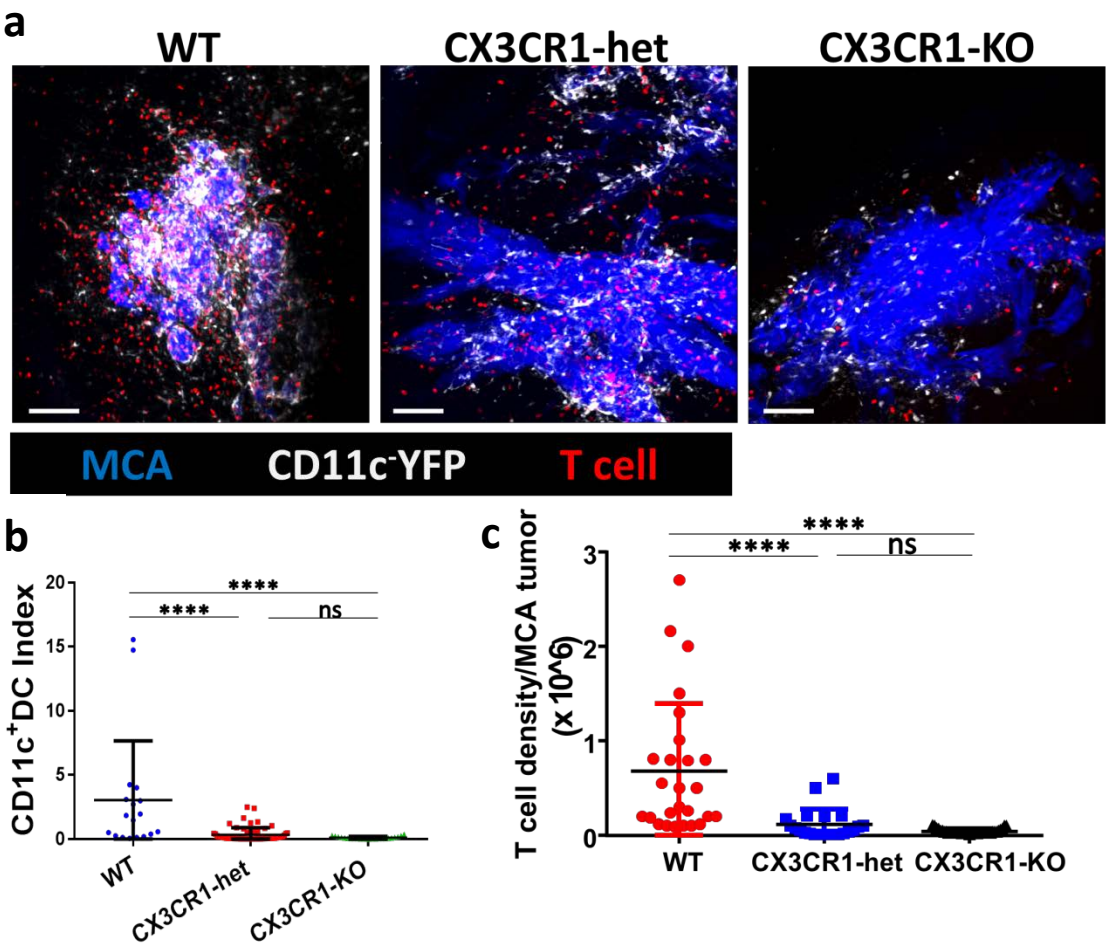

Figure 38. Fractalkine/CX3CR1 signaling is important for recruitment of DCs and T cells to the tumor.

a. Representative confocal images of endogenous CD11c-YFP cell and T cell localization in WT, CX3CR1-heterozygous, and CX3CR1-KO mice.

b. Density of CD11c-YFP cells in tumors analyzed in WT, CX3CR1-heterozygous, and CX3CR1-KO mice (DC index is defined as the volume of CD11c-YFP cells divided by the volume of the tumor). Each dot represents a tumor nodule (n = 3 mice per group; Mann-Whitney non-parametric test).

c. Density of total T cells recruited to tumor nodules in WT, CX3CR1-heterozygous, and CX3CR1-KO mice (n = 3 mice; Mann-Whitney non-parametric test).

Figure 39

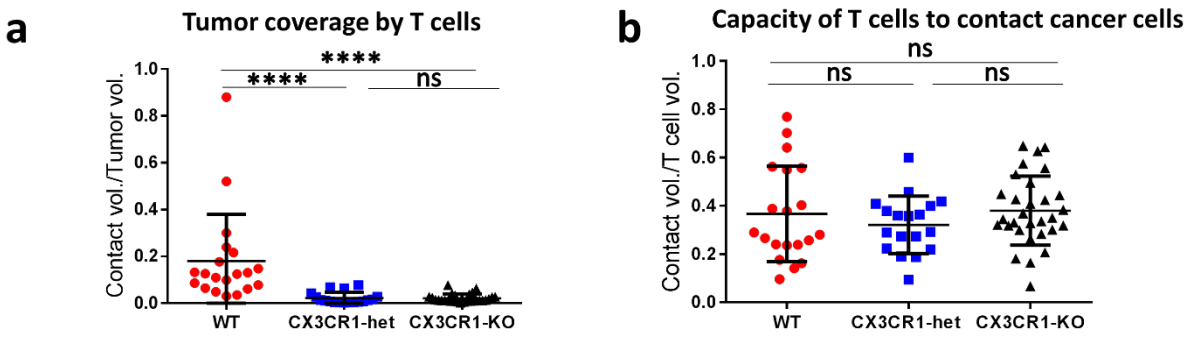

Figure 39. CX3CR1 controls tumor coverage by T cells but not extent of T cell surface contact to tumor

a. Extent of tumor surface covered by T cells, and **b.** Extent of T cell surface contacting tumor in wild type, CX3CR1-heterozygous, and CX3CR1-KO mice. Each dot represents the total surface of a single tumor nodule covered by or contacting T cells. (n = 2-3 mice/group; Mann-Whitney non-parametric test).

Figure 40

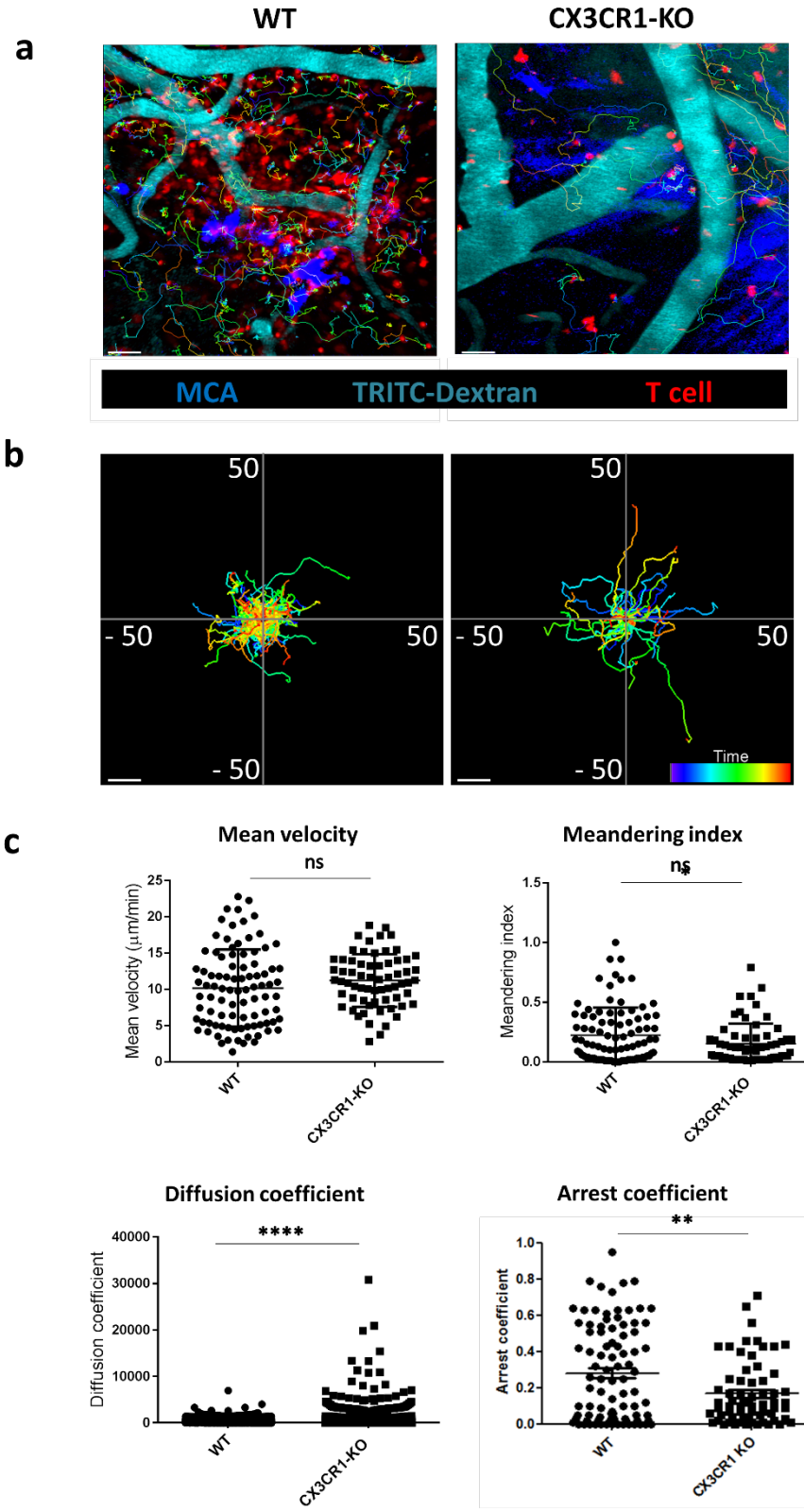
a
WT
CX3CR1-KO
MCA
TRITC-Dextran
T cell
b
50
- 50
50
- 50
Time
c
Mean velocity
ns
Mean velocity (µm/min)
WT
CX3CR1-KO
Meandering index
ns
Meandering index
Diffusion coefficient
****
Diffusion coefficient
Arrest coefficient
**
Arrest coefficient
CX3CR1 KO

Figure 40. CX3CR1 is important for T cell motility patterns in brain tumor.

a. Representative still images from intravital time-lapse imaging sessions showing MCA tumor (blue), blood vessels (hMW TRITC-dextran; cyan), and T cells (CD2-DsRed). T cell tracks are indicated by lines that are time color-coded.

b. Representative displacement tracks of T cells in MCA brain tumor-bearing WT or CX3CR1-KO mice. Displacement tracks are time color-coded.

c. T cell motility parameters in MCA brain tumor in WT or CX3CR1-KO mice including the mean velocity, meandering index, diffusion coefficient, and arrest coefficient. Each dot represents a T cell (n = 2 mice/ group; mean velocity, meandering index, and diffusion coefficient were analyzed by non-linear mixed effects regression model and arrest coefficient was analyzed by nested Mann-Whitney-Wilcoxon test).

Discussion

In this study, I found that T cell surveillance of brain tumor is controlled by the Fractalkine/CX3CR1 signaling axis and that this signaling pathway counteracts MCA brain tumor progression These findings are consistent with the results of a recent study in which CX3CR1 deficiency was shown to be important in increasing the survival of brain tumor-bearing mice in which orthotopic brain tumor was generated by using a GEMM brain tumor-derived cancer cell line[419]. In addition, lack of CX3CR1 was associated with increased recruitment of peripheral immune suppressive monocytes/macrophages increased in brain tumor[419]. However, they failed to identify any differences in *in situ* progression of brain tumor in the brains of CX3CR1-deficient mice in comparison with WT mice. Fractalkine expression was detected to be low or not expressed by tumor tissue or cancer cells indicating that fractalkine signaling was not responsible for recruitment of brain monocytes/macrophages. It appears that their focus on the accumulation of monocytes/macrophages inside the tumor core and their inability to identify the localization of DCs or T cells in their tumor model may have prevented interrogation of fractalkine in the peritumoral compartment as a key player in brain tumor progression. Here, I show that Fractalkine expression is increased especially at the margin of the tumor in both the MCA and GL261 model. This would indicate possible stress or damage to neurons adjacent to brain tumors, as neurons are known to constitutively express Fractalkine, and presumably upregulate this chemokine during inflammation. It is important to note that myeloid/T cell tumor infiltration has been observed in some studies to occur at the margins of tumor types studied[532-534], and consistently in chapter 4, characterization of tumor-infiltrating myeloid cells revealed that mature DCs expressing CX3CR1 are abundant at the tumor margin.

Whether this indicates a chemokine-based segregation of myeloid cells into different tumor compartments is an area of active investigation.

A key issue that was puzzling was that although the brain resident microglia show high expression of CX3CR1 in both steady state and in brain pathologies, they did not form clusters or aggregate around brain tumors as has been heavily documented in the literature[446,467,477,486,489,535,536]. One explanation for the findings in this thesis, as opposed to previous observations, may be that Fractalkine does not diffuse extensively into the brain parenchyma but is only locally upregulated and secreted around the tumor, and that the engraftment and invasion of tumor, for example MCA, from within the vasculature into the brain tissue allows for preferential secretion of Fractalkine into the circulation. This may then lead to the cascade of preferential recruitment of myeloid cells such as BM-derived monocytes rather than microglia. In support of this idea, I have observed multiple times that tumor-associated DCs are usually proximal to the brain vasculature. Another possibility is that steady state constitutive expression of membrane-bound Fractalkine in neurons and high expression of CX3CR1 in microglia may exist to tether microglia to neurons in order to enable an efficient physiologic neuron-pruning function for microglia and to also prevent potentially “neurotoxic” microglia from roaming free in the brain tissue[416,537,538]. Therefore, if this idea holds true, it is possible that relatively distal microglia from the tumor margins are not recruited because constitutively membrane-bound Fractalkine in intact neurons retain the capacity to tether microglia and prevent microglia recruitment to the tumor. In extension, it may be possible that in much larger tumors that have invaded significant regions of the brain, more microglia are recruited into the tumor, and that in CX3CR1-KO mice, microglia are untethered and able to infiltrate the tumor and

contribute to tumor progression; however, more work is needed to test these ideas. Alternative possibilities may involve the contribution of other chemokines and/or differences in chemokine signaling pathways between microglia and other myeloid cells such as DCs.

The decreased density of T cells and CD11c DCs in brain tumor in the absence of CX3CR1 implicates Fractalkine as a major regulator of DC and T cell surveillance in the tumor. In fact, analysis of T cell motility behavior in CX3CR1-KO mice showed altered patterns of T cell movement suggesting that Fractalkine signaling via CX3CR1 is important for the local migration of T cells in the tumor. However, if this pathway were dominant in deciding the recruitment of DCs and T cells, then such recruitment should be observed in melanoma brain tumor such as B16-F10 mouse tumor model. As this was not the case according to my observations in chapter 4, it indicates that there are other mechanisms that may be necessary for immune cell recruitment. Another explanation for differences in immune cell infiltration in cancer is their immunogenicity, which is an area of intense interest. Another possibility is that different cancer cells may vary in the extent to which they can induce cleavage and secretion of Fractalkine into the circulation. Therefore, more work is needed to evaluate the role of MMPs such as ADAM10 and 17 in the different tumor models as a potential mechanism underlying the differences in immune cell recruitment.

In human brain tumor patient specimens, CX3CR1 expression in CD14+ myeloid cells was reduced in both brain tumor tissues and in the peripheral blood, suggesting a similarity to our studies in mice in which CX3CR1-KO enhances brain tumor progression. However, a role for Fractalkine/CX3CR1 signaling in patient survival was unclear from preliminary analysis of TCGA datasets as the expression of CX3CR1 in

patient tissue was conducted in only very few patients and healthy tissues with insufficient statistical power. Regardless, there are several possibilities that might cause a reduction in the expression of CX3CR1 in CD14+ monocytes in human patient brain tumor including *de novo* genetic mutations, chemotherapy-induced downregulation, or preferential migration and localization of CX3CR1 low-expressing CD14+ monocytes in brain tumors that could have been preferentially sampled. In addition, CX3CR1 expression may be downregulated as a mechanism of tumor immune evasion or it may indicate disruption of fractalkine/CX3CR1 feedback loop. These possibilities will be dissected in future studies to gain better insight into the significance of reduced CX3CR1 expression on CD14+ monocytes in brain tumors of patients with GBM. Although more work needs to be done to elucidate the effect of reduced CX3CR1 mRNA expression in patients with GBM in functional human studies, the corresponding decrease in both brain myeloid cells and peripheral blood monocytes makes CX3CR1 expression an attractive tool for patient stratification for the purposes of prognostication, treatment, and follow-up.

Given these findings, the fractalkine/CX3CR1 chemokine pathway represents an attractive immunotherapeutic modulation pathway for guiding endogenous or adoptive transfer of T cells to brain tumor sites. Development of strategies modulating this pathway may be crucial in providing new immunotherapeutic strategies aimed at treating brain tumors.

CHAPTER 5: SUMMARY, GLOBAL DISCUSSION, AND FUTURE DIRECTIONS

5.1. Summary

Immune cells residing in tumor microenvironment play a critical role in tumor progression. In this thesis, I have documented important technical advances in intravital imaging of brain tumors that enable the visualization of immune cells in a near-physiological state. I have applied several innovative approaches and tumor models in elucidating the spatiotemporal dynamics of tumor-infiltrating T cells in relation to CD11c DCs. The method of *in situ* immune cell characterization in a novel myeloid cell mouse model reported here has revealed an unappreciated organization of myeloid cells in brain tumors. In addition, I have determined a mechanism of cellular control of T cell dynamics in the brain tumor microenvironment as well as a molecular chemokine cue that controls brain tumor progression, immune cell recruitment and migratory behavior. In sum, the data presented here provides a platform from which future studies could take off and in which multiple areas of cellular and molecular regulation could be better clarified and applied in the development of novel immunotherapy strategies.

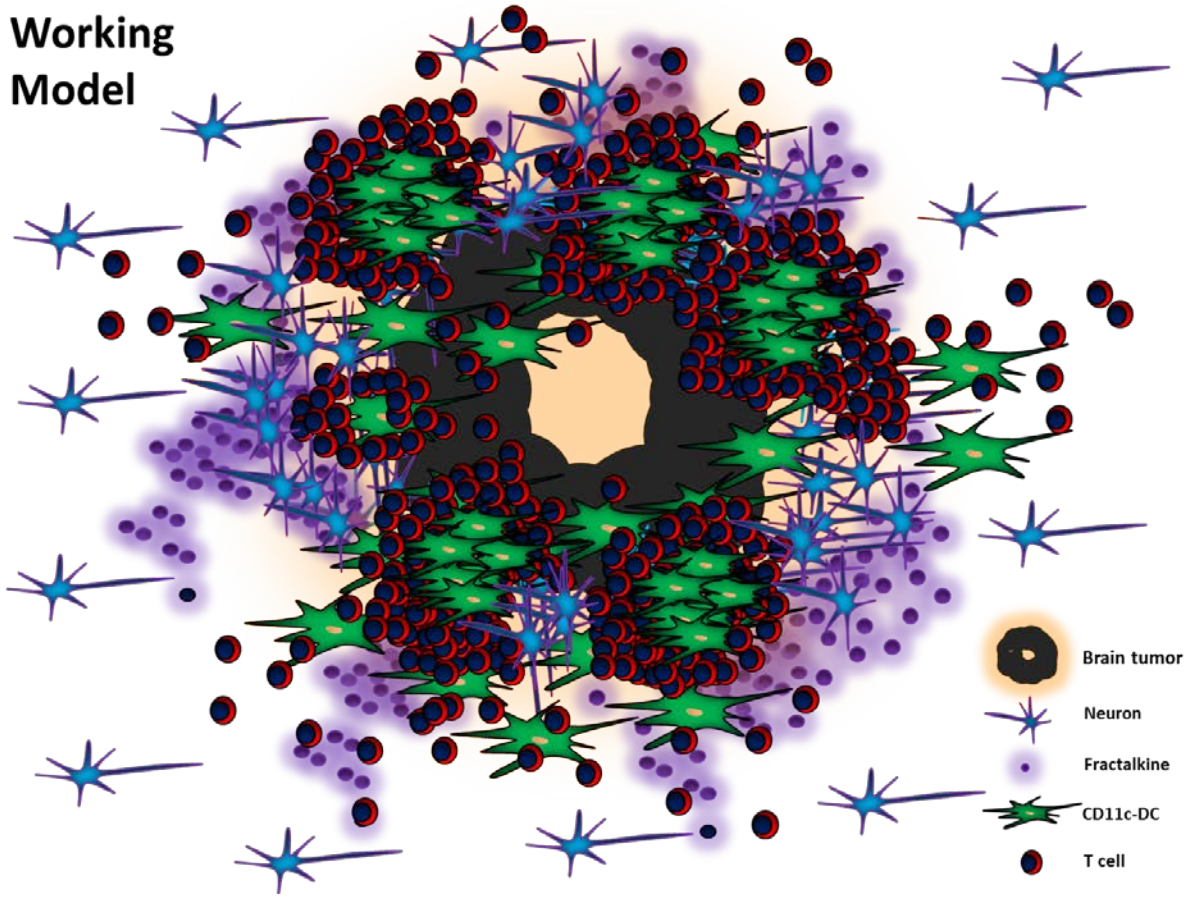

Figure 41. Model illustrating brain tumor immune surveillance.

The figure depicts a model in which growth of brain tumor causes damage of neurons and subsequent release of Fractalkine. DCs and T cells are recruited to the tumor, in part, by Fractalkine. DCs organize around the tumor margin and T cells form clusters around DCs. Other T cells migrate within the tumor.

5.2. Future implications of applying a near-physiological brain tumor imaging system

An elusive aspect of brain tumor immunology has been the lack of understanding of the reactivity of brain resident microglia to brain tumors beginning from a single cancer cell stage and the differential participation and contribution of resident and/or infiltrating myeloid immune cells in tumor progression. By using a new approach, I have clarified that microglia are generally non-reactive to cancer cell growth in the brain at early time points. Microglia were not recruited to the cancer cells, nor did they transform their morphology into an “activated” phenotype. In support of this, microglia somas were observed to remain relatively sessile despite appreciable tumor growth in brain tissue. Irrespective of the presence of cancer the microglia maintained probing activity, continuously extending and retracting dendritic processes toward vasculature and presumably other brain structures including neurons and astrocytes. Whether the scanning activity of microglia dendrites changes significantly in the presence of cancer cells in the brain was not apparent in the studies conducted here, but remains to be investigated. Even at later stages of advanced tumor growth, appreciable infiltration of microglia into the tumor was not observed. However, it is possible that a certain range of tumor size or brain tissue compression and/or damage unidentified here could trigger microglia to infiltrate into the tumor. Therefore, I am not able to absolutely exclude that microglia are active participants in brain tumor. This ambivalence is complicated by the fact that there is no appropriate technique available for the specific depletion of microglia to ascertain its real contribution to tumor progression. Some techniques that have been tested for depletion of microglia in mice brain include brain irradiation, Clodronate-liposome, Mac-1-Saporin, Colony Stimulating Factor 1 Receptor inhibitor (CSF1R; PLX5622), use of ganciclovir-mediated ablation on

tga20/CD11b Thymidine Kinase of Herpes Simplex Virus (HSVTK) transgenic mice, CX3CR1-DTR transgenic mice, and IL-34-KO mice[225,236,539-543]. Some of these systems have found use in the study of neurodegenerative diseases such as Alzheimer's or prion diseases where microglia but not extracranial myeloid cells are believed to play a major role in disease progression; however, none of these systems eliminate microglia specifically and most are sub-optimal in depletion efficacy. Also, microglia do not respond to irradiation strategies as they are radio-resistant[221,544]. At most, if an appreciable percentage of microglia is eliminated by any of the listed strategies, the depletion effect on extracranial myeloid cells in the periphery is disregarded. If the role of microglia is to be definitively distinguished from incoming myeloid cells in brain tumor studies, a system that targets only microglia for depletion will need to be established. Nevertheless, since myeloid cells such as monocytes but not microglia can be depleted by irradiation, combining this approach with chimeric reporter mouse bone marrow adoptive transfer experimental systems, in addition to the novel intravital near-physiological imaging system developed here, may help to partially answer this question. It is also possible that microglia may regulate brain tumor progression indirectly by interacting with other tumor immune infiltrates and this is an area of future study.

5.3. Outstanding questions on DC-T cell interactions

Anti-tumor immunity is known to depend on productive interactions between DCs and T cells in the lymph node[379,457]. Recently, however, there has been a paradigm shift from studying the *in vivo* dynamic interactions between DCs and T cells in the lymph node as a standard for understanding anti-tumor immune response to a new model involving real time visualization and mechanistic probing of DC-T cell

interactions in the tumor microenvironment [375,402,465,469,476]. This thesis has for the first time extended previous breakthroughs in imaging tumor DC-T cell interactions in tissues and organs such as the mammary tissue and skin to the brain. I have shown that there is robust infiltration of endogenous DCs and T cells to brain tumors and that their dynamics are correlated in space and time. Interestingly, T cells cluster around foci of DCs, maintain high migratory velocities even when proximal to DCs, and appear to make transient contacts with DCs. This is in contrast to previous studies that have employed model antigens such as ovalbumin to model tumor antigens and showed persistent interactions between DCs and T cells with long-lived contacts, that would suggest that prolonged DC/T cell interactions in an endogenous setting are infrequent [375,465]. Also, further cell tracking analysis revealed that T cells within clusters around DCs exhibit random motility when observed for short periods of imaging; however, they become highly confined around DCs in more prolonged observations especially in tumors undergoing rejection, which is not a known occurrence in human brain tumors. Apart from differences in cancer cell immunogenicity that may explain differences in interaction patterns of T cells with DCs, it will be important to determine whether migration of T cells around DCs is regulated by adhesion molecules like integrins or more diffusive molecules such as chemokines. Whether T cells receive differential levels of stimulation by the DCs or produce varying levels of cytotoxic molecules during tumor rejection versus progression was not investigated here, but should be examined in a future study.

Functional studies employing mouse models such as NFAT-GFP, Nurr77-GFP, or interferon-gamma (IFN-y)-GFP reporter transgenic mice in which the activation status of T cells can be observed in real time during cellular interactions will be useful

in determining the effect of DC-T cell interactions in either scenario. In addition, future application of technologies that visualize intracellular calcium flux in T cells will enable better understanding of potential DC-T cell immune synapses in tumor[393-395,545-548].

Reactivation of T cells in the tumor is a desired outcome in tumor immunotherapy[375]. Chronic unproductive activation or exhaustion of T cells in tumor has been well documented and targeted by checkpoint blockade immunotherapy[26,57]. However, little is known about the spatial interactions needed by T cells to integrate full activation signals for effective functioning *in vivo*. Even less is known about the molecular signals required for such interactions. An important question that remains unanswered is “how do T cells “find” DCs such as CD11c+ DCs to interact with within the multitude of different potential APCs in the tumor microenvironment and what factors lead to the formation of T cell clusters around DCs?” This is crucial to understand because it could guide therapeutic strategies that aim to enhance the recruitment of endogenous and exogenous transferred T cells to the tumor microenvironment.

Bear in mind that the novel triple myeloid reporter mouse established and evaluated here is an attempt to better understand the diverse myeloid cells *in situ* in tumor microenvironment; however, it likely does not reveal all myeloid cells that could potentially infiltrate brain tumor. In addition, although CD11c is highly expressed by DCs, some monocytes and macrophages express this marker. Therefore, to partly answer the question stated above, models that are engineered for visualization of spectrally distinct DC subsets such as conventional DCs in addition to macrophages, monocytes, and T cells will have to be established in order to delineate the interaction patterns of T cells within a diverse pool of myeloid cells.

Another equally pertinent question is how T cells migrate between DCs and the adjacent tumor and determine which cancer cell(s) to attack or kill; Do T cells kill better in prolonged interactions with tumor or in repeated on-off brief contacts? Do T cells that have previously killed continue in a killing “spree” (serial killing) or do they migrate back to DCs to be re-activated? Are lone T cells enough to effectively kill single cancer cells or does the killing efficacy increase in a T cell number-dependent manner in which more than one T cell makes contact with a cancer cell? Are cancer cells being killed when T cells are simultaneously contacting both DCs and cancer cells or can T cells kill cancer cells indirectly via DCs while maintaining DC-T cell contact? These are important questions that must be answered *in vivo* to better understand ways of improving T cell killing efficiency.

In observations documented here, active fragmentation of tumor and cancer cells was observed in association with T cells stably contacting DCs and/or tumor. An interesting speculation that arises from this is whether a mechanism of tumor killing by T cells involves initial disruption of adhesion molecules between cancer cells in the tumor before T cell-derived cytotoxic molecules are released or whether tumor fragmentation is only sequelae of a killing event. This seems plausible because the compact architecture of solid tumors may prevent effective T cell infiltration and killing. Therefore, if T cells are to engage cancer cells effectively, individual cancer cell surface area may have to be increased by mechanisms that cause disruption of cell-cell adhesion molecules in a tumor bulk. Whether T cells begin killing by first identifying and targeting weak links within the tumor is an interesting idea open for exploration.

Another important finding in this study is the dominant control exhibited by CD11c DCs on T cell retention and motility in brain tumor. This is in contrast with

previous studies in other tissues suggesting that T cells may be prevented from performing surveillance function in the tumor by being held in unproductive interactions with DCs[465]. In fact, when we adoptively transferred small numbers of T cells and DCs into brain tumor-bearing mice, T cells surprisingly localized in DC niches in the tumor, indicating that T cell homing and localization may actually be dependent on DCs. It also raises questions as to the functions played by specific myeloid cell populations in the tumor. Do some myeloid cell subsets synergize with DCs in retaining T cells? Do T cells exist in a Yin Yang situation in which their myeloid interaction partner is determined by the tumor cytokine milieu? Does the tumor host organ determine what interaction partners T cells will preferentially engage with? Even within the T cell population, the difference in the patterns of interaction between individual T cell subsets with tumor-associated myeloid cells is yet to be determined. It will be critical to evaluate the interaction patterns of Tregs and its potential myeloid cell partners in the tumor as this is an attractive T cell target for enhancing the efficacy of immunotherapy. Future studies should also determine the cellular and molecular regulators of Treg retention and motility as this may provide insight into potential targets applicable in both tumor immunology as well as autoimmune studies.

The neuronal chemokine Fractalkine has been implicated in cancer progression as well as in the regulation of immune cells[419]. The contextual elucidation of Fractalkine expression in brain tumor in relation to how tumor-associated myeloid cells are organized was achieved in this study. In observing robust Fractalkine expression at the margin of the tumor, it is tempting to speculate that the tumor directed tissue injury; in particular stress or damage impacted on adjacent neurons that may guide tumor immune surveillance. The idea that the innate immune system is capable of detecting

and responding to DAMPs via PRRs in host sterile tissue or noninfectious states lends support to this speculation[112,113,549-552].

There are several types of DAMPs including chromatin-associated high-mobility group box 1 (HMGB1), heat shock proteins (HSPs), deoxyribonucleotide adenine triphosphate (DNA), ribonucleotide adenine triphosphate (RNA), S100 molecules, purine metabolites such as adenosine triphosphate (ATP), and hyaluronan fragments[549,553-555]. Examples of PRRs utilized in the detection of DAMPs include Toll-like, RIG-I-like, and NOD-like receptor families. Interestingly, DAMP molecules such as S100 are expressed by neurons and glial cells and are utilized clinically to assess for brain injury[553-555]. In addition, pathways including ATP/purinergic receptors and HSPs are involved in neuronal and glial physiologic functions such as neurotransmission. Whether the signaling of these molecules engage innate myeloid cell PRRs at the margin of brain tumor, initiate innate immune responses and synergize with neuron-derived fractalkine to regulate T cell surveillance will be an interesting area to explore. In partial support of this idea, the data here shows that CX3CR1-GFP+ CD11c DCs and T cells organize around the margin of brain tumor, and in the absence of Fractalkine/CX3CR1 signaling, DCs and T cell numbers were decreased, and the motility of the few tumor-infiltrating T cells was more diffuse. Although it has long been established that the premise of immune surveillance is based on T cell recognition of tumor-associated antigens, it will be interesting to explore whether reaction to tissue injury in and of itself is enough to set off a parallel T cell surveillance mechanism in tumor. In fact, the immune infiltrates during wound healing bear strong similarity to those in tumors, and cancer has been suitably termed “a wound that never heals[35].” In this regard, groups of antigen non-specific T cells identified in tumor and named

“bystander T cells” have unveiled an interesting area in tumor immunology. Whether “bystander T cells” are recruited due to the tumor or tissue damage remains a matter of speculation. In support of the latter, a study showed that bystander T cells can be redirected to kill the stromal component (also a component of wounds) thereby causing tumor regression[556]. Nevertheless, one of the goals of future studies should be focused on elucidating the signals governing the recruitment of “bystander” T cells to the tumor, determine their interaction partners in the tumor and how they differ from antigen-experienced T cells, delineate the factors that regulate them, and potentially manipulate them for therapy.

5.4. Improvement in intravital imaging of immune cell dynamics in tumor

Generally, the extent of visualization during intravital imaging is limited by both the diffraction index of the tissue being imaged and the numerical aperture of the imaging objective[441,557,558]. In particular, intravital imaging in the brain is complicated by the layers of protective tissue and the high lipid content of brain cells, which increase light scattering and reduces the depth of tissue that can be sampled[441]. Although micro-endoscopes have been used for deep tissue imaging of tumor in mice brain, the traumatic nature of this approach may confound real immune cell behavior and function[559]. In addition, recent development of tissue “clearing”, which is a systematic process that has been applied to eliminate lipid from the brain and preserves only cellular architecture, has enabled high-resolution visualization of deep brain regions that were otherwise unreachable by previous techniques; however, such techniques can only be applied to non-living fixed brain tissues[560,561]. Another limitation in imaging is the numerical aperture of the imaging objective lens[561]. This limits sampling of immune cell interactions in large tumors located in a three-dimensional space and the

extent to which analysis can be done to understand the behavior of T cells in the tumor. In general, despite the advantage of two-photon microscopes over confocal imaging in terms of depth and other qualities, imaging large and deep areas of the intact brain still remains a challenge.

5.5. Significance of this study and implications for cancer immunotherapy

I have developed and applied a novel experimental system in illuminating the early immune cell events in brain tumor beginning at a single cell level. In combination with this, I have applied broadly conventional imaging approaches in studying immune cell dynamics in different brain tumors and elucidated DC-T cell interactions. Given the differences in immune cell recruitment and tumor progression in the tumor models used, it will be important to profile tumor cell genes from each tumor type as well as sequence the antigens presumably recognized by T cells to create a clearer picture of the differences between experimental tumor types and enhance studies that may be relevant in better understanding human tumors. GEMM tumor models are the gold standard for understanding biological phenomena and especially for translating research findings to the clinic. Therefore, it will be crucial to evaluate DC-T cell interactions in appropriate GEMM models that harbor genetic mutations that are known to drive progression of human tumors and possibly contribute to tumor immunogenicity.

I show here that myeloid cells are organized in distinct compartments within brain tumor microenvironment. Importantly, CD11c+ DCs reside mostly at the tumor margin. However, present analysis of tumor immune cell infiltration in patients with brain tumor is done using tumor biopsy specimen obtained from within the core of the tumor that may not truly reflect the immune infiltrates in the tumor microenvironment.

Therefore, the findings here should be translated to the clinic to guide neurosurgical biopsy procedures for immunological evaluation especially when immunotherapy strategies are being considered. I also show that CD11c+ DCs and T cells are correlated in space and that CD11c+ DCs control the retention and motility of effector T cells in brain tumors. Consistently, tissue-resident memory T cells have also been shown to be preferentially organized around DCs for prolonged periods after clearance of model viral infections in mice brain[371]. This has implications for brain tumor immunotherapy as interactions between T cells and DCs in brain tumors has been unappreciated as opposed to microglia and macrophages. Identifying and understanding potential molecular signals that control recruitment, retention, and survival of DCs in the tumor could present targets for modulating anti-tumor immune response, for example by specifically eliminating tumor-infiltrating DCs and associated T cells molecularly, and replacing the tumor microenvironment with “new” immune cells in addition to therapies that prevent tumor-mediated immune suppression. This strategy may find relevance in cellular transplantation in which whole body radiation, which could be injurious to normal tissue, is used to eliminate immune cells such as T cells before adoptive transfer of exogenous cells. Further, since DCs and T cells appear to work together during anti-tumor immune response, another strategy for tumor immunotherapy could entail adoptive transfer of competent antigen-presenting DCs and cytotoxic T cells serially or simultaneously into patients rather than conventional approaches employing either DCs of T cells exclusively. This strategy may aid in the persistence of adoptively transferred T cells in the tumor. Also, in addition to adoptive transfer of DCs, adjuvants such as Flt3-ligand vaccine (FVAX) may be used to stimulate increase in endogenous DC numbers in situations where exogenous DC cell

culture may produce low yield or alterations in DC functions[470]. Another avenue for application is in checkpoint blockade immunotherapy. The present goal for this type of therapy is to increase the percentage of patients that respond to this treatment strategy. Therefore, based on the data here, there is compelling reason to examine the composition of DCs in brain tumor or other tumor types in patients before initiating treatment or in patients who show partial or no response to treatment to determine whether lack of DCs may play a role in this regard. This could serve as a method of predicting treatment response. There is also support for combining DC treatment methods such as adoptive cell transfer or FVAX with T cell checkpoint blockade. However, more work needs to be done to better understand how DCs may regulate T cells in tumor during checkpoint blockade immunotherapy in preclinical models.

In addition, I have also demonstrated a role for Fractalkine signaling in brain tumor progression and in the control of tumor-infiltrating T cell recruitment and migration. Although I have not directly elaborated on the function of Fractalkine ligand in tumor progression or immune cell dynamics, this molecular pathway is an attractive target for modulating immune cells and potentially enhancing cancer immunotherapy. A major goal in adoptive T cell therapy in which infusion of exogenous T cell infiltrating lymphocytes or CAR T cells is done in patients with tumor, is to successfully direct the infused T cells to the tissue of interest. Thus, engineering CAR T cells with chemokine receptors such as CX3CR1 may help enhance cellular migration to the tumor. However, further studies are required to understand whether there is a functional significance to the changes in Fractalkine receptor CX3CR1, in GBM patients, and whether mouse observations are applicable in human brain tumor. Another aspect of this pathway that could be potentially modulated is the expression of ADAM10 and 17.

These MMPs are needed for Fractalkine cleavage and secretion into the circulation. Therefore, strategies that increase their expression may help maintain the secretion and levels of soluble Fractalkine in the circulation. This may assist in preventing downregulation of CX3CR1 expression in anti-tumor myeloid cells[562]. However, more work is required to better understand the regulating mechanisms involved in this process.

In sum, I have elucidated the dynamic behavior of immune cells in brain tumor and the studies conducted in this thesis have revealed novel cellular and molecular regulatory mechanisms in immune cell recruitment and interaction. This work paves way for exploration of other mechanisms involved in the regulation of brain tumor immune surveillance and potentially other cancer types.

BIBLIOGRAPHY

1. Janeway CA, Jr. How the immune system protects the host from infection. Microbes and infection / Institut Pasteur 2001;3:1167-71.
2. Medzhitov R, Janeway CA, Jr. Decoding the patterns of self and nonself by the innate immune system. Science 2002;296:298-300.
3. Yuan TL, Cantley LC. PI3K pathway alterations in cancer: variations on a theme. Oncogene 2008;27:5497-510.
4. Fruman DA, Rommel C. PI3K and cancer: lessons, challenges and opportunities. Nature reviews Drug discovery 2014;13:140-56.
5. Cizkova M, Susini A, Vacher S, et al. PIK3CA mutation impact on survival in breast cancer patients and in ERalpha, PR and ERBB2-based subgroups. Breast cancer research : BCR 2012;14:R28.
6. Li J, Yen C, Liaw D, et al. PTEN, a putative protein tyrosine phosphatase gene mutated in human brain, breast, and prostate cancer. Science 1997;275:1943-7.
7. Tomasetti C, Vogelstein B, Parmigiani G. Half or more of the somatic mutations in cancers of self-renewing tissues originate prior to tumor initiation. Proceedings of the National Academy of Sciences of the United States of America 2013;110:1999-2004.
8. Alexandrov LB, Nik-Zainal S, Wedge DC, et al. Signatures of mutational processes in human cancer. Nature 2013;500:415-21.
9. Alexandrov LB, Nik-Zainal S, Wedge DC, Campbell PJ, Stratton MR. Deciphering signatures of mutational processes operative in human cancer. Cell reports 2013;3:246-59.
10. Stratton MR, Campbell PJ, Futreal PA. The cancer genome. Nature 2009;458:719-24.
11. Pleasance ED, Cheetham RK, Stephens PJ, et al. A comprehensive catalogue of somatic mutations from a human cancer genome. Nature 2010;463:191-6.
12. Olivier M, Hollstein M, Hainaut P. TP53 mutations in human cancers: origins, consequences, and clinical use. Cold Spring Harbor perspectives in biology 2010;2:a001008.
13. Palmero EI, Achatz MI, Ashton-Prolla P, Olivier M, Hainaut P. Tumor protein 53 mutations and inherited cancer: beyond Li-Fraumeni syndrome. Current opinion in oncology 2010;22:64-9.
14. Puente XS, Pinyol M, Quesada V, et al. Whole-genome sequencing identifies recurrent mutations in chronic lymphocytic leukaemia. Nature 2011;475:101-5.
15. Cancer Genome Atlas N. Comprehensive molecular characterization of human colon and rectal cancer. Nature 2012;487:330-7.
16. Nik-Zainal S, Davies H, Staaf J, et al. Landscape of somatic mutations in 560 breast cancer whole-genome sequences. Nature 2016;534:47-54.
17. Stransky N, Egloff AM, Tward AD, et al. The mutational landscape of head and neck squamous cell carcinoma. Science 2011;333:1157-60.
18. Peifer M, Fernandez-Cuesta L, Sos ML, et al. Integrative genome analyses identify key somatic driver mutations of small-cell lung cancer. Nature genetics 2012;44:1104-10.
19. Pronobis MI, Peifer M. Wnt signaling: the many interfaces of beta-catenin. Current biology : CB 2012;22:R137-9.

20. Heukamp LC, Thor T, Schramm A, et al. Targeted expression of mutated ALK induces neuroblastoma in transgenic mice. Science translational medicine 2012;4:141ra91.
21. Hodis E, Watson IR, Kryukov GV, et al. A landscape of driver mutations in melanoma. Cell 2012;150:251-63.
22. Brennan CW, Verhaak RG, McKenna A, et al. The somatic genomic landscape of glioblastoma. Cell 2013;155:462-77.
23. Rohle D, Popovici-Muller J, Palaskas N, et al. An inhibitor of mutant IDH1 delays growth and promotes differentiation of glioma cells. Science 2013;340:626-30.
24. Dunn GP, Bruce AT, Ikeda H, Old LJ, Schreiber RD. Cancer immunoediting: from immunosurveillance to tumor escape. Nature immunology 2002;3:991-8.
25. Wu S, Powers S, Zhu W, Hannun YA. Substantial contribution of extrinsic risk factors to cancer development. Nature 2016;529:43-7.
26. Curran MA, Montalvo W, Yagita H, Allison JP. PD-1 and CTLA-4 combination blockade expands infiltrating T cells and reduces regulatory T and myeloid cells within B16 melanoma tumors. Proceedings of the National Academy of Sciences of the United States of America 2010;107:4275-80.
27. Joyce JA, Pollard JW. Microenvironmental regulation of metastasis. Nature reviews Cancer 2009;9:239-52.
28. Kitamura T, Qian BZ, Soong D, et al. CCL2-induced chemokine cascade promotes breast cancer metastasis by enhancing retention of metastasis-associated macrophages. The Journal of experimental medicine 2015;212:1043-59.
29. Nemunaitis J. Vaccines in cancer: GVAX, a GM-CSF gene vaccine. Expert review of vaccines 2005;4:259-74.
30. Quezada SA, Peggs KS, Curran MA, Allison JP. CTLA4 blockade and GM-CSF combination immunotherapy alters the intratumor balance of effector and regulatory T cells. The Journal of clinical investigation 2006;116:1935-45.
31. Tumeh PC, Harview CL, Yearley JH, et al. PD-1 blockade induces responses by inhibiting adaptive immune resistance. Nature 2014;515:568-71.
32. Zou W. Immunosuppressive networks in the tumour environment and their therapeutic relevance. Nature reviews Cancer 2005;5:263-74.
33. Rosenberg SA. IL-2: the first effective immunotherapy for human cancer. Journal of immunology 2014;192:5451-8.
34. Rosenberg SA, Packard BS, Aebersold PM, et al. Use of tumor-infiltrating lymphocytes and interleukin-2 in the immunotherapy of patients with metastatic melanoma. A preliminary report. The New England journal of medicine 1988;319:1676-80.
35. Dvorak HF. Tumors: wounds that do not heal. Similarities between tumor stroma generation and wound healing. The New England journal of medicine 1986;315:1650-9.
36. Winkler AE, Brotman JJ, Pittman ME, et al. CXCR3 enhances a T-cell-dependent epidermal proliferative response and promotes skin tumorigenesis. Cancer research 2011;71:5707-16.
37. Dvorak HF, Dickersin GR, Dvorak AM, Manseau EJ, Pyne K. Human breast carcinoma: fibrin deposits and desmoplasia. Inflammatory cell type and distribution. Microvasculature and infarction. Journal of the National Cancer Institute 1981;67:335-45.
38. Dvorak HF, Quay SC, Orenstein NS, et al. Tumor shedding and coagulation. Science 1981;212:923-4.

39. Leibovich SJ, Ross R. The role of the macrophage in wound repair. A study with hydrocortisone and antimacrophage serum. The American journal of pathology 1975;78:71-100.
40. Tremblay G. Stromal aspects of breast carcinoma. Experimental and molecular pathology 1979;31:248-60.
41. Knighton DR, Hunt TK, Scheuenstuhl H, Halliday BJ, Werb Z, Banda MJ. Oxygen tension regulates the expression of angiogenesis factor by macrophages. Science 1983;221:1283-5.
42. Swann JB, Vesely MD, Silva A, et al. Demonstration of inflammation-induced cancer and cancer immunoediting during primary tumorigenesis. Proceedings of the National Academy of Sciences of the United States of America 2008;105:652-6.
43. Ikeda H, Old LJ, Schreiber RD. The roles of IFN gamma in protection against tumor development and cancer immunoediting. Cytokine & growth factor reviews 2002;13:95-109.
44. Ramana CV, Gil MP, Schreiber RD, Stark GR. Stat1-dependent and -independent pathways in IFN-gamma-dependent signaling. Trends in immunology 2002;23:96-101.
45. Vesely MD, Schreiber RD. Cancer immunoediting: antigens, mechanisms, and implications to cancer immunotherapy. Annals of the New York Academy of Sciences 2013;1284:1-5.
46. Hanahan D, Weinberg RA. The hallmarks of cancer. Cell 2000;100:57-70.
47. Hanahan D, Weinberg RA. Hallmarks of cancer: the next generation. Cell 2011;144:646-74.
48. Smyth MJ, Godfrey DI, Trapani JA. A fresh look at tumor immunosurveillance and immunotherapy. Nature immunology 2001;2:293-9.
49. Williams CB, Yeh ES, Soloff AC. Tumor-associated macrophages: unwitting accomplices in breast cancer malignancy. NPJ breast cancer 2016;2.
50. Haribhai D, Ziegelbauer J, Jia S, et al. Alternatively Activated Macrophages Boost Induced Regulatory T and Th17 Cell Responses during Immunotherapy for Colitis. Journal of immunology 2016;196:3305-17.
51. Leek RD, Lewis CE, Whitehouse R, Greenall M, Clarke J, Harris AL. Association of macrophage infiltration with angiogenesis and prognosis in invasive breast carcinoma. Cancer research 1996;56:4625-9.
52. Stockmann C, Doedens A, Weidemann A, et al. Deletion of vascular endothelial growth factor in myeloid cells accelerates tumorigenesis. Nature 2008;456:814-8.
53. Yang J, Liao D, Chen C, et al. Tumor-associated macrophages regulate murine breast cancer stem cells through a novel paracrine EGFR/Stat3/Sox-2 signaling pathway. Stem cells 2013;31:248-58.
54. Condeelis J, Pollard JW. Macrophages: obligate partners for tumor cell migration, invasion, and metastasis. Cell 2006;124:263-6.
55. Chen Q, Zhang XH, Massague J. Macrophage binding to receptor VCAM-1 transmits survival signals in breast cancer cells that invade the lungs. Cancer cell 2011;20:538-49.
56. Hanson HL, Donermeyer DL, Ikeda H, et al. Eradication of established tumors by CD8+ T cell adoptive immunotherapy. Immunity 2000;13:265-76.
57. Hamid O, Robert C, Daud A, et al. Safety and tumor responses with lambrolizumab (anti-PD-1) in melanoma. The New England journal of medicine 2013;369:134-44.

58. Larkin J, Chiarion-Sileni V, Gonzalez R, et al. Combined Nivolumab and Ipilimumab or Monotherapy in Untreated Melanoma. The New England journal of medicine 2015;373:23-34.
59. Wolchok JD, Kluger H, Callahan MK, et al. Nivolumab plus ipilimumab in advanced melanoma. The New England journal of medicine 2013;369:122-33.
60. Ansell SM, Lesokhin AM, Borrello I, et al. PD-1 blockade with nivolumab in relapsed or refractory Hodgkin's lymphoma. The New England journal of medicine 2015;372:311-9.
61. Matsushita H, Vesely MD, Koboldt DC, et al. Cancer exome analysis reveals a T-cell-dependent mechanism of cancer immunoediting. Nature 2012;482:400-4.
62. Johanns TM, Miller CA, Dorward IG, et al. Immunogenomics of Hypermutated Glioblastoma: A Patient with Germline POLE Deficiency Treated with Checkpoint Blockade Immunotherapy. Cancer discovery 2016;6:1230-6.
63. Johanns TM, Ward JP, Miller CA, et al. Endogenous Neoantigen-Specific CD8 T Cells Identified in Two Glioblastoma Models Using a Cancer Immunogenomics Approach. Cancer immunology research 2016;4:1007-15.
64. Zolkind P, Dunn GP, Lin T, Griffith M, Griffith OL, Uppaluri R. Neoantigens in immunotherapy and personalized vaccines: Implications for head and neck squamous cell carcinoma. Oral oncology 2016.
65. Stoll G, Bindea G, Mlecnik B, Galon J, Zitvogel L, Kroemer G. Meta-analysis of organ-specific differences in the structure of the immune infiltrate in major malignancies. Oncotarget 2015;6:11894-909.
66. Stoll G, Zitvogel L, Kroemer G. Differences in the composition of the immune infiltrate in breast cancer, colorectal carcinoma, melanoma and non-small cell lung cancer: A microarray-based meta-analysis. Oncoimmunology 2016;5:e1067746.
67. Miloud T, Fiegler N, Suffner J, Hammerling GJ, Garbi N. Organ-specific cellular requirements for in vivo dendritic cell generation. Journal of immunology 2012;188:1125-35.
68. Carson MJ, Doose JM, Melchior B, Schmid CD, Ploix CC. CNS immune privilege: hiding in plain sight. Immunological reviews 2006;213:48-65.
69. Medawar PB. Immunity to homologous grafted skin; the fate of skin homografts transplanted to the brain, to subcutaneous tissue, and to the anterior chamber of the eye. British journal of experimental pathology 1948;29:58-69.
70. Stutman O. Chemical carcinogenesis in nude mice: comparison between nude mice from homozygous matings and heterozygous matings and effect of age and carcinogen dose. Journal of the National Cancer Institute 1979;62:353-8.
71. Stutman O. Tumor development after 3-methylcholanthrene in immunologically deficient athymic-nude mice. Science 1974;183:534-6.
72. Cserr HF, Harling-Berg CJ, Knopf PM. Drainage of brain extracellular fluid into blood and deep cervical lymph and its immunological significance. Brain pathology 1992;2:269-76.
73. Ifergan I, Kebir H, Alvarez JI, et al. Central nervous system recruitment of effector memory CD8+ T lymphocytes during neuroinflammation is dependent on alpha4 integrin. Brain : a journal of neurology 2011;134:3560-77.
74. Larochelle C, Alvarez JI, Prat A. How do immune cells overcome the blood-brain barrier in multiple sclerosis? FEBS letters 2011;585:3770-80.
75. McMenamin PG. Distribution and phenotype of dendritic cells and resident tissue macrophages in the dura mater, leptomeninges, and choroid plexus of the rat

brain as demonstrated in wholemount preparations. The Journal of comparative neurology 1999;405:553-62.
76. Ifergan I, Kebir H, Terouz S, et al. Role of Ninjurin-1 in the migration of myeloid cells to central nervous system inflammatory lesions. Annals of neurology 2011;70:751-63.
77. Greenwood J, Heasman SJ, Alvarez JI, Prat A, Lyck R, Engelhardt B. Review: leucocyte-endothelial cell crosstalk at the blood-brain barrier: a prerequisite for successful immune cell entry to the brain. Neuropathology and applied neurobiology 2011;37:24-39.
78. Cravens PD, Lipsky PE. Dendritic cells, chemokine receptors and autoimmune inflammatory diseases. Immunology and cell biology 2002;80:497-505.
79. Alvarez JI, Cayrol R, Prat A. Disruption of central nervous system barriers in multiple sclerosis. Biochimica et biophysica acta 2011;1812:252-64.
80. Cserr HF, Knopf PM. Cervical lymphatics, the blood-brain barrier and the immunoreactivity of the brain: a new view. Immunology today 1992;13:507-12.
81. Louis DN, Perry A, Reifenberger G, et al. The 2016 World Health Organization Classification of Tumors of the Central Nervous System: a summary. Acta neuropathologica 2016;131:803-20.
82. Louveau A, Smirnov I, Keyes TJ, et al. Structural and functional features of central nervous system lymphatic vessels. Nature 2015;523:337-41.
83. Bradstreet JJ, Ruggiero M, Pacini S. Commentary: Structural and functional features of central nervous system lymphatic vessels. Frontiers in neuroscience 2015;9:485.
84. Fecci PE, Heimberger AB, Sampson JH. Immunotherapy for primary brain tumors: no longer a matter of privilege. Clinical cancer research : an official journal of the American Association for Cancer Research 2014;20:5620-9.
85. Gedeon PC, Riccione KA, Fecci PE, Sampson JH. Antibody-based immunotherapy for malignant glioma. Seminars in oncology 2014;41:496-510.
86. Mitchell DA, Batich KA, Gunn MD, et al. Tetanus toxoid and CCL3 improve dendritic cell vaccines in mice and glioblastoma patients. Nature 2015;519:366-9.
87. Reardon DA, Gokhale PC, Klein SR, et al. Glioblastoma Eradication Following Immune Checkpoint Blockade in an Orthotopic, Immunocompetent Model. Cancer immunology research 2016;4:124-35.
88. Weller M, Fontana A. The failure of current immunotherapy for malignant glioma. Tumor-derived TGF-beta, T-cell apoptosis, and the immune privilege of the brain. Brain research Brain research reviews 1995;21:128-51.
89. Ceccarelli M, Barthel FP, Malta TM, et al. Molecular Profiling Reveals Biologically Discrete Subsets and Pathways of Progression in Diffuse Glioma. Cell 2016;164:550-63.
90. Ghazi SO, Stark M, Zhao Z, et al. Cell of origin determines tumor phenotype in an oncogenic Ras/p53 knockout transgenic model of high-grade glioma. Journal of neuropathology and experimental neurology 2012;71:729-40.
91. Lindberg N, Kastemar M, Olofsson T, Smits A, Uhrbom L. Oligodendrocyte progenitor cells can act as cell of origin for experimental glioma. Oncogene 2009;28:2266-75.
92. Liu C, Sage JC, Miller MR, et al. Mosaic analysis with double markers reveals tumor cell of origin in glioma. Cell 2011;146:209-21.

93. Modrek AS, Bayin NS, Placantonakis DG. Brain stem cells as the cell of origin in glioma. World journal of stem cells 2014;6:43-52.
94. Monje M, Mitra SS, Freret ME, et al. Hedgehog-responsive candidate cell of origin for diffuse intrinsic pontine glioma. Proceedings of the National Academy of Sciences of the United States of America 2011;108:4453-8.
95. Verhaak RG, Hoadley KA, Purdom E, et al. Integrated genomic analysis identifies clinically relevant subtypes of glioblastoma characterized by abnormalities in PDGFRA, IDH1, EGFR, and NF1. Cancer cell 2010;17:98-110.
96. Wang Q, Hu X, Hu B, et al. Tumor evolution of glioma intrinsic gene expression subtype associates with immunological changes in the microenvironment. bioRxiv 2016:052076.
97. Kalluri R, Weinberg RA. The basics of epithelial-mesenchymal transition. The Journal of clinical investigation 2009;119:1420-8.
98. Mani SA, Yang J, Brooks M, et al. Mesenchyme Forkhead 1 (FOXC2) plays a key role in metastasis and is associated with aggressive basal-like breast cancers. Proceedings of the National Academy of Sciences of the United States of America 2007;104:10069-74.
99. Chaffer CL, San Juan BP, Lim E, Weinberg RA. EMT, cell plasticity and metastasis. Cancer metastasis reviews 2016;35:645-54.
100. Fidler IJ. The Biology of Brain Metastasis: Challenges for Therapy. Cancer journal 2015;21:284-93.
101. Nathoo N, Chahlavi A, Barnett GH, Toms SA. Pathobiology of brain metastases. Journal of clinical pathology 2005;58:237-42.
102. Nguyen DX, Bos PD, Massague J. Metastasis: from dissemination to organ-specific colonization. Nature reviews Cancer 2009;9:274-84.
103. Shweikeh F, Bukavina L, Saeed K, et al. Brain metastasis in bone and soft tissue cancers: a review of incidence, interventions, and outcomes. Sarcoma 2014;2014:475175.
104. Choi HJ, Cho BC, Sohn JH, et al. Brain metastases from hepatocellular carcinoma: prognostic factors and outcome: brain metastasis from HCC. Journal of neuro-oncology 2009;91:307-13.
105. Hatzoglou V, Patel GV, Morris MJ, et al. Brain metastases from prostate cancer: an 11-year analysis in the MRI era with emphasis on imaging characteristics, incidence, and prognosis. Journal of neuroimaging : official journal of the American Society of Neuroimaging 2014;24:161-6.
106. Amita M, Sudeep G, Rekha W, Yogesh K, Hemant T. Brain metastasis from cervical carcinoma--a case report. MedGenMed : Medscape general medicine 2005;7:26.
107. Al-Shamy G, Sawaya R. Management of brain metastases: the indispensable role of surgery. Journal of neuro-oncology 2009;92:275-82.
108. Eichler AF, Loeffler JS. Multidisciplinary management of brain metastases. The oncologist 2007;12:884-98.
109. Berghoff AS, Fuchs E, Ricken G, et al. Density of tumor-infiltrating lymphocytes correlates with extent of brain edema and overall survival time in patients with brain metastases. Oncoimmunology 2016;5:e1057388.
110. Berghoff AS, Ricken G, Wilhelm D, et al. Tumor infiltrating lymphocytes and PD-L1 expression in brain metastases of small cell lung cancer (SCLC). Journal of neuro-oncology 2016;130:19-29.

111. Mogensen TH. Pathogen recognition and inflammatory signaling in innate immune defenses. Clinical microbiology reviews 2009;22:240-73, Table of Contents.
112. Tang D, Kang R, Coyne CB, Zeh HJ, Lotze MT. PAMPs and DAMPs: signal 0s that spur autophagy and immunity. Immunological reviews 2012;249:158-75.
113. Unlu S, Tang S, Wang E, et al. Damage associated molecular pattern molecule-induced microRNAs (DAMPmiRs) in human peripheral blood mononuclear cells. PloS one 2012;7:e38899.
114. Janeway CA, Jr., Medzhitov R. Innate immune recognition. Annual review of immunology 2002;20:197-216.
115. Litman GW, Rast JP, Fugmann SD. The origins of vertebrate adaptive immunity. Nature reviews Immunology 2010;10:543-53.
116. Han BW, Herrin BR, Cooper MD, Wilson IA. Antigen recognition by variable lymphocyte receptors. Science 2008;321:1834-7.
117. Burnet FM. The concept of immunological surveillance. Progress in experimental tumor research 1970;13:1-27.
118. Medawar PB. Immunity to homologous grafted skin; the relationship between the antigens of blood and skin. British journal of experimental pathology 1946;27:15-24.
119. Medawar PB. Immunity to homologous grafted skin; the suppression of cell division in grafts transplanted to immunized animals. British journal of experimental pathology 1946;27:9-14.
120. Burnet FM. Implications of immunological surveillance for cancer therapy. Israel journal of medical sciences 1971;7:9-16.
121. Prehn RT. Immunological surveillance versus immunological stimulation of oncogenesis--a formal proof of the stimulation hypothesis. Advances in experimental medicine and biology 1982;155:77-85.
122. Swann JB, Smyth MJ. Immune surveillance of tumors. The Journal of clinical investigation 2007;117:1137-46.
123. Prehn RT. Immunomodulation of tumor growth. The American journal of pathology 1974;77:119-22.
124. van der Bruggen P, Traversari C, Chomez P, et al. A gene encoding an antigen recognized by cytolytic T lymphocytes on a human melanoma. Science 1991;254:1643-7.
125. Ikehara S, Pahwa RN, Fernandes G, Hansen CT, Good RA. Functional T cells in athymic nude mice. Proceedings of the National Academy of Sciences of the United States of America 1984;81:886-8.
126. Caulfield MJ, Stanko D, Isaak DD. Athymic (nude) mice fail to delete functional self-reactive helper T cells. Thymus 1993;22:91-6.
127. Spiess S, Kuhrober A, Schirmbeck R, Arden B, Reimann J. Diversity of functional T-cell receptor delta-chain transcripts from bone marrow cells of athymic nude mice. Immunology 1993;78:252-9.
128. Spiess S, Kuhrober A, Schirmbeck R, Reimann J. Bone marrow cells of athymic nude mice express functional T cell receptor alpha chain transcripts rearranged to V delta 2, 3, 4, 5, 6 genes. European journal of immunology 1992;22:1939-42.
129. van den Broek ME, Kagi D, Ossendorp F, et al. Decreased tumor surveillance in perforin-deficient mice. The Journal of experimental medicine 1996;184:1781-90.
130. Dunn GP, Old LJ, Schreiber RD. The immunobiology of cancer immunosurveillance and immunoediting. Immunity 2004;21:137-48.

131. Gil MP, Bohn E, O'Guin AK, et al. Biologic consequences of Stat1-independent IFN signaling. Proceedings of the National Academy of Sciences of the United States of America 2001;98:6680-5.
132. Mittal D, Gubin MM, Schreiber RD, Smyth MJ. New insights into cancer immunoediting and its three component phases--elimination, equilibrium and escape. Current opinion in immunology 2014;27:16-25.
133. Chan SR, Rickert CG, Vermi W, et al. Dysregulated STAT1-SOCS1 control of JAK2 promotes mammary luminal progenitor cell survival and drives ERalpha(+) tumorigenesis. Cell death and differentiation 2014;21:234-46.
134. Kaplan DH, Shankaran V, Dighe AS, et al. Demonstration of an interferon gamma-dependent tumor surveillance system in immunocompetent mice. Proceedings of the National Academy of Sciences of the United States of America 1998;95:7556-61.
135. Street SE, Cretney E, Smyth MJ. Perforin and interferon-gamma activities independently control tumor initiation, growth, and metastasis. Blood 2001;97:192-7.
136. Street SE, Trapani JA, MacGregor D, Smyth MJ. Suppression of lymphoma and epithelial malignancies effected by interferon gamma. The Journal of experimental medicine 2002;196:129-34.
137. Smyth MJ, Thia KY, Street SE, MacGregor D, Godfrey DI, Trapani JA. Perforin-mediated cytotoxicity is critical for surveillance of spontaneous lymphoma. The Journal of experimental medicine 2000;192:755-60.
138. Shinkai Y, Rathbun G, Lam KP, et al. RAG-2-deficient mice lack mature lymphocytes owing to inability to initiate V(D)J rearrangement. Cell 1992;68:855-67.
139. Shankaran V, Ikeda H, Bruce AT, et al. IFNgamma and lymphocytes prevent primary tumour development and shape tumour immunogenicity. Nature 2001;410:1107-11.
140. Girardi M, Oppenheim DE, Steele CR, et al. Regulation of cutaneous malignancy by gammadelta T cells. Science 2001;294:605-9.
141. O'Sullivan T, Dunn GP, Lacoursiere DY, Schreiber RD, Bui JD. Cancer immunoediting of the NK group 2D ligand H60a. Journal of immunology 2011;187:3538-45.
142. O'Sullivan T, Saddawi-Konefka R, Vermi W, et al. Cancer immunoediting by the innate immune system in the absence of adaptive immunity. The Journal of experimental medicine 2012;209:1869-82.
143. Schreiber RD, Old LJ, Smyth MJ. Cancer immunoediting: integrating immunity's roles in cancer suppression and promotion. Science 2011;331:1565-70.
144. Dunn GP, Old LJ, Schreiber RD. The three Es of cancer immunoediting. Annual review of immunology 2004;22:329-60.
145. Alvarez JI, Dodelet-Devillers A, Kebir H, et al. The Hedgehog pathway promotes blood-brain barrier integrity and CNS immune quiescence. Science 2011;334:1727-31.
146. Alvarez JI, Katayama T, Prat A. Glial influence on the blood brain barrier. Glia 2013;61:1939-58.
147. Engelhardt B. Immune cell entry into the central nervous system: involvement of adhesion molecules and chemokines. Journal of the neurological sciences 2008;274:23-6.
148. Muldoon LL, Alvarez JI, Begley DJ, et al. Immunologic privilege in the central nervous system and the blood-brain barrier. Journal of cerebral blood flow and metabolism : official journal of the International Society of Cerebral Blood Flow and Metabolism 2013;33:13-21.

149. Ben-Zvi A, Lacoste B, Kur E, et al. Mfsd2a is critical for the formation and function of the blood-brain barrier. Nature 2014;509:507-11.
150. Hagan N, Ben-Zvi A. The molecular, cellular, and morphological components of blood-brain barrier development during embryogenesis. Seminars in cell & developmental biology 2015;38:7-15.
151. Ballabh P, Braun A, Nedergaard M. The blood-brain barrier: an overview: structure, regulation, and clinical implications. Neurobiology of disease 2004;16:1-13.
152. van Tellingen O, Yetkin-Arik B, de Gooijer MC, Wesseling P, Wurdinger T, de Vries HE. Overcoming the blood-brain tumor barrier for effective glioblastoma treatment. Drug resistance updates : reviews and commentaries in antimicrobial and anticancer chemotherapy 2015;19:1-12.
153. Osswald M, Blaes J, Liao Y, et al. Impact of Blood-Brain Barrier Integrity on Tumor Growth and Therapy Response in Brain Metastases. Clinical cancer research : an official journal of the American Association for Cancer Research 2016.
154. Milojkovic Kerklaan B, van Tellingen O, Huitema AD, et al. Strategies to target drugs to gliomas and CNS metastases of solid tumors. Journal of neurology 2016;263:428-40.
155. Agarwal S, Sane R, Gallardo JL, Ohlfest JR, Elmquist WF. Distribution of gefitinib to the brain is limited by P-glycoprotein (ABCB1) and breast cancer resistance protein (ABCG2)-mediated active efflux. The Journal of pharmacology and experimental therapeutics 2010;334:147-55.
156. Mrass P, Weninger W. Immune cell migration as a means to control immune privilege: lessons from the CNS and tumors. Immunological reviews 2006;213:195-212.
157. Engelhardt B. The blood-central nervous system barriers actively control immune cell entry into the central nervous system. Current pharmaceutical design 2008;14:1555-65.
158. Prendergast CT, Anderton SM. Immune cell entry to central nervous system--current understanding and prospective therapeutic targets. Endocrine, metabolic & immune disorders drug targets 2009;9:315-27.
159. Klonowski KD, Williams KJ, Marzo AL, Blair DA, Lingenheld EG, Lefrancois L. Dynamics of blood-borne CD8 memory T cell migration in vivo. Immunity 2004;20:551-62.
160. Engelhardt B, Kappos L. Natalizumab: targeting alpha4-integrins in multiple sclerosis. Neuro-degenerative diseases 2008;5:16-22.
161. Griffin DE, Levine B, Tyor WR, Irani DN. The immune response in viral encephalitis. Seminars in immunology 1992;4:111-9.
162. Alt C, Laschinger M, Engelhardt B. Functional expression of the lymphoid chemokines CCL19 (ELC) and CCL 21 (SLC) at the blood-brain barrier suggests their involvement in G-protein-dependent lymphocyte recruitment into the central nervous system during experimental autoimmune encephalomyelitis. European journal of immunology 2002;32:2133-44.
163. Barkauskas DS, Dixon Dorand R, Myers JT, et al. Focal transient CNS vessel leak provides a tissue niche for sequential immune cell accumulation during the asymptomatic phase of EAE induction. Exp Neurol 2015;266:74-85.
164. Engelhardt B, Ransohoff RM. Capture, crawl, cross: the T cell code to breach the blood-brain barriers. Trends in immunology 2012;33:579-89.
165. Hickey WF. Migration of hematogenous cells through the blood-brain barrier and the initiation of CNS inflammation. Brain pathology 1991;1:97-105.

166. Hickey WF, Hsu BL, Kimura H. T-lymphocyte entry into the central nervous system. Journal of neuroscience research 1991;28:254-60.
167. Ransohoff RM, Engelhardt B. The anatomical and cellular basis of immune surveillance in the central nervous system. Nature reviews Immunology 2012;12:623-35.
168. Vajkoczy P, Laschinger M, Engelhardt B. Alpha4-integrin-VCAM-1 binding mediates G protein-independent capture of encephalitogenic T cell blasts to CNS white matter microvessels. The Journal of clinical investigation 2001;108:557-65.
169. Laschinger M, Vajkoczy P, Engelhardt B. Encephalitogenic T cells use LFA-1 for transendothelial migration but not during capture and initial adhesion strengthening in healthy spinal cord microvessels in vivo. European journal of immunology 2002;32:3598-606.
170. Reboldi A, Coisne C, Baumjohann D, et al. C-C chemokine receptor 6-regulated entry of TH-17 cells into the CNS through the choroid plexus is required for the initiation of EAE. Nature immunology 2009;10:514-23.
171. Odoardi F, Sie C, Streyl K, et al. T cells become licensed in the lung to enter the central nervous system. Nature 2012;488:675-9.
172. Brooks WH, Netsky MG, Normansell DE, Horwitz DA. Depressed cell-mediated immunity in patients with primary intracranial tumors. Characterization of a humoral immunosuppressive factor. The Journal of experimental medicine 1972;136:1631-47.
173. Brooks WH, Caldwell HD, Mortara RH. Immune responses in patients with gliomas. Surgical neurology 1974;2:419-23.
174. Brooks WH, Roszman TL, Rogers AS. Impairment of rosette-forming T lymphocytes in patients with primary intracranial tumors. Cancer 1976;37:1869-73.
175. Roszman TL, Brooks WH. Immunobiology of primary intracranial tumours. III. Demonstration of a qualitative lymphocyte abnormality in patients with primary brain tumours. Clinical and experimental immunology 1980;39:395-402.
176. Heimberger AB, Kong LY, Abou-Ghazal M, et al. The role of tregs in human glioma patients and their inhibition with a novel STAT-3 inhibitor. Clinical neurosurgery 2009;56:98-106.
177. Vandenberk L, Van Gool SW. Treg infiltration in glioma: a hurdle for antiglioma immunotherapy. Immunotherapy 2012;4:675-8.
178. Sonabend AM, Rolle CE, Lesniak MS. The role of regulatory T cells in malignant glioma. Anticancer research 2008;28:1143-50.
179. El Andaloussi A, Lesniak MS. An increase in CD4+CD25+FOXP3+ regulatory T cells in tumor-infiltrating lymphocytes of human glioblastoma multiforme. Neuro-oncology 2006;8:234-43.
180. Kaur G, Han SJ, Yang I, Crane C. Microglia and central nervous system immunity. Neurosurgery clinics of North America 2010;21:43-51.
181. Weller RO, Djuanda E, Yow HY, Carare RO. Lymphatic drainage of the brain and the pathophysiology of neurological disease. Acta neuropathologica 2009;117:1-14.
182. Kikuchi T, Akasaki Y, Irie M, Homma S, Abe T, Ohno T. Results of a phase I clinical trial of vaccination of glioma patients with fusions of dendritic and glioma cells. Cancer immunology, immunotherapy : CII 2001;50:337-44.
183. Soling A, Rainov NG. Dendritic cell therapy of primary brain tumors. Molecular medicine 2001;7:659-67.

184. Sloan AE, Dansey R, Zamorano L, et al. Adoptive immunotherapy in patients with recurrent malignant glioma: preliminary results of using autologous whole-tumor vaccine plus granulocyte-macrophage colony-stimulating factor and adoptive transfer of anti-CD3-activated lymphocytes. Neurosurgical focus 2000;9:e9.
185. Ogden AT, Horgan D, Waziri A, et al. Defective receptor expression and dendritic cell differentiation of monocytes in glioblastomas. Neurosurgery 2006;59:902-9; discussion 9-10.
186. Tyrinova TV, Leplina OY, Mishinov SV, et al. Cytotoxic activity of ex-vivo generated IFNalpha-induced monocyte-derived dendritic cells in brain glioma patients. Cellular immunology 2013;284:146-53.
187. Gousias K, von Ruecker A, Voulgari P, Simon M. Phenotypical analysis, relation to malignancy and prognostic relevance of ICOS+T regulatory and dendritic cells in patients with gliomas. Journal of neuroimmunology 2013;264:84-90.
188. Tyrinova TV, Leplina OY, Tikhonova MA, et al. CCL19/CCL21-Dependent Chemotaxis of Dendritic Cells in Healthy Individuals and Patients with Brain Tumors. Bulletin of experimental biology and medicine 2015;158:785-8.
189. Lowenstein PR. Immunology of viral-vector-mediated gene transfer into the brain: an evolutionary and developmental perspective. Trends in immunology 2002;23:23-30.
190. Barker CF, Billingham RE. The role of afferent lymphatics in the rejection of skin homografts. The Journal of experimental medicine 1968;128:197-221.
191. Yang I, Han SJ, Kaur G, Crane C, Parsa AT. The role of microglia in central nervous system immunity and glioma immunology. Journal of clinical neuroscience : official journal of the Neurosurgical Society of Australasia 2010;17:6-10.
192. Barker CF, Billingham RE. Immunologically privileged sites. Advances in immunology 1977;25:1-54.
193. Louveau A, Harris TH, Kipnis J. Revisiting the Mechanisms of CNS Immune Privilege. Trends in immunology 2015;36:569-77.
194. Aspelund A, Antila S, Proulx ST, et al. A dural lymphatic vascular system that drains brain interstitial fluid and macromolecules. The Journal of experimental medicine 2015;212:991-9.
195. Alitalo K. The lymphatic vasculature in disease. Nature medicine 2011;17:1371-80.
196. Dejana E, Tournier-Lasserve E, Weinstein BM. The control of vascular integrity by endothelial cell junctions: molecular basis and pathological implications. Developmental cell 2009;16:209-21.
197. Kerjaschki D. The lymphatic vasculature revisited. The Journal of clinical investigation 2014;124:874-7.
198. Sweet DT, Jimenez JM, Chang J, et al. Lymph flow regulates collecting lymphatic vessel maturation in vivo. The Journal of clinical investigation 2015;125:2995-3007.
199. Foldi M, Gellert A, Kozma M, Poberai M, Zoltan OT, Csanda E. New contributions to the anatomical connections of the brain and the lymphatic system. Acta anatomica 1966;64:498-505.
200. Andres KH, von During M, Muszynski K, Schmidt RF. Nerve fibres and their terminals of the dura mater encephali of the rat. Anatomy and embryology 1987;175:289-301.

201. Raper D, Louveau A, Kipnis J. How Do Meningeal Lymphatic Vessels Drain the CNS? Trends in neurosciences 2016;39:581-6.
202. Louveau A, Da Mesquita S, Kipnis J. Lymphatics in Neurological Disorders: A Neuro-Lympho-Vascular Component of Multiple Sclerosis and Alzheimer's Disease? Neuron 2016;91:957-73.
203. Insug O, Ku G, Ertl HC, Blaszczyk-Thurin M. A dendritic cell vaccine induces protective immunity to intracranial growth of glioma. Anticancer research 2002;22:613-21.
204. Ni HT, Spellman SR, Jean WC, Hall WA, Low WC. Immunization with dendritic cells pulsed with tumor extract increases survival of mice bearing intracranial gliomas. Journal of neuro-oncology 2001;51:1-9.
205. Sica A, Saccani A, Mantovani A. Tumor-associated macrophages: a molecular perspective. International immunopharmacology 2002;2:1045-54.
206. Gordon S, Taylor PR. Monocyte and macrophage heterogeneity. Nature reviews Immunology 2005;5:953-64.
207. Hashimoto D, Chow A, Noizat C, et al. Tissue-resident macrophages self-maintain locally throughout adult life with minimal contribution from circulating monocytes. Immunity 2013;38:792-804.
208. Murray PJ, Wynn TA. Protective and pathogenic functions of macrophage subsets. Nature reviews Immunology 2011;11:723-37.
209. Goldmann T, Wieghofer P, Jordao MJ, et al. Origin, fate and dynamics of macrophages at central nervous system interfaces. Nature immunology 2016;17:797-805.
210. Jung S, Aliberti J, Graemmel P, et al. Analysis of fractalkine receptor CX(3)CR1 function by targeted deletion and green fluorescent protein reporter gene insertion. Molecular and cellular biology 2000;20:4106-14.
211. Tremblay ME, Stevens B, Sierra A, Wake H, Bessis A, Nimmerjahn A. The role of microglia in the healthy brain. The Journal of neuroscience : the official journal of the Society for Neuroscience 2011;31:16064-9.
212. Bulloch K, Miller MM, Gal-Toth J, et al. CD11c/EYFP transgene illuminates a discrete network of dendritic cells within the embryonic, neonatal, adult, and injured mouse brain. The Journal of comparative neurology 2008;508:687-710.
213. Schafer DP, Lehrman EK, Kautzman AG, et al. Microglia sculpt postnatal neural circuits in an activity and complement-dependent manner. Neuron 2012;74:691-705.
214. Nimmerjahn A, Kirchhoff F, Helmchen F. Resting microglial cells are highly dynamic surveillants of brain parenchyma in vivo. Science 2005;308:1314-8.
215. Fourgeaud L, Traves PG, Tufail Y, et al. TAM receptors regulate multiple features of microglial physiology. Nature 2016;532:240-4.
216. Hambardzumyan D, Gutmann DH, Kettenmann H. The role of microglia and macrophages in glioma maintenance and progression. Nature neuroscience 2016;19:20-7.
217. Davalos D, Grutzendler J, Yang G, et al. ATP mediates rapid microglial response to local brain injury in vivo. Nature neuroscience 2005;8:752-8.
218. Paolicelli RC, Bisht K, Tremblay ME. Fractalkine regulation of microglial physiology and consequences on the brain and behavior. Frontiers in cellular neuroscience 2014;8:129.
219. Murugan M, Ling EA, Kaur C. Glutamate receptors in microglia. CNS & neurological disorders drug targets 2013;12:773-84.

220. Hickey WF, Kimura H. Perivascular microglial cells of the CNS are bone marrow-derived and present antigen in vivo. Science 1988;239:290-2.
221. Mildner A, Schmidt H, Nitsche M, et al. Microglia in the adult brain arise from Ly-6ChiCCR2+ monocytes only under defined host conditions. Nature neuroscience 2007;10:1544-53.
222. Kokovay E, Cunningham LA. Bone marrow-derived microglia contribute to the neuroinflammatory response and express iNOS in the MPTP mouse model of Parkinson's disease. Neurobiology of disease 2005;19:471-8.
223. Simard AR, Rivest S. Bone marrow stem cells have the ability to populate the entire central nervous system into fully differentiated parenchymal microglia. FASEB journal : official publication of the Federation of American Societies for Experimental Biology 2004;18:998-1000.
224. Ginhoux F, Greter M, Leboeuf M, et al. Fate mapping analysis reveals that adult microglia derive from primitive macrophages. Science 2010;330:841-5.
225. Asai H, Ikezu S, Tsunoda S, et al. Depletion of microglia and inhibition of exosome synthesis halt tau propagation. Nature neuroscience 2015;18:1584-93.
226. Ginhoux F, Lim S, Hoeffel G, Low D, Huber T. Origin and differentiation of microglia. Frontiers in cellular neuroscience 2013;7:45.
227. Luo Y, Zhou H, Krueger J, et al. Targeting tumor-associated macrophages as a novel strategy against breast cancer. The Journal of clinical investigation 2006;116:2132-41.
228. Noy R, Pollard JW. Tumor-associated macrophages: from mechanisms to therapy. Immunity 2014;41:49-61.
229. Qian BZ, Pollard JW. Macrophage diversity enhances tumor progression and metastasis. Cell 2010;141:39-51.
230. Ojalvo LS, Whittaker CA, Condeelis JS, Pollard JW. Gene expression analysis of macrophages that facilitate tumor invasion supports a role for Wnt-signaling in mediating their activity in primary mammary tumors. Journal of immunology 2010;184:702-12.
231. Shi Y, Ping YF, Zhang X, Bian XW. Hostile takeover: glioma stem cells recruit TAMs to support tumor progression. Cell stem cell 2015;16:219-20.
232. Gabrusiewicz K, Ellert-Miklaszewska A, Lipko M, Sielska M, Frankowska M, Kaminska B. Characteristics of the alternative phenotype of microglia/macrophages and its modulation in experimental gliomas. PloS one 2011;6:e23902.
233. Rolny C, Mazzone M, Tugues S, et al. HRG inhibits tumor growth and metastasis by inducing macrophage polarization and vessel normalization through downregulation of PlGF. Cancer cell 2011;19:31-44.
234. Zhou W, Ke SQ, Huang Z, et al. Periostin secreted by glioblastoma stem cells recruits M2 tumour-associated macrophages and promotes malignant growth. Nature cell biology 2015;17:170-82.
235. Gabrusiewicz K, Rodriguez B, Wei J, et al. Glioblastoma-infiltrated innate immune cells resemble M0 macrophage phenotype. JCI insight 2016;1.
236. Pyonteck SM, Akkari L, Schuhmacher AJ, et al. CSF-1R inhibition alters macrophage polarization and blocks glioma progression. Nature medicine 2013;19:1264-72.
237. Quail DF, Bowman RL, Akkari L, et al. The tumor microenvironment underlies acquired resistance to CSF-1R inhibition in gliomas. Science 2016;352:aad3018.

238. Gabrusiewicz K, Hossain MB, Cortes-Santiago N, et al. Macrophage Ablation Reduces M2-Like Populations and Jeopardizes Tumor Growth in a MAFIA-Based Glioma Model. Neoplasia 2015;17:374-84.
239. Garris C, Pittet MJ. Therapeutically reeducating macrophages to treat GBM. Nature medicine 2013;19:1207-8.
240. Muller A, Brandenburg S, Turkowski K, Muller S, Vajkoczy P. Resident microglia, and not peripheral macrophages, are the main source of brain tumor mononuclear cells. International journal of cancer 2015;137:278-88.
241. D'Agostino PM, Gottfried-Blackmore A, Anandasabapathy N, Bulloch K. Brain dendritic cells: biology and pathology. Acta neuropathologica 2012;124:599-614.
242. Hussain SF, Yang D, Suki D, Aldape K, Grimm E, Heimberger AB. The role of human glioma-infiltrating microglia/macrophages in mediating antitumor immune responses. Neuro-oncology 2006;8:261-79.
243. Schartner JM, Hagar AR, Van Handel M, Zhang L, Nadkarni N, Badie B. Impaired capacity for upregulation of MHC class II in tumor-associated microglia. Glia 2005;51:279-85.
244. Ginzkey C, Eicker SO, Marget M, et al. Increase in tumor size following intratumoral injection of immunostimulatory CpG-containing oligonucleotides in a rat glioma model. Cancer immunology, immunotherapy : CII 2010;59:541-51.
245. Badie B, Schartner J, Prabakaran S, Paul J, Vorpahl J. Expression of Fas ligand by microglia: possible role in glioma immune evasion. Journal of neuroimmunology 2001;120:19-24.
246. Bowman RL, Joyce JA. Therapeutic targeting of tumor-associated macrophages and microglia in glioblastoma. Immunotherapy 2014;6:663-6.
247. Xu S, Wei J, Wang F, et al. Effect of miR-142-3p on the M2 macrophage and therapeutic efficacy against murine glioblastoma. Journal of the National Cancer Institute 2014;106.
248. Richards DM, Hettinger J, Feuerer M. Monocytes and macrophages in cancer: development and functions. Cancer microenvironment : official journal of the International Cancer Microenvironment Society 2013;6:179-91.
249. Hettinger J, Richards DM, Hansson J, et al. Origin of monocytes and macrophages in a committed progenitor. Nature immunology 2013;14:821-30.
250. Geissmann F, Jung S, Littman DR. Blood monocytes consist of two principal subsets with distinct migratory properties. Immunity 2003;19:71-82.
251. Carlin LM, Stamatiades EG, Auffray C, et al. Nr4a1-dependent Ly6C(low) monocytes monitor endothelial cells and orchestrate their disposal. Cell 2013;153:362-75.
252. Hanna RN, Carlin LM, Hubbeling HG, et al. The transcription factor NR4A1 (Nur77) controls bone marrow differentiation and the survival of Ly6C- monocytes. Nature immunology 2011;12:778-85.
253. Garcia MR, Ledgerwood L, Yang Y, et al. Monocytic suppressive cells mediate cardiovascular transplantation tolerance in mice. The Journal of clinical investigation 2010;120:2486-96.
254. Laoui D, Van Overmeire E, Movahedi K, et al. Mononuclear phagocyte heterogeneity in cancer: different subsets and activation states reaching out at the tumor site. Immunobiology 2011;216:1192-202.

255. Umemura N, Saio M, Suwa T, et al. Tumor-infiltrating myeloid-derived suppressor cells are pleiotropic-inflamed monocytes/macrophages that bear M1- and M2-type characteristics. Journal of leukocyte biology 2008;83:1136-44.
256. Pommier A, Lucas B, Prevost-Blondel A. Crucial role of inflammatory monocytes in antitumor immunity. Oncoimmunology 2013;2:e26384.
257. Pommier A, Audemard A, Durand A, et al. Inflammatory monocytes are potent antitumor effectors controlled by regulatory CD4+ T cells. Proceedings of the National Academy of Sciences of the United States of America 2013;110:13085-90.
258. Kuhn S, Yang J, Ronchese F. Monocyte-Derived Dendritic Cells Are Essential for CD8(+) T Cell Activation and Antitumor Responses After Local Immunotherapy. Frontiers in immunology 2015;6:584.
259. Hanna RN, Shaked I, Hubbeling HG, et al. NR4A1 (Nur77) deletion polarizes macrophages toward an inflammatory phenotype and increases atherosclerosis. Circulation research 2012;110:416-27.
260. Thomas G, Tacke R, Hedrick CC, Hanna RN. Nonclassical patrolling monocyte function in the vasculature. Arteriosclerosis, thrombosis, and vascular biology 2015;35:1306-16.
261. Hanna RN, Cekic C, Sag D, et al. Patrolling monocytes control tumor metastasis to the lung. Science 2015;350:985-90.
262. Steinman RM, Bonifaz L, Fujii S, et al. The innate functions of dendritic cells in peripheral lymphoid tissues. Advances in experimental medicine and biology 2005;560:83-97.
263. Hartgers FC, Figdor CG, Adema GJ. Towards a molecular understanding of dendritic cell immunobiology. Immunology today 2000;21:542-5.
264. Steinman RM, Adams JC, Cohn ZA. Identification of a novel cell type in peripheral lymphoid organs of mice. IV. Identification and distribution in mouse spleen. The Journal of experimental medicine 1975;141:804-20.
265. Banchereau J, Steinman RM. Dendritic cells and the control of immunity. Nature 1998;392:245-52.
266. Geijtenbeek TB, Krooshoop DJ, Bleijs DA, et al. DC-SIGN-ICAM-2 interaction mediates dendritic cell trafficking. Nature immunology 2000;1:353-7.
267. Geijtenbeek TB, Kwon DS, Torensma R, et al. DC-SIGN, a dendritic cell-specific HIV-1-binding protein that enhances trans-infection of T cells. Cell 2000;100:587-97.
268. Geijtenbeek TB, Torensma R, van Vliet SJ, et al. Identification of DC-SIGN, a novel dendritic cell-specific ICAM-3 receptor that supports primary immune responses. Cell 2000;100:575-85.
269. Swiggard WJ, Mirza A, Nussenzweig MC, Steinman RM. DEC-205, a 205-kDa protein abundant on mouse dendritic cells and thymic epithelium that is detected by the monoclonal antibody NLDC-145: purification, characterization, and N-terminal amino acid sequence. Cellular immunology 1995;165:302-11.
270. Inaba K, Swiggard WJ, Inaba M, et al. Tissue distribution of the DEC-205 protein that is detected by the monoclonal antibody NLDC-145. I. Expression on dendritic cells and other subsets of mouse leukocytes. Cellular immunology 1995;163:148-56.
271. Jiang W, Swiggard WJ, Heufler C, et al. The receptor DEC-205 expressed by dendritic cells and thymic epithelial cells is involved in antigen processing. Nature 1995;375:151-5.

272. Tan MC, Mommaas AM, Drijfhout JW, et al. Mannose receptor-mediated uptake of antigens strongly enhances HLA class II-restricted antigen presentation by cultured dendritic cells. European journal of immunology 1997;27:2426-35.
273. Weis WI, Taylor ME, Drickamer K. The C-type lectin superfamily in the immune system. Immunological reviews 1998;163:19-34.
274. Bonifaz L, Bonnyay D, Mahnke K, Rivera M, Nussenzweig MC, Steinman RM. Efficient targeting of protein antigen to the dendritic cell receptor DEC-205 in the steady state leads to antigen presentation on major histocompatibility complex class I products and peripheral CD8+ T cell tolerance. The Journal of experimental medicine 2002;196:1627-38.
275. Mahnke K, Schmitt E, Bonifaz L, Enk AH, Jonuleit H. Immature, but not inactive: the tolerogenic function of immature dendritic cells. Immunology and cell biology 2002;80:477-83.
276. Singh SK, Stephani J, Schaefer M, et al. Targeting glycan modified OVA to murine DC-SIGN transgenic dendritic cells enhances MHC class I and II presentation. Molecular immunology 2009;47:164-74.
277. Blum JS, Wearsch PA, Cresswell P. Pathways of antigen processing. Annual review of immunology 2013;31:443-73.
278. Savina A, Jancic C, Hugues S, et al. NOX2 controls phagosomal pH to regulate antigen processing during crosspresentation by dendritic cells. Cell 2006;126:205-18.
279. Hildner K, Edelson BT, Purtha WE, et al. Batf3 deficiency reveals a critical role for CD8alpha+ dendritic cells in cytotoxic T cell immunity. Science 2008;322:1097-100.
280. Edelson BT, Kc W, Juang R, et al. Peripheral CD103+ dendritic cells form a unified subset developmentally related to CD8alpha+ conventional dendritic cells. The Journal of experimental medicine 2010;207:823-36.
281. Li L, Kim S, Herndon JM, et al. Cross-dressed CD8alpha+/CD103+ dendritic cells prime CD8+ T cells following vaccination. Proceedings of the National Academy of Sciences of the United States of America 2012;109:12716-21.
282. Desch AN, Randolph GJ, Murphy K, et al. CD103+ pulmonary dendritic cells preferentially acquire and present apoptotic cell-associated antigen. The Journal of experimental medicine 2011;208:1789-97.
283. Satpathy AT, Kc W, Albring JC, et al. Zbtb46 expression distinguishes classical dendritic cells and their committed progenitors from other immune lineages. The Journal of experimental medicine 2012;209:1135-52.
284. Ashok D, Schuster S, Ronet C, et al. Cross-presenting dendritic cells are required for control of Leishmania major infection. European journal of immunology 2014;44:1422-32.
285. Mashayekhi M, Sandau MM, Dunay IR, et al. CD8alpha(+) dendritic cells are the critical source of interleukin-12 that controls acute infection by Toxoplasma gondii tachyzoites. Immunity 2011;35:249-59.
286. Edelson BT, Bradstreet TR, Hildner K, et al. CD8alpha(+) dendritic cells are an obligate cellular entry point for productive infection by Listeria monocytogenes. Immunity 2011;35:236-48.
287. Everts B, Tussiwand R, Dreesen L, et al. Migratory CD103+ dendritic cells suppress helminth-driven type 2 immunity through constitutive expression of IL-12. The Journal of experimental medicine 2016;213:35-51.
288. D'Agostino PM, Kwak C, Vecchiarelli HA, et al. Viral-induced encephalitis initiates distinct and functional CD103+ CD11b+ brain dendritic cell populations within

the olfactory bulb. Proceedings of the National Academy of Sciences of the United States of America 2012;109:6175-80.
289. Gottfried-Blackmore A, Kaunzner UW, Idoyaga J, Felger JC, McEwen BS, Bulloch K. Acute in vivo exposure to interferon-gamma enables resident brain dendritic cells to become effective antigen presenting cells. Proceedings of the National Academy of Sciences of the United States of America 2009;106:20918-23.
290. Murphy KM, Heimberger AB, Loh DY. Induction by antigen of intrathymic apoptosis of CD4+CD8+TCRlo thymocytes in vivo. Science 1990;250:1720-3.
291. Klein L, Kyewski B, Allen PM, Hogquist KA. Positive and negative selection of the T cell repertoire: what thymocytes see (and don't see). Nature reviews Immunology 2014;14:377-91.
292. Forster R, Schubel A, Breitfeld D, et al. CCR7 coordinates the primary immune response by establishing functional microenvironments in secondary lymphoid organs. Cell 1999;99:23-33.
293. Mori S, Nakano H, Aritomi K, Wang CR, Gunn MD, Kakiuchi T. Mice lacking expression of the chemokines CCL21-ser and CCL19 (plt mice) demonstrate delayed but enhanced T cell immune responses. The Journal of experimental medicine 2001;193:207-18.
294. Adema GJ, Hartgers F, Verstraten R, et al. A dendritic-cell-derived C-C chemokine that preferentially attracts naive T cells. Nature 1997;387:713-7.
295. Mempel TR, Henrickson SE, Von Andrian UH. T-cell priming by dendritic cells in lymph nodes occurs in three distinct phases. Nature 2004;427:154-9.
296. Chen L, Flies DB. Molecular mechanisms of T cell co-stimulation and co-inhibition. Nature reviews Immunology 2013;13:227-42.
297. Smith-Garvin JE, Koretzky GA, Jordan MS. T cell activation. Annual review of immunology 2009;27:591-619.
298. Pollizzi KN, Powell JD. Integrating canonical and metabolic signalling programmes in the regulation of T cell responses. Nature reviews Immunology 2014;14:435-46.
299. Riquelme E, Carreno LJ, Gonzalez PA, Kalergis AM. The duration of TCR/pMHC interactions regulates CTL effector function and tumor-killing capacity. European journal of immunology 2009;39:2259-69.
300. Elgueta R, Tobar JA, Shoji KF, et al. Gap junctions at the dendritic cell-T cell interface are key elements for antigen-dependent T cell activation. Journal of immunology 2009;183:277-84.
301. Marangoni F, Murooka TT, Manzo T, et al. The transcription factor NFAT exhibits signal memory during serial T cell interactions with antigen-presenting cells. Immunity 2013;38:237-49.
302. Moran AE, Holzapfel KL, Xing Y, et al. T cell receptor signal strength in Treg and iNKT cell development demonstrated by a novel fluorescent reporter mouse. The Journal of experimental medicine 2011;208:1279-89.
303. Au-Yeung BB, Zikherman J, Mueller JL, et al. A sharp T-cell antigen receptor signaling threshold for T-cell proliferation. Proceedings of the National Academy of Sciences of the United States of America 2014;111:E3679-88.
304. Carreno LJ, Riquelme EM, Gonzalez PA, et al. T-cell antagonism by short half-life pMHC ligands can be mediated by an efficient trapping of T-cell polarization toward the APC. Proceedings of the National Academy of Sciences of the United States of America 2010;107:210-5.

305. Bour-Jordan H, Bluestone JA. How suppressor cells led to anergy, costimulation, and beyond. Journal of immunology 2009;183:4147-9.
306. Bour-Jordan H, Bluestone JA. Regulating the regulators: costimulatory signals control the homeostasis and function of regulatory T cells. Immunological reviews 2009;229:41-66.
307. Lorenz U. SHP-1 and SHP-2 in T cells: two phosphatases functioning at many levels. Immunological reviews 2009;228:342-59.
308. Riley JL. PD-1 signaling in primary T cells. Immunological reviews 2009;229:114-25.
309. Barber DL, Wherry EJ, Masopust D, et al. Restoring function in exhausted CD8 T cells during chronic viral infection. Nature 2006;439:682-7.
310. Latchman Y, Wood CR, Chernova T, et al. PD-L2 is a second ligand for PD-1 and inhibits T cell activation. Nature immunology 2001;2:261-8.
311. Sharpe AH, Wherry EJ, Ahmed R, Freeman GJ. The function of programmed cell death 1 and its ligands in regulating autoimmunity and infection. Nature immunology 2007;8:239-45.
312. Zhai L, Lauing KL, Chang AL, et al. The role of IDO in brain tumor immunotherapy. Journal of neuro-oncology 2015;123:395-403.
313. Wainwright DA, Balyasnikova IV, Chang AL, et al. IDO expression in brain tumors increases the recruitment of regulatory T cells and negatively impacts survival. Clinical cancer research : an official journal of the American Association for Cancer Research 2012;18:6110-21.
314. Wainwright DA, Chang AL, Dey M, et al. Durable therapeutic efficacy utilizing combinatorial blockade against IDO, CTLA-4, and PD-L1 in mice with brain tumors. Clinical cancer research : an official journal of the American Association for Cancer Research 2014;20:5290-301.
315. Fecci PE, Ochiai H, Mitchell DA, et al. Systemic CTLA-4 blockade ameliorates glioma-induced changes to the CD4+ T cell compartment without affecting regulatory T-cell function. Clinical cancer research : an official journal of the American Association for Cancer Research 2007;13:2158-67.
316. Mathios D, Kim JE, Mangraviti A, et al. Anti-PD-1 antitumor immunity is enhanced by local and abrogated by systemic chemotherapy in GBM. Science translational medicine 2016;8:370ra180.
317. Kim JE, Patel MA, Mangraviti A, et al. Combination Therapy with Anti-PD-1, Anti-TIM-3, and Focal Radiation Results in Regression of Murine Gliomas. Clinical cancer research : an official journal of the American Association for Cancer Research 2017;23:124-36.
318. Fecci PE, Sweeney AE, Grossi PM, et al. Systemic anti-CD25 monoclonal antibody administration safely enhances immunity in murine glioma without eliminating regulatory T cells. Clinical cancer research : an official journal of the American Association for Cancer Research 2006;12:4294-305.
319. El Andaloussi A, Han Y, Lesniak MS. Prolongation of survival following depletion of CD4+CD25+ regulatory T cells in mice with experimental brain tumors. Journal of neurosurgery 2006;105:430-7.
320. Starbeck-Miller GR, Xue HH, Harty JT. IL-12 and type I interferon prolong the division of activated CD8 T cells by maintaining high-affinity IL-2 signaling in vivo. The Journal of experimental medicine 2014;211:105-20.

321. Das G, Sheridan S, Janeway CA, Jr. The source of early IFN-gamma that plays a role in Th1 priming. Journal of immunology 2001;167:2004-10.
322. Caretto D, Katzman SD, Villarino AV, Gallo E, Abbas AK. Cutting edge: the Th1 response inhibits the generation of peripheral regulatory T cells. Journal of immunology 2010;184:30-4.
323. Romagnani S. T-cell subsets (Th1 versus Th2). Annals of allergy, asthma & immunology : official publication of the American College of Allergy, Asthma, & Immunology 2000;85:9-18; quiz , 21.
324. Seki N, Miyazaki M, Suzuki W, et al. IL-4-induced GATA-3 expression is a time-restricted instruction switch for Th2 cell differentiation. Journal of immunology 2004;172:6158-66.
325. Villarino AV, Gallo E, Abbas AK. STAT1-activating cytokines limit Th17 responses through both T-bet-dependent and -independent mechanisms. Journal of immunology 2010;185:6461-71.
326. Murugaiyan G, Saha B. Protumor vs antitumor functions of IL-17. Journal of immunology 2009;183:4169-75.
327. Muranski P, Boni A, Antony PA, et al. Tumor-specific Th17-polarized cells eradicate large established melanoma. Blood 2008;112:362-73.
328. Esensten JH, Wofsy D, Bluestone JA. Regulatory T cells as therapeutic targets in rheumatoid arthritis. Nature reviews Rheumatology 2009;5:560-5.
329. Penaranda C, Bluestone JA. Is antigen specificity of autoreactive T cells the key to islet entry? Immunity 2009;31:534-6.
330. Putnam AL, Brusko TM, Lee MR, et al. Expansion of human regulatory T-cells from patients with type 1 diabetes. Diabetes 2009;58:652-62.
331. Dooms H, Abbas AK. Revisiting the role of IL-2 in autoimmunity. European journal of immunology 2010;40:1538-40.
332. Barron L, Dooms H, Hoyer KK, et al. Cutting edge: mechanisms of IL-2-dependent maintenance of functional regulatory T cells. Journal of immunology 2010;185:6426-30.
333. Perry JS, Lio CW, Kau AL, et al. Distinct contributions of Aire and antigen-presenting-cell subsets to the generation of self-tolerance in the thymus. Immunity 2014;41:414-26.
334. Klein L, Emmerich J, d'Cruz L, Aschenbrenner K, Khazaie K. Selection and behavior of CD4+ CD25+ T cells in vivo: lessons from T cell receptor transgenic models. Current topics in microbiology and immunology 2005;293:73-87.
335. Zhou X, Bailey-Bucktrout SL, Jeker LT, et al. Instability of the transcription factor Foxp3 leads to the generation of pathogenic memory T cells in vivo. Nature immunology 2009;10:1000-7.
336. Bluestone JA, Kuchroo V. Autoimmunity. Current opinion in immunology 2009;21:579-81.
337. Su MA, Stenerson M, Liu W, et al. The role of X-linked FOXP3 in the autoimmune susceptibility of Turner Syndrome patients. Clinical immunology 2009;131:139-44.
338. Bluestone JA, Mackay CR, O'Shea JJ, Stockinger B. The functional plasticity of T cell subsets. Nature reviews Immunology 2009;9:811-6.
339. Kretschmer K, Apostolou I, Hawiger D, Khazaie K, Nussenzweig MC, von Boehmer H. Inducing and expanding regulatory T cell populations by foreign antigen. Nature immunology 2005;6:1219-27.

340. Brusko TM, Bluestone JA. Regulatory T cells directed to the site of the action. Proceedings of the National Academy of Sciences of the United States of America 2009;106:20553-4.
341. Curiel TJ, Coukos G, Zou L, et al. Specific recruitment of regulatory T cells in ovarian carcinoma fosters immune privilege and predicts reduced survival. Nature medicine 2004;10:942-9.
342. Chen ML, Pittet MJ, Gorelik L, et al. Regulatory T cells suppress tumor-specific CD8 T cell cytotoxicity through TGF-beta signals in vivo. Proceedings of the National Academy of Sciences of the United States of America 2005;102:419-24.
343. Kastenmuller W, Gasteiger G, Subramanian N, et al. Regulatory T cells selectively control CD8+ T cell effector pool size via IL-2 restriction. Journal of immunology 2011;187:3186-97.
344. Heimberger AB, Abou-Ghazal M, Reina-Ortiz C, et al. Incidence and prognostic impact of FoxP3+ regulatory T cells in human gliomas. Clinical cancer research : an official journal of the American Association for Cancer Research 2008;14:5166-72.
345. Fecci PE, Mitchell DA, Whitesides JF, et al. Increased regulatory T-cell fraction amidst a diminished CD4 compartment explains cellular immune defects in patients with malignant glioma. Cancer research 2006;66:3294-302.
346. Grauer OM, Nierkens S, Bennink E, et al. CD4+FoxP3+ regulatory T cells gradually accumulate in gliomas during tumor growth and efficiently suppress antiglioma immune responses in vivo. International journal of cancer 2007;121:95-105.
347. Jordan JT, Sun W, Hussain SF, DeAngulo G, Prabhu SS, Heimberger AB. Preferential migration of regulatory T cells mediated by glioma-secreted chemokines can be blocked with chemotherapy. Cancer immunology, immunotherapy : CII 2008;57:123-31.
348. Kong LY, Wei J, Sharma AK, et al. A novel phosphorylated STAT3 inhibitor enhances T cell cytotoxicity against melanoma through inhibition of regulatory T cells. Cancer immunology, immunotherapy : CII 2009;58:1023-32.
349. Humphries W, Wang Y, Qiao W, et al. yuDetecting the percent of peripheral blood mononuclear cells displaying p-STAT-3 in malignant glioma patients. Journal of translational medicine 2009;7:92.
350. Paglia P, Chiodoni C, Rodolfo M, Colombo MP. Murine dendritic cells loaded in vitro with soluble protein prime cytotoxic T lymphocytes against tumor antigen in vivo. The Journal of experimental medicine 1996;183:317-22.
351. Wheeler CJ, Yu JS, Black KL. Cellular immunity in the treatment of brain tumors. Clinical neurosurgery 2004;51:132-9.
352. Liu G, Ying H, Zeng G, Wheeler CJ, Black KL, Yu JS. HER-2, gp100, and MAGE-1 are expressed in human glioblastoma and recognized by cytotoxic T cells. Cancer research 2004;64:4980-6.
353. Yu JS, Liu G, Ying H, Yong WH, Black KL, Wheeler CJ. Vaccination with tumor lysate-pulsed dendritic cells elicits antigen-specific, cytotoxic T-cells in patients with malignant glioma. Cancer research 2004;64:4973-9.
354. Rooney CM, Smith CA, Ng CY, et al. Infusion of cytotoxic T cells for the prevention and treatment of Epstein-Barr virus-induced lymphoma in allogeneic transplant recipients. Blood 1998;92:1549-55.
355. Rooney CM, Heslop HE, Brenner MK. EBV specific CTL: a model for immune therapy. Vox sanguinis 1998;74 Suppl 2:497-8.

356. Celluzzi CM, Mayordomo JI, Storkus WJ, Lotze MT, Falo LD, Jr. Peptide-pulsed dendritic cells induce antigen-specific CTL-mediated protective tumor immunity. The Journal of experimental medicine 1996;183:283-7.
357. Andreasson K, Eriksson M, Tegerstedt K, Ramqvist T, Dalianis T. CD4+ and CD8+ T cells can act separately in tumour rejection after immunization with murine pneumotropic virus chimeric Her2/neu virus-like particles. PloS one 2010;5:e11580.
358. Peters PJ, Borst J, Oorschot V, et al. Cytotoxic T lymphocyte granules are secretory lysosomes, containing both perforin and granzymes. The Journal of experimental medicine 1991;173:1099-109.
359. Pipkin ME, Lieberman J. Delivering the kiss of death: progress on understanding how perforin works. Current opinion in immunology 2007;19:301-8.
360. Smyth MJ, Street SE, Trapani JA. Cutting edge: granzymes A and B are not essential for perforin-mediated tumor rejection. Journal of immunology 2003;171:515-8.
361. Zamarin D, Holmgaard RB, Ricca J, et al. Intratumoral modulation of the inducible co-stimulator ICOS by recombinant oncolytic virus promotes systemic anti-tumour immunity. Nature communications 2017;8:14340.
362. Huang Y, Ma C, Zhang Q, et al. CD4+ and CD8+ T cells have opposing roles in breast cancer progression and outcome. Oncotarget 2015;6:17462-78.
363. Ahmadzadeh M, Johnson LA, Heemskerk B, et al. Tumor antigen-specific CD8 T cells infiltrating the tumor express high levels of PD-1 and are functionally impaired. Blood 2009;114:1537-44.
364. Yuan J, Adamow M, Ginsberg BA, et al. Integrated NY-ESO-1 antibody and CD8+ T-cell responses correlate with clinical benefit in advanced melanoma patients treated with ipilimumab. Proceedings of the National Academy of Sciences of the United States of America 2011;108:16723-8.
365. Curran MA, Kim M, Montalvo W, Al-Shamkhani A, Allison JP. Combination CTLA-4 blockade and 4-1BB activation enhances tumor rejection by increasing T-cell infiltration, proliferation, and cytokine production. PloS one 2011;6:e19499.
366. Savage PA, Vosseller K, Kang C, et al. Recognition of a ubiquitous self antigen by prostate cancer-infiltrating CD8+ T lymphocytes. Science 2008;319:215-20.
367. Pedicord VA, Montalvo W, Leiner IM, Allison JP. Single dose of anti-CTLA-4 enhances CD8+ T-cell memory formation, function, and maintenance. Proceedings of the National Academy of Sciences of the United States of America 2011;108:266-71.
368. Liu S, Lizee G, Lou Y, et al. IL-21 synergizes with IL-7 to augment expansion and anti-tumor function of cytotoxic T cells. International immunology 2007;19:1213-21.
369. Schluns KS, Lefrancois L. Cytokine control of memory T-cell development and survival. Nature reviews Immunology 2003;3:269-79.
370. Steinbach K, Vincenti I, Kreutzfeldt M, et al. Brain-resident memory T cells represent an autonomous cytotoxic barrier to viral infection. The Journal of experimental medicine 2016;213:1571-87.
371. Wakim LM, Woodward-Davis A, Bevan MJ. Memory T cells persisting within the brain after local infection show functional adaptations to their tissue of residence. Proceedings of the National Academy of Sciences of the United States of America 2010;107:17872-9.
372. Breart B, Lemaitre F, Celli S, Bousso P. Two-photon imaging of intratumoral CD8+ T cell cytotoxic activity during adoptive T cell therapy in mice. The Journal of clinical investigation 2008;118:1390-7.

373. Henrickson SE, Mempel TR, Mazo IB, et al. In vivo imaging of T cell priming. Science signaling 2008;1:pt2.
374. Zal T, Chodaczek G. Intravital imaging of anti-tumor immune response and the tumor microenvironment. Seminars in immunopathology 2010;32:305-17.
375. Engelhardt JJ, Boldajipour B, Beemiller P, et al. Marginating dendritic cells of the tumor microenvironment cross-present tumor antigens and stably engage tumor-specific T cells. Cancer cell 2012;21:402-17.
376. Sakadzic S, Demirbas U, Mempel TR, et al. Multi-photon microscopy with a low-cost and highly efficient Cr:LiCAF laser. Optics express 2008;16:20848-63.
377. Sumen C, Mempel TR, Mazo IB, von Andrian UH. Intravital microscopy: visualizing immunity in context. Immunity 2004;21:315-29.
378. Mempel TR, Scimone ML, Mora JR, von Andrian UH. In vivo imaging of leukocyte trafficking in blood vessels and tissues. Current opinion in immunology 2004;16:406-17.
379. Hugues S, Fetler L, Bonifaz L, Helft J, Amblard F, Amigorena S. Distinct T cell dynamics in lymph nodes during the induction of tolerance and immunity. Nature immunology 2004;5:1235-42.
380. Germain RN, Robey EA, Cahalan MD. A decade of imaging cellular motility and interaction dynamics in the immune system. Science 2012;336:1676-81.
381. Pittet MJ, Mempel TR. Regulation of T-cell migration and effector functions: insights from in vivo imaging studies. Immunological reviews 2008;221:107-29.
382. Bromley SK, Mempel TR, Luster AD. Orchestrating the orchestrators: chemokines in control of T cell traffic. Nature immunology 2008;9:970-80.
383. Henrickson SE, Mempel TR, Mazo IB, et al. T cell sensing of antigen dose governs interactive behavior with dendritic cells and sets a threshold for T cell activation. Nature immunology 2008;9:282-91.
384. Henrickson SE, Perro M, Loughhead SM, et al. Antigen availability determines CD8(+) T cell-dendritic cell interaction kinetics and memory fate decisions. Immunity 2013;39:496-507.
385. Babich A, Burkhardt JK. Coordinate control of cytoskeletal remodeling and calcium mobilization during T-cell activation. Immunological reviews 2013;256:80-94.
386. Tan YX, Manz BN, Freedman TS, Zhang C, Shokat KM, Weiss A. Inhibition of the kinase Csk in thymocytes reveals a requirement for actin remodeling in the initiation of full TCR signaling. Nature immunology 2014;15:186-94.
387. Kumari S, Curado S, Mayya V, Dustin ML. T cell antigen receptor activation and actin cytoskeleton remodeling. Biochimica et biophysica acta 2014;1838:546-56.
388. Reicher B, Barda-Saad M. Multiple pathways leading from the T-cell antigen receptor to the actin cytoskeleton network. FEBS letters 2010;584:4858-64.
389. Sechi AS, Buer J, Wehland J, Probst-Kepper M. Changes in actin dynamics at the T-cell/APC interface: implications for T-cell anergy? Immunological reviews 2002;189:98-110.
390. Cannon JL, Burkhardt JK. The regulation of actin remodeling during T-cell-APC conjugate formation. Immunological reviews 2002;186:90-9.
391. Gerard A, Beemiller P, Friedman RS, Jacobelli J, Krummel MF. Evolving immune circuits are generated by flexible, motile, and sequential immunological synapses. Immunological reviews 2013;251:80-96.
392. Beemiller P, Krummel MF. Regulation of T-cell receptor signaling by the actin cytoskeleton and poroelastic cytoplasm. Immunological reviews 2013;256:148-59.

393. Gascoigne NR, Zal T, Yachi PP, Hoerter JA. Co-receptors and recognition of self at the immunological synapse. Current topics in microbiology and immunology 2010;340:171-89.
394. Le Borgne M, Raju S, Zinselmeyer BH, et al. Real-Time Analysis of Calcium Signals during the Early Phase of T Cell Activation Using a Genetically Encoded Calcium Biosensor. Journal of immunology 2016;196:1471-9.
395. Gwack Y, Feske S, Srikanth S, Hogan PG, Rao A. Signalling to transcription: store-operated Ca2+ entry and NFAT activation in lymphocytes. Cell calcium 2007;42:145-56.
396. Mues M, Bartholomaus I, Thestrup T, et al. Real-time in vivo analysis of T cell activation in the central nervous system using a genetically encoded calcium indicator. Nature medicine 2013;19:778-83.
397. Krummel MF, Allison JP. Pillars article: CD28 and CTLA-4 have opposing effects on the response of T cells to stimulation. The journal of experimental medicine. 1995. 182: 459-465. Journal of immunology 2011;187:3459-65.
398. Mempel TR, Bauer CA. Intravital imaging of CD8+ T cell function in cancer. Clinical & experimental metastasis 2009;26:311-27.
399. Leimgruber A, Berger C, Cortez-Retamozo V, et al. Behavior of endogenous tumor-associated macrophages assessed in vivo using a functionalized nanoparticle. Neoplasia 2009;11:459-68, 2 p following 68.
400. Halle S, Keyser KA, Stahl FR, et al. In Vivo Killing Capacity of Cytotoxic T Cells Is Limited and Involves Dynamic Interactions and T Cell Cooperativity. Immunity 2016;44:233-45.
401. Honda T, Egen JG, Lammermann T, Kastenmuller W, Torabi-Parizi P, Germain RN. Tuning of antigen sensitivity by T cell receptor-dependent negative feedback controls T cell effector function in inflamed tissues. Immunity 2014;40:235-47.
402. Boissonnas A, Fetler L, Zeelenberg IS, Hugues S, Amigorena S. In vivo imaging of cytotoxic T cell infiltration and elimination of a solid tumor. The Journal of experimental medicine 2007;204:345-56.
403. Boissonnas A, Fetler L, Amigorena S. [Stepwise strategy adopted by cytotoxic T cells to eliminate solid tumors]. Medecine sciences : M/S 2007;23:570-2.
404. Han A, Glanville J, Hansmann L, Davis MM. Corrigendum: Linking T-cell receptor sequence to functional phenotype at the single-cell level. Nature biotechnology 2015;33:210.
405. Luster AD, Alon R, von Andrian UH. Immune cell migration in inflammation: present and future therapeutic targets. Nature immunology 2005;6:1182-90.
406. Cyster JG. Chemokines and cell migration in secondary lymphoid organs. Science 1999;286:2098-102.
407. Baggiolini M, Dewald B, Moser B. Human chemokines: an update. Annual review of immunology 1997;15:675-705.
408. Schumann K, Lammermann T, Bruckner M, et al. Immobilized chemokine fields and soluble chemokine gradients cooperatively shape migration patterns of dendritic cells. Immunity 2010;32:703-13.
409. Umehara H, Goda S, Imai T, et al. Fractalkine, a CX3C-chemokine, functions predominantly as an adhesion molecule in monocytic cell line THP-1. Immunology and cell biology 2001;79:298-302.
410. Harrison JK, Jiang Y, Chen S, et al. Role for neuronally derived fractalkine in mediating interactions between neurons and CX3CR1-expressing microglia.

Proceedings of the National Academy of Sciences of the United States of America 1998;95:10896-901.
411. Vitale S, Cambien B, Karimdjee BF, et al. Tissue-specific differential antitumour effect of molecular forms of fractalkine in a mouse model of metastatic colon cancer. Gut 2007;56:365-72.
412. Garton KJ, Gough PJ, Blobel CP, et al. Tumor necrosis factor-alpha-converting enzyme (ADAM17) mediates the cleavage and shedding of fractalkine (CX3CL1). The Journal of biological chemistry 2001;276:37993-8001.
413. Imai T, Hieshima K, Haskell C, et al. Identification and molecular characterization of fractalkine receptor CX3CR1, which mediates both leukocyte migration and adhesion. Cell 1997;91:521-30.
414. Staumont-Salle D, Fleury S, Lazzari A, et al. CX3CL1 (fractalkine) and its receptor CX3CR1 regulate atopic dermatitis by controlling effector T cell retention in inflamed skin. The Journal of experimental medicine 2014;211:1185-96.
415. Landsman L, Bar-On L, Zernecke A, et al. CX3CR1 is required for monocyte homeostasis and atherogenesis by promoting cell survival. Blood 2009;113:963-72.
416. Cardona AE, Pioro EP, Sasse ME, et al. Control of microglial neurotoxicity by the fractalkine receptor. Nature neuroscience 2006;9:917-24.
417. Fuhrmann M, Bittner T, Jung CK, et al. Microglial Cx3cr1 knockout prevents neuron loss in a mouse model of Alzheimer's disease. Nature neuroscience 2010;13:411-3.
418. Lee S, Varvel NH, Konerth ME, et al. CX3CR1 deficiency alters microglial activation and reduces beta-amyloid deposition in two Alzheimer's disease mouse models. The American journal of pathology 2010;177:2549-62.
419. Feng X, Szulzewsky F, Yerevanian A, et al. Loss of CX3CR1 increases accumulation of inflammatory monocytes and promotes gliomagenesis. Oncotarget 2015;6:15077-94.
420. Helmchen F, Denk W. Deep tissue two-photon microscopy. Nature methods 2005;2:932-40.
421. Theer P, Hasan MT, Denk W. Two-photon imaging to a depth of 1000 microm in living brains by use of a Ti:Al2O3 regenerative amplifier. Optics letters 2003;28:1022-4.
422. Svoboda K, Denk W, Kleinfeld D, Tank DW. In vivo dendritic calcium dynamics in neocortical pyramidal neurons. Nature 1997;385:161-5.
423. Helmchen F, Svoboda K, Denk W, Tank DW. In vivo dendritic calcium dynamics in deep-layer cortical pyramidal neurons. Nature neuroscience 1999;2:989-96.
424. Svoboda K, Helmchen F, Denk W, Tank DW. Spread of dendritic excitation in layer 2/3 pyramidal neurons in rat barrel cortex in vivo. Nature neuroscience 1999;2:65-73.
425. Nimmerjahn A, Kirchhoff F, Kerr JN, Helmchen F. Sulforhodamine 101 as a specific marker of astroglia in the neocortex in vivo. Nature methods 2004;1:31-7.
426. Hoffman RM. In vivo imaging of metastatic cancer with fluorescent proteins. Cell death and differentiation 2002;9:786-9.
427. Barretto RP, Schnitzer MJ. In vivo microendoscopy of the hippocampus. Cold Spring Harbor protocols 2012;2012:1092-9.
428. Chen BE, Trachtenberg JT, Holtmaat AJ, Svoboda K. Long-term, high-resolution imaging in the neocortex in vivo. CSH protocols 2008;2008:pdb prot4902.

429. Irla M, Guenot J, Sealy G, Reith W, Imhof BA, Serge A. Three-dimensional visualization of the mouse thymus organization in health and immunodeficiency. Journal of immunology 2013;190:586-96.
430. Liarski VM, Kaverina N, Chang A, et al. Cell distance mapping identifies functional T follicular helper cells in inflamed human renal tissue. Science translational medicine 2014;6:230ra46.
431. Ziegler-Heitbrock HW, Fingerle G, Strobel M, et al. The novel subset of CD14+/CD16+ blood monocytes exhibits features of tissue macrophages. Eur J Immunol 1993;23:2053-8.
432. Dolmans MM, Michaux N, Camboni A, et al. Evaluation of Liberase, a purified enzyme blend, for the isolation of human primordial and primary ovarian follicles. Hum Reprod 2006;21:413-20.
433. Nikodemova M, Watters JJ. Efficient isolation of live microglia with preserved phenotypes from adult mouse brain. J Neuroinflammation 2012;9:147.
434. Lindstrom MJ, Bates DM. Nonlinear mixed effects models for repeated measures data. Biometrics 1990:673-87.
435. Thompson PG, Smouse PE, Scofield DG, Sork VL. What seeds tell us about birds: a multi-year analysis of acorn woodpecker foraging movements. Movement Ecology 2014;2:12.
436. Abbott NJ, Ronnback L, Hansson E. Astrocyte-endothelial interactions at the blood-brain barrier. Nature reviews Neuroscience 2006;7:41-53.
437. Saris SC, Rosenberg SA, Friedman RB, Rubin JT, Barba D, Oldfield EH. Penetration of recombinant interleukin-2 across the blood-cerebrospinal fluid barrier. Journal of neurosurgery 1988;69:29-34.
438. Beck DW, Vinters HV, Hart MN, Cancilla PA. Glial cells influence polarity of the blood-brain barrier. Journal of neuropathology and experimental neurology 1984;43:219-24.
439. Prat A, Biernacki K, Wosik K, Antel JP. Glial cell influence on the human blood-brain barrier. Glia 2001;36:145-55.
440. Liu C, Wu CA, Yang QF, et al. Macrophages Mediate the Repair of Brain Vascular Rupture through Direct Physical Adhesion and Mechanical Traction. Immunity 2016;44:1162-76.
441. Mostany R, Portera-Cailliau C. A craniotomy surgery procedure for chronic brain imaging. Journal of visualized experiments : JoVE 2008.
442. Lathia JD, Gallagher J, Myers JT, et al. Direct in vivo evidence for tumor propagation by glioblastoma cancer stem cells. PloS one 2011;6:e24807.
443. Mostany R, Portera-Cailliau C. A method for 2-photon imaging of blood flow in the neocortex through a cranial window. Journal of visualized experiments : JoVE 2008.
444. Ricard C, Debarbieux FC. Six-color intravital two-photon imaging of brain tumors and their dynamic microenvironment. Frontiers in cellular neuroscience 2014;8:57.
445. Ricard C, Stanchi F, Rodriguez T, Amoureux MC, Rougon G, Debarbieux F. Dynamic quantitative intravital imaging of glioblastoma progression reveals a lack of correlation between tumor growth and blood vessel density. PloS one 2013;8:e72655.
446. Ricard C, Tchoghandjian A, Luche H, et al. Phenotypic dynamics of microglial and monocyte-derived cells in glioblastoma-bearing mice. Scientific reports 2016;6:26381.

447. Kienast Y, von Baumgarten L, Fuhrmann M, et al. Real-time imaging reveals the single steps of brain metastasis formation. Nature medicine 2010;16:116-22.
448. Winkler F, Kienast Y, Fuhrmann M, et al. Imaging glioma cell invasion in vivo reveals mechanisms of dissemination and peritumoral angiogenesis. Glia 2009;57:1306-15.
449. Madden KS, Zettel ML, Majewska AK, Brown EB. Brain tumor imaging: live imaging of glioma by two-photon microscopy. Cold Spring Harbor protocols 2013;2013.
450. Fumagalli S, Coles JA, Ejlerskov P, et al. In vivo real-time multiphoton imaging of T lymphocytes in the mouse brain after experimental stroke. Stroke; a journal of cerebral circulation 2011;42:1429-36.
451. Chen X, Nadiarynkh O, Plotnikov S, Campagnola PJ. Second harmonic generation microscopy for quantitative analysis of collagen fibrillar structure. Nature protocols 2012;7:654-69.
452. Zipfel WR, Williams RM, Webb WW. Nonlinear magic: multiphoton microscopy in the biosciences. Nature biotechnology 2003;21:1369-77.
453. Zipfel WR, Williams RM, Christie R, Nikitin AY, Hyman BT, Webb WW. Live tissue intrinsic emission microscopy using multiphoton-excited native fluorescence and second harmonic generation. Proceedings of the National Academy of Sciences of the United States of America 2003;100:7075-80.
454. Zhang L, Lapierre A, Roy B, et al. Imaging glioma initiation in vivo through a polished and reinforced thin-skull cranial window. Journal of visualized experiments : JoVE 2012.
455. Stence N, Waite M, Dailey ME. Dynamics of microglial activation: a confocal time-lapse analysis in hippocampal slices. Glia 2001;33:256-66.
456. Blond D, Campbell SJ, Butchart AG, Perry VH, Anthony DC. Differential induction of interleukin-1beta and tumour necrosis factor-alpha may account for specific patterns of leukocyte recruitment in the brain. Brain research 2002;958:89-99.
457. Roberts EW, Broz ML, Binnewies M, et al. Critical Role for CD103+/CD141+ Dendritic Cells Bearing CCR7 for Tumor Antigen Trafficking and Priming of T Cell Immunity in Melanoma. Cancer cell 2016.
458. Katzman SD, O'Gorman WE, Villarino AV, et al. Duration of antigen receptor signaling determines T-cell tolerance or activation. Proceedings of the National Academy of Sciences of the United States of America 2010;107:18085-90.
459. Inaba K, Metlay JP, Crowley MT, Steinman RM. Dendritic cells pulsed with protein antigens in vitro can prime antigen-specific, MHC-restricted T cells in situ. The Journal of experimental medicine 1990;172:631-40.
460. Aloisi F, Ria F, Penna G, Adorini L. Microglia are more efficient than astrocytes in antigen processing and in Th1 but not Th2 cell activation. Journal of immunology 1998;160:4671-80.
461. Graeber MB, Scheithauer BW, Kreutzberg GW. Microglia in brain tumors. Glia 2002;40:252-9.
462. Miller MJ, Hejazi AS, Wei SH, Cahalan MD, Parker I. T cell repertoire scanning is promoted by dynamic dendritic cell behavior and random T cell motility in the lymph node. Proceedings of the National Academy of Sciences of the United States of America 2004;101:998-1003.
463. Saederup N, Cardona AE, Croft K, et al. Selective chemokine receptor usage by central nervous system myeloid cells in CCR2-red fluorescent protein knock-in mice. PloS one 2010;5:e13693.

464. Gerner MY, Kastenmuller W, Ifrim I, Kabat J, Germain RN. Histo-cytometry: a method for highly multiplex quantitative tissue imaging analysis applied to dendritic cell subset microanatomy in lymph nodes. Immunity 2012;37:364-76.
465. Boissonnas A, Licata F, Poupel L, et al. CD8+ tumor-infiltrating T cells are trapped in the tumor-dendritic cell network. Neoplasia 2013;15:85-94.
466. Aloisi F, Ria F, Adorini L. Regulation of T-cell responses by CNS antigen-presenting cells: different roles for microglia and astrocytes. Immunology today 2000;21:141-7.
467. Li W, Graeber MB. The molecular profile of microglia under the influence of glioma. Neuro-oncology 2012;14:958-78.
468. Zhu W, Carney KE, Pigott VM, et al. Glioma-mediated microglial activation promotes glioma proliferation and migration: roles of Na+/H+ exchanger isoform 1. Carcinogenesis 2016.
469. Broz ML, Binnewies M, Boldajipour B, et al. Dissecting the tumor myeloid compartment reveals rare activating antigen-presenting cells critical for T cell immunity. Cancer cell 2014;26:638-52.
470. Broz ML, Krummel MF. The emerging understanding of myeloid cells as partners and targets in tumor rejection. Cancer immunology research 2015;3:313-9.
471. Tussiwand R, Lee WL, Murphy TL, et al. Compensatory dendritic cell development mediated by BATF-IRF interactions. Nature 2012;490:502-7.
472. Hume DA, Freeman TC. Transcriptomic analysis of mononuclear phagocyte differentiation and activation. Immunological reviews 2014;262:74-84.
473. Hume DA, Mabbott N, Raza S, Freeman TC. Can DCs be distinguished from macrophages by molecular signatures? Nature immunology 2013;14:187-9.
474. Hume DA. Macrophages as APC and the Dendritic Cell Myth. Journal of immunology 2008;181:5829-35.
475. Yona S, Kim KW, Wolf Y, et al. Fate mapping reveals origins and dynamics of monocytes and tissue macrophages under homeostasis. Immunity 2013;38:79-91.
476. Headley MB, Bins A, Nip A, et al. Visualization of immediate immune responses to pioneer metastatic cells in the lung. Nature 2016;531:513-7.
477. Szulzewsky F, Arora S, de Witte L, et al. Human glioblastoma-associated microglia/monocytes express a distinct RNA profile compared to human control and murine samples. Glia 2016;64:1416-36.
478. a Dzaye OD, Hu F, Derkow K, et al. Glioma Stem Cells but Not Bulk Glioma Cells Upregulate IL-6 Secretion in Microglia/Brain Macrophages via Toll-like Receptor 4 Signaling. Journal of neuropathology and experimental neurology 2016;75:429-40.
479. Zhang ZM, Yang Z, Zhang Z. Distribution and characterization of tumor-associated macrophages/microglia in rat C6 glioma. Oncology letters 2015;10:2442-6.
480. van der Vos KE, Abels ER, Zhang X, et al. Directly visualized glioblastoma-derived extracellular vesicles transfer RNA to microglia/macrophages in the brain. Neuro-oncology 2016;18:58-69.
481. Mieczkowski J, Kocyk M, Nauman P, et al. Down-regulation of IKKbeta expression in glioma-infiltrating microglia/macrophages is associated with defective inflammatory/immune gene responses in glioblastoma. Oncotarget 2015;6:33077-90.
482. Choi J, Stradmann-Bellinghausen B, Yakubov E, Savaskan NE, Regnier-Vigouroux A. Glioblastoma cells induce differential glutamatergic gene expressions in human tumor-associated microglia/macrophages and monocyte-derived macrophages. Cancer biology & therapy 2015;16:1205-13.

483. Szulzewsky F, Pelz A, Feng X, et al. Glioma-associated microglia/macrophages display an expression profile different from M1 and M2 polarization and highly express Gpnmb and Spp1. PloS one 2015;10:e0116644.
484. Hattermann K, Sebens S, Helm O, et al. Chemokine expression profile of freshly isolated human glioblastoma-associated macrophages/microglia. Oncology reports 2014;32:270-6.
485. Sasaki A, Yokoo H, Tanaka Y, Homma T, Nakazato Y, Ohgaki H. Characterization of microglia/macrophages in gliomas developed in S-100beta-v-erbB transgenic rats. Neuropathology : official journal of the Japanese Society of Neuropathology 2013;33:505-14.
486. Engler JR, Robinson AE, Smirnov I, et al. Increased microglia/macrophage gene expression in a subset of adult and pediatric astrocytomas. PloS one 2012;7:e43339.
487. Zheng PP, van der Weiden M, van der Spek PJ, Vincent AJ, Kros JM. Isocitrate dehydrogenase 1R132H mutation in microglia/macrophages in gliomas: indication of a significant role of microglia/macrophages in glial tumorigenesis. Cancer biology & therapy 2012;13:836-9.
488. Levy A, Blacher E, Vaknine H, Lund FE, Stein R, Mayo L. CD38 deficiency in the tumor microenvironment attenuates glioma progression and modulates features of tumor-associated microglia/macrophages. Neuro-oncology 2012;14:1037-49.
489. Okada M, Saio M, Kito Y, et al. Tumor-associated macrophage/microglia infiltration in human gliomas is correlated with MCP-3, but not MCP-1. International journal of oncology 2009;34:1621-7.
490. Eistere W, Hilbe W, Stauder R, Bechter O, Fend F, Thaler J. An aggressive subtype of B-CLL is characterized by strong CD44 expression and lack of CD11c. British journal of haematology 1996;93:661-9.
491. Wang Y, Xu B, Hu WW, et al. High expression of CD11c indicates favorable prognosis in patients with gastric cancer. World journal of gastroenterology 2015;21:9403-12.
492. Benvenuti F, Lagaudriere-Gesbert C, Grandjean I, et al. Dendritic cell maturation controls adhesion, synapse formation, and the duration of the interactions with naive T lymphocytes. Journal of immunology 2004;172:292-301.
493. Egen JG, Rothfuchs AG, Feng CG, Horwitz MA, Sher A, Germain RN. Intravital imaging reveals limited antigen presentation and T cell effector function in mycobacterial granulomas. Immunity 2011;34:807-19.
494. Mantovani A. Chemokines in neoplastic progression. Seminars in cancer biology 2004;14:147-8.
495. Mantovani A, Allavena P, Sozzani S, Vecchi A, Locati M, Sica A. Chemokines in the recruitment and shaping of the leukocyte infiltrate of tumors. Seminars in cancer biology 2004;14:155-60.
496. Zlotnik A, Burkhardt AM, Homey B. Homeostatic chemokine receptors and organ-specific metastasis. Nature reviews Immunology 2011;11:597-606.
497. Ozawa PM, Ariza CB, Ishibashi CM, et al. Role of CXCL12 and CXCR4 in normal cerebellar development and medulloblastoma. International journal of cancer 2016;138:10-3.
498. Calatozzolo C, Canazza A, Pollo B, et al. Expression of the new CXCL12 receptor, CXCR7, in gliomas. Cancer biology & therapy 2011;11:242-53.

499. Hattermann K, Held-Feindt J, Lucius R, et al. The chemokine receptor CXCR7 is highly expressed in human glioma cells and mediates antiapoptotic effects. Cancer research 2010;70:3299-308.
500. Berahovich RD, Zabel BA, Lewen S, et al. Endothelial expression of CXCR7 and the regulation of systemic CXCL12 levels. Immunology 2014;141:111-22.
501. Hattermann K, Mentlein R, Held-Feindt J. CXCL12 mediates apoptosis resistance in rat C6 glioma cells. Oncology reports 2012;27:1348-52.
502. Zhu X, Fujita M, Snyder LA, Okada H. Systemic delivery of neutralizing antibody targeting CCL2 for glioma therapy. Journal of neuro-oncology 2011;104:83-92.
503. do Carmo A, Patricio I, Cruz MT, Carvalheiro H, Oliveira CR, Lopes MC. CXCL12/CXCR4 promotes motility and proliferation of glioma cells. Cancer biology & therapy 2010;9:56-65.
504. Uemae Y, Ishikawa E, Osuka S, et al. CXCL12 secreted from glioma stem cells regulates their proliferation. Journal of neuro-oncology 2014;117:43-51.
505. Walters MJ, Ebsworth K, Berahovich RD, et al. Inhibition of CXCR7 extends survival following irradiation of brain tumours in mice and rats. British journal of cancer 2014;110:1179-88.
506. Gatti M, Pattarozzi A, Bajetto A, et al. Inhibition of CXCL12/CXCR4 autocrine/paracrine loop reduces viability of human glioblastoma stem-like cells affecting self-renewal activity. Toxicology 2013;314:209-20.
507. Vakilian A, Khorramdelazad H, Heidari P, Sheikh Rezaei Z, Hassanshahi G. CCL2/CCR2 signaling pathway in glioblastoma multiforme. Neurochemistry international 2017;103:1-7.
508. Brown CE, Vishwanath RP, Aguilar B, et al. Tumor-derived chemokine MCP-1/CCL2 is sufficient for mediating tumor tropism of adoptively transferred T cells. Journal of immunology 2007;179:3332-41.
509. Zhou M, Bracci PM, McCoy LS, et al. Serum macrophage-derived chemokine/CCL22 levels are associated with glioma risk, CD4 T cell lymphopenia and survival time. International journal of cancer 2015;137:826-36.
510. Carrillo-de Sauvage MA, Gomez A, Ros CM, et al. CCL2-expressing astrocytes mediate the extravasation of T lymphocytes in the brain. Evidence from patients with glioma and experimental models in vivo. PloS one 2012;7:e30762.
511. Laudati E, Curro D, Navarra P, Lisi L. Blockade of CCR5 receptor prevents M2 microglia phenotype in a microglia-glioma paradigm. Neurochemistry international 2017.
512. Pham K, Luo D, Liu C, Harrison JK. CCL5, CCR1 and CCR5 in murine glioblastoma: immune cell infiltration and survival rates are not dependent on individual expression of either CCR1 or CCR5. Journal of neuroimmunology 2012;246:10-7.
513. Brandenburg S, Muller A, Turkowski K, et al. Resident microglia rather than peripheral macrophages promote vascularization in brain tumors and are source of alternative pro-angiogenic factors. Acta neuropathologica 2016;131:365-78.
514. Liu C, Luo D, Reynolds BA, et al. Chemokine receptor CXCR3 promotes growth of glioma. Carcinogenesis 2011;32:129-37.
515. Wang L, Qin H, Li L, et al. Overexpression of CCL20 and its receptor CCR6 predicts poor clinical prognosis in human gliomas. Medical oncology 2012;29:3491-7.
516. Hattermann K, Held-Feindt J, Ludwig A, Mentlein R. The CXCL16-CXCR6 chemokine axis in glial tumors. Journal of neuroimmunology 2013;260:47-54.

517. Chen L, Liu X, Zhang HY, et al. Upregulation of chemokine receptor CCR10 is essential for glioma proliferation, invasion and patient survival. Oncotarget 2014;5:6576-83.
518. Pu Y, Li S, Zhang C, Bao Z, Yang Z, Sun L. High expression of CXCR3 is an independent prognostic factor in glioblastoma patients that promotes an invasive phenotype. Journal of neuro-oncology 2015;122:43-51.
519. Bazan JF, Bacon KB, Hardiman G, et al. A new class of membrane-bound chemokine with a CX3C motif. Nature 1997;385:640-4.
520. Ludwig A, Hundhausen C, Lambert MH, et al. Metalloproteinase inhibitors for the disintegrin-like metalloproteinases ADAM10 and ADAM17 that differentially block constitutive and phorbol ester-inducible shedding of cell surface molecules. Combinatorial chemistry & high throughput screening 2005;8:161-71.
521. Mizuno T, Kawanokuchi J, Numata K, Suzumura A. Production and neuroprotective functions of fractalkine in the central nervous system. Brain research 2003;979:65-70.
522. Liu C, Luo D, Streit WJ, Harrison JK. CX3CL1 and CX3CR1 in the GL261 murine model of glioma: CX3CR1 deficiency does not impact tumor growth or infiltration of microglia and lymphocytes. Journal of neuroimmunology 2008;198:98-105.
523. Mason SD, Joyce JA. Proteolytic networks in cancer. Trends in cell biology 2011;21:228-37.
524. Held-Feindt J, Hattermann K, Muerkoster SS, et al. CX3CR1 promotes recruitment of human glioma-infiltrating microglia/macrophages (GIMs). Experimental cell research 2010;316:1553-66.
525. Matsubara T, Ono T, Yamanoi A, Tachibana M, Nagasue N. Fractalkine-CX3CR1 axis regulates tumor cell cycle and deteriorates prognosis after radical resection for hepatocellular carcinoma. Journal of surgical oncology 2007;95:241-9.
526. Shulby SA, Dolloff NG, Stearns ME, Meucci O, Fatatis A. CX3CR1-fractalkine expression regulates cellular mechanisms involved in adhesion, migration, and survival of human prostate cancer cells. Cancer research 2004;64:4693-8.
527. Lee YS, Morinaga H, Kim JJ, et al. The fractalkine/CX3CR1 system regulates beta cell function and insulin secretion. Cell 2013;153:413-25.
528. Ohta M, Tanaka F, Yamaguchi H, Sadanaga N, Inoue H, Mori M. The high expression of Fractalkine results in a better prognosis for colorectal cancer patients. International journal of oncology 2005;26:41-7.
529. Depner M, Kormann MS, Klopp N, et al. CX3CR1 polymorphisms are associated with atopy but not asthma in German children. International archives of allergy and immunology 2007;144:91-4.
530. Faure S, Meyer L, Costagliola D, et al. Rapid progression to AIDS in HIV+ individuals with a structural variant of the chemokine receptor CX3CR1. Science 2000;287:2274-7.
531. McDermott DH, Colla JS, Kleeberger CA, et al. Genetic polymorphism in CX3CR1 and risk of HIV disease. Science 2000;290:2031.
532. Halama N, Michel S, Kloor M, et al. Localization and density of immune cells in the invasive margin of human colorectal cancer liver metastases are prognostic for response to chemotherapy. Cancer research 2011;71:5670-7.

533. Bindea G, Mlecnik B, Tosolini M, et al. Spatiotemporal dynamics of intratumoral immune cells reveal the immune landscape in human cancer. Immunity 2013;39:782-95.
534. Jochems C, Schlom J. Tumor-infiltrating immune cells and prognosis: the potential link between conventional cancer therapy and immunity. Experimental biology and medicine 2011;236:567-79.
535. Geranmayeh F, Scheithauer BW, Spitzer C, Meyer FB, Svensson-Engwall AC, Graeber MB. Microglia in gemistocytic astrocytomas. Neurosurgery 2007;60:159-66; discussion 66.
536. Wierzba-Bobrowicz T, Kuchna I, Matyja E. Reaction of microglial cells in human astrocytomas (preliminary report). Folia neuropathologica / Association of Polish Neuropathologists and Medical Research Centre, Polish Academy of Sciences 1994;32:251-2.
537. Limatola C, Ransohoff RM. Modulating neurotoxicity through CX3CL1/CX3CR1 signaling. Frontiers in cellular neuroscience 2014;8:229.
538. Lauro C, Catalano M, Di Paolo E, et al. Fractalkine/CX3CL1 engages different neuroprotective responses upon selective glutamate receptor overactivation. Frontiers in cellular neuroscience 2014;8:472.
539. Spangenberg EE, Green KN. Inflammation in Alzheimer's disease: Lessons learned from microglia-depletion models. Brain, behavior, and immunity 2016.
540. Acharya MM, Green KN, Allen BD, et al. Elimination of microglia improves cognitive function following cranial irradiation. Scientific reports 2016;6:31545.
541. Zhu C, Herrmann US, Falsig J, et al. A neuroprotective role for microglia in prion diseases. The Journal of experimental medicine 2016;213:1047-59.
542. Yao Y, Echeverry S, Shi XQ, et al. Dynamics of spinal microglia repopulation following an acute depletion. Scientific reports 2016;6:22839.
543. Wang YM, Szretter KJ, Vermi W, et al. IL-34 is a tissue-restricted ligand of CSF1R required for the development of Langerhans cells and microglia. Nature immunology 2012;13:753-+.
544. Xiao Y, Jin J, Chang M, et al. Peli1 promotes microglia-mediated CNS inflammation by regulating Traf3 degradation. Nature medicine 2013;19:595-602.
545. Beemiller P, Jacobelli J, Krummel MF. Integration of the movement of signaling microclusters with cellular motility in immunological synapses. Nature immunology 2012;13:787-95.
546. Wulfing C, Rabinowitz JD, Beeson C, Sjaastad MD, McConnell HM, Davis MM. Kinetics and extent of T cell activation as measured with the calcium signal. The Journal of experimental medicine 1997;185:1815-25.
547. Feske S. Calcium signalling in lymphocyte activation and disease. Nature reviews Immunology 2007;7:690-702.
548. Gwack Y, Srikanth S, Feske S, et al. Biochemical and functional characterization of Orai proteins. The Journal of biological chemistry 2007;282:16232-43.
549. Russo MV, McGavern DB. Immune Surveillance of the CNS following Infection and Injury. Trends in immunology 2015;36:637-50.
550. Bianchi ME. DAMPs, PAMPs and alarmins: all we need to know about danger. Journal of leukocyte biology 2007;81:1-5.
551. Manson J, Thiemermann C, Brohi K. Trauma alarmins as activators of damage-induced inflammation. Brit J Surg 2012;99:12-20.

552. Kigerl KA, Vaccari JPD, Dietrich WD, Popovich PG, Keane RW. Pattern recognition receptors and central nervous system repair. Exp Neurol 2014;258:5-16.
553. Castagna C, Viglietti-Panzica C, Panzica GC. Protein S100 immunoreactivity in glial cells and neurons of the Japanese quail brain. J Chem Neuroanat 2003;25:195-212.
554. Nygren De Boussard C, Fredman P, Lundin A, Andersson K, Edman G, Borg J. S100 in mild traumatic brain injury. Brain injury 2004;18:671-83.
555. Zongo D, Ribereau-Gayon R, Masson F, et al. S100-B protein as a screening tool for the early assessment of minor head injury. Annals of emergency medicine 2012;59:209-18.
556. Schietinger A, Philip M, Liu RB, Schreiber K, Schreiber H. Bystander killing of cancer requires the cooperation of CD4(+) and CD8(+) T cells during the effector phase. The Journal of experimental medicine 2010;207:2469-77.
557. Corbin K, Pinkard H, Peck S, Beemiller P, Krummel MF. Assessing and benchmarking multiphoton microscopes for biologists. Methods in cell biology 2014;123:135-51.
558. Thornton EE, Krummel MF, Looney MR. Live imaging of the lung. Current protocols in cytometry / editorial board, J Paul Robinson, managing editor [et al] 2012;Chapter 12:Unit12 28.
559. Barretto RP, Ko TH, Jung JC, et al. Time-lapse imaging of disease progression in deep brain areas using fluorescence microendoscopy. Nature medicine 2011;17:223-8.
560. Chung K, Wallace J, Kim SY, et al. Structural and molecular interrogation of intact biological systems. Nature 2013;497:332-7.
561. Tomer R, Ye L, Hsueh B, Deisseroth K. Advanced CLARITY for rapid and high-resolution imaging of intact tissues. Nature protocols 2014;9:1682-97.
562. Ansel KM, Ngo VN, Hyman PL, et al. A chemokine-driven positive feedback loop organizes lymphoid follicles. Nature 2000;406:309-14.

VITA

Felix Ijeoma Nwajei was born in Zaria, Kaduna State, Nigeria, to Felix O. Nwajei and Felicia N. Nwajei. He completed his pre-medical and medical studies at University of Lagos Nigeria, earning a degree in Medicine. He was a medical/surgical intern at the Lagos University Teaching Hospital and then Research Fellow at the University of Texas MD Anderson Cancer Center department of neurosurgery before being admitted at the University of Texas Graduate School of Biomedical Sciences at Houston in January 2012. He joined the laboratory of Dr. Tomasz Zal at the Immunology Department in July 2012, where he completed his dissertation work.